LEUPHANA
UNIVERSITÄT LÜNEBURG

Einfluss unterschiedlicher Lichtspektren und Temperaturen auf die Biomassen- und Wertstoffproduktion in Mikroalgen

Der Fakultät Nachhaltigkeit

der Leuphana Universität Lüneburg zur Erlangung des Grades

doctor rerum naturalium

– Dr. rer. nat. –

vorgelegte Dissertation von

Mark Helamieh

geboren am 13. November 1984 in Aachen

Eingereicht am: 30.06.2023

Mündliche Verteidigung (Disputation) am: 10.01.2024

Betreuer und Erstgutachter: Prof. Dr. Klaus Kümmerer
(Leuphana Universität Lüneburg)

Zweitgutachterin: Prof. Dr. Vicky Temperton
(Leuphana Universität Lüneburg)

Drittgutachterin: Prof. Dr. Sigrun Reumann
(Universität Hamburg)

Die einzelnen Beiträge zur kumulativen Dissertation wurden wie folgt veröffentlicht:

Helamieh, M., Gebhardt, A., Reich, M., Kuhn, F., Kerner, M., & Kümmerer, K. (2021). Growth and fatty acid composition of *Acutodesmus obliquus* under different light spectra and temperatures. *Lipids*, 56(5), 485-498. DOI: 10.1002/lipd.12316.

Helamieh, M., Reich, M., Bory, S., Rohne, P., Riebesell, U., Kerner, M., & Kümmerer K. (2022). Blue-green light is required for a maximized fatty acid unsaturation and pigment concentration in the microalga *Acutodesmus obliquus*. *Lipids*, 57(4-5), 221-232. DOI: 10.1002/lipd.12343.

Helamieh, M., Reich, M., Rohne, P., Riebesell, U., Kerner, M., & Kümmerer, K. (2023). Impact of green and blue-green light on the growth, pigment concentration, and fatty acid unsaturation in the microalga *Monoraphidium braunii*. *Photochemistry and Photobiology*. Veröffentlicht im Oktober 2023. DOI:10.1111/php.13873.

Veröffentlichungsjahr: 2024

PER ASPERA AD ASTRA

-Lucius Annaeus Seneca-

Zusammenfassung

Mikroalgen können bei den internationalen Bemühungen zur Begrenzung der CO_2-Emissionen einen wichtigen Beitrag leisten. In der Photosynthese der Mikroalgen wird, wie auch bei Landpflanzen, das CO_2 aus der Atmosphäre in Biomasse fixiert. Im Gegensatz zu Landpflanzen können Mikroalgen zudem exponentiell wachsen, haben geringere Anforderungen an die Wasserqualität und konkurrieren nicht mit Agrarflächen, die begrenzt und für die Nahrungsmittelsicherheit der Weltbevölkerung erforderlich sind. Die produzierte Mikroalgenbiomasse kann als regenerative Ressource zu Biokraftstoffen wie Biogas und Biodiesel umgewandelt und somit als Energieträger genutzt werden. Zudem können Mikroalgen auch bei der biotechnologischen Produktion kommerziell relevanter Wertstoffe wie Pigmenten und Omega-3-Fettsäuren für die Nahrungsmittelindustrie Anwendung finden. Mit dem Ziel der Steigerung dieser Wertstoffe stand die Untersuchung des Einflusses der Kultivierungsparameter Licht und Temperatur auf das Wachstum und die Zusammensetzung der Mikroalgenbiomasse im Mittelpunkt dieser Dissertation. Insbesondere der Einfluss unterschiedlicher Lichtspektren auf das Wachstum und die Wertstoffproduktion in Mikroalgen wird in der Literatur kontrovers diskutiert und wurde daher detailliert untersucht. Zusätzlich wurde überprüft, ob sich die gewonnenen Erkenntnisse auch auf Landpflanzen übertragen lassen.

Im Rahmen dieser Promotion wurde erstmals systematisch der Einfluss unterschiedlicher Temperaturen und Lichtspektren im zeitlichen Verlauf der Kultivierung auf Mikroalgen untersucht. Hierbei konnten distinkte Spektralbereiche sowie Temperaturen ermittelt werden, die für eine maximale Produktion von Biomasse und Pigmenten sowie einem maximalen Desaturierungsgrad der Fettsäuren erforderlich sind. Die in dieser Arbeit gewonnenen Erkenntnisse tragen zu einem besseren Verständnis der Biochemie von photosynthetischen Organismen bei. Dieses Wissen ist bereits in die Entwicklung eines Hybridsystems zur komplementären Nutzung des Sonnenlichts für die Photovoltaik und Biomassenproduktion eingeflossen und könnte künftig bei der gezielten Produktion von Wertstoffen mittels Mikroalgen weitere Anwendungen finden.

In den Untersuchungen wurden Mikroalgen sowie zusätzlich Rapspflanzen (*Brassica napus* L.) unter verschiedenen Bedingungen kultiviert und die Biomassenkonzentration sowie die Fettsäure- und Pigmentkomposition zu festgelegten Zeitpunkten untersucht. Mit einer modifizierten Folch-Extraktion wurden die Fettsäuren extrahiert, umgeestert und mittels Gaschromatografie mit Elektronenstoßionisation Massenspektrometrie (GC-EI/MS) analysiert. Die Analyse der Photosynthesepigmente erfolgte durch Hochleistungsflüssigkeitschromatografie gekoppelt mit einem UV/VIS Spektrometer (HPLC-UV/VIS).

Zunächst wurde die grüne Mikroalge *Acutodesmus obliquus* (Turpin) bei unterschiedlichen Temperaturen mit blauem, grünem und rotem Licht unterschiedlicher Photonenflussdichte kultiviert. Die Bestrahlung mit blauem Licht führte unter allen Bedingungen zur geringsten Biomassenproduktion. Demgegenüber bewirkte die Behandlung mit rotem Licht bei allen Experimenten eine höhere

Biomassenproduktion. Die Biomassenproduktion unter grünem Licht war dagegen sehr variabel und abhängig von den Rahmenbedingungen. Entgegen der klassischen Lehrmeinung ließ sich mit diesem Spektralbereich insbesondere bei hohen Photonenflussdichten und hohen Biomassenkonzentrationen ein höheres Wachstum als mit rotem Licht erzielen. In nachfolgenden Untersuchungen wurde zudem festgestellt, dass die Biomassenkonzentration im Vergleich zur Behandlung mit rotem Licht signifikant erhöht ist, wenn das Lichtspektrum neben langwelligeren Anteilen zusätzlich noch kurzwelligere Spektralanteile unter 550 nm enthält. Diese Ergebnisse wurden mehrfach an *A. obliquus* und bei der nah verwandten Grünalge *Monoraphidium braunii* (Nägeli) reproduziert.

Bei der Fettsäureanalyse war ein starker Einfluss der Parameter Temperatur und Lichtspektrum auf die Fettsäurekomposition in *A. obliquus* feststellbar. So bewirkte eine niedrige Kultivierungstemperatur einen erhöhten prozentualen Anteil der mehrfach ungesättigten Fettsäuren (PUFAs) 16:4, 18:3 und 18:4. Eine starke Erhöhung der prozentualen Anteile dieser PUFAs wurde ebenfalls bei Kultivierung mit grünem und blauem Licht gegenüber rotem Licht festgestellt. Umgekehrt waren die relativen Proportionen der ungesättigten Fettsäuren mit niedrigerem Desaturierungsgrad (16:1, 16:2, 16:3, 18:1 und 18:2) unter rotem Licht gegenüber grünem und blauem Licht erhöht. Weil der Spektralbereich zwischen 450 und 550 nm (blaugrünes Licht) im grünen und blauen Licht, nicht jedoch im roten Licht enthalten ist, wurde geschlossen, dass dieser Spektralanteil für den Einbau von Doppelbindungen in die Kohlenwasserstoffkette der Fettsäuren in *A. obliquus* relevant ist. Im weiteren Verlauf der Arbeit wurde diese Beobachtung bei *A. obliquus* reproduziert und durch die Kultivierung mit spezifischen Lichtspektren auf einen Spektralbereich von 470–520 nm eingegrenzt. Zudem wurde auch eine maximale Konzentration aller in *A. obliquus* identifizierten Pigmente bei Kultivierung mit blaugrünem Licht gemessen. Da sowohl die PUFAs 16:4 und 18:3 als auch die Pigmente vorwiegend in der Thylakoidmembran vorkommen, wurde die Hypothese entwickelt, dass blaugrünes Licht eine physiologische Reaktion bewirkt, die zu einer erhöhten Bildung von Thylakoidmembranen führt.

Im letzten Teil der Arbeit wurde überprüft, ob die an *A. obliquus* gewonnenen Erkenntnisse auf die phylogenetisch nah verwandte Grünalgenart *M. braunii* und auf die Landpflanze *B. napus* übertragen werden können. Bei *M. braunii* wurde, ähnlich wie bei *A. obliquus*, ein maximaler Desaturierungsgrad der Fettsäuren und eine maximale Konzentration der Photosynthesepigmente bei Behandlung mit blaugrünem Licht gemessen. Zudem konnten Hinweise dafür gefunden werden, dass blaugrünes Licht ebenfalls relevant für die Desaturierung der Fettsäuren in den Folgeblättern von *B. napus* ist.

Abstract

Due to international efforts to reduce the emission of CO_2, microalgae-based industrial products are expected to gain importance. Like land plants, microalgae can fix CO_2 into biomass by photosynthesis. Additionally, microalgae have several advantages compared to land plants, such as potentially exponential growth, a lower water quality requirement, and the fact that they do not compete for arable land with land-based crops. The different components of algal biomass can be used to produce renewable biofuels, such as biogas and biodiesel. Furthermore, microalgae can be used as a production platform for valuable compounds, e.g., pigments, and omega-3 fatty acids for the food industry. This work was focused on the impact of the parameters of temperature and light on the growth and biomass composition in microalgae. In particular, the impact of different light spectra on the growth and production of valuable compounds in microalgae has only been sparsely studied. Therefore, a systematic investigation of the effects of different light spectra on microalgal growth, fatty acid composition, and pigment concentration was carried out. Subsequently, it was tested if the effects identified in microalgae might be applicable to land plants.

In this thesis, a systematic investigation of the impact of temperature and light spectra on microalgae cultivation was performed. The light spectra and temperatures that are required for maximized biomass production, pigment concentration, and fatty acid unsaturation in microalgae were identified. This knowledge brings new insights into the biochemistry of photosynthetic organisms. In addition, these data were subsequently used for developing a hybrid system for the comprehensive use of sunlight in one system for photovoltaic and biomass production. Furthermore, future applications might include the targeted production of valuable compounds in microalgae.

Microalgae and canola plants (*Brassica napus* L.) were cultivated under different conditions for systematic investigation. After defined cultivation times, samples were taken to analyse the biomass concentration, fatty acid, and pigment composition. A modified Folch extraction was applied to isolate the fatty acids of microalgae and canola leaves. Subsequently, a qualitative characterization of the fatty acid composition was performed by gas chromatography coupled with electron impact ionization mass spectrometry (GC-EI/MS). Additionally, the microalgal pigments were quantitatively characterized using high-performance liquid chromatography with diode array detection (HPLC-UV/VIS).

In the first part of this work, the green microalga, *Acutodesmus obliquus* (Turpin), was cultivated under different temperatures and photon flux densities, with blue, green, and red light. Blue light cultivation resulted in the lowest biomass production under all tested conditions. Thus, the red light treatment led to higher biomass production than the blue light treatment. The biomass production under green light was highly dependent on biomass concentration and photon flux density. Contrary to the common opinion in plant physiology, green light led to the highest biomass production under high light conditions and high biomass concentrations. In addition, it was observed that a spectral combination of red and

blue light can outperform monochromatic red light in terms of biomass production at medium photon flux densities. These results were reproduced multiple times with *A. obliquus* and the closely related species *Monoraphidium braunii* (Nägeli).

The results of the fatty acid analysis in *A. obliquus* showed a strong impact of the parameter temperature and light spectrum on the fatty acid composition. The shares of the polyunsaturated fatty acid (PUFA) 16:4, 18:3, and 18:4 were higher for low cultivation temperatures and blue-green light between 450 and 550 nm. In contrast, the shares of the lower desaturated fatty acids 16:1, 16:2, 16:3, 18:1, and 18:2 were maximized if blue-green light was not applied during cultivation.

In the second part of this work, the waveband that affects fatty acid unsaturation in *A. obliquus* was identified with a higher spectral resolution (470–520 nm). Furthermore, a link was found between blue-green light application and a maximized concentration of all identified photosynthetic pigments in *A. obliquus*. These pigments, as well as the PUFAs 16:4 and 18:3, are contained in high proportions in thylakoid membranes. Therefore, it was assumed that blue-green light might trigger a physiological reaction that increases thylakoid membranes in microalgae. In the last part of this work, it was investigated whether blue-green light might also trigger similar effects in the closely related green microalga *M. braunii* and the land plant *B. napus*. The results of these experiments indicate that blue-green light-triggered effects related to fatty acid unsaturation and pigment concentration are widespread among photosynthetic organisms.

Danksagung

Ich möchte Prof. Dr. Kümmerer für das Ermöglichen dieser Arbeit danken. Vielen Dank für die wegweisende Unterstützung bei meiner Forschungsarbeit und bei der Veröffentlichung meiner Publikationen.

Mein Dank gilt zudem Prof. Dr. Vicky Temperton und Prof. Sigrun Reumann für die Begutachtung dieser Arbeit.

Ein herzliches Dankeschön geht an Dr. Marco Reich für die Betreuung in der Promotion. Danke Marco, auch für Deine stets positive, motivierende Art und die angenehme Zusammenarbeit.

Danke an Dr. Oliver Olson für die kritische Durchsicht dieser Arbeit.

Ich danke Herrn Dr. Kerner, Geschäftsführer der SSC GmbH, für die finanzielle Förderung im Rahmen des interdisziplinären Forschunsgprojektes HYPP (BBSR Akt. 10.08.18.7-17.02). Damit verbunden war eine intensive Zusammenarbeit mit Norbert Osterthun sowie Dr. Martin Vehse und Dr. Kai Gehrke von der DLR Next Energy e.V. in Oldenburg sowie den Forschenden der SSC GmbH auf der Freilandanlage der SSC in Hamburg Reitbrook.

Für die gemeinsame Zeit bei SSC GmbH danke ich Dr. Rahmania Darmawan, Dr. Mathilde Foix-Cablé, Dr. Stefan Hindersin und Theo Reymann.

Ich danke Dieter Stengel und Christoph Stegen für den technischen Support bei meinem Versuchsaufbau.

Herzlichen Dank an Karen Kratschmer für die administrative Unterstützung, die generelle Hilfsbereitschaft sowie die vielen guten Gespräche.

Vielen Dank an Dr. Benjamin M. Delory, Sophie Bory und Dr. Thomas Niemeyer für die Kooperation und angenehme Zusammenarbeit beim Rapsprojekt.

Danke an Astrid V. Lindner für den engen Austausch von Ideen sowie die gemeinsame Zeit am Institut und im Büro.

Danke an meine Studierenden: Sophie Bory, Annkathrin Gebhardt, Hannes Diers, Josi Steinke, Melina Wulf, Dominik Franke, Stina Krings, Mareike Schmidt und Sarah Beyer.

Zudem möchte ich auch noch allen anderen Mitarbeiterinnen und Mitarbeitern des Instituts für die gute Zusammenarbeit danken.

Ein besonderer Dank geht an meine Freunde und meine Familie für Ihre Unterstützung. Insbesondere danke ich meinem Vater, der während meines Studiums verstarb. Vielen Dank für Dein Vertrauen in mich und die Rückendeckung zu allen Zeiten.

Inhaltsverzeichnis

Abbildungsverzeichnis

Tabellenverzeichnis

Abkürzungsverzeichnis

ALA	Alpha-Linolensäure
ANOVA	einfaktorielle Varianzanalyse
ATP	Adenosintriphosphat
C	Kohlenstoff
CO_2	Kohlenstoffdioxid
DAD	Diodanarray-Detektor
DLR	Deutsches Institut für Luft- und Raumfahrt
EPA	Eicosapentaensäure
GC-EI/MS	Gaschromatografie mit Elektronenstoßionisation Massenspektrometrie (engl.: *gas chromatography coupled with electron impact ionization mass spectrometry*)
HPLC	Hochleistungsflüssigkeitschromatografie (engl.: *high-performance liquid chromatography*)
HYPP	Hybridsysteme aus Photosynthese und Photovoltaik
IS	Interner Standard
MZCH	Microalgae and Zygnematophyceae Collection Hamburg
NADPH	Nicotinamid-Adenin-Dinukleotid-Phosphat-Hydrid
NPZ	Norddeutschen Pflanzenzucht Hans-Georg Lembke KG
OD_{750}	Optische Dichte bei 750 nm
PBR	Photobioreaktor
PUFA	Mehrfach ungesättigte Fettsäuren (engl.: *polyunsaturated fatty acids*)
PV	Photovoltaik
SSC	Strategic Science Consult
TS	Trockensubstanz
UV/VIS	Ultraviolett /visuell
% v/v	Volumenprozent

Publikationsverzeichnis

Veröffentlichungen in Fachzeitschriften:

Helamieh, M., Reich, M., Rohne, P., Riebesell, U., Kerner, M., & Kümmerer, K. (2023). Impact of green and blue-green light on the growth, pigment concentration, and fatty acid unsaturation in the microalga *Monoraphidium braunii*. *Photochemistry and Photobiology*. Veröffentlicht im Oktober 2023. DOI:10.1111/php.13873. (Im Prüfungsexemplar noch als unveröffentlichtes Manuskript).

Krimech, A., Cherifi, O., Helamieh, M., Wulf, M., Krohn, I., Nachtigall, K., Hejajj, A., Naaila, O., Zidan, K., Oudra, B., Riebesell, U., Kerner, M. & Mandi, L. (2022). Algal biomass production in different types of wastewaters under extreme conditions of light and temperature. *Desalination and Water Treatment*, 260, 253-264. DOI: 10.5004/dwt.2022.28379.

Helamieh, M., Reich, M., Bory, S., Rohne, P., Riebesell, U., Kerner, M., & Kümmerer, K. (2022). Blue-green light is required for a maximized fatty acid unsaturation and pigment concentration in the microalga *Acutodesmus obliquus*. *Lipids*, *57*(4-5), 221-232. DOI: 10.1002/lipd.12343.

Krimech, A., Helamieh, M., Wulf, M., Krohn, I., Riebesell, U., Cherifi, O., Mandi, L, & Kerner, M. (2022). Differences in adaptation to light and temperature extremes of *Chlorella sorokiniana* strains isolated from a wastewater lagoon. *Bioresource Technology*, 350, 126931. DOI: 10.1016/j.biortech.2022.126931.

Helamieh, M., Gebhardt, A., Reich, M., Kuhn, F., Kerner, M., & Kümmerer, K. (2021). Growth and fatty acid composition of *Acutodesmus obliquus* under different light spectra and temperatures. *Lipids*, 56(5), 485-498. DOI.:10.1002/lipd.12316.

Konferenzbeiträge:

Osterthun, N., Helamieh, M., Berends, D., Neugebohrn, N., Gehrke, K., Vehse, M., Kerner, M., & Agert, C. (2021). Influence of spectrally selective solar cells on microalgae growth in photo-bioreactors. In *AIP Conference Proceedings*, 2361, No. 1, 070001. AIP Publishing LLC. DOI.:10.1063/5.0054814.

Osterthun, N., Helamieh, M., Neugebohrn, N., Gehrke, K., Kerner, M., Vehse, M., & Agert, C. (2020). Nano-absorber based spectrally selective solar cells for the application in photo-bioreactors. In *AIP Conference Proceedings*. Poster auf der AgriVoltaics 2020 (14.-16. Okt. 2020).

Sonstige Veröffentlichungen:

Helamieh, M., Gehrke, K., Osterthun, N., Vehse, M., & Kerner, M. (2021): Photosynthese und Photovoltaik in hybriden Fassadensystemen. Entwicklung semitransparenter Photovoltaikmodule für gebäudeintegrierte Hybridsysteme aus Photosynthese und Photovoltaik zur komplementären Nutzung des Sonnenlichts. BBSR-Online-Publikation. Edited by Bundesinstitut für Bau-, Stadt- und Raumforschung (BBSR) im Bundesamt für Bauwesen und Raumordnung (BBR), Bonn. Aktenzeichen: 10.08.18.7-17.02 Projektlaufzeit: 04.2017–08.2019.

1 Einleitung

1.1 Photosynthese

Die oxygene Photosynthese liefert die energetischen Grundlagen für höheres Leben auf diesem Planeten [1], [2]. In diesem Stoffwechselweg wird anorganischer Kohlenstoff in Form von CO_2 in organischer Substanz fixiert und zu Kohlenhydraten reduziert. In eukaryotischen Organismen ist die Photosynthese dabei in den Chloroplasten verortet [3]. Dieses Zellorganell wurde im Verlauf der Evolution vermutlich durch die Endosymbiose eines prokaryotischen Cyanobakteriums in die eukaryotische Zelle aufgenommen [4]. Nach außen hin ist dieses Zellkompartiment durch mehrere Membranen abgegrenzt. Der Innenraum gliedert sich in das sogenannte Stroma und die Thylakoide. Das Stroma ist dabei die Cytoplasma-Matrix der Chloroplasten. Die Thylakoidmembranen sind dagegen ein ausgedehntes Membransystem innerhalb der Chloroplasten. In diesen Membranen befinden sich die Lichtsammelkomplexe sowie die Reaktionszentren mit den akzessorischen Pigmenten der Photosynthese [3], [5]. Zudem grenzen die Thylakoidmembranen das Stroma vom Thylakoidinnenraum, dem Lumen, ab. In den Thylakoiden ist die Lichtreaktion der Photosynthese lokalisiert, an dessen Ende die Bildung des reduzierenden Äquivalents Nicotinamid-Adenin-Dinukleotid-Phosphat-Hydrid (NADPH) sowie des Adenosintriphosphats (ATP) mit Hilfe der Lichtenergie steht. Diese Moleküle werden im sogenannten Calvin-Zyklus im Stroma zur finalen Fixierung des CO_2 in Kohlenhydraten benötigt. Die so entstandenen Kohlenstoffgerüste dienen in der belebten Natur als Energieressource und organische Substanz [3]. Diese organische Substanz bildet heute die Grundlage für die Nahrungsmittelketten dieses Planeten. Zudem decken derzeit die aus photosynthetisch produzierter Biomasse hervorgehenden fossilen Energieträger den Großteil des Energiebedarfs der Menschheit [6], [7]. Der Ursprung der Photosynthese reicht mehr als 3,5 Mrd. Jahre zurück. In etwa aus dieser Zeit stammen erste geologische Ablagerungen, die auf die Photosynthese hindeuten [8], [9]. Es waren wahrscheinlich die Vorfahren der heute noch rezenten prokaryotischen Cyanobakterien, die erstmalig durch diesen Prozess Sauerstoff freisetzten [10]. Dadurch veränderte sich die Gaszusammensetzung der Erdatmosphäre, was überhaupt erst eine Besiedlung der Erdoberfläche für höhere Lebensformen ermöglichte [11]. Im weiteren Verlauf verbreitete sich die Photosynthese auch unter den eukaryotischen Organismen [12], [13]. Heute ist die Photosynthese weit verbreitet in unterschiedlichen Domänen des Lebens. So kommt sie nach wie vor in den prokaryotischen Cyanobakterien, aber auch in verschiedenen eukaryotischen Organismen wie den Landpflanzen und Algen vor [7], [14].

1.2 Algen

Algen sind in Bezug auf die Formenvielfalt und den Stoffwechsel eine besonders diverse Gruppe photoautotropher Organismen [15]–[17]. Im Gegensatz zu den Landpflanzen sind Algen keine geschlossene monophyletische Gruppe in der Systematik der Organismen. Unter dem Begriff Alge

werden vielmehr aquatische, einfach strukturierte eukaryotische Organismen, die primär Photosynthese treiben, zusammengefasst. Den Algen werden zum Teil phylogenetisch weit entfernte Organismen zugeordnet [18]. Die Algen-Untergruppe der Grünalgen (Chlorobionta) geht dagegen auf einen gemeinsamen Vorfahren zurück und wird phylogenetisch in ein enges Verwandtschaftsverhältnis zu den Landpflanzen gestellt [19]. Morphologisch wird zwischen Makroalgen, die einen ohne optische Hilfsmittel sichtbaren vielzelligen Organismus bilden, und Mikroalgen, die nur mikroskopisch erkennbare Strukturen – meist einzelne Zellen – bilden, unterschieden [20]–[22]. Auch unter den Mikroalgen ist die morphologische, genetische und metabolische Diversität sehr hoch. [23], [24]. Es kommen mehrzellige Formen vor. Die meisten Vertreter umfassen allerdings einzellige oder lose Verbände aus wenigen Zellen, deren Größe ca. 5-20 µm beträgt [22], [25], [26].

1.3 Wertstoffe in Mikroalgen

Durch die photoautotrophe Lebensweise können Mikroalgen zur Produktion von nachwachsenden Biokraftstoffen wie Biogas und Biodiesel genutzt werden [27]. Viele Mikroalgen enthalten einen sehr hohen Anteil an gesättigten Fettsäuren, was sie daher zu geeigneten Kandidaten für die Produktion von Biodiesel macht [28]. Im Gegensatz zu Agrarpflanzen wie z.B. Raps bieten Mikroalgen einige Vorteile. So können Mikroalgen höhere Wachstumsraten haben und benötigen zudem keine Ackerflächen. Damit konkurrieren sie nicht mit Nahrungspflanzen um die Agrarflächen [29], [30]. Weiterhin stellen sie geringere Anforderungen an die Wasserqualität als Nutzpflanzen und die Kultivierung ist auch mit Abwasser möglich [31], [32]. Die Inhaltsstoffe von Mikroalgen können aber auch als Wertstoffe für die Lebens- und Futtermittelindustrie oder als Kosmetikprodukte verwendet werden [33]. Eine Kategorie an Wertstoffen aus Mikroalgen sind Pigmente und Antioxidantien. Insbesondere die Pigmente Astaxanthin und Lutein kommen in industriell relevanten Mengen in vielen Mikroalgen vor [34], [35]. Aufgrund ihrer Eigenschaften als Antioxidantien und Farbstoffe haben diese Substanzen diverse industrielle Anwendungen, z.B. bei der Produktion von Zuchtlachsen oder als Nahrungsergänzungsmittel [36], [37]. In einigen Mikroalgen konnte zudem ein hoher Anteil an Omega-3-Fettsäuren wie beispielsweise Alpha-Linolensäure (18:3, ALA) beobachtet werden [38], [39]. Diese mehrfach ungesättigten Fettsäuren (engl.: *polyunsaturated fatty acids*) (PUFAs) haben eine essenzielle Bedeutung für die menschliche Ernährung [40], [41]. Auch das Verhältnis von Omega-3 zu Omega-6-Fettsäuren ist für eine gesunde Ernährung entscheidend. In modernen Nahrungsmitteln sind hohe Gehalte an Omega-6-Fettsäuren vorherrschend, was ursächlich für die erhöhte Neigung zu sogenannten Wohlstandskrankheiten wie Herz-Kreislauf-Erkrankungen, Krebs und Autoimmunerkrankungen in der westlichen Welt sein könnte [42], [43]. Im Gegensatz dazu sind Omega-3-Fettsäuren wie Eicosapentaensäure (EPA) und Docosahexaensäure (DHA) wichtige Ausgangssubstanzen für die Biosynthese von Hormonen. Diese Omega-3-Fettsäuren werden zudem mit neuroprotektiven Eigenschaften in Verbindung gebracht [43]. Im menschlichen Körper erfolgt die Biosynthese von EPA und DHA aus Linolsäure (18:2) und ALA [43]. Aus diesem Grund gibt es Bestrebungen, Lebensmittel

mit hohem Anteil an Omega-3-Fettsäuren herzustellen [44]. Bisher wird der Großteil der Omega-3-Fettsäuren durch Meeresprodukte wie Fisch abgedeckt. Aufgrund der unterschiedlichen Nachteile, die aus der Überfischung der Weltmeere und der Fischzucht resultieren, sind alternative Gewinnungsmöglichkeiten erforderlich [45], [46]. Mikroalgen könnten in diesem Bereich künftig als erneuerbare Alternative bei der Produktion von nahrungsrelevanten Fettsäuren eine wichtige Rolle einnehmen [47]. Weiterhin bietet sich durch Auswahl der Kultivierungsparameter die Möglichkeit, den Stoffwechsel und somit die Produktion der Wertstoffe in Algen zu modifizieren. Beispielsweise kann sich durch Verringerung der Kultivierungstemperatur der PUFA-Anteil in Mikroalgen erhöhen. Durch diese Modifikation der Fettsäurekomposition stellen Mikroorganismen die Fluidität der Lipidmembranen bei geringeren Temperaturen sicher [48], [49]. In ähnlicher Weise kann die Produktion von Fettsäuren durch Variation des Parameters Licht modifiziert werden [49]–[51].

1.4 Licht und Wachstum

Für photosynthetische Organismen ist Licht ein entscheidender Umweltreiz. Es liefert wichtige Informationen und ist die energetische Grundlage für den Metabolismus [52], [53]. In Bezug auf die Lichtintensität ist bei Mikroalgen bekannt, dass niedrige Strahlungsintensitäten energetisch effizienter genutzt werden können als Starklicht [54], [55]. Bei hohen Strahlungsintensitäten kann es zudem durch Schädigung des Photosystems zur sogenannten Photoinhibition kommen, die sich weiterhin negativ auf die photosynthetische Effizienz auswirken kann. In Photobioreaktoren (PBR) tritt diese Schadwirkung durch Starklicht insbesondere bei niedrigen Biomassenkonzentrationen auf [3], [29], [54], [56]. Die energetische Nutzungseffizienz der Lichtspektralbereiche durch Photosynthese treibende Organismen wird dagegen in der Literatur kontrovers diskutiert [55]–[57]. In der älteren Literatur dominierte die Einschätzung, dass vorwiegend blaues und rotes Licht effektiv in der Photosynthese genutzt werden, weil diese Spektralbereiche mit den Absorptionsmaxima des Chlorophylls korrelieren [56], [57]. Zu blauem Licht ist allerdings bekannt, dass weitere akzessorische Pigmente wie Carotinoide und Xanthophylle ebenfalls in diesem Spektralbereich absorbieren [58]. Die durch diese Pigmente absorbierte Lichtenergie wird mittels strahlungsloser Relaxation in Wärme umgewandelt und steht dadurch energetisch der Photosynthese nicht mehr zur Verfügung [3]. Dem grünen Licht wurde aufgrund der geringeren Absorption des Chlorophylls in diesem Spektralbereich eine eher untergeordnete Rolle zugewiesen. In den letzten Jahren setzt sich allerdings zunehmend die Erkenntnis durch, dass schwach absorbierte Wellenlängenbereiche unter bestimmten Bedingungen sehr effektiv durch Photosynthese treibende Organismen genutzt werden können [55], [56], [59]. Allerdings wurde bei eukaryotischen Mikroalgen noch keine systematische Untersuchung der Parameter Lichtspektrum, Lichtintensität und Biomassenkonzentration durchgeführt.

1.5 Lichtspektren und Wertstoffe

Neben der photosynthetischen Nutzung hat Licht im Stoffwechsel von Landpflanzen eine wichtige Funktion bei der Regulation von Entwicklungs- und Stoffwechselvorgängen. Bei Landpflanzen sind in diesem Zusammenhang verschiedene Spektralbereiche bekannt, die durch spezifische Photorezeptoren perzipiert werden können und wichtige physiologische Reize für die Pflanzen darstellen. Insbesondere blaues Licht spielt bei morphologischen Prozessen von Landpflanzen eine wichtige Rolle und ist für die Pflanzenentwicklung essenziell [53], [60]. Auch bei Mikroalgen scheint blaues Licht eine wichtige Funktion bei morphologischen und physiologischen Vorgängen zu haben. So hat der kurzwellige Spektralbereich eine zentrale Rolle als Trigger von Zellteilungsprozessen in Mikroalgen [61]. Bei verschiedenen Grünalgenarten werden unterschiedliche Komponenten des Stickstoff-Metabolismus sowie der Transport von Nitrat und Hydrogencarbonat über die Cytoplasmamembran durch blaues Licht aktiviert [62]–[64]. Für die Algenart *Monoraphidium braunii* ist zudem beschrieben worden, dass blaues Licht die Expression verschiedener Enzyme des Stickstoffmetabolismus steigert [65]. Auch die Aktivität von Enzymen, die eine direkte Decarboxylierung von Fettsäuren in Mikroalgen katalysieren, wird durch blaues Licht beeinflusst. Dadurch ergibt sich die Möglichkeit, den Algenstoffwechsel mit Hilfe von Lichtspektren zu beeinflussen. Beispielsweise kann durch blaues Licht die Produktion von Alkanen in Mikroalgen direkt angeregt werden, was künftig bei der Herstellung von Biokraftstoffen aus Mikroalgen genutzt werden könnte [66], [67]. Auch ist bekannt, dass bei Pflanzen eine Lichtregulation von Fettsäure-Desaturase codierenden Genen erfolgt [68]. Die entsprechenden Enzyme bewirken die Desaturierung von Fettsäuren. Daher ist deren Aktivität entscheidend für das Verhältnis von ungesättigten zu gesättigten Fettsäuren [69]. Ob diese Regulation allerdings durch bestimmte Lichtspektralbereiche getriggert wird, ist nicht bekannt. Eine Studie, die die Fettsäurekomposition von Mikroalgen bei unterschiedlichen Lichtspektren untersucht hat, liefert jedoch Hinweise dafür, dass tatsächlich distinkte Wellenlängenbereiche des Lichts einen höheren prozentualen Anteil bestimmter PUFAs in Mikroalgen bewirken [50]. In Bezug auf die Photosynthesepigmente ist in der Literatur bekannt, dass blaues Licht die Produktion in vielen phylogenetisch entfernten Algenarten fördert [70]–[72]. Bei *Clamydomonas reinhardti* konnte eine Erhöhung des Transkriptlevels der enzymcodierenden Gene, die an der Biosynthese von Carotinoiden beteiligt sind, unter dem Einfluss von blauem Licht festgestellt werden [73]. Eine systematische Analyse der Komposition der Algenpigmente zusammen mit der Fettsäurekomposition bei Bestrahlung mit unterschiedlichen Lichtspektren im zeitlichen Kultivierungsverlauf wurde an Mikroalgen bisher allerdings noch nicht durchgeführt.

1.6 Hybridsysteme aus Photosynthese und Photovoltaik

Künftig können dezentrale gebäudeintegrierte Energiekonzepte einen wichtigen Beitrag zur Energiesicherheit im urbanen Bereich leisten [74]. Dabei werden Photovoltaik (PV) und Solarthermie bereits heute zur Beheizung und Elektrizitätsgewinnung an Gebäuden eingesetzt [75], [76]. In diesem Feld ergibt sich eine weitere Anwendung von Mikroalgen. Auf der internationalen Bauausstellung in

Hamburg wurde im Jahr 2013 erstmalig das Konzept einer Bioenergiefassade an einem Wohngebäude, dem sogenannten Algenhaus, realisiert. Hierbei wird das Sonnenlicht mehrfach genutzt. In der Bioenergiefassade sind an einer Wohngebäudefassade, PBR auf einer Fläche von ca. 200 m^2 in einem Volumen von 3500 Litern integriert, die eine Biomassenproduktion, mittels Photosynthese treibender Mikroalgen ermöglichen. Diese Biomasse kann in einem nachgeschalteten Biogasreaktor in Methangas umgewandelt werden, wobei sich mit diesem dann zusammen mit der thermischen Energie der Sonne das Gebäude beheizen lässt. Gleichzeitig können die Mikroalgen die im Haus entstehenden Rauchgasemissionen zur Biomassenproduktion verwenden, wodurch sich zusätzlich die CO_2-Emissionen des Gebäudes verringern. Weiterhin wurden auch die Abwässer des Gebäudes bereits erfolgreich für die Biomassenproduktion am Algenhaus genutzt [31], [77], [78]. Mikroalgen können in diesem Zusammenhang auch einen wichtigen Beitrag zum Erreichen der 17 Ziele für eine nachhaltige Entwicklung der Vereinten Nationen leisten. Insbesondere zur Reduktion der CO_2-Emissionen (Ziel 13), der Herstellung von sauberem Wasser (Ziel 6), aber auch bei der Produktion von Biokraftstoffen (Ziel 2) [79]–[81]. Die Effizienz von solchen Mikroalgen PBR-Systemen wird künftig auch darüber entscheiden, in welchem Ausmaße Mikroalgen einen Beitrag zum Green Deal der Europäischen leisten können [82]. Zur Steigerung der Lichtkonversionseffizienz soll künftig der Bioenergiefassade zusätzlich eine semitransparente Solarzelle zur Elektrizitätsgewinnung vorgeschaltet werden (Abbildung 1). Im interdisziplinären Projekt „Hybridsysteme aus Photosynthese und Photovoltaik“ (HYPP) erfolgte die Entwicklung eines Hybridsystems aus Photosynthese und PV. Die Forschungsarbeit wurde von den

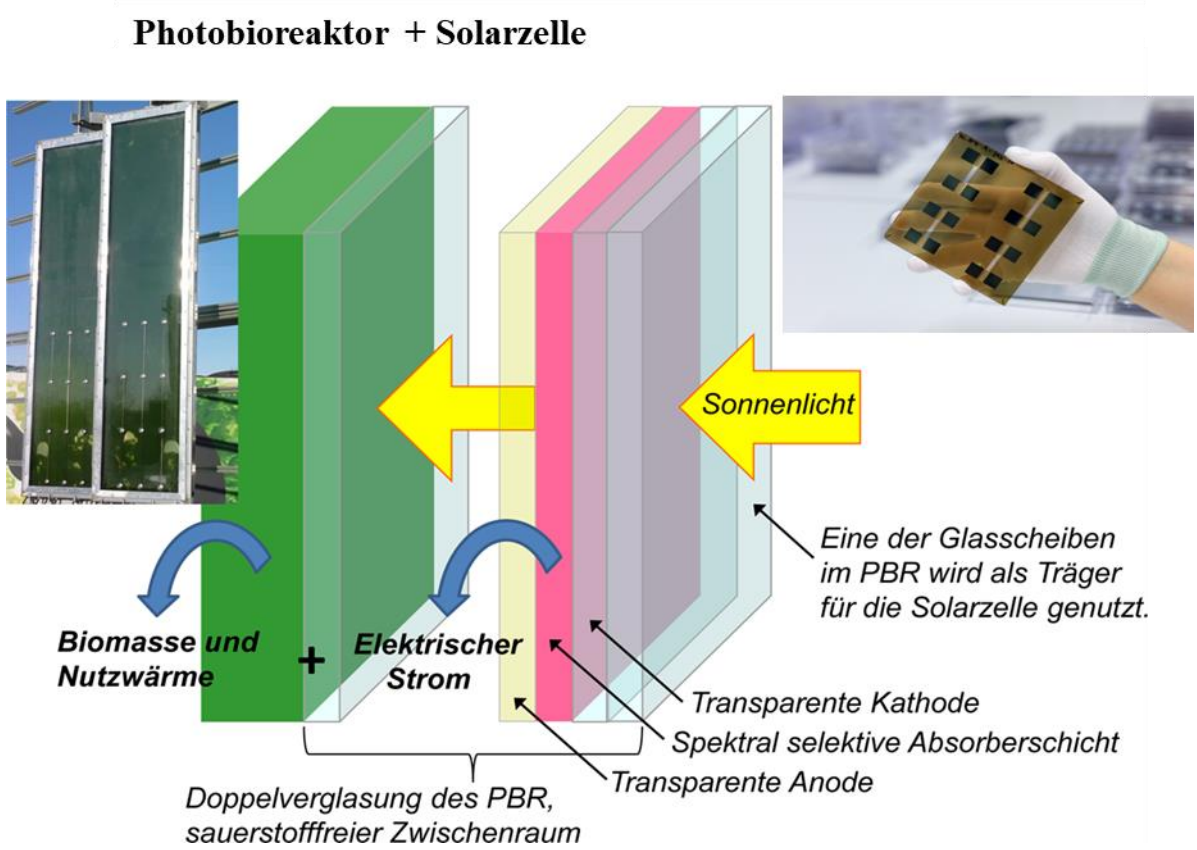

Abbildung 1: Geplantes Hybridsystem [83]

Unternehmen Strategic Science Consult (SSC) GmbH, Hamburg und dem Deutschen Institut für Luft- und Raumfahrt (DLR) aus Oldenburg durchgeführt [83]. Dafür fand eine neuartige semitransparente Solarzelle, basierend auf amorphem Germanium, Anwendung. Diese Technologie wurde durch die DLR in Oldenburg entwickelt. Dadurch ist eine komplementäre Nutzung des Sonnenlichts für PV und Photosynthese möglich. Insbesondere kann durch Auswahl der Schichtdicke des Germanium-Absorbers die Transmission der Solarzellen genau auf die Lichterfordernisse der Algen abgestimmt werden [84]. Zu diesem Zweck erfolgte die Untersuchung der Auswirkungen von spektralselektiver Kultivierung auf das Wachstum und den Stoffwechsel von Mikroalgen. Hierbei sollten Spektralbereiche identifiziert werden, die zu einem optimalen Mikroalgenwachstum und einer erhöhten Bildung von bioaktiven industriell relevanten Substanzen in Mikroalgen führen.

2 Ziele und Aufbau der Arbeit

2.1 Zielstellung

Der Einfluss unterschiedlicher Lichtspektren und Temperaturen auf das Wachstum und die Wertstoffproduktion bei Mikroalgen wurde bisher nicht hinreichend untersucht. In dieser Arbeit soll daher eine systematische Analyse des Einflusses verschiedener Lichtspektren und Temperaturen auf die Biomassenproduktion und die Biomassenzusammensetzung von Mikroalgen erfolgen. Dadurch soll insbesondere das Verständnis lichtgesteuerter biochemischer Prozesse in Mikroalgen vertieft und eine Wissensgrundlage für die Steuerung des Algenstoffwechsels durch den Parameter Licht geschaffen werden. Optimalerweise soll eine Identifizierung distinkter Licht-Spektralbereiche erfolgen, die eine maximale Biomassenproduktion sowie eine optimale Fettsäure- und Pigmentzusammensetzung für industrielle Zwecke bewirken. Dieses Wissen fand im Projekt HYPP (1.6) Anwendung und wurde zu einer optimalen Abstimmung der PV-Transmission auf die Erfordernisse der Algen im geplanten Hybridsystem genutzt. Daraus leiten sich folgende Unterziele der Arbeit ab:

1) Untersuchung der Auswirkungen von distinkten Spektralbereichen, Biomassenkonzentration und Photonenflussdichte auf das Wachstum von *A. obliquus.*

2) Beschreibung distinkter Lichtspektren für eine optimale Biomassenproduktion von *A. obliquus*.

3) Benennung von Lichtspektren, die wichtig für eine hohe Produktion bzw. einen hohen prozentualen Anteil von industriell relevanten Pigmenten und Fettsäuren in *A. obliquus* sind.

4) Testung der Übertragbarkeit der an *A. obliquus* gewonnenen Erkenntnisse auf andere Algenarten und Landpflanzen.

5) Anwendung der in 1–4 gewonnenen Erkenntnisse im geplanten Hybridsystem.

2.2 Aufbau

Die praktischen Arbeiten erfolgten im Zeitraum von April 2018 bis August 2021 an der Leuphana Universität Lüneburg am Institut für Nachhaltige Chemie und Stoffliche Ressourcen unter der Leitung von Herrn Prof. Dr. Kümmerer. Die dabei entstandenen Daten wurden in drei Manuskripte zusammengefasst und bilden die Grundlage dieser Dissertation. Alle drei Manuskripte wurden als internationale Veröffentlichungen mit Peer-Review Verfahren publiziert. Zudem konnten weitere Resultate, die im Zusammenhang mit dem Projekt HYPP und der Arbeit bei der SSC GmbH entstanden sind, in weiteren projektbezogenen Veröffentlichungen publiziert werden (siehe Publikationsverzeichnis). Diese werden in der Dissertation nicht im Detail beschrieben, weil sie nur eine begrenzte thematische Überschneidung mit der Fragestellung in dieser Arbeit haben.

Publikation 1

Helamieh, M., Gebhardt, A., Reich, M., Kuhn, F., Kerner, M., & Kümmerer, K. (2021). Growth and fatty acid composition of *Acutodesmus obliquus* under different light spectra and temperatures. *Lipids*, 56(5), 485-498. DOI: 10.1002/lipd.12316.

Publikation 2

Helamieh, M., Reich, M., Bory, S., Rohne, P., Riebesell, U., Kerner, M., & Kümmerer K. (2022). Blue-green light is required for a maximized fatty acid unsaturation and pigment concentration in the microalga *Acutodesmus obliquus*. *Lipids*, 57(4-5), 221-232. DOI: 10.1002/lipd.12343.

Publikation 3

Helamieh, M., Reich, M., Rohne, P., Riebesell, U., Kerner, M., & Kümmerer, K. (2023). Impact of green and blue-green light on the growth, pigment concentration, and fatty acid unsaturation in the microalga *Monoraphidium braunii*. *Photochemistry and Photobiology*. Veröffentlicht im Oktober 2023. DOI:10.1111/php.13873. (Im Prüfungsexemplar noch als unveröffentlichtes Manuskript).

3 Methoden

Im folgenden Kapitel wird das methodische Vorgehen und die Konzeption der Versuche der Forschungsarbeiten zusammenfassend beschrieben. Detailliertere Beschreibungen mit der Auflistung der verwendeten Materialien sind in den dieser Dissertation zugrunde liegenden Publikationen 1–3 aufgeführt.

3.1 Algenkultivierung

In den Algenexperimenten wurden die Mikroalgenstämme *Acutodesmus obliquus* (syn. *Scenedesmus obliquus*, *Tetradesmus obliquus*) (Nr. U169) aus der Algensammlung (Microalgae and Zygnematophyceae Collection Hamburg MZCH) und *Monoraphidium braunii* SAG-202-7b aus der Sammlung von Algenkulturen der Universität Göttingen (SAG) verwendet.

3.1.1 Vorbehandlung der Algen

Die Algenkultur wurde auf einer Agarplatte mit Kulturmedium und 1 % Agarose ausgestrichen und bei Raumtemperatur und Raumbeleuchtung gelagert. Um ausreichend Biomasse für die Algenexperimente zu erhalten, wurden Einzelkolonien von diesen Agarplatten ausgewählt und steril in 50 ml Kolben mit flüssigem Kulturmedium überführt. Diese Kolben wurden mit Wattestopfen abgedichtet und als Schüttelkultur bei 50 µmol m^{-2} s^{-1} Photonenflussdichte für etwa drei Wochen vorbehandelt. Die so vorbereitete Flüssigkultur wurde 5 Tage vor Versuchsbeginn steril in eine 1 l Laborglasflasche mit Kulturmedium überführt. In diesem Gefäß wurde die Flüssigkultur als sogenannte Vorkultur mit einem CO_2-Druckluftgemisch (5 % v/v) und 150 µmol m^{-2} s^{-1} Weißlicht behandelt und mit Hilfe eines Magnetrührers homogenisiert.

3.1.2 Lichtquellen und optische Filter

Zur Vorkultivierung wurde eine Ringleuchte mit weißem Licht verwendet (Sylvania T9 circline, 32 W). Als Strahlungsquellen in den Kultivierungsexperimenten wurden Gasentladungslampen (MSR 575 HR CT) verwendet, die vor der Kultivierungseinheit positioniert waren. Die Gasentladungslampen emittieren ein elektromagnetisches Spektrum, das ähnlich dem der Sonne ist. Allerdings wurden die Wellenlängen unterhalb von 380 nm durch das Acrylglas der Kultivierungseinheit absorbiert (Abbildung 2a). Mittels optischer Filterfolien bzw. durch Abkleben der Frontseite des Acrylglasbeckens mit Aluminiumfolie konnten unterschiedliche Lichtspektren bzw. Dunkelproben in einem Versuchsansatz nebeneinander getestet werden. Hierbei wurden die optischen Filterfolien „*medium yellow*“, „*deep straw*“, „*light blue*“, „*dark green*“ und „*light red*“ (LEE-Filters, England) an der Frontseite der Kultivierungseinheit fixiert. Die aus der Kombination der optischen Filterfolien mit den Gasentladungslampen resultierenden Spektren werden folgend als weißes Licht (400–700 nm)

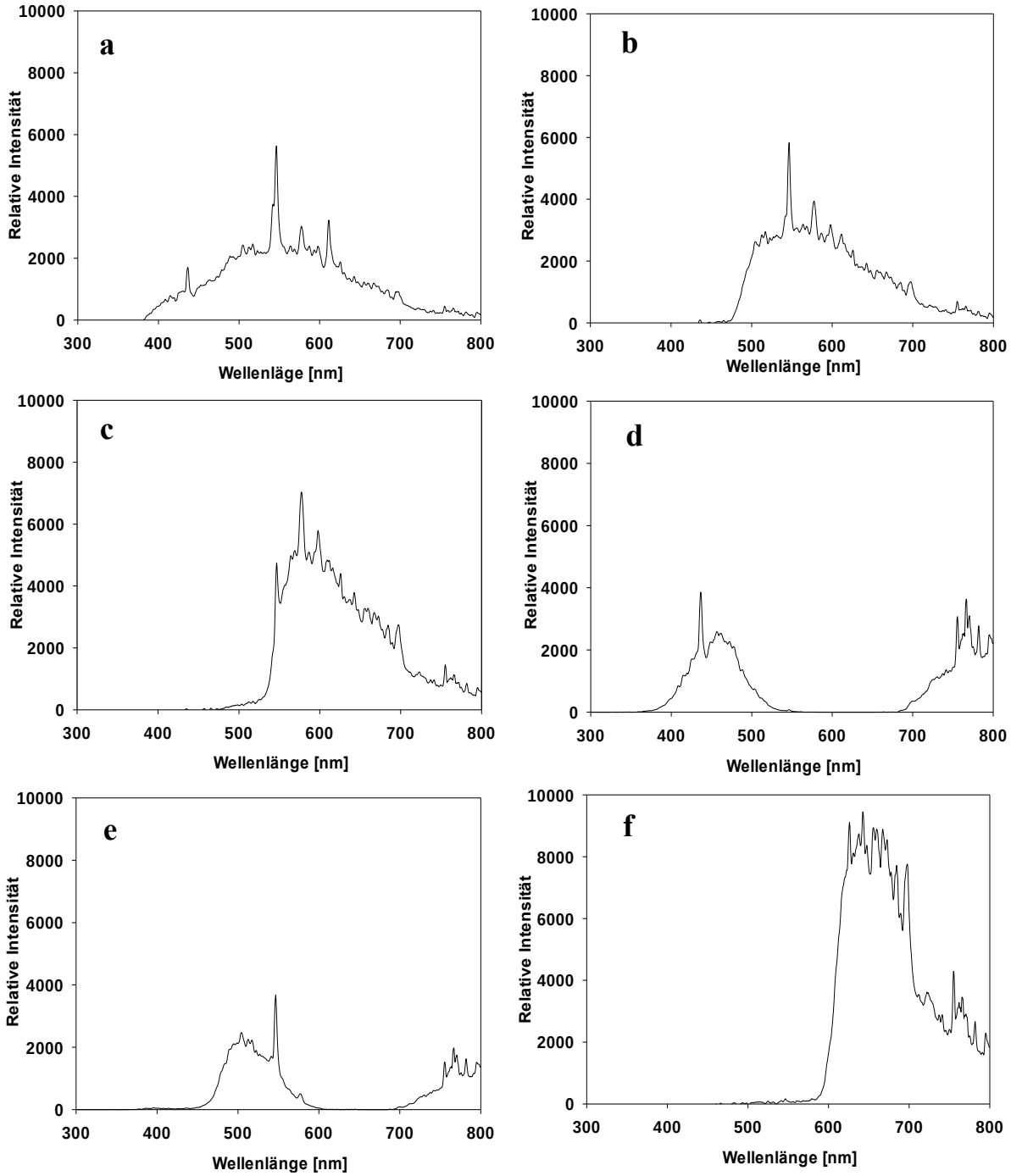

Abbildung 2: Verwendete Lichtspektren. Die Lichtspektren resultierten aus dem Emissionsspektrum der Gasentladungslampen (MSR 575 HR CT) in Kombination mit dem Acrylglas der Kultivierungseinheit: weißes Licht (a), und optischen Filterfolien (LEE-Filters, England): gelbes Licht (b), oranges Licht (c), blaues Licht (d), grünes Licht (e) und rotes Licht (f). Die relativen Emissionsspektren ($J\lambda$,rel in counts) wurden mittels UV-Vis Spektrometer (BLACK-Comet, StellarNET, Tampa, USA) im Wellenlängenbereich λ = 300 bis 800 nm (Integrationszeit = 10 ms) ermittelt.

(ungefiltertes Licht), gelbes Licht (470–700 nm), oranges Licht (520–700 nm), blaues Licht (400–540 nm), grünes Licht (450–600 nm), und rotes Licht (580–700 nm) bezeichnet (Abbildung 2 a-f).

Vor den jeweiligen Algen-Kultivierungsexperimenten wurden alle verwendeten Lichtspektren auf einheitliche Photonenflussdichten eingestellt, um ausschließlich die Auswirkungen der Lichtspektren zu

untersuchen. Die Photonenflüsse wurden mit Hilfe eines UV/VIS Spektrometers (BlackComet, StellarNET, Tampa, USA) innerhalb von 400-700 nm gemessen. Zur Aufnahme der Lichtspektren wurde der Wellenlängenbereich von 300-800 nm berücksichtigt.

3.1.3 Kultivierungseinheit

Zur einheitlichen Kultivierung der Mikroalgen wurde eine Mikroalgen-Kultivierungseinheit in Zusammenarbeit mit der SSC GmbH und der Leuphana-Werkstatt konzipiert und gebaut. In ihr können bis zu zwölf Röhrenreaktoren und damit maximal vier unterschiedliche Lichtbedingungen in Triplikaten untersucht werden. In den Röhrenreaktoren erfolgte die Kultivierung der Mikroalgen im Kulturmedium, begast mit einem CO_2 Druckluft Gemisch (5 % v/v) bei einem Volumenstrom von 200 ml Min^{-1}. Als Röhren wurden große Reagenzgläser mit einer Länge von 490 mm, einem Durchmesser von 40 mm und einem maximalen Füllvolumen von 350 ml verwendet. Die Reaktoren waren dabei mit einem Verschlussstopfen aus Kunststoff versehen, der über zwei Löcher eine Be- und Entgasung ermöglichte. Die Begasung erfolgte durch Kunststoffröhrchen, die in die Röhrenreaktoren eingelassen waren. Die Reaktoren standen dabei senkrecht in Haltevorrichtungen, die einen sicheren Stand in einem wassergefüllten Acrylglas-Becken ermöglichten. Zudem stellten diese Haltevorrichtungen sicher, dass Licht ausschließlich von der Frontseite auf die Röhrenreaktoren traf. Das Wasser im Acrylglas-Becken konnte durch einen sekundären Wasserkreislauf mit Hilfe eines externen Durchlaufkühlers genau temperiert werden.

3.2 Rapskultivierung

Zur Untersuchung unterschiedlicher Lichtspektren an Landpflanzen wurden Rapspflanzen spektralselektiv kultiviert. Zu diesem Zweck wurde *Brassica napus* var. Medicus, Herkunft: Norddeutsche Pflanzenzucht Hans-Georg Lembke KG (NPZ), verwendet. Die Untersuchungen erfolgten in enger Zusammenarbeit mit Dr. Benjamin Delory vom Institut für Ökologie der Leuphana Universität Lüneburg.

3.2.1 Versuchsbedingungen

Die Kultivierung der Rapspflanzen erfolgte im Gewächshaus der Leuphana Universität Lüneburg. Es wurden jeweils 5 Rapssamen pro Blumentopf in insgesamt 30 Töpfen mit zuvor ausgesiebter Blumenerde (Maschenweite 2 mm) ausgesät. Nach der Keimung erfolgte eine Auswahl der Sämlinge für die weiteren Experimente. Sämlinge, die in der Topfmitte und zudem gut ausgewachsen waren, wurden präferiert. Die Kultivierung erfolgte bei drei unterschiedlichen Lichtbedingungen (jeweils 10 Pflanzen pro Lichtbedingung). Als Lichtquelle diente in allen drei Gruppen die Sonne. Die solare Photonenflussdichte und die Temperaturen wurde im gesamten Versuchszeitraum vom 17. September bis zum 05. November 2020 kontinuierlich aufgezeichnet. Die Photonenflussmessung erfolgte mit einem Aufzeichnungsintervall von einem Wert pro 10 Minuten (HOBO-Datenlogger mit S-LIA-M003

Abbildung 3: Experimenteller Aufbau der Rapskultivierung. Auf den Rolltischen befinden sich unter den optischen Filtervorrichtungen die Töpfe mit den Rapspflanzen.

PAR-Sensor, Onset Computer Corporation, Bourne, USA) und einem Wert pro Stunde bei der Temperaturmessung (Voltcraft DL-120TH Thermometer, Hirschau, Germany) (siehe Abbildung 9 im Anhang). Für alle drei Gruppen wurden spezielle optische Filtervorrichtungen für die Töpfe konstruiert (Abbildung 3). In der ersten Gruppe erfolgte die Verhüllung mittels Filterfolie „*LEE light red*“ (3.1.2). Diese Filterfolie war optisch nur für den Spektralbereich von 580 nm bis 700 nm durchlässig. Die Transmission dieser Filterfolie lag bei 38 %. Mit dieser Gruppe wurde der Einfluss von rotem Licht getestet. In der zweiten Gruppe wurde der Einfluss von ungefiltertem Sonnenlicht untersucht. Zur Sicherstellung konstanter Gas- und Feuchtigkeitsbedingungen kam allerdings eine optisch transparente Kunststofffolie (Transmission bei 89 %) zum Einsatz. In einer dritten Gruppe wurde Sonnenlicht mit einem Pflanzen-Kultivierungsnetz und der durchsichtigen Kunststofffolie abgeschwächt (Transmission 28 %). Das Kultivierungsnetz ermöglichte eine gleichmäßige Abschwächung des Sonnenlichts ohne Auswirkungen auf das Lichtspektrum. Diese Gruppe diente als Weißlichtkontrolle mit ähnlicher Lichtintensität wie bei der rotlichtbehandelten Gruppe. Die Töpfe mit den unterschiedlichen Filterfolien wurden im Gewächshaus auf Tabletts gelagert, die auf Rolltischen positioniert waren (Abbildung 3). Auf jedem Tisch waren jeweils zwei Töpfe aus jeder Gruppe gelagert und die Anordnung der Rolltische wurde täglich variiert. Dadurch sollten eventuelle Positions- oder Schatteneffekte einzelner Gruppen vermieden werden. Alle 2–3 Tage wurden die Pflanzen mit 200 ml Wasser versorgt. Die Filterkonstruktionen ermöglichten eine Bewässerung ohne Entfernung der Filterfolien. Die Ernte der Rapspflanzen erfolgte, nachdem alle Pflanzen mindestens zwei Folgeblätter entwickelt hatten. Die Kotyledonen (Keimblätter) wurden nicht mitberücksichtigt. Für die Fettsäureextraktion wurden die

geernteten Blätter mit flüssigem Stickstoff bei -80 °C schockgefroren und zu einem Pulver gemörsert. Die auf diese Weise pulverisierten Blätter wurden bei für die Fettsäureextraktion (3.4.2) verwendet.

3.3 Studienkonzeption

Die Algenexperimente erfolgten alle als Batch-Kultur. Im Fokus der Arbeit stand die Fragestellung, welche Bereiche des elektromagnetischen Spektrums für das Wachstum und den Stoffwechsel der Mikroalgen erhöhte Relevanz haben. Dafür wurde in der ersten Studie der Einfluss von blauem, grünem und rotem Licht auf das Algenwachstum exemplarisch an der Mikroalge *A. obliquus* untersucht. Diese Versuche wurden bei drei unterschiedlichen Photonenflussdichten durchgeführt. Die Kultivierungsexperimente bei mittlerer Photonenflussdichte erfolgten zudem bei unterschiedlichen Temperaturen. Zur Untersuchung des Einflusses der Parameter Licht und Temperatur wurden bei den Versuchen in zeitlich dichter Folge Proben der Algenbiomasse aus den Kultivierungsexperimenten entnommen und nachfolgend die Fettsäurekomposition analysiert. In der ersten Studie wurden daher auch die Wechselwirkung der Parameter Temperatur und Lichtspektrum auf den Fettsäurestoffwechsel untersucht (Publikation 1).

Nachfolgend wurde eine Folgestudie konzipiert. Hierbei stand eine detaillierte Untersuchung der Fettsäurekomposition in *A. obliquus* bei unterschiedlichen Lichtbedingungen im Vordergrund. Im Detail sollte der Einfluss des Wellenlängenbereiches zwischen 450 und 550 nm auf die Fettsäurekomposition näher untersucht werden. Insbesondere, weil sich dieser in der ersten Studie als relevant für die Desaturierung von Fettsäuren in *A. obliquus* erwiesen hatte. Weiterhin wurden zusätzlich in Zusammenarbeit mit dem GEOMAR Helmholtz-Zentrum für Ozeanforschung in Kiel die Photosynthesepigmente der Proben aus den Kultivierungsexperimenten quantifiziert. Hierbei sollte untersucht werden, ob auch ein Einfluss des Lichtspektrums auf die Pigmentproduktion in *A. obliquus* feststellbar ist (Publikation 2).

In der dritten Studie wurden die an der Algenart *A. obliquus* gewonnenen Erkenntnisse bei einer weiteren Grünalgenart getestet. Insbesondere wurde untersucht, ob der beobachtete Einfluss des Spektralbereichs zwischen 450 und 550 nm auf die Entsättigung der Fettsäuren auf die Spezies *A. obliquus* beschränkt ist oder ob dieser spektrale Effekt auch in anderen Algen nachgewiesen werden kann. Dafür wurde die Grünalge *M. braunii* ausgewählt. Diese Versuche wurden bei einheitlicher Temperatur und Photonenflussdichte mit blauem, grünem, rotem und zusätzlich weißem Licht durchgeführt, wobei die Fettsäurekomposition sowie die Pigmentkonzentration im Nachgang vergleichend untersucht wurden (Publikation 3).

Im letzten Teil der Arbeit wurde zudem untersucht, ob es Hinweise dafür gibt, dass die bei Algen beobachteten spektralen Effekte auf die Fettsäurekomposition auch bei Landpflanzen vorkommen. Daher wurden in Zusammenarbeit mit der Ökologie der Leuphana Universität Lüneburg *B. napus*

spektralselektiv im Gewächshaus kultiviert. Nach Ausbildung der Haupttriebe der Pflanzen wurde im Nachgang die Fettsäurekomposition der Laubblätter untersucht (unveröffentlichte Daten).

3.4 Analyse der Biomasse

Während der Versuche wurden täglich Proben aus der Algenkultur zur Untersuchung der Trockensubstanz (TS), Fettsäurekomposition und Pigmentanalyse entnommen.

3.4.1 Trockensubstanzbestimmung

Die TS-Bestimmung bei den Algenexperimenten erfolgte gravimetrisch. Durch Messung der Optischen Dichte bei 750 nm (OD_{750}) konnte die TS rechnerisch ermittelt werden. Vor Beginn jeder Versuchsreihe wurde zu diesem Zweck eine TS-OD_{750} Korrelation aus der Biomasse der Vorkultur erstellt.

3.4.2 Fettsäureaufbereitung und Fettsäureanalytik

Zur Abtrennung der Zellkomponenten (Proteine, Zellfragmente etc.) von den Lipiden wurde eine abgewandelte Folch-Extraktion angewandt [85]. Zu diesem Zweck wurde bei den Experimenten mit *A. obliquus* eine TS von 2,5 mg und bei den Experimenten mit *M. braunii* eine TS von 0,015 g für die Extraktion verwendet. Bei der Analyse der Rapsblätter wurden dafür 0,03 g der schockgefrorenen und pulverisierten Blätter eingesetzt (3.2.1). Als interne Standards (IS) wurden bei den Extraktionen bei *A. obliquus* und *B. napus* 20 µmol Heptadecansäure und bei *M. braunii* 20 µmol Heneicosansäure vor der Extraktion zugegeben. Im Anschluss wurden die so extrahierten freien Fettsäuren mit Methanol bei 100 °C für 1 h im sauren zu den entsprechenden Methylestern verestert bzw. es erfolgte eine Umesterung der Triglyceride zu den entsprechenden Methylestern. Die Analyse der Fettsäuren erfolgte mittels Gaschromatografie mit Elektronenstoßionisation Massenspektrometrie (GC-EI/MS). Das Temperaturprogramm sowie die Details der Methode sind in der ersten Publikation näher beschrieben.

3.4.3 Pigmentanalytik

Die Pigmentanalyse wurde in Zusammenarbeit mit dem GEOMAR Helmholtz-Zentrum in Kiel durchgeführt. Die Analyse erfolgte dort mittels Hochleistungsflüssigkeitschromatografie gekoppelt mit einem Spektrometer mit ultraviolettem und sichtbarem Licht (HPLC-DAD) [86]. Die Details der Methode können in der zweiten Publikation eingesehen werden.

3.5 Statistik

Die statistischen Methoden sind in den jeweiligen Publikationen genau beschrieben. Bei der Auswertung der Daten von *B. napus* wurden 10 Replikate getestet und ein Wilcoxon-Vorzeichen-Rang-Test mit Bonferroni-Korrektur angewandt. Die statistische Signifikanz wird in den Abbildungen mittels *Compact Letter Display* dargestellt.

4 Ergebnisse und Diskussion

Im folgenden Kapitel werden der Inhalt der drei Publikationen sowie noch unveröffentlichte Daten vorgestellt und diskutiert.

4.1 Einfluss von Lichtspektrum, Photonenflussdichte und Temperatur auf *Acutodesmus obliquus*

In der ersten Publikation wurden die Ergebnisse der ersten Studie thematisiert. In dieser wurde die Grünalge *A. obliquus* parallel mit blauem, grünem und rotem Licht für 96 h kultiviert (Abbildung 2d-f). Diese Kultivierungsexperimente wurden bei unterschiedlichen Temperaturen (20 °C, 30 °C und 35 °C) mit einheitlicher Photonenflussdichte bei allen verwendeten Lichtspektren (480 µmol m^{-2} s^{-1}) durchgeführt. Nach Kultivierungsstart wurden in enger zeitlicher Folge Proben entnommen und die Biomassenkonzentration sowie die Fettsäurekomposition im zeitlichen Verlauf untersucht (Publikation 1).
Zusätzlich wurden zwei weitere Kultivierungsexperimente mit *A obliquus* bei 30 °C, photonengleich mit 120 sowie 800 µmol m^{-2} s^{-1} bei allen Lichtspektren durchgeführt. Hierbei wurde die Biomassenkonzentration im Zeitraum von 96 h und 225 h erfasst (Daten unveröffentlicht).

4.1.1 Wachstum

In Bezug auf das Wachstum wurde bei Kultivierung mit blauem Licht unter allen getesteten Bedingungen immer die geringste Biomassenproduktion beobachtet. Demgegenüber bewirkte rotes Licht bei allen Experimenten eine höhere Biomassenproduktion als blaues Licht (Abbildung 4a-c). Die Biomassenproduktion bei Kultivierung unter grünem Licht erwies sich als sehr variabel und stark abhängig von weiteren Parametern. Bei geringen Photonenflussdichten und geringen Biomassenkonzentrationen führte die Bestrahlung mit grünem Licht zu ähnlich niedrigem Biomassenzuwachs wie blaues Licht (Abbildung 4a). Im Gegensatz dazu wurden mit grünem Licht bei hohen Photonenflussdichten und hohen Biomassenkonzentrationen höhere Werte als mit rotem oder blauem Licht erzielt (Abbildung 4c).

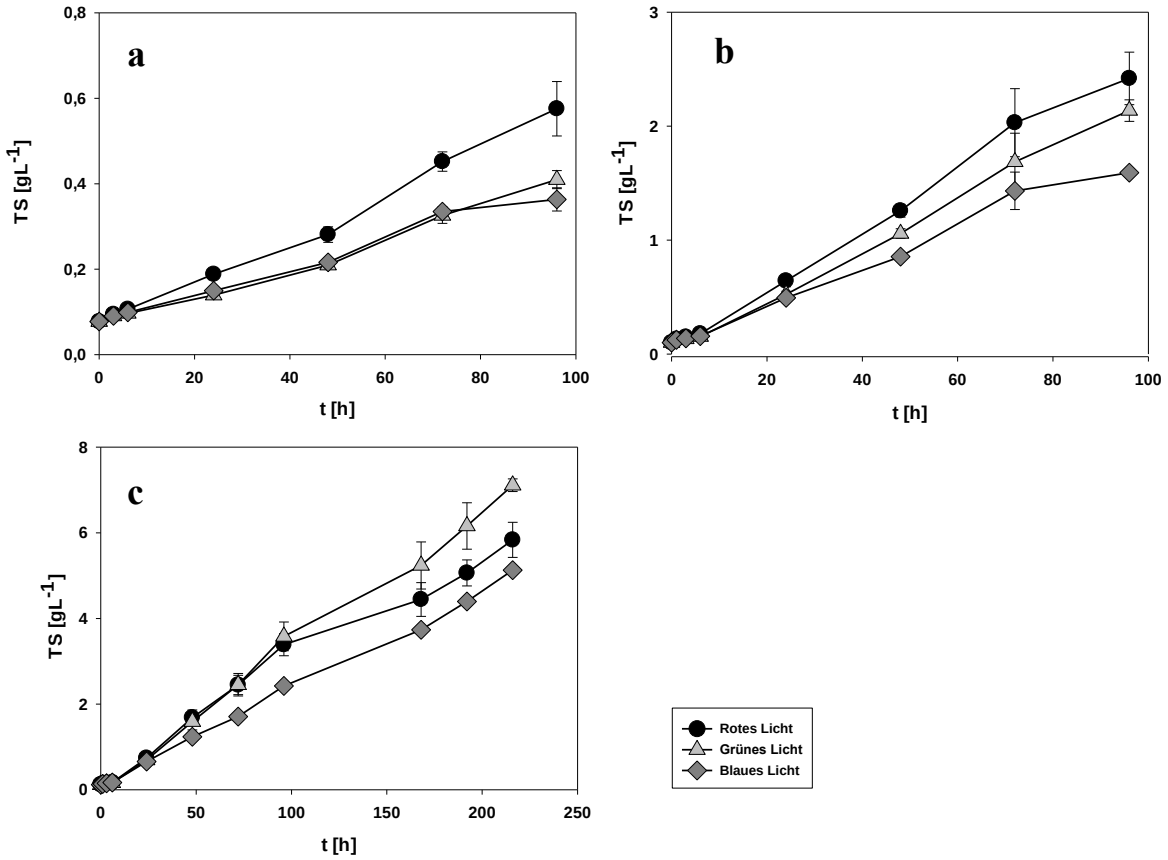

Abbildung 4: Biomassenkonzentration von *Acutodesmus obliquus*, kultiviert mit rotem Licht (580-700 nm), grünem Licht (450-600 nm) und blauem Licht (400-540 nm) bei 30 °C. Die Kultivierungen wurden jeweils bei Photonenflussdichten von 120 µmol m^{-2} s^{-1} (a), 480 µmol m^{-2} s^{-1} (b) und 800 µmol m^{-2} s^{-1} (c) durchgeführt. Die Trockensubstanz (TS) wurde aus der linearen Korrelation mit der Optischen Dichte bei 750 nm errechnet. Zu beachten sind die unterschiedlichen Skalierungen. Die Datenpunkte entsprechen Mittelwerten und Standardabweichungen aus Triplikaten.

Die hohe Biomassenproduktion der Algenkultur bei Bestrahlung mit rotem Licht wird dadurch erklärt, dass dieser Spektralbereich sehr effizient durch Chlorophyll a und Chlorophyll b absorbiert wird und daher effektiv für die Photosynthese genutzt werden kann. Das verwendete rote Licht hat insbesondere eine große Überlappung mit dem zweiten Absorptionsmaximum des Chlorophylls (Abbildung 2f) [3], [87]. Auch das eingesetzte blaue Licht hat eine spektrale Überlappung mit dem ersten Absorptionsmaximum des Chlorophylls (Abbildung 2d). Das geringe Algenwachstum unter blauem Licht kann allerdings durch eine gleichzeitige Absorption verschiedener, in den Algen enthaltener Xanthophylle und Carotinoide erklärt werden. Diese konkurrieren mit dem Chlorophyll um die Anregungsenergie. Die auf die Xanthophylle übertragene Lichtenergie geht meist durch quantenmechanische Wärmeübergänge verloren und steht somit nicht mehr für die Photosynthese und die Biomassenproduktion zur Verfügung [57], [88].

Die Beobachtung, dass grünes Licht auch effizient zum Algenwachstum beitragen kann, steht im Widerspruch zu klassischen Vorstellungen der Pflanzenphysiologie. In dieser Arbeit konnte jedoch bei hoher Photonenflussdichte (800 µmol m^{-2} s^{-1}) und hohen Biomassenkonzentrationen (über 3g L^{-1}) sogar die höchste Biomassenproduktion mit grünem Licht erzielt werden (Abbildung 4c). Diese Resultate

stehen jedoch im Einklang mit neuesten Studien [55], [56], [59]. Demnach kann grünes Licht aufgrund der geringeren Absorption der Algenpigmente in diesem Spektralbereich tiefer in hochdichte Algenlösungen eindringen als rotes und blaues Licht. Im Vergleich mit stärker absorbierten Spektralbereichen wird mit grünem Licht ein größeres Algensuspensionsvolumen und damit einhergehend mehr Algenzellen mit geringerer Strahlungsenergie versorgt. Dies führt insbesondere bei hohen Photonenflussdichten und hohen Biomassenkonzentrationen zu einer für die Algen energetisch besser nutzbaren Lichtverteilung [55]. Das ist insbesondere auch der Fall, weil Mikroalgen Schwachlicht deutlich effizienter als Starklicht nutzen können [29], [54]. Zudem wurde angenommen, dass die Absorption von grünem Licht bei hohen Strahlungsintensitäten einen weiteren Vorteil haben könnte. Eine Überanregung des Photosystems, durch zu hohe Strahlungsenergie kann bei Photosynthese treibenden Organismen eine Photoinhibition bewirken. Diese kann zu einer Schädigung des Photosystems und zu reduzierter Biomasssenproduktion führen [3]. Durch die geringere Absorption der einzelnen Algenzellen könnte grünes Licht auch bei hohen Lichtintensitäten kaum schädliche Auswirkungen haben. Diese Zusammenhänge haben in den letzten Jahren zunehmend Eingang in die Literatur gefunden. Gleichwohl dominiert in der pflanzenphysiologischen Literatur noch immer die Einschätzung, dass grünes Licht kaum Relevanz für die Photosynthese und das Algenwachstum hat. Mit dieser Studie konnte daher ein wichtiger Beitrag zum Verständnis der komplexen Rolle von grünem Licht für das Wachstum und die Photosynthese von Mikroalgen geleistet werden. Zudem wurden die genannten Zusammenhänge erstmalig mit breiten Lichtspektren an eukaryotischen Algen untersucht und die Ergebnisse vernetzend mit existierender Literatur diskutiert.

4.1.2 Fettsäurekomposition

Insgesamt konnten bei der Fettsäureanalyse 14 Fettsäuren identifiziert werden. Die Fettsäure 16:1 wurde dabei in zwei konfigurationsisomeren Formen identifiziert (16:1 $^{\Delta 9}$-cis/trans). Für den Vergleich der relativen Proportionen wurden die prozentualen Anteile der beiden isomeren Formen zusammengefasst. Die Fettsäurekomposition in dieser Studie steht dabei im Einklang mit den Ergebnissen vorheriger Analysen, die an diesem Algenstamm durchgeführt wurden [89]. Bei der Untersuchung ließ sich ein starker Einfluss der Parameter Temperatur und Lichtspektrum auf die prozentualen Verhältnisse der Fettsäuren feststellen. Die Effekte betrafen insbesondere die ungesättigten Fettsäuren mit 16 und 18 C-Atomen.

Wenn die Kultivierungstemperatur höher war als 25 °C, die Temperatur während der Vorkultivierung, war eine sukzessive Verringerung der prozentualen Anteile der PUFAs 16:4, 18:3 und 18:4 zu beobachten. Umgekehrt stieg der prozentuale Anteil dieser PUFAs im zeitlichen Verlauf der Kultivierung, wenn die Kultivierungstemperatur unterhalb von 25 °C lag. Die Konstanthaltung der Fluidität der Zellmembranen bei veränderter Temperatur wird in vielen Mikroorganismen durch Variation des Saturierungsgrades der Membranlipide ermöglicht [48]. Dies konnte somit auch in *A. obliquus* nachgewiesen werden.

Weiterhin konnte ein starker Effekt der Lichtspektren auf die Fettsäurekomposition entdeckt werden. Im Vergleich waren die prozentualen Anteile der PUFAs 16:4, 18:3 und 18:4, gemessen am Gesamtanteil der Fettsäuren, in *A. obliquus* unter rotem Licht zu allen Zeitpunkten verringert gegenüber blauem und grünem Licht (Abbildung 5a-c). Im Gegensatz dazu waren die relativen Proportionen der Fettsäuren mit höherem Saturierungsgrad (16:1, 16:2, 16:3, 18:1 und 18:2) bei Kultivierung mit rotem Licht zu allen Zeitpunkten erhöht gegenüber grünem und blauem Licht (1. Publikation).

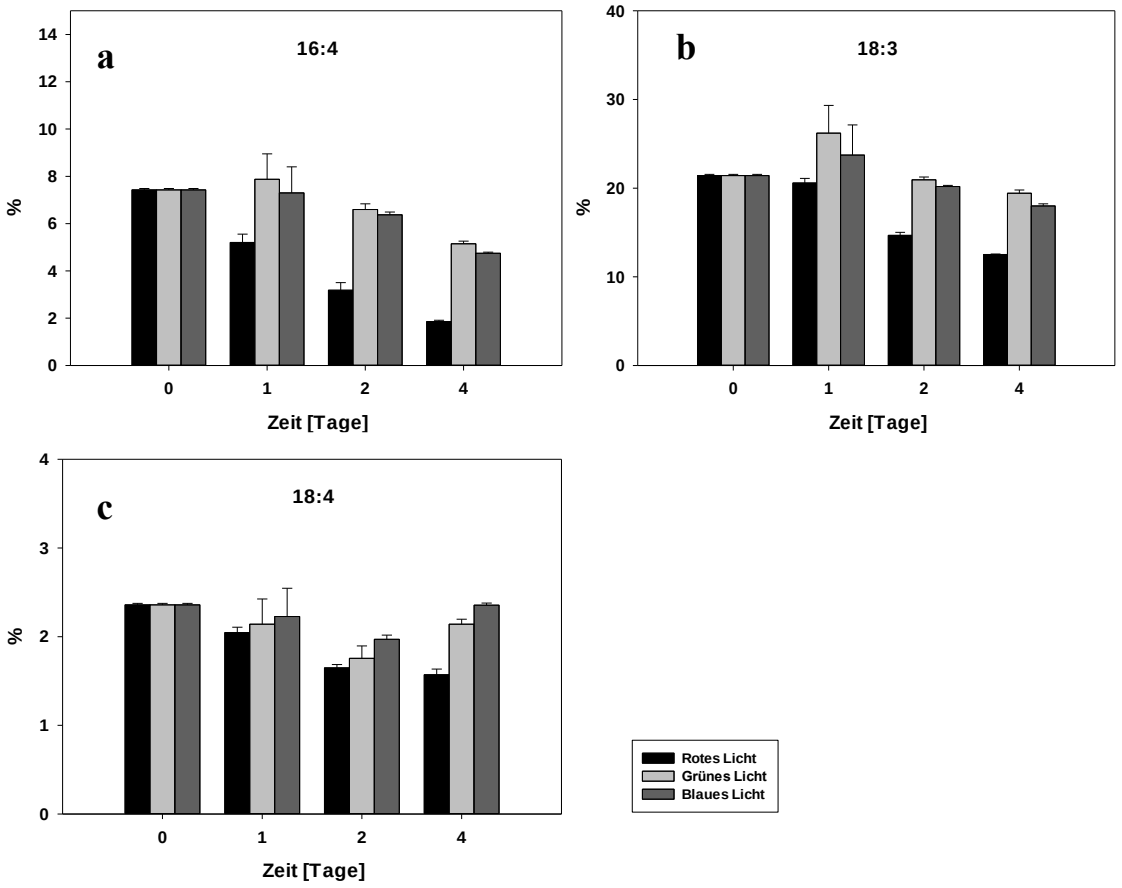

Abbildung 5: Relative Proportionen [%] der Fettsäuren 16:4 (a), 18:3 (b) und 18:4 (c) in *Acutodesmus obliquus* mit 480 µmol m^{-2} s^{-1} rotem Licht (580-700 nm), grünem Licht (450-600 nm) und blauem Licht (400-540 nm) bei 30 °C. Zu beachten sind die unterschiedlichen Skalierungen. Aufgetragen sind jeweils Mittelwerte und Standardabweichungen aus Triplikaten.

Dieser Effekt von Lichtspektren auf die Fettsäurekomposition von Organismen ist in der Literatur bisher unbekannt und wurde in dieser Arbeit erstmalig beschrieben. Die Änderungen in den Proportionen der PUFAs 16:4, 18:3 und 18:4 gegenüber den Fettsäuren 16:1, 16:2, 16:3, 18:1 und 18:2 weisen auf eine veränderte Enzymaktivität als Ursache hin. Aus der Literatur ist bekannt, dass die Entsättigung der Fettsäuren sukzessive durch Enzyme, die spezifisch eine weitere Doppelbindung im Molekül einfügen, katalysiert wird. Diese sogenannten Fettsäure-Desaturasen werden in ihrer katalytischen Aktivität zum Teil durch Umweltreize wie Licht und Temperatur beeinflusst [68], [90]. Jedoch ist noch unbekannt, ob Fettsäure-Desaturasen spezifisch durch bestimmte Lichtspektren beeinflusst werden. Aufgrund der vorliegenden Daten wird angenommen, dass die Aktivität von Fettsäure-Desaturasen in *A. obliquus* durch blaues und grünes Licht sowie Kältereize stimuliert wird. Blaues und grünes Licht teilen einen

gemeinsamen Spektralbereich (450-550 nm), dieser fehlt allerdings im roten Licht (Abbildung 2d-f). Daher wird angenommen, dass Fettsäure-Desaturasen spezifisch durch blaugrünes Licht (450–550 nm) und Kälte stimuliert werden, wodurch sich das Verhältnis der Fettsäuren in *A. obliquus* zugunsten der höher desaturierten Fettsäuren (16:4, 18:3 und 18:4) verändert. Dafür sprechen jedenfalls die erhöhten Werte der PUFAs 16:4, 18:3 und 18:4 bei Versuchen mit niedrigen Kultivierungstemperaturen und mit blaugrünem Licht (450-550 nm). Ob auch rotes Licht gegenüber Dunkelheit einen positiven Einfluss auf die Fettsäure-Desaturierung hat, konnte aufgrund der bisherigen Daten nicht beurteilt werden. Auch eine negative Regulation der Fettsäure-Desaturasen durch rotes Licht gegenüber blauem und grünem Licht konnte nicht ausgeschlossen werden. Diese Fragestellungen sollten daher Gegenstand von Folgestudien sein (4.2). Die Erhöhung des prozentualen Anteils der PUFA 16:4, 18:3 und 18:4 in *A. obliquus* durch blaugrünes Licht und Kälte könnte zudem mit einer vermehrten Bildung von Thylakoidmembranen in den Chloroplasten der Algen einhergehen. Dafür spricht insbesondere der bekannte Umstand, dass in den Thylakoiden diese Fettsäuren in höheren Anteilen vorkommen [50]. Ferner könnte es sich bei dieser physiologischen Reaktion um eine adaptive Kompensationsreaktion handeln. Durch eine Erhöhung der Menge an Thylakoidmembranen, die auch die Photosysteme und Lichtsammelantennen beinhalten, könnte die Lichtabsorption der Algen erhöht werden [3]. Auf diese Weise könnten die Algen auch die schwächer absorbierten Spektralbereiche besser nutzen, was auch einen weiteren Erklärungsansatz für das hohe Wachstum unter grünem Licht (4.1.1) liefern könnte.

4.2 Einfluss von blaugrünem Licht auf *Acutodesmus obliquus.*

In der zweiten Studie sollten die Erkenntnisse der ersten Veröffentlichung erweitert werden. Im ersten Teil der Studie wurden weißes und rotes Licht sowie Dunkelproben (mit und ohne Glukose) getestet. Die zusätzliche Verwendung von Dunkelproben ermöglichte es, die Fragestellung zu untersuchen, ob rotes Licht einen Einfluss auf die Entsättigung der Fettsäuren in *A. obliquus* hat. Im zweiten Teil wurde der Einfluss des Spektralbereiches zwischen 450 und 550 nm auf die Fettsäurekomposition genauer untersucht. Zu diesem Zweck wurde ungefiltertes weißes Licht zusammen mit rotem, gelbem und orangem Licht verwendet (Abbildung 2a-c,f). Die Algenkultivierung wurde einheitlich bei 15 °C und 210 µmol m^{-2} s^{-1} durchgeführt. Zudem wurde zusätzlich die Pigmentkomposition von *A. obliquus* untersucht. Alle in dieser Studie generierten Daten wurden veröffentlicht (Publikation 2).

4.2.1 Wachstum

In dieser Studie lag der Fokus nicht auf der Untersuchung des Algenwachstums, gleichwohl konnte eine wichtige Beobachtung beim Algenwachstum gemacht werden. Bei Behandlung mit Lichtspektren, die neben dem langwelligen Spektralanteil um 600 nm noch kurzwelligere Spektralanteile unterhalb von 550 nm enthielten, ließ sich immer ein deutlich höheres Algenwachstum beobachten als unter monochromatischem rotem Licht (580-700 nm). Es konnte nicht genau geklärt werden, warum diese spektrale Komposition gegenüber rotem Licht zu einem höheren Wachstum führte. Es wird jedoch

angenommen, dass kurzwelligere Spektralanteile des sichtbaren Lichts als Trigger für den Metabolismus der Algen relevant sind und kombiniert mit langwelligen visuellen Spektralanteilen zur gesteigerten Biomassenproduktion führen. Hinweise dafür liefern zudem die Analysen der Fettsäure- und Pigmentkomposition (4.2.2, 4.2.3).

4.2.2 Fettsäurekomposition

Bei diesen Untersuchungen war erneut ein starker Einfluss der Lichtbedingungen auf die Fettsäurekomposition zu beobachten. Signifikante Unterschiede betrafen insbesondere die Fettsäuren 16:4 und 18:3 (Abbildung 6). Es konnten die Resultate aus der ersten Studie bestätigt werden, durch eine feinere Abstufung der eingesetzten Lichtspektren war es jedoch möglich, den für die Desaturierung der Fettsäuren relevante Spektralbereich auf 470-520 nm einzugrenzen. Nur wenn dieser im Lichtspektrum enthalten war, konnte ein erhöhter prozentualer Anteil der Fettsäuren 16:4 und 18:3 beobachtet werden (Abbildung 6a-b). Dieser Spektralanteil ist im weißen Licht und im gelben Licht, nicht jedoch im orangen Licht, roten Licht und in den Dunkelproben enthalten (Abbildung 2a-c,f). Keine signifikanten Unterschiede in den Fettsäureproportionen waren zwischen den mit rotem Licht kultivierten Proben und den heterotrophen Dunkelproben zu beobachten (Abbildung 6a).

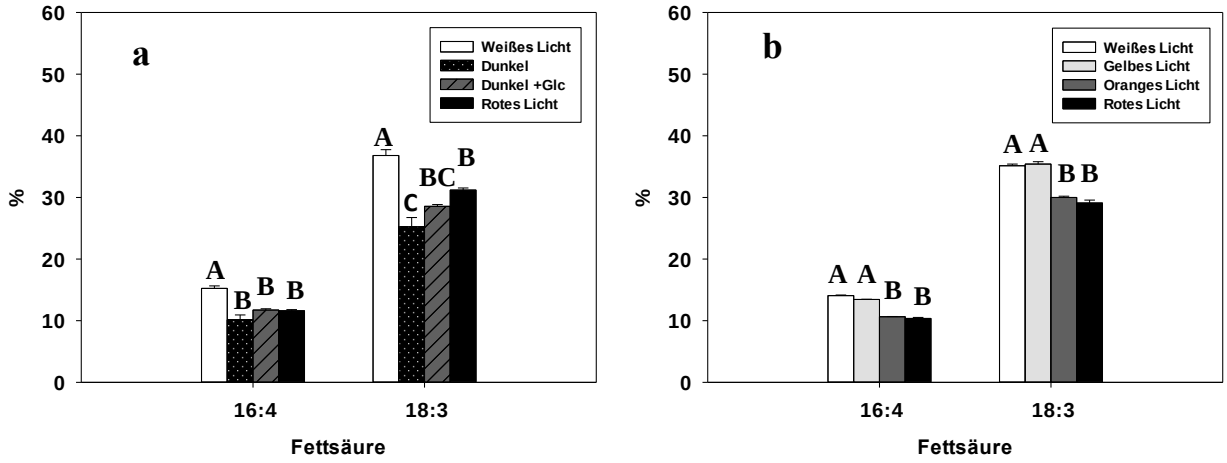

Abbildung 6: Relative Proportionen [%] der Fettsäuren 16:4 and 18:3 in *A. obliquus*, kultiviert mit weißem Licht (400–700 nm), Dunkelansatz ohne oder mit 2 gL^{-1} Glucose (Glc) und rotem Licht (580–700 nm) (a) sowie weißes Licht (400–700 nm), gelbes Licht (470–700 nm), oranges Licht (520–700 nm) und rotes Licht (580–700 nm) (b). Die Experimente wurden bei 210 µmol m^{-2} s^{-1} (wenn Licht verwendet wurde) und 15 °C durchgeführt. Angegeben sind jeweils die Mittelwerte und Standardfehler von zwei (a) bzw. drei (b) unabhängigen Experimenten. Die Buchstaben (A–C) zeigen signifikante Unterschiede ($p \leq 0.05$) zwischen den Gruppen an.

Eine positive oder negative regulatorische Funktion von rotem Licht auf die Fettsäure-Entsättigung konnte somit nicht festgestellt werden. Daher wird eine positive Regulation durch den Spektralbereich zwischen 470 und 520 nm auf die Desaturierung der Fettsäuren als plausible Erklärung für die Unterschiede bei der Fettsäuren-Desaturierung angenommen.

4.2.3 Pigmentkomposition

Durch die Pigmentanalyse konnten neben Chlorophyll a und Chlorophyll b zudem noch die Carotinoide und Xanthophylle Lutein, Violaxanthin, Neoxanthin und Beta-Carotin identifiziert werden. Die Komposition und Konzentrationen der Pigmente entsprach im Wesentlichen denen von anderen Studien mit *A. obliquus* [31], [70]. Ähnlich wie es bei Proportionen der PUFAs 16:4 und 18:3 der Fall ist (4.2.2), konnte bei den Pigmenten ein Zusammenhang zwischen der Anwendung von blaugrünem Licht und einer maximalen Pigmentkonzentration festgestellt werden. Die gleichzeitige Erhöhung der Pigmentkonzentrationen und relativen Prozente der PUFAs 16:4 und 18:3 lieferte weitere Indizien dafür, dass blaugrünes Licht zu einer erhöhten Bildung von Thylakoidmembranen in den Algen führt, insbesondere weil sowohl hochungesättigte PUFAs als auch Pigmente vorwiegend in diesen Membransystemen vorkommen [3], [50].

4.3 Einfluss verschiedener Lichtspektren auf *Monoraphidium braunii*

Im Vordergrund stand im letzten Teil der Arbeit die Frage, ob die bei *A. obliquus* beschriebenen spektralselektiven Effekte auf diese Spezies beschränkt oder weiter verbreitet unter den Grünalgen und Landpflanzen sind. Zu diesem Zweck wurde zunächst die Grünalge *M. braunii* bei weißem, blauem, grünem und rotem Licht bei 25 °C und 210 µmol m^{-2} s^{-1} kultiviert und die Fettsäure- und Pigmentkomposition analysiert. Diese Spezies wurde aufgrund eines engen phylogenetischen Verwandtschaftsverhältnisses zu *A. obliquus* sowie bei dieser Art bereits identifizierter blaulichtregulierter Stoffwechselprozesse ausgewählt [62], [63], [65], [91]. Die generierten Daten sind in eine weitere Publikation eingeflossen und dort im Detail beschrieben (3. Publikation).

4.3.1 Wachstum

Bei der Biomassenproduktion von *M. braunii* wurden ähnliche Resultate wie bei den vorherigen Studien mit *A. obliquus* erzielt. Im Vergleich der Teilspektren wurde bei Kultivierung mit blauem Licht die geringste Biomassenproduktion gemessen. Im direkten Vergleich wurde dagegen mit rotem und grünem Licht eine höhere Biomassenproduktion als mit blauem Licht verzeichnet. Die Biomassenproduktionen unter grünem und rotem Licht unterschieden sich nicht signifikant. Allerdings wurden die höchsten Biomassenproduktionen nach 96 h Kultivierungsdauer bei Bestrahlung mit weißem Licht beobachtet. Ähnlich wie bei den Untersuchungen an *A. obliquus* (4.2.1) konnte somit die höchste Biomassenproduktion bei einem Lichtspektrum beobachtet werden, das sowohl langwellige Spektralanteile über 600 nm als auch kurzwelligere Spektralanteile unter 550 nm enthält. Dies ist auch bei weiteren spektralselektiven Experimenten an Algen beobachtet worden, die im Zusammenhang mit dem Projekt HYPP (1.6) durchgeführt und auch bereits veröffentlicht wurden [92].

4.3.2 Fettsäurekomposition

Es wurden bei dieser Algenart hohe prozentuale Anteile der nahrungsmittelrelevanten PUFAs 18:2 und 18:3 gemessen, der prozentuale PUFA-Gesamtanteil lag bei über 55 %. Bei einigen Fettsäuren konnten zudem unterschiedliche isomere Formen detektiert werden. Dies betraf die Fettsäuren 16:1, 16:3 und 18:1. In dieser Studie wurden die Isomeren allerdings nicht weiter mittels Standards identifiziert. Für den Vergleich der Fettsäureproportionen wurden die relativen Anteile der Isomeren der Fettsäure zusammengefasst. Auch bei *M. braunii* konnte ein starker Einfluss des Lichtspektrums auf die Fettsäurekomposition beobachtet werden. Insbesondere die relativen prozentualen Anteile der kommerziell relevanten Fettsäure 18:3 waren bei Kultivierung mit blauem, grünem und weißem Licht gegenüber der Kultivierung mit rotem Licht signifikant erhöht. Dagegen waren die ungesättigten Fettsäuren, 18:1 und 18:2 unter rotem Licht gegenüber den mit den anderen Lichtspektren kultivierten Algen erhöht (Abbildung 7a).

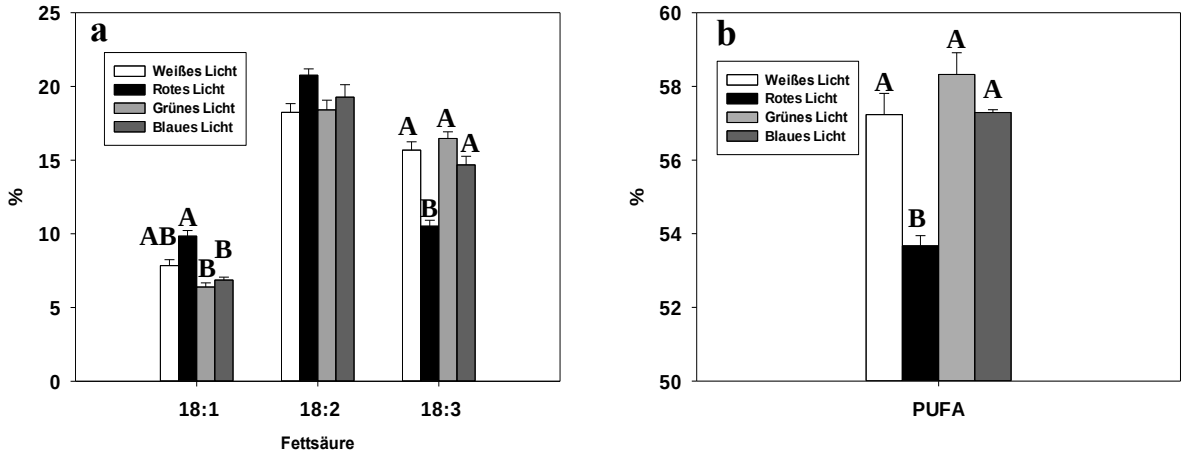

Abbildung 7: Relative Proportionen [%] der Fettsäuren 18:1, 18:2 und 18:3 (a) und der summierte prozentuale Anteil mehrfach ungesättigter Fettsäuren [PUFA] (b) in *Monoraphidium braunii*. Kultiviert wurde für 96 h mit 210 µmol m^{-2} s^{-1} weißem Licht (400-700 nm), rotem Licht (580-700 nm), grünem Licht (450-600 nm) und blauem Licht (400-550 nm) bei 25 °C. Aufgetragen sind jeweils Mittelwerte und Standardfehler aus zwei unabhängigen Experimenten. Unterschiedliche Buchstaben (A-B) zeigen signifikante Unterschiede ($p \leq 0.05$) zwischen den Gruppen an.

Alle eingesetzten Spektren mit der Ausnahme von rotem Licht enthielten dabei den blaugrünen Spektralbereich zwischen 450 und 550 nm. Ähnlich wie zuvor in *A. obliquus* bewirkte eine Bestrahlung mit Licht dieses Spektralbereichs gegenüber rotem Licht einen höheren prozentualen Anteil der Fettsäure 18:3 (Abbildung 7a). Unter den gleichen Bedingungen wurde allerdings ein niedrigerer prozentualer Anteil der Fettsäuren 18:2 und 18:1 gemessen (Abbildung 7a). Weiterhin wurde bei allen verwendeten Lichtspektren, außer bei rotem Licht, ein höherer prozentualer Anteil der summierten PUFAs beobachtet (Abbildung 7b). Die Bestrahlung mit Wellenlängen zwischen 450 und 550 nm bewirkt bei *M. braunii* daher gegenüber rotem Licht einerseits eine Erhöhung des relativen Anteils der PUFAs (Abbildung 7b) und andererseits einen erhöhten Desaturierungsgrad unter den PUFAs (Abbildung 7a). Dieser spektrale Effekt auf die Fettsäurekomposition wurde in dieser Dissertation zuvor

auch an der phylogenetisch mit *M. braunii* eng verwandten Grünalge *A. obliquus* entdeckt und im Detail beschrieben (4.1.2 und 4.2.2). Auch in *M. braunii* ist eine positive Regulation einer Fettsäure-Desaturase durch den Spektralanteil von 450-550 nm eine schlüssige Erklärung für die Unterschiede im Saturierungsgrad der Fettsäuren.

4.3.3 Pigmentkomposition

Bei der Pigmentanalyse konnten die Pigmente Chlorophyll a, Chlorophyll b, Lutein, Neoxanthin, Violaxanthin und Alpha-Carotin in *M. braunii* nachgewiesen und quantifiziert werden. Die Pigmente wurden in für diese Spezies typischen Konzentrationen und Proportionen gemessen [93]. Die Konzentration aller Pigmente war bei Bestrahlung mit Lichtspektren, die blaugrünes Licht zwischen 450 und 550 nm enthielten, höher als unter rotem Licht (Abbildung 8a-b). In der Literatur ist bekannt, dass blaues Licht die Synthese von Chlorophyll und einigen Xanthophyllen steigert [70]–[72].

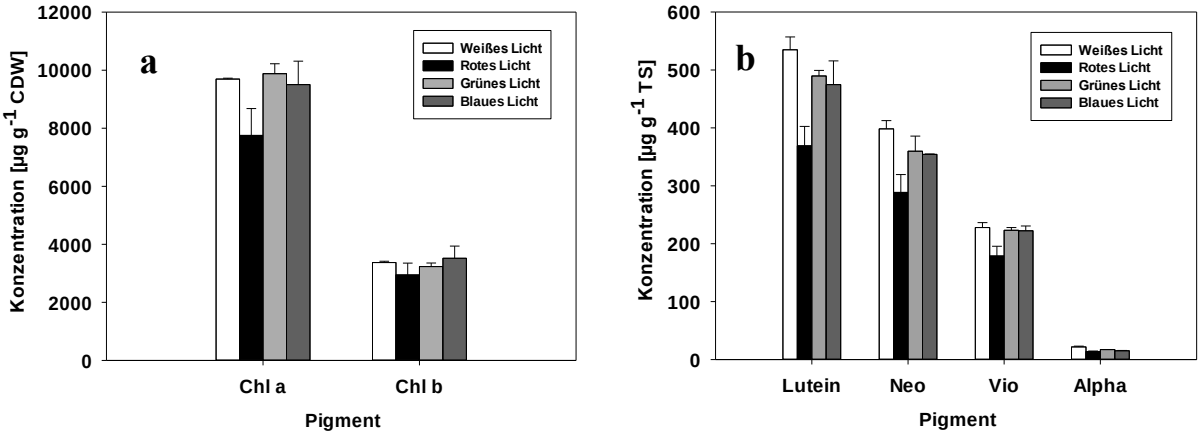

Abbildung 8: Ergebnisse der HPLC-DAD Analyse bei *Monoraphidium braunii*. Chl a: Chlorophyll a; Chl b: Chlorophyll b (a). Vio: Violaxanthin; Neo: Neoxanthin; Alpha: Alpha-Carotin (b). TS: Trockensubstanz. Kultiviert wurde für 96 h mit 210 µmol m^{-2} s^{-1} weißem Licht (400-700 nm), rotem Licht (580-700 nm), grünem Licht (450-600 nm) und blauem Licht (400-550 nm) bei 25 °C. Zu beachten sind die unterschiedlichen Skalierungen links und rechts. Aufgetragen sind jeweils Mittelwerte und Standardfehler aus zwei unabhängigen Experimenten.

In dieser Studie konnte ebenfalls eine erhöhte Pigmentkonzentration bei Bestrahlung mit blaugrünem Licht beobachtet werden. Eine ähnliche Auswirkung von blaugrünem Licht auf die Pigmentkomposition wurde auch bei *A. obliquus* festgestellt und dort besprochen (4.2.3).

4.4 Fettsäurekomposition in *Brassica napus* L.

Viele bekannte photosensitive Effekte sind im Stammbaum des Lebens hochkonserviert [94], [95]. Daher könnte der in den Mikroalgen *A. obliquus* und *M. braunii* beschriebene Effekt auf die Fettsäurekomposition ebenfalls weit verbreitet unter den Photosynthese treibenden Organismen sein. Abschließend wurde daher noch eine Untersuchung der Fettsäurekomposition an spektralselektiv kultivierten Landpflanzen (*B. napus*), durchgeführt. Dafür wurden in Zusammenarbeit mit der Ökologie der Leuphana Universität Lüneburg Rapspflanzen (*B. napus*) im Gewächshaus spektralselektiv

kultiviert und die Fettsäurekomposition nachfolgend analysiert. Es wurde insbesondere untersucht, ob auch in Landpflanzen kurzwelligere Strahlung für die Entsättigung der Fettsäuren eine Relevanz hat. Dafür wurden Rapspflanzen zum einen mit ungefiltertem Sonnenlicht und zum anderen mit rotem Licht (580–700 nm) behandelt. Zudem wurde noch eine Weißlichtgruppe mit vergleichbarer Photonenflussdichte zur Rotlichtgruppe verwendet. Im Anschluss wurde die Fettsäurekomposition der Folgeblätter in den drei Gruppen vergleichend analysiert. Auf die Wachstumsresultate wird in dieser Arbeit aus thematischen Gründen nicht weiter eingegangen, alle identifizierten Fettsäuren sind in Tabelle 1 aufgeführt. Für die Fettsäuren 16:1, 18:1 wurden zudem Isomere detektiert, diese wurden allerdings nicht mittels Standards identifiziert.

Tabelle 1: Fettsäureprofil der Folgeblätter von *Brassica napus* L.. Die Pflanzen wurden zuvor vom 17.09.2020-05.11.2020 im Gewächshaus mit ungefiltertem Sonnenlicht kultiviert. Angegeben sind die Mittelwerte und Standardabweichung aus 10 biologischen Replikaten. Gesättigte Fettsäuren (SFA), einfach ungesättigte Fettsäuren (MUFA) und mehrfach ungesättigte Fettsäuren (PUFA).

Fettsäure	**%**	**Fettsäure**	**%**
12:0	≤1	18:1 Isomer	≤1
14:0	≤1	19:0	≤1
15:0	≤1	18:2 $^{\Delta 9,12}$	7,3 ± 0,7
16:0	29,1 ± 2,1	18:3 $^{\Delta 9,12,15}$	39,4 ± 2,0
16:1 Isomer	≤1	20:0	≤1
16:1 Isomer	≤1	22:0	≤1
16:2 $^{\Delta 7,10}$	≤1	24:0	≤1
17:0	≤1		
16:3 $^{\Delta 7,10,13}$	13,9 ± 0,6	SFA	36,8
18:0	4,7 ± 0,5	MUFA	2,1
18:1 Isomer	≤1	PUFA	61,1

Die Fettsäuren 18:3, 16:0, 16:3 und 18:2 konnten in hohen prozentualen Anteilen gemessen werden und bei diesen gab es zudem signifikante Unterschiede zwischen allen drei getesteten Bedingungen (Tabelle 2). Die Fettsäuren 16:3 und 18:3 waren in *B. napus* die am höchsten desaturierten Fettsäuren.

Tabelle 2: Relative Proportionen [%] der Fettsäuren 16:0, 16:3, 18:2 und 18:3 in *Brassica napus* L.. Die Pflanzen wurden zuvor vom 17.09.2020-05.11.2020 im Gewächshaus mit ungefiltertem Sonnenlicht (Weiß), durch Kultivierungsnetz abgeschwächtes Sonnenlicht (Netz) und mit roter Filterfolie gefiltertes Sonnenlicht kultiviert (Rot). Angegeben sind die Mittelwerte und Standardabweichung aus 10 biologischen Replikaten. Unterschiedliche Buchstaben im Index (a-c) zeigen signifikante Unterschiede ($p \leq 0.05$) zwischen den Gruppen an.

	16:0 [%]	**16:3 [%]**	**18:2 [%]**	**18:3 [%]**
Weiß	29,1 ±2,1^{c}	13,9 ±0.6^{a}	7,3 ±0.7^{c}	39,4 ±2,0 ^{a}
Netz	30,9 ±1.0^{b}	11,9 ±0.8^{b}	10,9 ±0.5^{b}	35,6 ±1,1^{b}
Rot	33,1 ±1.1^{a}	10,8 ±0.6^{c}	11,1 ±0.5^{a}	33,4 ±1.3^{c}

Der höchste prozentuale Anteil der PUFAs 16:3 und 18:3 konnte bei Behandlung mit weißem Licht beobachtet werden. Ein niedrigerer Prozentsatz dieser PUFAs wurde bei der Kultivierung der mittels Kultivierungsnetz abgeschwächten Rapsblätter ermittelt (Tabelle 2). Das Lichtspektrum dieser beiden Gruppen ist gleich, die aufgetretenen Unterschiede gehen daher sehr wahrscheinlich auf die Unterschiede in der Strahlungsintensität zurück. Der geringste prozentuale Anteil der Fettsäuren 16:3 und 18:3 wurde jedoch bei den Rapspflanzen gemessen, die mit einer roten Filterfolie abgedeckt waren (Tabelle 2). Da die Strahlungsintensität bei dieser Gruppe ähnlich hoch war wie bei den unter dem Kultivierungsnetz aufgewachsenen Pflanzen, gehen die Unterschiede in diesem Fall sehr wahrscheinlich auf die Unterschiede in den Lichtspektren zurück. Die Rotlichtfolie ist intransparent für Licht unterhalb von 580 nm. Die beobachteten Unterschiede könnten daher ein Indiz dafür sein, dass bei den Folgeblättern von *B. napus* der kurzwellige visuelle Spektralanteil für eine Entsättigung der Fettsäuren Relevanz hat und dieser Effekt auch bei Landpflanzen vorkommt. Dieser blaulichtregulierte Prozess wäre somit weit verbreitet unter Photosynthese treibenden Organismen und könnte sogar auch bei heterotrophen Organismen vorkommen. Diese Daten wurden bisher noch nicht veröffentlicht.

5 Fazit und Ausblick

In dieser Arbeit wurde der Einfluss unterschiedlicher Temperaturen und Lichtspektren auf den Stoffwechsel von Mikroalgen untersucht. Dabei wurden Teilspektren und Temperaturen identifiziert, die eine maximale Bildung von industriell relevanten Pigmenten, einen maximalen prozentualen Anteil PUFAs und zugleich ein optimales Algenwachstum ermöglichen. Diese Erkenntnisse konnten das grundlegende Verständnis licht- und temperaturgesteuerter Prozesse in Photosynthese treibenden Organismen vertiefen. Zudem kann durch die Erkenntnisse dieser Arbeit das Zusammenspiel und die Effizienz von Mikroalgen PBR-Systemen mit mehreren integrierten Anwendungen optimiert und dadurch ein wichtiger praktischer Beitrag für eine nachhaltige Entwicklung geleistet werden. So konnten Lichtspektren definiert werden, die eine optimale gemeinsame Nutzung des Sonnenlichts für die PV und die Kultivierung von Mikroalgen in PBR auf gleicher Nutzfläche ermöglichen. Insbesondere in Regionen mit hoher solarer Strahlung könnten diese Systeme dadurch synergistisch, platzsparend und effizient zusammen betrieben werden.

Bei hohen Biomassenkonzentrationen und Starklicht wurde mit grünem Licht die höchste Biomassenproduktion unter den Teilspektren erzielt. Mit diesem Spektralbereich kann bei Starklicht und hohen Algendichten im PBR eine sehr effiziente Nutzung des Lichts erfolgen. Diese Erkenntnisse könnten künftig bei der Algenproduktion in Regionen mit hohen solaren Photonenflüssen, z.B. durch Teilabschattung mit Grünlichtfiltern oder im industriellen Maßstab mittels grüner Leuchtdioden Anwendung finden. Die höchste Biomassenproduktion bei mittleren Photonenflüssen konnte bei Bestrahlung von Spektren mit einer Mischung aus rotem Licht (600–700 nm) und einem kurzwelligen Spektralanteil unter 550 nm beobachtet werden. Zudem konnte blaugrünes Licht (450–550 nm) als wichtiger Trigger für eine maximierte Bildung von Photosynthesepigmenten und einen erhöhten Grad der Desaturierung von Fettsäuren in Grünalgen identifiziert werden. Dieses Wissen könnte künftig biotechnologisch zur stimulierten Produktion spezifischer Fettsäuren für die Biokraftstoff- oder Nahrungsmittel-Produktion angewandt werden. Durch Spektren ohne blaugrünes Licht ließe sich etwa eine Fettsäurekomposition mit niedrigem Desaturierungsgrad für die Herstellung von Biodiesel erzielen. So ist für die Produktion von Biodiesel ein niedriger Grad der Desaturierung von Fettsäuren notwendig. Daher könnte mit rotem Licht (600–700 nm) und zusätzlich einer hohen Kultivierungstemperatur (30–40°C) optimale Resultate erzielt werden. Diese Kombination ermöglicht eine vergleichsweise hohe Biomassenproduktion der Algen sowie eine optimale Fettsäurekomposition für die Herstellung von Biodiesel. Damit könnte ein wichtiger Beitrag zu einer effizienteren großtechnischen Produktion von Biokraftstoffen aus Algen und zum Ziel 7 (saubere Energie) der Vereinten Nationen geleistet werden. Zur Stimulation eines hohen Anteils der Omega-3-Fettsäure 18:3 und einer erhöhten Pigmentkonzentration wären dagegen eine Bestrahlung mit einem Spektralanteil zwischen 450 und 550 nm und eine geringere Kultivierungstemperatur erforderlich. In diesem Fall ist eine spektrale Kombination zusammen mit rotem Licht (600-700 nm) sinnvoll, weil diese gleichzeitig zu einer

optimalen Biomassenproduktion der Algen führt. Da eine geringere Kultivierungstemperatur mit einer reduzierten Biomassenproduktion einhergeht, müsste im Einzelfall entschieden werden, ob der Fokus auf die Wertstoffproduktion oder das Algenwachstum gelegt werden soll. Alternativ könnte auch sequenziell kultiviert und die Kultivierungstemperatur erst im letzten Kultivierungsintervall entsprechend reduziert werden. Abgeleitet von den Erkenntnissen dieser Arbeit, könnte der physiologische Wert der Algenbiomasse für die Anwendung in der Aquakultur und der Nahrungsmittelindustrie gezielt gesteigert werden, was einen Beitrag zur Nahrungsmittelsicherheit leisten kann. Im Freiland lassen sich die Lichtbedingungen sehr einfach durch die Applikation entsprechender Lichtfilterfolien auf die Algenreaktoren umsetzen.

Weiterhin wurden bei Experimenten mit *B. napus* Hinweise dafür gefunden, dass kurzwellige visuelle Strahlung auch bei Landpflanzen eine wichtige Funktion bei der Fettsäure-Desaturierung hat. Diese spektralen Effekte waren bisher in der Literatur unbekannt. Als Ursache für die erhöhten Pigmentkonzentrationen und die höhere Desaturierung der Fettsäuren wird eine positive Regulation von Fettsäure-Desaturasen und eine erhöhte Bildung von Thylakoid Membranen durch blaugrünes Licht angenommen. Ob blaugrünes Licht diese physiologischen Reaktionen tatsächlich stimuliert, sollte Gegenstand von Folgeuntersuchungen sein. Eine Transkriptomanalyse der codierenden Gene für Fettsäure-Desaturasen bei Mikroalgen sowie Enzymassays der aufgereinigten Desaturase-Proteine könnten bei dieser Fragestellung Klarheit liefern. Zur Untersuchung der Auswirkung von blaugrünem Licht auf die Bildung von Thylakoidmembranen könnten elektronenmikroskopische Aufnahmen der pflanzlichen Chloroplasten weitere Einblicke ermöglichen.

Mit Hilfe der Daten aus dieser Dissertation konnte zudem bereits eine Vorgabe für das Transmissionsspektrum der semitransparenten Solarzellen im geplanten Hybridsystem erstellt werden. Daraufhin wurden semitransparente Solarzellen-Dummys mit Transmissionsmaxima bei 460 und 600 nm von der DLR in Oldenburg hergestellt. Diese Dummys simulieren die Transmission der geplanten Germanium-basierten und semitransparenten Solarzelle. Mit diesen PV-Dummys wurden im Rahmen des Projekts HYPP bereits Wachstumsexperimente an *A. obliquus* durchgeführt. Es ließen sich dabei höhere photosynthetische Effizienzen erreichen als mit dem roten Spektralbereich zwischen 600 und 700 nm, der vorwiegend bei semitransparenten siliziumbasierten Solarzellen transmittiert wird.

6 Literaturverzeichnis

[1] Shen, J. R. (2015). The structure of photosystem II and the mechanism of water oxidation in photosynthesis. *Annual review of plant biology*, *66*, 23-48.

[2] Nelson, N. (2011). Photosystems and global effects of oxygenic photosynthesis. *Biochimica et Biophysica Acta (BBA)-Bioenergetics*, *1807*(8), 856-863.

[3] Heldt, H. W., & Piechulla, B. (2021). *Plant biochemistry*. Academic Press.

[4] McFadden, G. I. (2001). Chloroplast origin and integration. *Plant physiology*, *125*(1), 50-53.

[5] Sarafis, V. (1998). Chloroplasts: a structural approach. *Journal of Plant Physiology*, *152*(2-3), 248-264.

[6] Johnson, M. P. (2017). Correction: Photosynthesis. *Essays in Biochemistry*, *61*(4), 429.

[7] Blankenship, R. E. (2010). Early evolution of photosynthesis. *Plant physiology*, *154*(2), 434-438.

[8] Blankenship, R. E. (2002). Origin and evolution of photosynthesis. *Molecular Mechanisms of Photosynthesis*, 220-257.

[9] Awramik, S. M. (1992). The oldest records of photosynthesis. *Photosynthesis research*, *33*, 75-89.

[10] Sánchez-Baracaldo, P., & Cardona, T. (2020). On the origin of oxygenic photosynthesis and Cyanobacteria. *New Phytologist*, *225*(4), 1440-1446.

[11] Garcia-Pichel, F., Lombard, J., Soule, T., Dunaj, S., Wu, S. H., & Wojciechowski, M. F. (2019). Timing the evolutionary advent of cyanobacteria and the later great oxidation event using gene phylogenies of a sunscreen. *MBio*, *10*(3), e00561-19.

[12] Archibald, J. M. (2009). The origin and spread of eukaryotic photosynthesis: evolving views in light of genomics. *Botanica Marina*, *52*(2), 95–103.

[13] Fehling, J., Stoecker, D., & Baldauf, S. L. (2007). Photosynthesis and the eukaryote tree of life. *Evolution of primary producers in the sea*, 75-107.

[14] Gupta, R. S. (2012). Origin and spread of photosynthesis based upon conserved sequence features in key bacteriochlorophyll biosynthesis proteins. *Molecular biology and evolution*, *29*(11), 3397-3412.

[15] Pooja, S. (2014). Algae used as medicine and food-a short review. *Journal of Pharmaceutical Sciences and Research*, *6*(1), 33.

[16] Harwood, J. L., & Guschina, I. A. (2009). The versatility of algae and their lipid metabolism. *Biochimie*, *91*(6), 679-684.

[17] Douglas, S. E., Raven, J. A., & Larkum, A. W. (2003). The algae and their general characteristics. *Photosynthesis in Algae*, 1-10.

[18] Bhattacharya, D., & Medlin, A. L. (1998). Algal phylogeny and the origin of land plants. *Plant physiology*, *116*(1), 9-15.

[19] Leliaert, F., Smith, D. R., Moreau, H., Herron, M. D., Verbruggen, H., Delwiche, C. F., & De Clerck, O. (2012). Phylogeny and molecular evolution of the green algae. *Critical reviews in plant sciences*, *31*(1), 1-46.

[20] Khan, M. I., Shin, J. H., & Kim, J. D. (2018). The promising future of microalgae: current status, challenges, and optimization of a sustainable and renewable industry for biofuels, feed, and other products. *Microbial cell factories*, *17*(1), 1-21.

[21] Pereira, L. (2021). Macroalgae. *Encyclopedia*, *1*(1), 177-188.

[22] Ebenezer, V., Medlin, L. K., & Ki, J. S. (2012). Molecular detection, quantification, and diversity evaluation of microalgae. *Marine biotechnology*, *14*, 129-142.

[23] Hildebrand, M., Abbriano, R. M., Polle, J. E., Traller, J. C., Trentacoste, E. M., Smith, S. R., & Davis, A. K. (2013). Metabolic and cellular organization in evolutionarily diverse microalgae as related to biofuels production. *Current opinion in chemical biology*, *17*(3), 506-514.

[24] Gimpel, J. A., Henríquez, V., & Mayfield, S. P. (2015). In metabolic engineering of eukaryotic microalgae: potential and challenges come with great diversity. *Frontiers in microbiology*, *6*, 1376.

[25] Muylaert, K., Bastiaens, L., Vandamme, D., & Gouveia, L. (2017). Harvesting of microalgae: Overview of process options and their strengths and drawbacks. *Microalgae-based biofuels and bioproducts*, 113-132.

[26] Wang, B., Li, Y., Wu, N., & Lan, C. Q. (2008). CO_2 bio-mitigation using microalgae. *Applied microbiology and biotechnology*, *79*, 707-718.

[27] Anto, S., Mukherjee, S. S., Muthappa, R., Mathimani, T., Deviram, G., Kumar, S. S., Verma, T.M., & Pugazhendhi, A. (2020). Algae as green energy reserve: Technological outlook on biofuel production. *Chemosphere*, *242*, 125079.

[28] Piligaev, A. V., Sorokina, K. N., Bryanskaya, A. V., Peltek, S. E., Kolchanov, N. A., & Parmon, V. N. (2015). Isolation of prospective microalgal strains with high saturated fatty acid content for biofuel production. *Algal Research*, *12*, 368-376.

[29] Hindersin, S., Leupold, M., Kerner, M., & Hanelt, D. (2013). Irradiance optimization of outdoor microalgal cultures using solar tracked photobioreactors. *Bioprocess and biosystems engineering*, *36*, 345-355.

[30] Miranda, M. T., Sepúlveda, F. J., Arranz, J. I., Montero, I., & Rojas, C. V. (2018). Physical-energy characterization of microalgae *Scenedesmus* and experimental pellets. *Fuel*, *226*, 121-126.

[31] Admirasari, R., Hindersin, S., von Schwartzenberg, K., & Hanelt, D. (2022). Nutritive capability of anaerobically digested black water increases productivity of *Tetradesmus obliquus*: domestic wastewater as an alternative nutrient resource. *Bioresource Technology Reports*, *17*, 100905.

[32] Posten, C., & Schaub, G. (2009). Microalgae and terrestrial biomass as source for fuels—a process view. *Journal of biotechnology*, *142*(1), 64-69.

[33] Spolaore, P., Joannis-Cassan, C., Duran, E., & Isambert, A. (2006). Commercial applications of microalgae. *Journal of bioscience and bioengineering*, *101*(2), 87-96.

[34] Zheng, H., Wang, Y., Li, S., Nagarajan, D., Varjani, S., Lee, D. J., & Chang, J. S. (2022). Recent advances in lutein production from microalgae. *Renewable and Sustainable Energy Reviews*, *153*, 111795.

[35] Lorenz, R. T., & Cysewski, G.R. (2000). Commercial potential for *Haematococcus* microalgae as a natural source of astaxanthin. *Trends in Biotechnology*, *18*, 160-167.

[36] Sun, Z., Li, T., Zhou, Z. G., & Jiang, Y. (2015). Microalgae as a source of lutein: chemistry, biosynthesis, and carotenogenesis. *Microalgae biotechnology*, 37-58.

[37] Johnson, E. A., & An, G. H. (1991). Astaxanthin from microbial sources. *Critical reviews in Biotechnology*, *11*(4), 297-326.

[38] Maltsev, Y., & Maltseva, K. (2021). Fatty acids of microalgae: Diversity and applications. *Reviews in Environmental Science and Bio/Technology*, *20*, 515-547.

[39] de Oliveira, C. Y. B., Viegas, T. L., Lopes, R. G., Cella, H., Menezes, R. S., Soares, A. T., Filho, N.R.A., & Derner, R. B. (2020). A comparison of harvesting and drying methodologies on fatty acids composition of the green microalga *Scenedesmus obliquus*. *Biomass and Bioenergy*, *132*, 105437.

[40] Crawford, M., Galli, C., Visioli, F., Renaud, S., Simopoulos, A. P., & Spector, A. A. (2000). Role of plant-derived omega–3 fatty acids in human nutrition. *Annals of Nutrition and Metabolism*, *44*(5-6), 263-265.

[41] La Guardia, M., Giammanco, S., Di Majo, D., Tabacchi, G., Tripoli, E., & Giammanco, M. (2005). Omega 3 fatty acids: biological activity and effects on human health. *Panminerva medica*, *47*(4), 245-257.

[42] Simopoulos, A. P. (2002). The importance of the ratio of omega-6/omega-3 essential fatty acids. *Biomedicine & pharmacotherapy*, *56*(8), 365-379.

[43] Shanab, S. M. M., Hafez, R. M., & Fouad, A. S. (2018). A review on algae and plants as potential source of arachidonic acid. *Journal of advanced research*, *11*, 3-13.

[44] Kamal-Eldin, A., & Yanishlieva, N. V. (2002). *N*-3 fatty acids for human nutrition: stability considerations. *European journal of lipid science and technology*, *104*(12), 825-836.

[45] Worm, B., Barbier, E. B., Beaumont, N., Duffy, J. E., Folke, C., Halpern, B. S., Jackson, J. B. C., Lotze, H. K., Micheli, F., Palumbi, S. R., Sala, E., Selkoe, K. A., Stachowicz, J. J., & Watson, R. (2006). Services impacts of biodiversity loss on ocean ecosystem. *Science*, *314*, 787.

[46] Blanco Gonzalez, E., & de Boer, F. (2017). The development of the Norwegian wrasse fishery and the use of wrasses as cleaner fish in the salmon aquaculture industry. *Fisheries Science*, *83*, 661-670.

[47] Adarme-Vega, T. C., Lim, D. K., Timmins, M., Vernen, F., Li, Y., & Schenk, P. M. (2012). Microalgal biofactories: a promising approach towards sustainable omega-3 fatty acid production. *Microbial cell factories*, *11*(1), 1-10.

[48] Patterson, G. W. (1970). Effect of culture temperature on fatty acid composition of *Chlorella sorokiniana*. *Lipids*, *5*(7), 597-600.

[49] Degraeve-Guilbault, C., Pankasem, N., Gueirrero, M., Lemoigne, C., Domergue, F., Kotajima, T., Suzuki, I., Joubes, J, & Corellou, F. (2021). Temperature acclimation of the picoalga *Ostreococcus tauri* triggers early fatty-acid variations and involves a plastidial ω3-desaturase. *Frontiers in Plant Science*, *12*, 639330.

[50] Hultberg, M., Jönsson, H. L., Bergstrand, K. J., & Carlsson, A. S. (2014). Impact of light quality on biomass production and fatty acid content in the microalga *Chlorella vulgaris*. *Bioresource technology*, *159*, 465-467.

[51] Abomohra, A. E. F., Shang, H., El-Sheekh, M., Eladel, H., Ebaid, R., Wang, S., & Wang, Q. (2019). Night illumination using monochromatic light-emitting diodes for enhanced microalgal growth and biodiesel production. *Bioresource technology*, *288*, 121514.

[52] Fortunato, A. E., Annunziata, R., Jaubert, M., Bouly, J. P., & Falciatore, A. (2015). Dealing with light: the widespread and multitasking cryptochrome/photolyase family in photosynthetic organisms. *Journal of plant physiology*, *172*, 42-54.

[53] Fankhauser, C., & Chory, J. (1997). Light control of plant development. *Annual review of cell and developmental biology*, *13*(1), 203-229.

[54] Hindersin, S., Leupold, M., Kerner, M., & Hanelt, D. (2014). Key parameters for outdoor biomass production of *Scenedesmus obliquus* in solar tracked photobioreactors. *Journal of applied phycology*, *26*, 2315-2325.

[55] Ooms, M. D., Graham, P. J., Nguyen, B., Sargent, E. H., & Sinton, D. (2017). Light dilution via wavelength management for efficient high-density photobioreactors. *Biotechnology and bioengineering*, *114*(6), 1160-1169.

[56] de Mooij, T., de Vries, G., Latsos, C., Wijffels, R. H., & Janssen, M. (2016). Impact of light color on photobioreactor productivity. *Algal research*, *15*, 32-42.

[57] Wilhelm, C., Krámer, P., & Wild, A. (1985). Effect of different light qualities on the ultrastructure, thylakoid membrane composition and assimilation metabolism of *Chlorella fusca*. *Physiologia Plantarum*, *64*(3), 359-364.

[58] Ruban, A. V., Horton, P., & Young, A. J. (1993). Aggregation of higher plant xanthophylls: differences in absorption spectra and in the dependency on solvent polarity. *Journal of Photochemistry and Photobiology B: Biology*, *21*(2-3), 229-234.

[59] Mattos, E. R., Singh, M., Cabrera, M. L., & Das, K. C. (2015). Enhancement of biomass production in *Scenedesmus bijuga* high-density culture using weakly absorbed green light. *Biomass and Bioenergy*, *81*, 473-478.

[60] Christie, J. M., & Briggs, W. R. (2001). Blue light sensing in higher plants. *Journal of Biological Chemistry*, *276*(15), 11457-11460.

[61] Münzner, P., & Voigt, J. (1992). Blue light regulation of cell division in *Chlamydomonas reinhardtii*. *Plant Physiology*, *99*(4), 1370.

[62] Giráldez, N., Aparicio, P. J., & Quiñones, M. A. (2000). Limiting CO_2 levels induce a blue light-dependent HCO_3^- uptake system in *Monoraphidium braunii*. *Journal of experimental botany*, *51*(345), 807-815.

[63] Aparicio, P. J., & Quiñones, M. A. (1991). Blue light, a positive switch signal for nitrate and nitrite uptake by the green alga *Monoraphidium braunii*. *Plant physiology*, *95*(2), 374-378.

[64] Quiñones, M. A., Galván, A., Fernández, E., & Aparicio, P. J. (1999). Blue-light requirement for the biosynthesis of an NO_2^- transport system in the *Chlamydomonas reinhardtii* nitrate transport mutant S10. *Plant, Cell & Environment*, *22*(9), 1169-1175.

[65] Quiñones, M. A., & Aparicio, P. J. (1990). Blue light activation of nitrate reductase and blue light promotion of the biosynthesis of nitrite reductase in *Monoraphidium braunii*. *Inorganic Nitrogen in Plants and Microorganisms: Uptake and Metabolism* (pp. 171-177). Springer Berlin Heidelberg.

[66] Moulin, S. L., Beyly-Adriano, A., Cuiné, S., Blangy, S., Légeret, B., Floriani, M., Burlacot, A., Sorigué, D., Samire, P., Li-Beisson, Y., Peltier, G., & Beisson, F. (2021). Fatty acid photodecarboxylase is an ancient photoenzyme that forms hydrocarbons in the thylakoids of algae. *Plant Physiology*, *186*(3), 1455-1472.

[67] Heyes, D. J., Lakavath, B., Hardman, S. J., Sakuma, M., Hedison, T. M., & Scrutton, N. S. (2020). Photochemical mechanism of light-driven fatty acid photodecarboxylase. *ACS catalysis*, *10*(12), 6691-6696.

[68] Collados, R., Andreu, V., Picorel, R., & Alfonso, M. (2006). A light-sensitive mechanism differently regulates transcription and transcript stability of ω3 fatty-acid desaturases (FAD3, FAD7 and FAD8) in soybean photosynthetic cell suspensions. *FEBS letters*, *580*(20), 4934-4940.

[69] Los, D. A., & Murata, N. (1998). Structure and expression of fatty acid desaturases. *Biochimica et Biophysica Acta (BBA)-Lipids and Lipid Metabolism*, *1394*(1), 3-15.

[70] Ho, S. H., Chan, M. C., Liu, C. C., Chen, C. Y., Lee, W. L., Lee, D. J., & Chang, J. S. (2014). Enhancing lutein productivity of an indigenous microalga *Scenedesmus obliquus* FSP-3 using light-related strategies. *Bioresource technology*, *152*, 275-282.

[71] Fu, W., Guðmundsson, Ó., Paglia, G., Herjólfsson, G., Andrésson, Ó. S., Palsson, B. Ø., & Brynjólfsson, S. (2013). Enhancement of carotenoid biosynthesis in the green microalga *Dunaliella salina* with light-emitting diodes and adaptive laboratory evolution. *Applied microbiology and biotechnology*, *97*, 2395-2403.

[72] Sharmila, D., Suresh, A., Indhumathi, J., Gowtham, K., & Velmurugan, N. (2018). Impact of various color filtered LED lights on microalgae growth, pigments and lipid production. *European Journal of Biotechnology and Bioscience*, *6*(6), 1-7.

[73] Bohne, F., & Linden, H. (2002). Regulation of carotenoid biosynthesis genes in response to light in *Chlamydomonas reinhardtii*. *Biochimica et Biophysica Acta (BBA)-Gene Structure and Expression*, *1579*(1), 26-34.

[74] Adil, A. M., & Ko, Y. (2016). Socio-technical evolution of Decentralized Energy Systems: A critical review and implications for urban planning and policy. *Renewable and Sustainable Energy Reviews*, *57*, 1025-1037.

[75] Li, D., Liu, G., & Liao, S. (2015). Solar potential in urban residential buildings. *Solar Energy*, *111*, 225-235.

[76] Ramos, A., Chatzopoulou, M. A., Guarracino, I., Freeman, J., & Markides, C. N. (2017). Hybrid photovoltaic-thermal solar systems for combined heating, cooling and power provision in the urban environment. *Energy conversion and management*, *150*, 838-850.

[77] Aßmus, E., Weller, B., Walter, F., & Kerner, M. (2018). Fassadenelemente einer Bioenergiefassade–Entwicklung eines Prototyps. *ce/papers*, *2*(1), 211-220.

[78] Kerner, M. (2017, January). Anaerobic domestic waste water treatment coupled to a bioreactor facade for the production of biogas, heat and biomass. In *Powerskin Conference: proceedings*.

[79] Olabi, A. G., Shehata, N., Sayed, E. T., Rodriguez, C., Anyanwu, R. C., Russell, C., & Abdelkareem, M. A. (2022). Role of microalgae in achieving sustainable development goals and circular economy. *Science of The Total Environment*, 158689.

[80] Vereinte Nationen (2023). Ziele für nachhaltige Entwicklung. Online verfügbar unter https://unric.org/de/17ziele/, 22.02.2023.

[81] Oliveira, C. Y. B., Jacob, A., Nader, C., Oliveira, C. D. L., Matos, Â. P., Araújo, E. S., Shabnam, N., Ashok, B., & Gálvez, A. O. (2022). An overview on microalgae as renewable resources for meeting sustainable development goals. *Journal of Environmental Management*, *320*, 115897.

[82] Vindel, J. M., Trincado, E., & Sánchez-Bayón, A. (2021). European union green deal and the opportunity cost of wastewater treatment projects. *Energies*, *14*(7), 1994.

[83] Kerner, M. (2017). Entwicklung semitransparenter Photovoltaikmodule für gebäudeintegrierte Hybridsysteme aus Photosynthese und Photovoltaik zur komplementären Nutzung des Sonnenlichts. *Projektantrag SSC (Strategic Science Consult) GmbH*.

[84] Osterthun, N., Neugebohrn, N., Gehrke, K., Vehse, M., & Agert, C. (2021). Spectral engineering of ultrathin germanium solar cells for combined photovoltaic and photosynthesis. *Optics Express*, *29*(2), 938-950.

[85] Reich, M., Hannig, C., Al-Ahmad, A., Bolek, R., & Kümmerer, K. (2012). A comprehensive method for determination of fatty acids in the initial oral biofilm (pellicle). *Journal of lipid research*, *53*(10), 2226-2230.

[86] Van Heukelem, L., & Thomas, C. S. (2001). Computer-assisted high-performance liquid chromatography method development with applications to the isolation and analysis of phytoplankton pigments. *Journal of Chromatography A*, *910*(1), 31-49.

[87] Sandmann, G. (1991). Light-dependent switch from formation of poly-cis carotenes to all-trans carotenoids in the *Scenedesmus mutant* C-6D. *Archives of microbiology*, *155*, 229-233.

[88] Niyogi, K. K., Björkman, O., & Grossman, A. R. (1997). The roles of specific xanthophylls in photoprotection. *Proceedings of the National Academy of Sciences*, *94*(25), 14162-14167.

[89] Abomohra, A. E. F., Wagner, M., El-Sheekh, M., & Hanelt, D. (2013). Lipid and total fatty acid productivity in photoautotrophic fresh water microalgae: screening studies towards biodiesel production. *Journal of applied phycology*, *25*, 931-936.

[90] Kis, M., Zsiros, O., Farkas, T., Wada, H., Nagy, F., & Gombos, Z. (1998). Light-induced expression of fatty acid desaturase genes. *Proceedings of the National Academy of Sciences*, *95*(8), 4209-4214.

[91] Krienitz, L., Ustinova, I., Friedl, T., & Huss, V. A. (2001). Traditional generic concepts versus 18S rRNA gene phylogeny in the green algal family Selenastraceae (Chlorophyceae, Chlorophyta). *Journal of phycology*, *37*(5), 852-865.

[92] Osterthun, N., Helamieh, M., Berends, D., Neugebohrn, N., Gehrke, K., Vehse, M., Kerner, M., & Agert, C. (2021, June). Influence of spectrally selective solar cells on microalgae growth in photo-bioreactors. In *AIP Conference Proceedings* (Vol. 2361, No. 1, p. 070001). AIP Publishing LLC.

[93] Cordero, B. F., Obraztsova, I., Couso, I., Leon, R., Vargas, M. A., & Rodriguez, H. (2011). Enhancement of lutein production in *Chlorella sorokiniana* (Chorophyta) by improvement of culture conditions and random mutagenesis. *Marine drugs*, *9*(9), 1607-1624.

[94] Falciatore, A., & Bowler, C. (2005). The evolution and function of blue and red light photoreceptors. *Current topics in developmental biology*, *68*, 317-350.

[95] Paul, K. N., Saafir, T. B., & Tosini, G. (2009). The role of retinal photoreceptors in the regulation of circadian rhythms. *Reviews in endocrine and metabolic disorders*, *10*, 271-278.

7 Anhang

7.1 Wachstumsbedingungen der Versuche mit *Brassica napus* L.

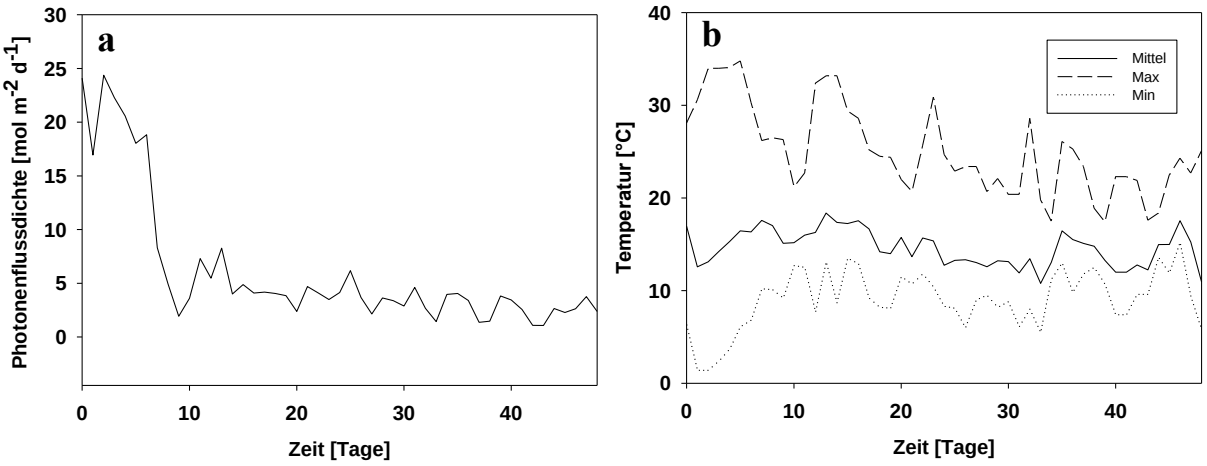

Abbildung 9: Wachstumsbedingungen der Versuche mit *Brassica napus* L.. Dargestellt sind die summierten täglichen Photonenflüsse (a) sowie die Temperaturdaten (b) der Rapsversuche im Zeitraum vom 17.09.-2020-05.11.2020. Mittel (Mittlere Temperatur), Max, (Maximale Temperatur) und Min (Minimale Temperatur).

8 Publikationen, die aus der Dissertation hervorgegangen sind

Publikation 1

Growth and Fatty composition of *Acutodesmus obliquus* under different light spectra and temperatures

Mark Helamieh; Annkathrin Gebhardt; Marco Reich; Friedericke Kuhn; Martin Kerner; Klaus Kümmerer

2021

Lipids, 56(5), 485-498.

DOI: 10.1002/lipd.12316

Received: 1 March 2021 | Revised: 1 June 2021 | Accepted: 9 June 2021

DOI: 10.1002/lipd.12316

ORIGINAL ARTICLE

AOCS WILEY

Growth and fatty acid composition of *Acutodesmus obliquus* under different light spectra and temperatures

Mark Helamieh[1,2] | Annkathrin Gebhardt[2] | Marco Reich[1] | Friedericke Kuhn[3] | Martin Kerner[2] | Klaus Kümmerer[1]

[1]Institute of Sustainable and Environmental Chemistry, Leuphana University of L neburg, L neburg, Germany

[2]Strategic Science Consult Ltd., Hamburg, Germany

[3]Institute of Experimental Business Psychology, Leuphana University of L neburg, L neburg, Germany

Correspondence
Mark Helamieh, Leuphana University of L neburg, Universitätsallee 1, 21335 L neburg, Germany.
Email: m.helamieh@ssc-hamburg.de; mark.helamieh@stud.leuphana.de

Abstract

The combined impact of temperature and light spectra on the fatty acid (FA) composition in microalgae has been sparsely investigated. The aim of this study was to investigate the interactions of light and temperature on the FA composition in Acutodesmus obliquus. For this purpose, A. obliquus was cultivated with different temperatures (20, 30, and 35°C), as well as broad light spectra (blue, green, and red light). Growth and FA composition were monitored daily. Microalgal FA were extracted, and a qualitative characterization was done by gas chromatography coupled with electron impact ionization mass spectrometry (GC-EI/MS). Compared to red light, green and blue light caused a higher percentage of the polyunsaturated fatty acids (PUFA) 16:4, 18:3, and 18:4, at all temperatures. The highest total percentage of these PUFA were observed at the lowest cultivation temperature and blue and green light. These data imply that a combination of lower temperatures and blue-green light (450–550 nm) positively influences the activity of specific FA-desaturases in A. obliquus. Additionally, a lower 16:1 trans/cis ratio was observed upon green and blue light treatment and lower cultivation temperatures. Remarkably, green light treatment resulted in a comparably high growth under all tested conditions. Therefore, a higher content of green light, compared to blue light might additionally lead to a higher biomass concentration. Microalgae cultivation with low temperatures and green light might therefore result in a suitable FA composition for the food industry and a comparably high biomass production.

KEYWORDS

blue-green light, cis-trans isomers, fatty acid desaturases, microalgae, polyunsaturated fatty acids

1 | INTRODUCTION

Microalgae are a group of photosynthetic microorganisms of high diversity (Metting, 1996). While adapting to various environments, plenty of bioactive substances have evolved (Metting, 1996; Pulz & Gross, 2004). Today, various microalgal substances e.g., antioxidants, carotenoids, as well as proteins, are of high importance in various sectors, such as pharmacy, cosmetic, and food industry (Pulz & Gross, 2004; Vanthoor-Koopmans et al., 2013). Due to the high fatty acid (FA) content, several microalgae species are also considered an interesting platform for a targeted FA production in the biofuel and food industry (Abomohra et al., 2013; Adarme-Vega et al., 2012; El-Sheekh et al., 2013). A high content of saturated fatty acids (SFA) is required for biofuel production, whereas a high content of polyunsaturated fatty acids (PUFA) is suitable for applications in the food industry (Piligaev

Abbreviations: CDW, cell dry weight; EI, electron impact; EPA, eicosapentanoic acid; FA, fatty acid; FAME, fatty acid methyl ester; GC, gas chromatography; IS, internal standard; MS, mass spectrometry; MUFA, monounsaturated fatty acids; PUFA, polyunsaturated fatty acids; RT, retention time; SFA, saturated fatty acids; SIM, selected ion monitoring.

et al., 2015; Riediger et al., 2009; Ruxton et al., 2004). Omega-3 FA such as linolenic acid (18:3), and the omega-6 FA, linoleic acid (18:2), are the basis for longer-chain PUFA, such as eicosapentanoic acid (EPA) and can be used as supplements for human diet (Brenna, 2002). Besides the degree of unsaturation, the ratio of these two FA is essential for healthy nutrition as well. Several diseases are caused by a high ratio of omega-6/omega-3 FA (Simopoulos, 2004). Another cause of adverse health effects are trans FA (Gebauer et al., 2007; Mozaffarian et al., 2006). Trans-isomers of unsaturated FA are naturally present in several microbial food products and in industrially processed vegetable oils, such as margarine (Dhaka et al., 2011; Kuhnt et al., 2011; Sommerfeld, 1983). Hence, to produce a suitable FA composition in microalgae for applications in the food or biofuel industry, a regulation of the FA metabolism during microalgae cultivation is of high importance.

It is well known that the FA metabolism in microalgae can be influenced by cultivation with selected parameters (Breuer et al., 2012; Mandotra et al., 2016). For instance, the total lipid content in microalgae can be raised by nitrogen-limiting conditions in the cultivation media. However, this results in reduced growth, which counterbalances the total lipid yield (El-Sheekh et al., 2013). More recent studies showed an elevation of the lipid content without compromising the microalgae growth (Abomohra et al., 2018, 2019, 2020; Abomohra & Almutairi, 2020; Almarashi et al., 2020; Esakkimuthu et al., 2020). For example, the utilization of phytohormones and the integration of seaweeds anaerobic digestate were shown to increase both growth and lipid production (Abomohra & Almutairi, 2020; Esakkimuthu et al., 2020). In a very novel approach, it was also shown, that a pretreatment of microalgae with low-dose cold atmospheric plasma (CAAP) resulted in an enhancement of growth and lipid content in *Chlorella vulgaris* (Almarashi et al., 2020). Variation of the cultivation temperature is another factor to influence the FA metabolism in microalgae. Beside the lipid content, also the degree of saturation and the FA composition can be influenced by the microalgae cultivation conditions. One of the underlying mechanisms of temperature adaptation in plants, microorganisms, and green algae is the modification of the degree of FA saturation to regulate the cell membrane fluidity (Alfonso et al., 2001; Collados et al., 2006; de Mendoza & Cronan Jr, 1983; Degraeve-Guilbault et al., 2021; Patterson, 1970).

Another important parameter to influence FA production in microalgae is light. It is known that light regulates the activity and triggers the expression of various FA-desaturases (Berestovoy et al., 2020; Collados et al., 2006; Kis et al., 1998). Most studies on microalgae had focused on the effect of the light intensity on biomass production and FA composition. However, the light spectrum can influence various metabolic processes in microalgae as well. Additional night illumination with colored light-emitting diodes was also shown to influence the fatty acid composition (Abomohra et al., 2019). Especially, blue light can trigger several enzymatic reactions in microalgae (Aparicio et al., 1994; Giráldez et al., 1998). It was also shown that exposure to green light increases the percentage of PUFA in *Chlorella vulgaris* (Hultberg et al., 2014) and the expression level of omega-3 desaturases in *Chlorella sp*. (Osman et al., 2018). Therefore, the influence of green, blue, and red light on the FA composition is subject to further investigation. Moreover, there is only little knowledge about the combined effects of temperature and light spectrum on the FA composition in microalgae.

This study aims to investigate the combined impact of the light spectrum and temperature on the FA composition in *Acutodesmus obliquus*. The green microalga *A. obliquus* was chosen due to its beneficial FA profile and high growth rate (Abomohra et al., 2013; El-Sheekh et al., 2013; Hindersin et al., 2013). In order to evaluate the growth and FA profile, *A. obliquus* was cultivated at 20, 30, and 35°C in three successive experiments. In all experiments, the cultivation tubes were irradiated with red light, blue light, and green light. Produced biomass of *A. obliquus* was assessed and the FA profile was analyzed by gas chromatography coupled with electron impact ionization mass spectrometry (GC-EI/MS). It could be shown that temperature and light spectrum have a major impact on the FA composition in *A. obliquus*.

2 | MATERIALS AND METHODS

2.1 | Chemicals

The cultivation medium for *A. obliquus* was composed of Flory Basis Fertilizer 1 (Euflor, Germany) and KNO_3 (Fisher Scientific, Germany) and kept at a pH of 7.0 ± 0.5 with the usage of HCl (Fisher Scientific, Germany) and NaOH (Fisher Scientific, Germany). Culture medium was prepared in distilled water for all cultivation experiments. The internal standard (IS), heptadecanoic acid (17:0) was purchased from Sigma Aldrich (Taufkirchen, Germany). Hydrochloric acid, chloroform, methanol, and n-hexane for the FA extractions were purchased from Carl Roth (Karlsruhe, Germany) in GC ultragrade.

2.2 | Microalgae preparation

The microalgae strain *A. obliquus* (No. U169) from the Microalgae and Zygnematophyceae Collection Hamburg (MZCH, previously SVCK) microalgae collection

of the University of Hamburg was used. Microalgae precultivations were done in Schott flasks at 25°C and a constant photon flux density of 150 μmol m^{-2} s^{-1} emitted by a Sylvania T9 circline, 32 W fluorescent tube with a white light spectrum. The precultures were aerated with CO_2-enriched air (5% v/v) and stirred by using a magnetic stirrer. The cultivation medium was composed of 2 g L^{-1} Flory Basis I (Euroflor, Germany) and 3.22 g L^{-1} KNO_3 and kept at a pH of 7 ± 0.5 daily by manual adjustment. Cell dry weight (CDW) was determined gravimetrically, and a correlation of CDW and optical density at 750 nm (OD_{750}) was set up for each experiment from different dilution steps of the culture of each respective experiment (Chen et al., 2012; Girard et al., 2014; Reymann et al., 2020). The defined volume was filtered, subsequently dried at 80°C for 24 h and the measured CDW was set into relation with the respective OD_{750}. It was previously tested that the filters kept constant weight after 3–8 h, depending on the applied biomass.

2.3 | Cultivation device

Cultivation experiments were performed in glass tubes of a length of 490 mm and a diameter of 40 mm each holding a volume of 350 ml. Up to 12 glass tubes were submerged into a transparent acrylic glass water bath and kept in a vertical position in black acrylic brackets. These brackets prevented ambient light from reaching the tubes from the back and the sides. All tubes were irradiated from the front side of the water bath with metal halide lamps (Philips MSR HR CT, 575 W), which emit a sun-like light spectrum (Figure 1a). Different light spectra were generated by optical filter foils: light red, dark green, and dark blue (LEE-Filters, England) which were fixed to the outer front side of the water bath. The resulting spectra of the metal halide lamps, and the LEE filters were measured and adjusted to an equal photon flux density, respectively (Figure 1b–d, Table 1). Absolute photon fluxes were determined by a UV–Vis spectrometer (BLACK-Comet, StellarNET, Tempa, USA) within a range of λ = 400–700 nm.

2.4 | Experimental conditions

Pre-cultures were diluted to an OD_{750} of 0.2 for each experiment, which was determined by a UV/VIS spectrometer (Pharmacia LKB Ultrospec III). The cultivation was started with a volume of 350 ml of microalgae suspension. Microalgal growth was monitored via the OD_{750}, which was measured directly after sampling. The CDW was calculated from the OD_{750} by using the coefficient determined from the linear correlation between OD_{750} and CDW:

$$CDW = 0.5246 \times OD_{750} - 0.0464.$$

After inoculation, batch cultivation started in triplicates for a duration of 96 h. The microalgae were irradiated constantly with a photon flux density of 480 μmol m^{-2} s^{-1} ± 51 μmol m^{-2} s^{-1} at all experiments of different wavebands (Figure 1b–d and Table 1). The microalgae suspension was mixed by aeration with humidified and CO_2-enriched air (5% v/v) and an airflow of 0.2 L min^{-1}. The temperature in the water bath was kept at 20°C ± 0.5°C, 30°C ± 0.5°C, and 35°C ± 0.5°C by a chiller (AD15R-30, VWR European) in three successive experiments (Table 1). The pH was kept at pH 7 ± 0.5 manually and adjusted daily by the addition of 1 M HCl or 1 M NaOH. Samples for the FA analysis were taken from the preculture. After the cultivation was started, samples were taken after 1, 3, 6, 24, 48, 72, and 96 h of cultivation. For the GC–MS measurements, 3–20 ml samples were taken, depending on the biomass concentration, and subsequently stored at −80°C prior to analysis.

2.5 | Sample preparation and FA analysis

Samples were thawed, homogenized, and the volume of microalgae suspension, containing 0.0025 g CDW, determined via OD_{750} -CDW-correlation, was used for the FA-extraction. Heptadecanoic acid was used as IS and a stock solution of 1.0 mg ml^{-1} was prepared. The samples were centrifuged at 5137*g* for 20 s (Rotanta 460R, Hettich Zentrifugen, Tuttlingen, Germany), the supernatant was discarded, and 20 μmol of the IS stock solution dissolved in hexane were added to the pellet. A modified Folch extraction (Reich et al., 2012, 2013), in which the pellet was resuspended in a $CHCl_3$ /MeOH mixture (2:1, v/v), was applied. Upon full resuspension, the samples were shaken at 200 rpm (IKA HS 501 digital, Jahnke and Kunkel and Co IKA Labortechnik, Staufen, Germany) for 1 h. Afterward, they were centrifuged for 20 s at 5137*g* (Rotanta 460R, Hettich Zentrifugen, Tuttlingen, Germany), and the supernatant containing the extracted lipids was collected in a glass tube. This procedure was repeated twice with shaking times of 3 and 12 h. Previous test extractions showed highest FA yields with three extraction steps. In a further extraction, less than 0.1% of extracted FA of the first three extractions were found. The supernatants, containing virtually all extractable lipids were all transferred and collected in one glass tube, and the solvents were evaporated under a constant and gentle stream of nitrogen. The transesterification was performed according to the method of Ichiara and Fukubayashi (Ichihara & Fukubayashi, 2010). The dried lipid extracts

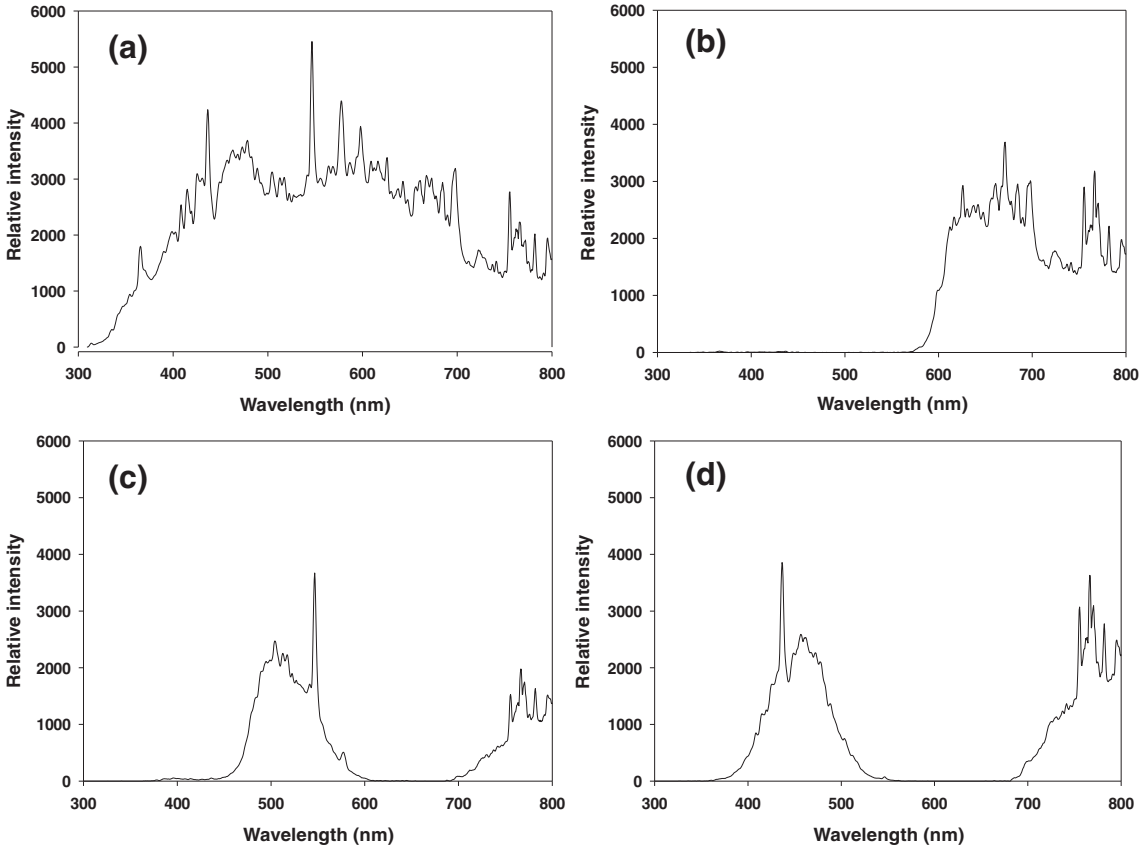

FIGURE 1 The light spectrum of the MSR 575 HR CT metal halide lamp. Unfiltered (a); in combination with the optical foils: light red (b); dark green (c), and dark blue (d) (Lee filters, England). The relative emission spectra ($J_{\lambda,rel}$ in counts) were determined by a UV–vis spectrometer (BLACK-comet, StellarNET, Tempa, USA) within a range of $\lambda = 300$ to 800 nm (integration time = 10 ms)

TABLE 1 Test conditions during the different experiments

Experiment	Conditions	Red light	Green light	Blue light
1	Temperature (°C)	20 ± 0.5	20 ± 0.5	20 ± 0.5
	Photon flux (μmol m^{-2} s^{-1})	469 ± 51	487 ± 27	482 ± 7
2	Temperature (°C)	30 ± 0.5	30 ± 0.5	30 ± 0.5
	Photon flux (μmol m^{-2} s^{-1})	469 ± 51	487 ± 27	482 ± 7
3	Temperature (°C)	35 ± 0.5	35 ± 0.5	35 ± 0.5
	Photon flux (μmol m^{-2} s^{-1})	469 ± 51	487 ± 27	482 ± 7

Note: The temperatures and the estimated accuracies of measurement. Values for the photon fluxes represent means ± standard deviation of triplicates.

were resuspended in 0.2 ml of chloroform, 2 ml of methanol were added, and acidified with 0.1 ml of concentrated hydrochloric acid (35% w/w). This solution was transferred into a screw-capped glass tube, overlaid with nitrogen, and the tube was tightly closed. Upon vortexing, the tube was heated to 100°C for 1 h and subsequently cooled down at room temperature for 10 min. In order to extract the fatty acid methyl esters (FAME), 2 ml of hexane and 2 ml of water were added, the tube was vortexed, and the hexane phase was collected after phase separation. This solution was diluted 1:10 with hexane, of which 1 μl was injected for GC–MS analysis.

2.6 | Instrumental conditions (GC)

GC/EI-MS was performed with a Thermo Scientific™ ISQ™ 7000 Single Quadrupole GC–MS system. The samples (1 μl) were injected with an autosampler, and the injector was operated in splitless mode and kept at 260°C. For the separation of the target compounds, a TRACE™ TR FAME fused silica capillary column (0.25 mm, 0,25 μm × 30 m) with helium as carrier gas was used with a constant pressure of 100 kPa and a flow of 1,5 ml min^{-1}. The oven temperature was set to start at 60°C for 1 min, followed by a ramp rate of 6.5°C min^{-1} until the final temperature of 260°C was

reached and then held for 8 min. The electron energy was 70 eV, the ion source was set to 270°C, and the mass range of m/z 60–400 was recorded in the full scan mode. Fragment ions included m/z 74, m/z 79, m/z 81, and m/z 87 for the FAME that were detected during the measurement in the GC/EI-MS selected ion monitoring (SIM) mode (Reich et al., 2013). A chromatogram with retention times (RT) of the identified FA is shown in Figure 2.

2.7 | Data evaluation

The mass spectra and the RT were used for the qualitative analysis of the separated FAME. The peak area ratio of the identified FAME was set into relation with the respective area of the IS, and the share of each FA (in %) was calculated. All samples were taken and measured in triplicates, and the mean values ± standard deviation were calculated.

Additionally, to the in-depth descriptive analysis and visualization of the data, analysis of variance with repeated measures were conducted to examine statistical effects of the light spectrum on the CDW, the percentage of the FA 16:4, 18:3, 18:4, and the isomers of the FA 16:1.

As the samples were taken in triplicates, degrees of freedom for statistical analyses were limited. Missing values were replaced with means of existent values. The individual samples were randomly grouped to test the effect of light spectrum on the dependent variables in a within-subjects design. As such sufficient data were obtained to test assumptions for a repeated-measures ANOVA and the analysis was conducted respectively. In the interpretation of results, the focus lies on the spectral effects on dependent variables, and not on conclusions on the growth. For statistical inference, conservative measures of Greenhouse–Geisser corrected values due to the small sample size are reported. Furthermore, measures included in the ANOVA concerned the measurement timepoints after 24, 48, and 96 h of cultivation.

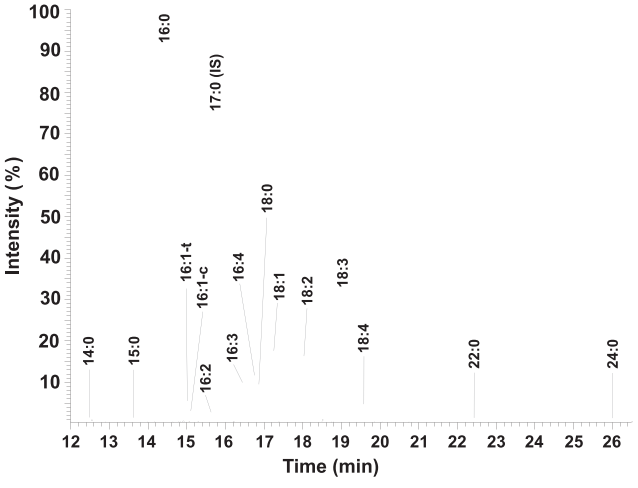

FIGURE 2 GC/MS chromatogram of *Acutodesmus obliquus* acquired in SIM mode. The sample was taken after 5 days of cultivation with 150 μmol m^{-2} s^{-1} white light at 25°C

3 | RESULTS

3.1 | Microalgal growth

The biomass concentration was determined daily for the whole cultivation period (Figure 3a–c). The light spectrum strongly influenced the growth patterns of *A. obliquus*. In all experiments, the red light regime resulted in the highest increase of biomass after 96 h of cultivation. A maximum of 2.42 g L^{-1} CDW was observed after 96 h cultivation at 30°C and under red light (Figure 3b).

Blue light treatment resulted in the lowest amount of produced CDW at all tested temperatures. Irradiation with blue light resulted in a 34.3%–36.8% reduced biomass production in 96 h compared to red light, in all experiments (Figure 3a–c). Biomass production under green light was higher than under blue light, but still 11.6%–16.8% lower than under red light (Figure 3a–c). Nevertheless, the green light regime resulted in a relatively high amount of produced biomass. The highest CDW was measured for all spectra at a temperature of 30°C (Figure 3b). In comparison, the maximum CDW were decreased by 21.1% at 20°C and 12.4% at 35°C, after 96 h cultivation (Figure 3a,c).

Results of the main ANOVA further show that the main effect of light spectrum on the CDW was highly significant with large effect sizes across all temperature conditions. The effect of the light spectra on CDW was highest at 35°C at $F(1.1; 2.1) = 68.8$ at $p = 0.01$ with a large effect of partial $eta^2 = 0.98$. Within-subject contrasts show that CDW is significantly different under blue light condition than under red light condition under all temperature conditions. The difference is also significant for green and red light conditions at 35°C.

3.2 | Fatty acids

In this study, a total of 14 FA were identified in *A. obliquus*, which are shown in Figure 2 and Table 2. The FA 14:0, 15:0, 22:0, and 24:0 were always found in low share (<1%) and were therefore dismissed for further study. The cis/trans (c/t) isomers of unsaturated FA were summed up for the comparison of the relative FA relations. Strong variations of 16:1 (c/t) isomers were found, and the relative changes toward different test conditions are separately shown in Section 3.5.

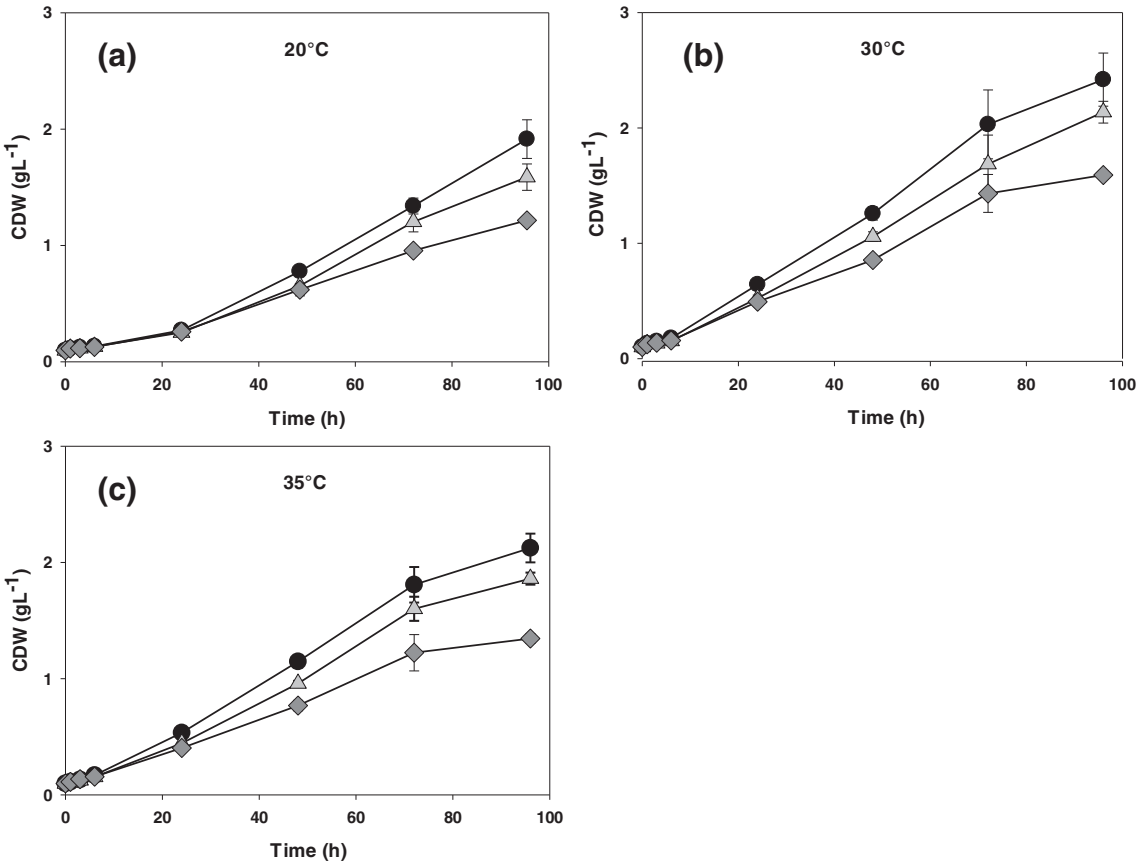

FIGURE 3 Biomass production of *Acutodesmus obliquus* exposed to 480 μmol m^{-2} s^{-1} red light (circle; 580–720 nm), green light (triangle; 450–600 nm), and blue light (diamonds; 380–540 nm) at 20°C (a), 30°C (b) and 35°C (c). The cell dry weight (CDW) was determined by a correlation with the optical density at 750 nm. Values represent means ± standard deviation of triplicates

TABLE 2 Fatty acid (FA) profile of Acutodesmus obliquus

FA	%	FA	%
14:0	≤1	$18:1^{\Delta9}$	7.8 ± 0.1
15:0	≤1	$18:2^{\Delta9,12}$	10.2 ± 0.1
16:0	38.2 ± 0.9	$18:3^{\Delta9,12,15}$	21.9 ± 0.5
$16:1^{\Delta9}$ -trans	1.4 ± 0.1	$18:4^{\Delta6,9,12,15}$	2.4 ± 0.1
$16:1^{\Delta9}$ -cis	1.1 ± 0.1	22:0	≤1
$16:2^{\Delta7,10}$	1.0 ± 0.1	24:0	≤1
$16:3^{\Delta7,10,13}$	5.2 ± 0.1	SFA	41.4
$16:4^{\Delta4,7,10,13}$	7.5 ± 0.2	MUFA	10.3
18:0	2.1 ± 0.2	PUFA	48.3

Note: The samples were taken after 5 days of cultivation with 150 μmol m^{-2} s^{-1} white light at 25°C. Values represent means ± standard deviation of triplicates.

3.3 | Effect of light spectrum on the degree of saturation

The light spectrum had a strong impact on the FA composition. In all experiments, red light caused a lower degree of desaturation, in comparison to blue and green light. The relative proportions of the 16:4, 18:3, and 18:4 FA decreased by up to 64% under a red light regime compared to green- and blue-light treatments (Figure 4a–c). Accordingly, the percentage of the lower desaturated FA increased (Figure 5b–d). These differences in the degree of desaturation were already detectable after 1 and 3 h of cultivation (data not shown). Nevertheless, it became evident in all experiments after 24 h of cultivation (Figures 4a–c, 5b–d, 6a–c and 7a–c). The SFA were not affected by the light spectrum (Figures 5a and 7d).

3.4 | Impact of temperature and light spectrum on the degree of saturation

In this study, a strong impact of the temperature on the degree of FA saturation of *A. obliquus* was observed. These temperature-triggered FA changes interacted with the aforementioned light related FA changes. The precultures of all experiments were cultivated at 25°C (see Section 2.2). The cultivation at 20°C resulted in a maximum increase of the PUFA 16:4, 18:3, and 18:4 by 37.9%, 32.8%, and 23.1% of the relative amounts, respectively

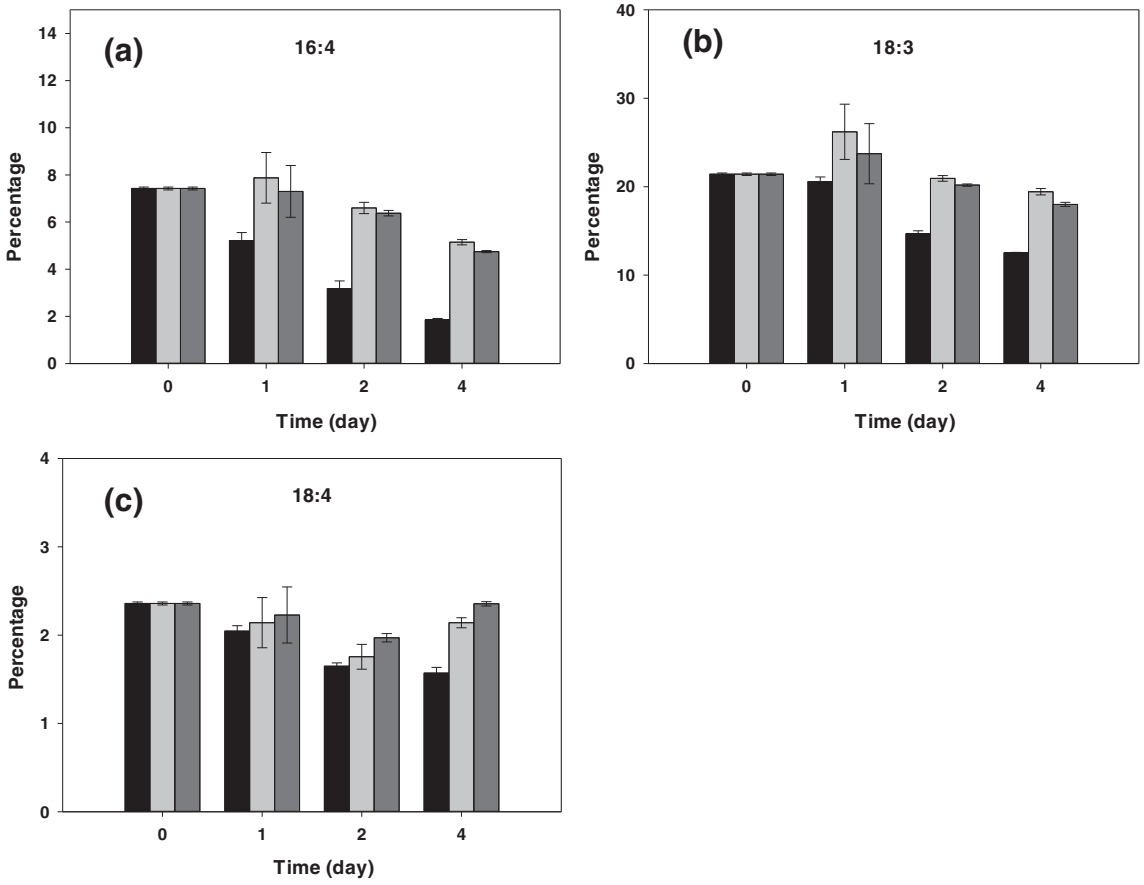

FIGURE 4 Relative proportions (%) of the fatty acids 16:4 (a), 18:3 (b) and 18:4 (c) in *Acutodesmus obliquus*, cultivated at a photon flux density of 480 μmol m^{-2} s^{-1} red light (black columns; 580–720 nm), green light (light gray colums, 450–600 nm), blue light (dark gray columns; 380–540 nm), and a temperature of 30°C. values represent means ± standard deviation of triplicates

(Figure 6a–c). However, this increase was significantly less expressed during cultivation under red light regime, compared to the blue- and green light groups (Figure 6a–c).

The cultivation at 30°C and red light resulted in a reduction of the PUFA 16:4, 18:3, and 18:4 after 96 h of cultivation by up to 74.97%, 41.55%, and 43.47% (Figure 4a–c), respectively. This decrease was significantly less expressed in the green and blue light groups (Figure 4a–c). Cultivation at 35°C resulted in a maximum decrease of 16:4, 18:3, and 18:4 by 75.57%, 35.51%, and 64.76%, respectively, after 96 h of cultivation with red light (Figure 7a–c). However, this temperature-triggered decrease was also less expressed under green as well as blue light at 35°C (Figure 7a–c). Still, this was not significant for all measured timepoints.

In summary, results show that exposure to red light and higher temperatures (30 and 35°C) resulted in lower relative shares of the PUFA 16:4, 18:3, and 18:4, whereas exposure to blue or green light and low temperatures (20°C) gave rise to elevated shares (Figures 4a–c, 6a–c and 7a–c). No impact of the light spectrum was found on the relative proportions of SFA. In contrast, high temperatures 35 and 30°C resulted in an elevation of the relative amounts of the FA 16:0 by up to 23.2% (35°C) and 11.7% (30°C) in the course of the experiment (Figures 5a and 7d). At a cultivation temperature of 20°C, the relative amount of the FA 16:0 was maintained at a level of the preculture (data not shown).

Repeated-measures ANOVA exposed a significant effect of the light spectrum on the FA 16:4, 18:3, and 18:4 across all temperature conditions. This effect was the largest at a temperature of 30°C, at $F(1.4; 2.8) = 308.4$ at $p = 0.001$ with a large effect size of partial $eta^2 = 0.99$. Furthermore, the differences in FA composition are significant for green light against red light conditions across all temperatures in the experiment. The FA composition under blue light significantly differed from that under red light under 20 and 30°C; however, there are no significant differences regarding the FA composition between red and blue light under 35°C.

3.5 | cis-trans isomerism of the fatty acid 16:1

Both cis and trans isomers of the FA 16:1 were identified in *A. obliquus*. The light spectrum and temperature

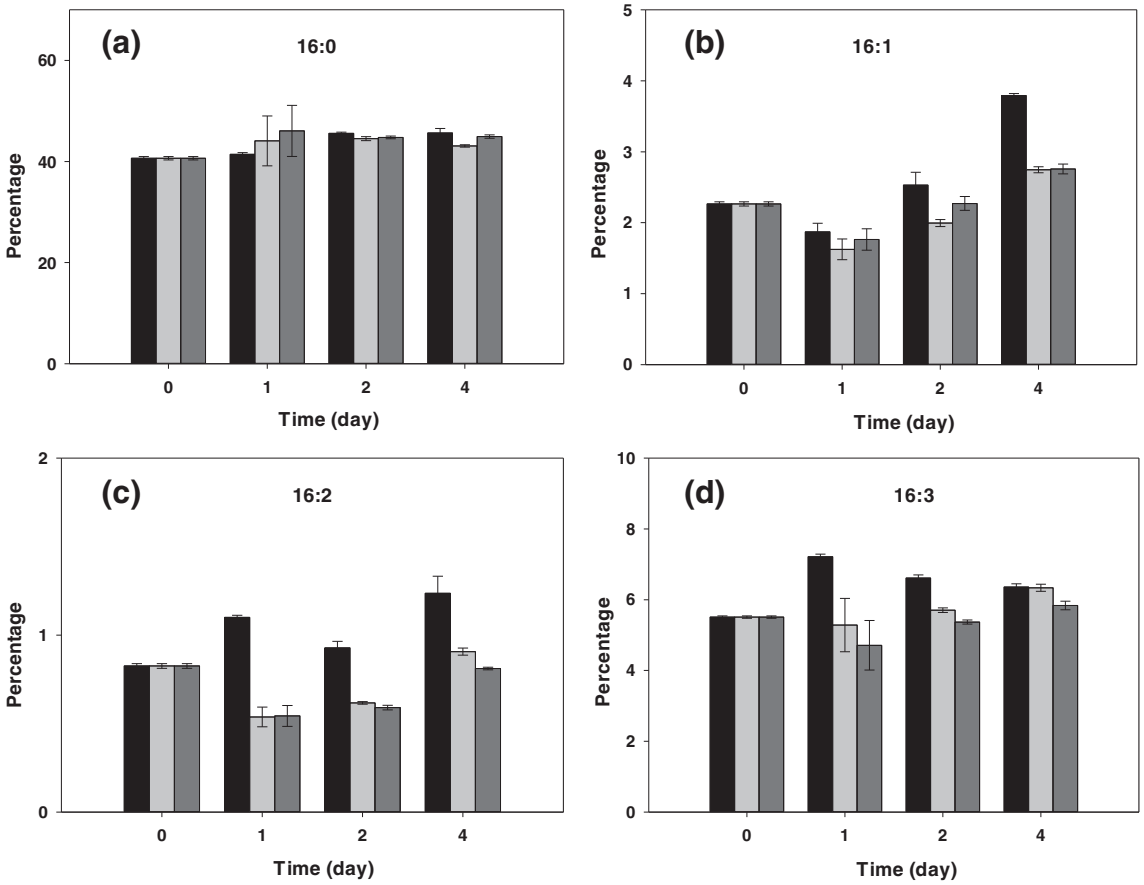

FIGURE 5 Relative proportions (%) of the fatty acids 16:0 (a), 16:1 (b), 16:2 (c), and 16:3 (d) in *Acutodesmus obliquus*, cultivated at a photon flux density of 480 μmol m^{-2} s^{-1} red light (black columns; 580–720 nm), green light (light gray columns; 450–600 nm), blue light (dark gray columns; 380–540 nm), and a temperature of 30°C. values represent means ± standard deviation of triplicates

had a strong impact on the 16:1 c/t ratio. A significant difference between samples irradiated with red light and the ones irradiated with green light was found (Figures 8 and 9). In contrast, no strong differences between the green light- and blue light-treated samples were observed, which is why the data of the blue light cultivations are not shown and discussed together with the green light cultivation data.

Results of the repeated-measures ANOVA show significant effects of the light spectrum on cis-trans isomerism of the FA 16:1 across all temperature conditions. Here, the effect was largest at 20°C with F (1;2) = 4629 at $p = 0.001$ with a larger effect size of partial $eta^2 = 1$. Within-subject contrasts show that these differences are significant for green light compared to red light conditions, and for blue light compared to red light conditions, across all temperatures in the experimental setup.

The relative percentage of the 16:1c increased from 44.4% in the preculture to 76.4% after 96 h of cultivation at 20°C in the blue and green light group (Figure 9b). However, no such increase was observed in the red-light group at the same temperature (Figure 9a). Upon cultivation with 35°C, the relative percentage of the 16:1c decreased from 42.8% in the preculture to 30.8%–33.2% for all tested spectra (Figure 8a,b). Over the time course of all experiments, the relative percentage of the 16:1c was significantly reduced in the red-light group, with respect to the green light- and blue light-treated samples (Figures 8a,b and 9a,b). Independent of the influences of temperature and light spectrum, a third effect was observed. In all experiments, a strong increase of the 16:1 c was evident in the first 24 h of cultivation (Figures 8a,b and 9a,b). In the first hours of cultivation, biomass concentration was always under 1 g L^{-1} (Figure 3a–c). In the following 72 h, the CDW in all experimental approaches increased to higher values, combined with a concomitant reduction of the relative percentage of the 16:1c isomers (Figures 3a-c, 8a,b and 9a,b). This leads to the conclusion that the 16:1c/t ratio is also influenced by the biomass concentration.

Presumably, the isomeric ratio changes are also influenced by temperature. While the maximum percentage of the 16:1 c was reached after 24–48 h of cultivation time with 20°C (Figure 9a,b), the maximum value of the 30°C cultivation was reached after 3–6 h (data not shown) and 1–3 h in the case of 35°C

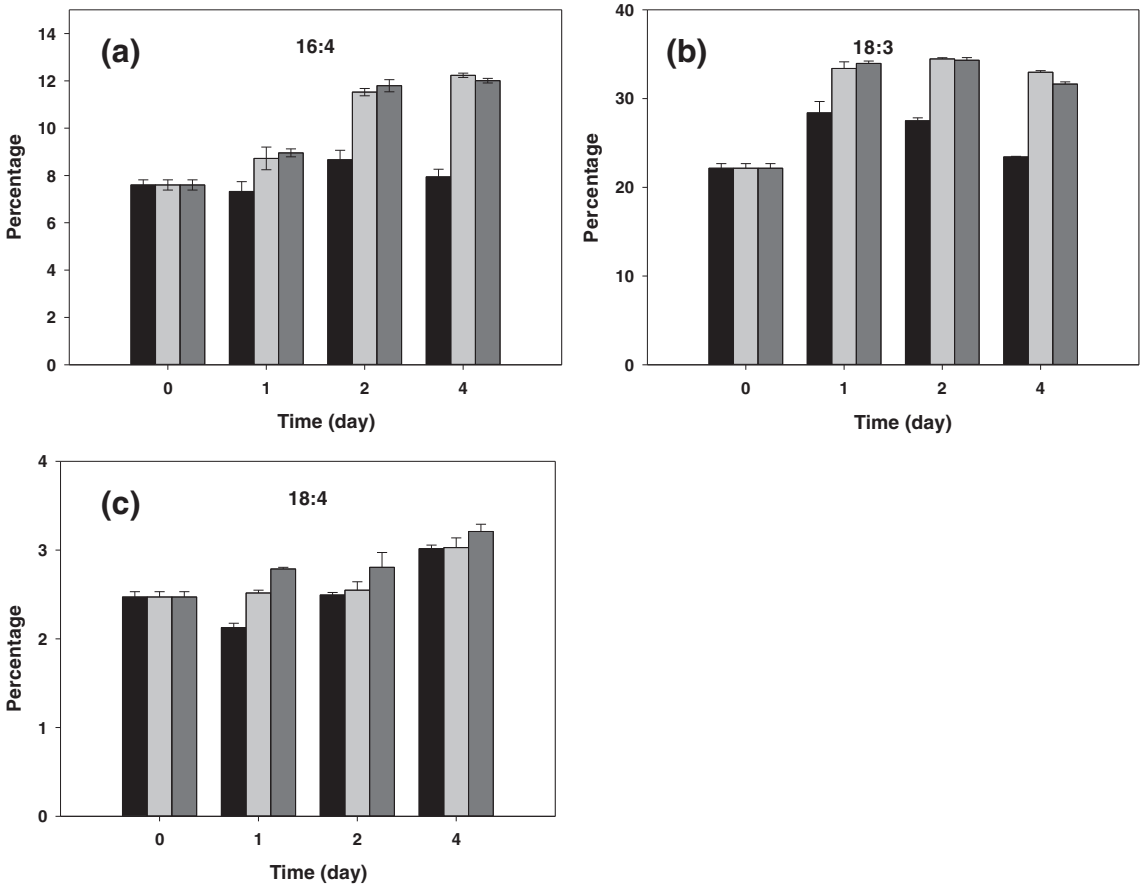

FIGURE 6 Relative proportions (%) of the fatty acids 16:4 (a), 18:3 (b), and 18:4 (c) in *Acutodesmus obliquus*, cultivated at a photon flux density of 480 μmol m^{-2} s^{-1} red light (black columns; 580–720 nm), green light (light gray columns; 450–600 nm), blue light (dark gray columns; 380–540 nm), and a temperature of 20°C. values represent means ± standard deviation of triplicates

(Figure 8a,b). In general, lower temperatures, blue-green light as well as a low biomass concentration resulted in a high relative percentage of 16:1c. In contrast, red light, higher temperatures, and higher biomass concentrations gave rise to a lower 16:1c/t ratio.

4 | DISCUSSION

In general, a maximum biomass of 2.42 g L^{-1} CDW was reached with a cultivation temperature of 30°C and red light (Figure 3b). This temperature is close to the optimum growth temperature for *A. obliquus* (Hindersin et al., 2013). The maximum of produced biomass was reduced by 21.1% and 12.4% at cultivation temperatures of 20 and 35°C, compared to the 30°C cultivation (Figure 3a–c). Among all tested temperatures, the maximum of produced biomass for *A. obliquus* was observed under red-light conditions (Figure 3a–c). The red light spectrum, (wavelength between 600 and 700 nm, Figure 1b), is effectively absorbed by the main photosynthesis pigments in microalgae (Sandmann, 1991). Therefore, the growth results might be related to the high absorption of these wavebands by chlorophyll a. The utilized blue light has a high overlap with the chlorophyll a absorption maximum at 430 nm (Figure 1d). Nevertheless, blue light regime caused the lowest amounts of produced biomass of all tested light spectra at all tested temperatures (Figure 3a–c). Beside chlorophyll a, carotenoids and xanthophylls also absorb light at this waveband in *A. obliquus* (Niyogi et al., 1997). These pigments mainly convert light energy into heat and, therefore, may reduce the contribution of this waveband to the biomass production (Wilhelm et al., 1985). This can provide an explanation for the low performance under blue light regime. Contrary to common assumptions, green light treatment resulted in a relatively high amount of produced biomass at all tested temperatures. A comparably high biomass production was reached with green compared to red light (Figure 3a–c). Due to the low absorption of this waveband, many studies on microalgae postulate that green light only has a low contribution to biomass production in microalgae (Kim et al., 2013, 2014). However, more recent studies have shown that light spectra that are weakly absorbed by microalgae can outperform all other light spectra in biomass productivity

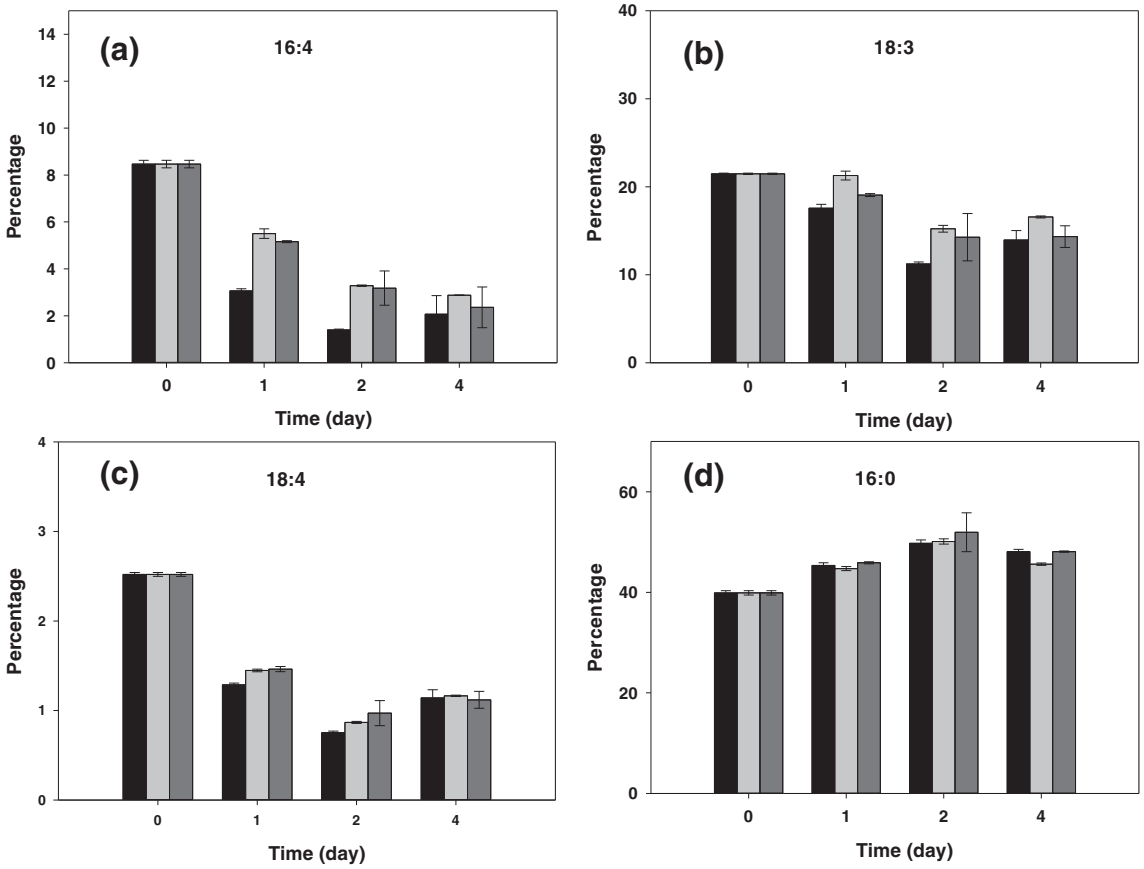

FIGURE 7 Relative proportions (%) of the fatty acids 16:4 (a), 18:3 (b), 18:4 (c) and 16:0 (d) in *Acutodesmus obliquus*, cultivated at a photon flux density of 480 μmol m^{-2} s^{-1} red light (black columns; 580–720 nm), green light (light gray columns; 450–600 nm), blue light (dark gray columns; 380–540 nm), and a temperature of 35°C. values represent means ± standard deviation of triplicates

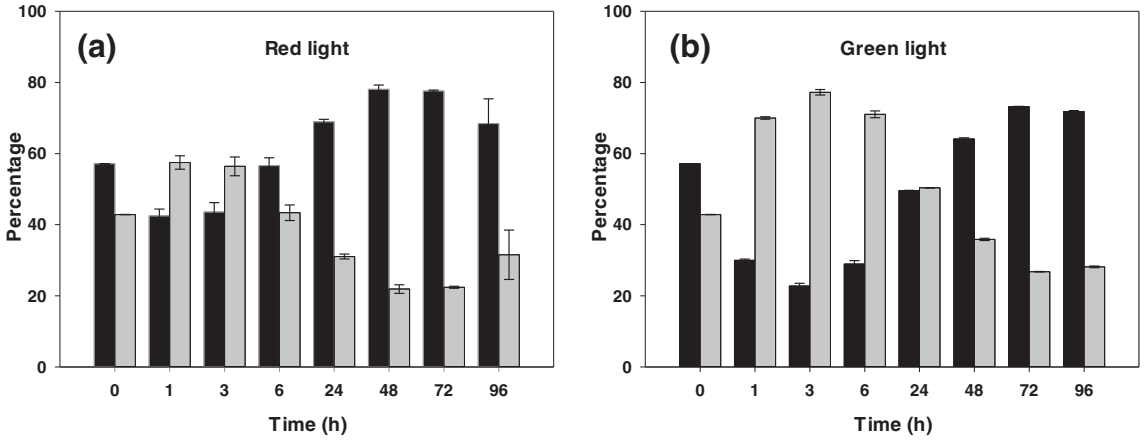

FIGURE 8 Relative amounts of the 16:1 trans (black columns) and 16:1 cis (gray columns) isomers in *Acutodesmus obliquus* after cultivation at a photon flux density of 480 μmol m^{-2} s^{-1} red light (580–720 nm) (a), green light (450–600 nm) (b), and a temperature of 35°C. values represent means ± standard deviation of triplicates

(Mattos et al., 2015; de Mooij et al., 2016; Ooms et al., 2017). In another study on the green microalga *Scenedesmus bijuga*, green light treatment resulted in the highest biomass production of all tested light spectra (Mattos et al., 2015). Due to the close phylogenetical relation of *A. obliquus* and *Scenedesmus bijuga*, it might be reasonable to compare the growth results of this species with the ones received for *A. obliquus* in this study. Additionally, the tests in both studies were performed with a similar

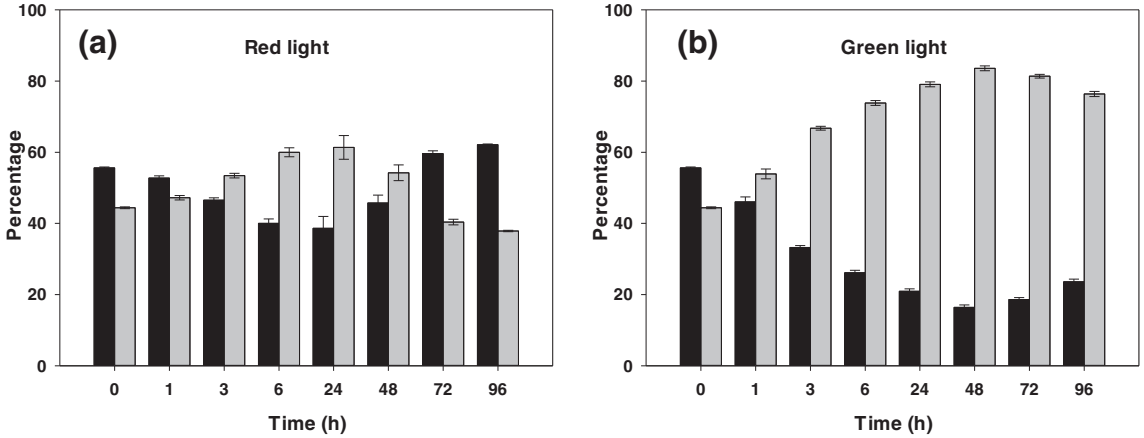

FIGURE 9 Relative amounts of the 16:1 trans (black columns) and 16:1 cis (gray columns) isomers in *Acutodesmus obliquus* upon cultivation at a photon flux density of 480 μmol m^{-2} s^{-1} red light (580–720 nm) (a), green light (450–600 nm) (b), and a temperature of 20°C. values represent means ± standard deviation of triplicates (a)

photon flux density. In both cases, the green light spectrum between 500 and 600 nm was shown to have a strong contribution to microalgal growth, because green light penetrates deeper into plant leaves and microalgae suspensions, which results in a dilution of the light energy and more efficient light into biomass conversion (Clark & Lister, 1975; de Mooij et al., 2016; Mattos et al., 2015; Ooms et al., 2017; Sun et al., 1998). Especially under conditions of high-density of the microalgae cultures and high light intensities, weakly absorbed wavebands can outperform blue and red light, in terms of photosynthetic efficiency (de Mooij et al., 2016; Mattos et al., 2015; Ooms et al., 2017). Additionally, green light irradiation causes shade avoidance responses in plants (Zhang et al., 2011). Recent findings in the FA profile of *Chlorella vulgaris* hint toward a compensatory increase of the chloroplasts and thylakoid membranes, upon green light treatment (Hultberg et al., 2014). This increase of the light harvesting structures might also be a shade avoidance effect and could contribute to a more efficient use of weakly absorbed wavebands in microalgae. Thus, our data support new findings in microalgae research, which postulate a high contribution of green light to the biomass production under certain conditions.

In this study, 14 FA were identified in *A. obliquus*. This FA composition is in accordance with previous analyses of the same strain (Abomohra et al., 2013). It could be shown that lower cultivation temperatures resulted in a lower degree of FA unsaturation in *A. obliquus*. The relative percentage of the PUFA 16:4, 18:3, and 18:4 were highest at a cultivation temperature of 20°C, and decreased with higher temperatures (30 and 35°C) (Figures 6a–c, 4a–c and 7a-c). It is well known that many organisms raise their degree of FA unsaturation at lower temperatures in order to maintain the cell membrane fluidity (Alfonso et al., 2001; Collados et al., 2006; de Mendoza & Cronan Jr, 1983; Degraeve-Guilbault et al., 2021; Patterson, 1970). Our data suggest that these temperature-triggered changes of FA unsaturation in *A. obliquus* are performed by the ratio change of the FA 16:4, 18:3, and 18:4 and lower desaturated FA. PUFA in plants, algae, and cyanobacteria are synthesized sequentially by specific FA-desaturases from FA of lower degree of desaturation (Cherif et al., 1975; Kis et al., 1998). Furthermore, it was observed that some of these specific FA-desaturases are regulated by light (Collados et al., 2006; Kis et al., 1998). Therefore, we assumed that the FA-desaturases that catalyze the desaturation of the 18:2 and 16:3, in *A. obliquus* are regulated by a combination of light color and temperature. We suggest that the activity of these specific FA-desaturases is positively regulated by a combination of blue-green light and lower temperatures. This seems to be an explanation for the higher ratio of the FA 16:4, 18:3, and 18:4 toward lower desaturated FA, at blue and green light treatment and lower temperatures.

Notably, red-light regime always resulted in the lowest relative shares of the PUFA 16:4, 18:3, and 18:4 and thus an overall lower degree of FA unsaturation at all tested temperatures (Figures 4a-c, 6a–c, and 7a–c). These light-spectrum-triggered changes in the FA composition, indicate that blue-green light is required for the temperature-related FA adaptations in *A. obliquus*, presumably by activation of FA-desaturases. Furthermore, enzymes are already known to be activated by blue and green light in the microalga *Monoraphidium braunii* (Aparicio & Qui ones, 1991). However, little is known about the influence of FA-desaturases by different light spectra. Merely, one very recent study showed an elevated expression level of omega-3 desaturases upon green light treatment in *Chlorella sp*. (Osman et al., 2018). Our experimental setup provides an opportunity to detect the spectral response waveband of the light receptor. Compared to red light, blue and green

light treatment generally resulted in a higher degree of FA unsaturation in *A. obliquus*. The used blue and green light spectra share a waveband between 450 and 550 nm, whereas the used red light comprised light wavelengths higher than 570 nm (Figure 1b–d). Therefore, one can conclude that the FA-desaturases in *A. obliquus* are most likely influenced or even activated by the light waveband between 450 and 550 nm.

Not only the FA composition but also the cis/trans ratio of the FA 16:1 was influenced by the parameters light and temperature. To the authors best knowledge, these effects on the isomeric composition of the FA composition in microalgae have never been discussed in literature before. Blue-green light treatment and lower cultivation temperatures gave rise to a higher 16:1 cis/trans ratio. Furthermore, a higher 16:1 cis/trans ratio was found in the first hours of cultivation (Figure 8 and Figure 9). This might be related to a higher relative light exposition at this time of the cultivation. Due to the low CDW in the first 24 h of cultivation, intershading effects of the microalgae were minimal (Figure 3a–c). Light intensity might therefore also contribute to 16:1 cis/trans ratio changes in *A. obliquus*. The FA 16:1 can be further desaturated to FA of higher degree of desaturation, by specific FA-desaturases (Cherif et al., 1975). One explanation for these isomeric changes might be therefore an enzymatic discrimination of one isomer by these specific FA-desaturases, which results in the 16:1 cis/trans ratio changes. This would explain the accelerated ratio changes at high cultivation temperatures, compared to lower cultivation temperatures (Figures 8 and 9). Up to a certain temperature, enzymatic reactions are catalyzed faster at higher temperatures (Holleman & Wiberg, 2007).

In summary, the right choice of cultivation parameters can influence the FA composition in *A. obliquus*. A tailored light spectrum, with a high content of green light between 500 and 600 nm and a low cultivation temperature might, therefore, be a new approach to combine a high biomass production with a suitable FA composition for the food industry. Conversely, a reduced degree of FA unsaturation is a beneficial feature for FA in the biofuel production. In this case, a high cultivation temperature and red light treatment can promote a suitable FA composition in microalgae. Moreover, the heat tolerance of microalgae might be raised by reducing the degree of FA unsaturation in microalgae with red light. In a study on *Arabidopsis thaliana*, a FA-desaturase was genetically deactivated by knockout mutations. This resulted in a lower degree of unsaturation and concomitantly a higher heat tolerance of this organism (Hugly et al., 1989). The light spectrum-triggered FA changes might be an object of further studies. It can be of particular interest to investigate if the observed FA changes are only a special case in microalgae or if it is also applicable to land plants, and perhaps even heterotrophic organisms. These new insights can lead to many applications and innovations in and beyond the field of microalgae technology.

ACKNOWLEDGMENTS

We want to thank PD Dr. Klaus von Schwartzenberg and the staff of the Microalgae and Zygnematophyceae Collection Hamburg (MZCH, previously SVCK) microalgae collection of the University of Hamburg for giving us the chance to work with one of their microalgae strains. A special thanks goes to Christoph Stegen of the technical support team of the Leuphana University L neburg. Thanks to his excellent technical support and expertise we were able to improve our experimental setup for the microalgae cultivation. The authors thank Josi Steinke and Hannes Diers for their contribution in the microalgae cultivations and the sample preparations.

CONFLICT OF INTEREST

The authors declare that they have no conflict of interest.

AUTHOR CONTRIBUTIONS

All authors have made a scientific contribution and approved the final draft of the manuscript.

M.H. Conceived and designed the study. Carried out the research. Analyzed the data. Wrote the first draft of the manuscript.

A.G. Carried out the research. Analysis of data.

M.R. Supervision and support in the methodology part. Analysis and interpretation of data. Contribution to the writing process. Editing and review of manuscript.

F.K. Analysis of data and made the statistical work. Contribution to the writing process.

M.K. Analysis of data. Contribution to the writing process. Supervision of the study.

K.K. Analysis of data. Contribution to the writing process. Supervision of the study.

REFERENCES

Abomohra AEF, Almutairi AW. A close-loop integrated approach for microalgae cultivation and efficient utilization of agar-free seaweed residues for enhanced biofuel recovery. Bioresour Technol. 2020;317:124027.

Abomohra AEF, Wagner M, El-Sheekh M, Hanelt D. Lipid and total fatty acid productivity in photoautotrophic fresh water microalgae: screening studies towards biodiesel production. J Appl Phycol. 2013;25:931–6.

Abomohra AEF, Eladel H, El-Esawi M, Wang S, Wang Q, He Z, et al. Effect of lipid-free microalgal biomass and waste glycerol on growth and lipid production of *Scenedesmus obliquus*: innovative waste recycling for extraordinary lipid production. Bioresour Technol. 2018;249:992–9.

Abomohra AEF, Shang H, El-Sheekh M, Eladel H, Ebaid R, Wang S, et al. Night illumination using monochromatic light-emitting diodes for enhanced microalgal growth and biodiesel production. Bioresour Technol. 2019;288:121514.

Abomohra AEF, El-Naggar AH, Alaswad SO, Elsayed M, Li M, Li W. Enhancement of biodiesel yield from a halophilic green microalga isolated under extreme hypersaline conditions through

stepwise salinity adaptation strategy. Bioresour Technol. 2020; 310:123462.
Adarme-Vega TC, Lim DK, Timmins M, Vernen F, Li Y, Schenk PM. Microalgal biofactories: a promising approach towards sustainable omega-3 fatty acid production. Microb Cell Fact. 2012; 11:96.
Alfonso M, Yruela I, Almárcegui S, Torrado E, P rez MA, Picorel R. Unusual tolerance to high temperatures in a new herbicide-resistant D1 mutant from *Glycine max* (L.) Merr. Cell cultures deficient in fatty acid desaturation. Planta. 2001;212:573–82.
Almarashi JQ, El-Zohary SE, Ellabban MA, Abomohra AEF. Enhancement of lipid production and energy recovery from the green microalga *Chlorella vulgaris* by inoculum pretreatment with low-dose cold atmospheric pressure plasma (CAPP). Energ Conver Manage. 2020;204:112314.
Aparicio PJ, Qui ones MA. Blue light, a positive switch signal for nitrate and nitrite uptake by the green alga Monoraphidium braunii. Plant Physiol. 1991;95:374–8.
Aparicio PJ, Witt FG, Ramirez JM, Quinones MA, Balandin T. Blue-light-induced pH changes associated with NO3−, NO2− and cl− uptake by the green alga Monoraphidium braunii. Plant Cell Environ. 1994;17:1323–30.
Berestovoy MA, Pavlenko OS, Goldenkova-Pavlova IV. Plant fatty acid desaturases: role in the life of plants and biotechnological potential. Biol Bull Rev. 2020;10:127–39.
Brenna JT. Efficiency of conversion of α-linolenic acid to long chain n-3 fatty acids in man. Curr Opin Clin Nutr Metabol Care. 2002; 5:127–32.
Breuer G, Lamers PP, Martens DE, Draaisma RB, Wijffels RH. The impact of nitrogen starvation on the dynamics of triacylglycerol accumulation in nine microalgae strains. Bioresour Technol. 2012;124:217–26.
Chen X, Huang C, Liu T. Harvesting of microalgae Scenedesmus sp. using polyvinylidene fluoride microfiltration membrane. Desalin Water Treat. 2012;45:177–81.
Cherif A, Dubacq J, Mache R, Oursel A, Tremolieres A. Biosynthesis of α-linolenic acid by desaturation of oleic and linoleic acids in several organs of higher and lower plants and in algae. Phytochemistry. 1975;14:703–6.
Clark JB, Lister GR. Photosynthetic action spectra of trees: I. comparative photosynthetic action spectra of one deciduous and four coniferous tree species as related to photorespiration and pigment complements. Plant Physiol. 1975;55:401–6.
Collados R, Andreu V, Picorel R, Alfonso M. A light-sensitive mechanism differently regulates transcription and transcript stability of ω3 fatty-acid desaturases (FAD3, FAD7 and FAD8) in soybean photosynthetic cell suspensions. FEBS Lett. 2006;580:4934–40.
Degraeve-Guilbault C, Pankasem N, Gueirrero M, Lemoigne C, Domergue F, Kotajima T, et al. Temperature acclimation of the picoalga *Ostreococcus tauri* triggers early fatty-acid variations and involves a plastidial ω3-desaturase. Front Plant Sci. 2021;12: 1–17.
Dhaka V, Gulia N, Ahlawat KS, Khatkar BS. Trans fats—sources, health risks and alternative approach-a review. J Food Sci Technol. 2011;48:534–54.
El-Sheekh M, Abomohra AEF, Hanelt D. Optimization of biomass and fatty acid productivity of *Scenedesmus obliquus* as a promising microalga for biodiesel production. World J Microbiol Biotechnol. 2013;29:915–22.
Esakkimuthu S, Krishnamurthy V, Wang S, Hu X, Swaminathan K, Abomohra AEF. Application of p-coumaric acid for extraordinary lipid production in Tetradesmus obliquus: a sustainable approach towards enhanced biodiesel production. Renew Energy. 2020;157:368–76.
Gebauer SK, Psota TL, Kris-Etherton PM. The diversity of health effects of individual trans fatty acid isomers. Lipids. 2007;42: 787–99.
Giráldez N, Aparicio PJ, Qui ones MA. Blue light requirement for HC03 uptake and its action Spectrum in Monoraphidium braunii. Photochem Photobiol. 1998;68:420–6.
Girard JM, Roy ML, Hafsa MB, Gagnon J, Faucheux N, Heitz M, et al. Mixotrophic cultivation of green microalgae *Scenedesmus obliquus* on cheese whey permeate for biodiesel production. Algal Res. 2014;5:241–8.
Hindersin S, Leupold M, Kerner M, Hanelt D. Irradiance optimization of outdoor microalgal cultures using solar tracked photobioreactors. Bioprocess Biosyst Eng. 2013;36:345–55.
Holleman AF, Wiberg E. Lehrbuch der anorganischen chemie. 102nd ed.; 2007. Berlin, Germany: de Gruyter.
Hugly S, Kunst L, Somerville C. Enhanced thermal tolerance of photosynthesis and altered chloroplast ultrastructure in a mutant of Arabidopsis deficient in lipid desaturation. Plant Physiol. 1989; 90:1134–42.
Hultberg M, Jönsson HL, Bergstrand KJ, Carlsson AS. Impact of light quality on biomass production and fatty acid content in the microalga *Chlorella vulgaris*. Bioresour Technol. 2014;159:465–7.
Ichihara KI, Fukubayashi Y. Preparation of fatty acid methyl esters for gas-liquid chromatography. J Lipid Res. 2010;51:635–40.
Kim TH, Lee Y, Han SH, Hwang SJ. The effects of wavelength and wavelength mixing ratios on microalgae growth and nitrogen, phosphorus removal using Scenedesmus sp. for wastewater treatment. Bioresour Technol. 2013;130:75–80.
Kim CW, Sung MG, Nam K, Moon M, Kwon JH, Yang JW. Effect of monochromatic illumination on lipid accumulation of *Nannochloropsis gaditana* under continuous cultivation. Bioresour Technol. 2014;159:30–5.
Kis M, Zsiros O, Farkas T, Wada H, Nagy F, Gombos Z. Light-induced expression of fatty acid desaturase genes. Proc Natl Acad Sci. 1998;95:4209–14.
Kuhnt K, Baehr M, Rohrer C, Jahreis G. Trans fatty acid isomers and the trans-9/trans-11 index in fat containing foods. Eur J Lipid Sci Technol. 2011;113:1281–92.
Mandotra SK, Kumar P, Suseela MR, Nayaka S, Ramteke PW. Evaluation of fatty acid profile and biodiesel properties of microalga *Scenedesmus abundans* under the influence of phosphorus, pH and light intensities. Bioresour Technol. 2016;201: 222–9.
Mattos ER, Singh M, Cabrera ML, Das KC. Enhancement of biomass production in *Scenedesmus bijuga* high-density culture using weakly absorbed green light. Biomass Bioenergy. 2015;81: 473–8.
de Mendoza D, Cronan JE Jr. Thermal regulation of membrane lipid fluidity in bacteria. Trends Biochem Sci. 1983;8:49–52.
Metting FB. Biodiversity and application of microalgae. J Ind Microbiol. 1996;17:477–89.
de Mooij T, de Vries G, Latsos C, Wijffels RH, Janssen M. Impact of light color on photobioreactor productivity. Algal Res. 2016;15: 32–42.
Mozaffarian D, Katan MB, Ascherio A, Stampfer MJ, Willett WC. Trans fatty acids and cardiovascular disease. N Engl J Med. 2006;354:1601–13.
Niyogi KK, Björkman O, Grossman AR. The roles of specific xanthophylls in photoprotection. Proc Natl Acad Sci. 1997;94: 14162–7.
Ooms MD, Graham PJ, Nguyen B, Sargent EH, Sinton D. Light dilution via wavelength management for efficient high-density photobioreactors. Biotechnol Bioeng. 2017;114:1160–9.
Osman SM, Chuah TS, Loh SH, San Cha T, Ahmad A. Light-color-induced changes in fatty acid biosynthesis in Chlorella sp. strain Ks-ma2 in early stationary growth phase. BIOTROPIA Southeast Asian J Trop Biol. 2018;25:33–42.
Patterson GW. Effect of culture temperature on fatty acid composition of *Chlorella sorokiniana*. Lipids. 1970;5:597–600.
Piligaev AV, Sorokina KN, Bryanskaya AV, Peltek SE, Kolchanov NA, Parmon VN. Isolation of prospective microalgal

strains with high saturated fatty acid content for biofuel production. Algal Res. 2015;12:368–76.
Pulz O, Gross W. Valuable products from biotechnology of microalgae. Appl Microbiol Biotechnol. 2004;65:635–48.
Reich M, Hannig C, Al-Ahmad A, Bolek R, K mmerer K. A comprehensive method for determination of fatty acids in the initial oral biofilm (pellicle). J Lipid Res. 2012;53:2226–30.
Reich M, K mmerer K, Al-Ahmad A, Hannig C. Fatty acid profile of the initial oral biofilm (pellicle): an in-situ study. Lipids. 2013;48: 929–37.
Reymann T, Kerner M, K mmerer K. Assessment of the biotic and abiotic elimination processes of five micropollutants during cultivation of the green microalgae *Acutodesmus obliquus*. Bioresour Technol Rep. 2020;11:100512.
Riediger ND, Othman RA, Suh M, Moghadasian MH. A systemic review of the roles of n-3 fatty acids in health and disease. J Am Diet Assoc. 2009;109:668–79.
Ruxton CHS, Reed SC, Simpson MJA, Millington KJ. The health benefits of omega-3 polyunsaturated fatty acids: a review of the evidence. J Hum Nutr Diet. 2004;17:449–59.
Sandmann G. Light-dependent switch from formation of poly-cis carotenes to all-trans carotenoids in the Scenedesmus mutant C-6D. Arch Microbiol. 1991;155:229–33.
Simopoulos AP. Omega-6/omega-3 essential fatty acid ratio and chronic diseases. Food Rev Intl. 2004;20:77–90.
Sommerfeld M. Trans unsaturated fatty acids in natural products and processed foods. Prog Lipid Res. 1983;22:221–33.
Sun J, Nishio JN, Vogelmann TC. Green light drives CO2 fixation deep within leaves. Plant Cell Physiol. 1998;39:1020–6.
Vanthoor-Koopmans M, Wijffels RH, Barbosa MJ, Eppink MH. Biorefinery of microalgae for food and fuel. Bioresour Technol. 2013;135:142–9.
Wilhelm C, Krámer P, Wild A. Effect of different light qualities on the ultrastructure, thylakoid membrane composition and assimilation metabolism of *Chlorella fusca*. Physiol Plant. 1985;64:359–64.
Zhang T, Maruhnich SA, Folta KM. Green light induces shade avoidance symptoms. Plant Physiol. 2011;157:1528–36.

SUPPORTING INFORMATION

Additional supporting information may be found online in the Supporting Information section at the end of this article.

How to cite this article: Helamieh M, Gebhardt A, Reich M, Kuhn F, Kerner M, K mmerer K. Growth and fatty acid composition of *Acutodesmus obliquus* under different light spectra and temperatures. Lipids. 2021;1–14. https://doi.org/10.1002/lipd.12316

```
 DATASET ACTIVATE DataSet1.

SAVE OUTFILE='C:\Users\Frieda\Downloads\Mark\Data.sav'
  /COMPRESSED.
SORT CASES  BY Temperature.
SPLIT FILE SEPARATE BY Temperature.

* Encoding: UTF-8.


GLM CDW_red_T1 CDW_green_T1 CDW_blue_T1 CDW_red_T2 CDW_green_T2 CDW_blue_T2
 CDW_red_T3 CDW_green_T3 CDW_blue_T3
  /WSFACTOR=time 3 Polynomial lightcolour 3 Simple(1)
  /METHOD=SSTYPE(3)
  /PRINT=DESCRIPTIVE ETASQ OPOWER
  /CRITERIA=ALPHA(.05)
  /WSDESIGN=time lightcolour time*lightcolour.
```

General Linear Model

Notes

Output Created		28-FEB-2021 15:03:45
Comments		
Input	Data	C:\Users\Frieda\Downloads\Mark\Data.sav
	Active Dataset	DataSet1
	Filter	<none>
	Weight	<none>
	Split File	Temperature
	N of Rows in Working Data File	9
Missing Value Handling	Definition of Missing	User-defined missing values are treated as missing.
	Cases Used	Statistics are based on all cases with valid data for all variables in the model.

Notes

Syntax		GLM CDW_red_T1 CDW_green_T1 CDW_blue_T1 CDW_red_T2 CDW_green_T2 CDW_blue_T2 CDW_red_T3 CDW_green_T3 CDW_blue_T3 /WSFACTOR=time 3 Polynomial lightcolour 3 Simple(1) /METHOD=SSTYPE(3) /PRINT=DESCRIPTIVE ETASQ OPOWER /CRITERIA=ALPHA(.05) /WSDESIGN=time lightcolour time*lightcolour.
Resources	Processor Time	00:00:00,05
	Elapsed Time	00:00:00,08

Within-Subjects Factors

Measure: MEASURE_1

time	lightcolour	Dependent Variable
1	1	CDW_red_T1
	2	CDW_green_T1
	3	CDW_blue_T1
2	1	CDW_red_T2
	2	CDW_green_T2
	3	CDW_blue_T2
3	1	CDW_red_T3
	2	CDW_green_T3
	3	CDW_blue_T3

Temperature = 1,00

Between-Subjects Factors[a]

a. Temperature = 1,00

Descriptive Statistics[a]

	Mean	Std. Deviation	N
CDW_red_T1	,2733	,00577	3
CDW_green_T1	,2533	,00577	3
CDW_blue_T1	,2600	,00000	3
CDW_red_T2	,7767	,01528	3
CDW_green_T2	,6500	,02000	3
CDW_blue_T2	,6167	,05132	3
CDW_red_T3	1,9167	,16503	3
CDW_green_T3	1,5900	,11533	3
CDW_blue_T3	1,2133	,01528	3

a. Temperature = 1,00

Multivariate Tests[a,b]

Effect		Value	F	Hypothesis df	Error df
time	Pillai's Trace	1,000	1318,051[c]	2,000	1,000
	Wilks' Lambda	,000	1318,051[c]	2,000	1,000
	Hotelling's Trace	2636,102	1318,051[c]	2,000	1,000
	Roy's Largest Root	2636,102	1318,051[c]	2,000	1,000
lightcolour	Pillai's Trace	,972	17,338[c]	2,000	1,000
	Wilks' Lambda	,028	17,338[c]	2,000	1,000
	Hotelling's Trace	34,675	17,338[c]	2,000	1,000
	Roy's Largest Root	34,675	17,338[c]	2,000	1,000
time * lightcolour	Pillai's Trace	.[d]	.	.	.
	Wilks' Lambda	.[d]	.	.	.
	Hotelling's Trace	.[d]	.	.	.
	Roy's Largest Root	.[d]	.	.	.

Multivariate Tests[a,b]

Effect		Sig.	Partial Eta Squared	Noncent. Parameter	Observed Power[e]
time	Pillai's Trace	,019	1,000	2636,102	,990
	Wilks' Lambda	,019	1,000	2636,102	,990
	Hotelling's Trace	,019	1,000	2636,102	,990
	Roy's Largest Root	,019	1,000	2636,102	,990
lightcolour	Pillai's Trace	,167	,972	34,675	,235
	Wilks' Lambda	,167	,972	34,675	,235
	Hotelling's Trace	,167	,972	34,675	,235
	Roy's Largest Root	,167	,972	34,675	,235
time * lightcolour	Pillai's Trace	.	.	.	.
	Wilks' Lambda	.	.	.	.
	Hotelling's Trace	.	.	.	.
	Roy's Largest Root	.	.	.	.

a. Temperature = 1,00

b. Design: Intercept
Within Subjects Design: time + lightcolour + time * lightcolour

c. Exact statistic

d. Cannot produce multivariate test statistics because of insufficient residual degrees of freedom.

e. Computed using alpha = ,05

Mauchly's Test of Sphericity[a,b]

Measure: MEASURE_1

Within Subjects Effect	Mauchly's W	Approx. Chi-Square	df	Sig.	Epsilon[c] Greenhouse-Geisser
time	,173	1,754	2	,416	,547
lightcolour	,860	,151	2	,927	,877
time * lightcolour	,000	.	9	.	,324

Mauchly's Test of Sphericity[a,b]

Measure: MEASURE_1

Within Subjects Effect	Epsilon[c] Huynh-Feldt	Lower-bound
time	,709	,500
lightcolour	1,000	,500
time * lightcolour	,674	,250

Tests the null hypothesis that the error covariance matrix of the orthonormalized transformed dependent variables is proportional to an identity matrix.

a. Temperature = 1,00

b. Design: Intercept
Within Subjects Design: time + lightcolour + time * lightcolour

c. May be used to adjust the degrees of freedom for the averaged tests of significance. Corrected tests are displayed in the Tests of Within-Subjects Effects table.

Tests of Within-Subjects Effects[a]

Measure: MEASURE_1

Source		Type III Sum of Squares	df	Mean Square
time	Sphericity Assumed	8,072	2	4,036
	Greenhouse-Geisser	8,072	1,095	7,373
	Huynh-Feldt	8,072	1,418	5,690
	Lower-bound	8,072	1,000	8,072
Error(time)	Sphericity Assumed	,013	4	,003
	Greenhouse-Geisser	,013	2,189	,006
	Huynh-Feldt	,013	2,837	,005
	Lower-bound	,013	2,000	,007
lightcolour	Sphericity Assumed	,385	2	,193
	Greenhouse-Geisser	,385	1,754	,220
	Huynh-Feldt	,385	2,000	,193
	Lower-bound	,385	1,000	,385
Error(lightcolour)	Sphericity Assumed	,030	4	,007
	Greenhouse-Geisser	,030	3,507	,009
	Huynh-Feldt	,030	4,000	,007
	Lower-bound	,030	2,000	,015
time * lightcolour	Sphericity Assumed	,402	4	,100
	Greenhouse-Geisser	,402	1,298	,309
	Huynh-Feldt	,402	2,695	,149
	Lower-bound	,402	1,000	,402
Error(time*lightcolour)	Sphericity Assumed	,039	8	,005
	Greenhouse-Geisser	,039	2,595	,015
	Huynh-Feldt	,039	5,390	,007
	Lower-bound	,039	2,000	,019

Tests of Within-Subjects Effects[a]

Measure: MEASURE_1

Source		F	Sig.	Partial Eta Squared
time	Sphericity Assumed	1233,355	,000	,998
	Greenhouse-Geisser	1233,355	,000	,998
	Huynh-Feldt	1233,355	,000	,998
	Lower-bound	1233,355	,001	,998
Error(time)	Sphericity Assumed			
	Greenhouse-Geisser			
	Huynh-Feldt			
	Lower-bound			
lightcolour	Sphericity Assumed	25,768	,005	,928
	Greenhouse-Geisser	25,768	,008	,928
	Huynh-Feldt	25,768	,005	,928
	Lower-bound	25,768	,037	,928
Error(lightcolour)	Sphericity Assumed			
	Greenhouse-Geisser			
	Huynh-Feldt			
	Lower-bound			
time * lightcolour	Sphericity Assumed	20,842	,000	,912
	Greenhouse-Geisser	20,842	,026	,912
	Huynh-Feldt	20,842	,002	,912
	Lower-bound	20,842	,045	,912
Error(time*lightcolour)	Sphericity Assumed			
	Greenhouse-Geisser			
	Huynh-Feldt			
	Lower-bound			

Tests of Within-Subjects Effects[a]

Measure: MEASURE_1

Source		Noncent. Parameter	Observed Power[b]
time	Sphericity Assumed	2466,710	1,000
	Greenhouse-Geisser	1350,158	1,000
	Huynh-Feldt	1749,445	1,000
	Lower-bound	1233,355	1,000
Error(time)	Sphericity Assumed		
	Greenhouse-Geisser		
	Huynh-Feldt		
	Lower-bound		
lightcolour	Sphericity Assumed	51,536	,986
	Greenhouse-Geisser	45,191	,968
	Huynh-Feldt	51,536	,986
	Lower-bound	25,768	,730
Error(lightcolour)	Sphericity Assumed		
	Greenhouse-Geisser		
	Huynh-Feldt		
	Lower-bound		
time * lightcolour	Sphericity Assumed	83,368	1,000
	Greenhouse-Geisser	27,046	,807
	Huynh-Feldt	56,172	,995
	Lower-bound	20,842	,656
Error(time*lightcolour)	Sphericity Assumed		
	Greenhouse-Geisser		
	Huynh-Feldt		
	Lower-bound		

a. Temperature = 1,00

b. Computed using alpha = ,05

Tests of Within-Subjects Contrasts[a]

Measure: MEASURE_1

Source	time	lightcolour	Type III Sum of Squares	df	Mean Square
time	Linear		2,579	1	2,579
	Quadratic		,112	1	,112
Error(time)	Linear		,003	2	,001
	Quadratic		,001	2	,001
lightcolour		Level 2 vs. Level 1	,224	1	,224
		Level 3 vs. Level 1	,769	1	,769
Error(lightcolour)		Level 2 vs. Level 1	,041	2	,021
		Level 3 vs. Level 1	,024	2	,012
time * lightcolour	Linear	Level 2 vs. Level 1	,141	1	,141
		Level 3 vs. Level 1	,714	1	,714
	Quadratic	Level 2 vs. Level 1	,004	1	,004
		Level 3 vs. Level 1	,079	1	,079
Error(time*lightcolour)	Linear	Level 2 vs. Level 1	,048	2	,024
		Level 3 vs. Level 1	,032	2	,016
	Quadratic	Level 2 vs. Level 1	,009	2	,004
		Level 3 vs. Level 1	,014	2	,007

Tests of Within-Subjects Contrasts[a]

Measure: MEASURE_1

Source	time	lightcolour	F	Sig.	Partial Eta Squared
time	Linear		1796,645	,001	,999
	Quadratic		150,104	,007	,987
Error(time)	Linear				
	Quadratic				
lightcolour		Level 2 vs. Level 1	10,905	,081	,845
		Level 3 vs. Level 1	63,284	,015	,969
Error(lightcolour)		Level 2 vs. Level 1			
		Level 3 vs. Level 1			
time * lightcolour	Linear	Level 2 vs. Level 1	5,861	,137	,746
		Level 3 vs. Level 1	44,083	,022	,957
	Quadratic	Level 2 vs. Level 1	1,000	,423	,333
		Level 3 vs. Level 1	11,532	,077	,852
Error(time*lightcolour)	Linear	Level 2 vs. Level 1			
		Level 3 vs. Level 1			
	Quadratic	Level 2 vs. Level 1			
		Level 3 vs. Level 1			

Tests of Within-Subjects Contrasts[a]

Measure: MEASURE_1

Source	time	lightcolour	Noncent. Parameter	Observed Power[b]
time	Linear		1796,645	1,000
	Quadratic		150,104	,999
Error(time)	Linear			
	Quadratic			
lightcolour		Level 2 vs. Level 1	10,905	,442
		Level 3 vs. Level 1	63,284	,957
Error(lightcolour)		Level 2 vs. Level 1		
		Level 3 vs. Level 1		
time * lightcolour	Linear	Level 2 vs. Level 1	5,861	,286
		Level 3 vs. Level 1	44,083	,889
	Quadratic	Level 2 vs. Level 1	1,000	,095
		Level 3 vs. Level 1	11,532	,459
Error(time*lightcolour)	Linear	Level 2 vs. Level 1		
		Level 3 vs. Level 1		
	Quadratic	Level 2 vs. Level 1		
		Level 3 vs. Level 1		

a. Temperature = 1,00

b. Computed using alpha = ,05

Tests of Between-Subjects Effects[a]

Measure: MEASURE_1

Transformed Variable: Average

Source	Type III Sum of Squares	df	Mean Square	F	Sig.	Partial Eta Squared
Intercept	6,334	1	6,334	5681,312	,000	1,000
Error	,002	2	,001			

Tests of Between-Subjects Effects[a]

Measure: MEASURE_1

Transformed Variable: Average

Source	Noncent. Parameter	Observed Power[b]
Intercept	5681,312	1,000
Error		

a. Temperature = 1,00

b. Computed using alpha = ,05

Temperature = 2,00

Between-Subjects Factors[a]

a. Temperature = 2,00

Descriptive Statistics[a]

	Mean	Std. Deviation	N
CDW_red_T1	,6433	,05033	3
CDW_green_T1	,5233	,02887	3
CDW_blue_T1	,4933	,00577	3
CDW_red_T2	1,2600	,05568	3
CDW_green_T2	1,0567	,04041	3
CDW_blue_T2	,8567	,01155	3
CDW_red_T3	2,4200	,23302	3
CDW_green_T3	2,1400	,09539	3
CDW_blue_T3	1,5933	,01155	3

a. Temperature = 2,00

Multivariate Tests[a,b]

Effect		Value	F	Hypothesis df	Error df
time	Pillai's Trace	1,000	13108,983[c]	2,000	1,000
	Wilks' Lambda	,000	13108,983[c]	2,000	1,000
	Hotelling's Trace	26217,967	13108,983[c]	2,000	1,000
	Roy's Largest Root	26217,967	13108,983[c]	2,000	1,000
lightcolour	Pillai's Trace	,984	30,270[c]	2,000	1,000
	Wilks' Lambda	,016	30,270[c]	2,000	1,000
	Hotelling's Trace	60,541	30,270[c]	2,000	1,000
	Roy's Largest Root	60,541	30,270[c]	2,000	1,000
time * lightcolour	Pillai's Trace	.[d]	.	.	.
	Wilks' Lambda	.[d]	.	.	.
	Hotelling's Trace	.[d]	.	.	.
	Roy's Largest Root	.[d]	.	.	.

Multivariate Tests[a,b]

Effect		Sig.	Partial Eta Squared	Noncent. Parameter	Observed Power[e]
time	Pillai's Trace	,006	1,000	26217,967	1,000
	Wilks' Lambda	,006	1,000	26217,967	1,000
	Hotelling's Trace	,006	1,000	26217,967	1,000
	Roy's Largest Root	,006	1,000	26217,967	1,000
lightcolour	Pillai's Trace	,127	,984	60,541	,305
	Wilks' Lambda	,127	,984	60,541	,305
	Hotelling's Trace	,127	,984	60,541	,305
	Roy's Largest Root	,127	,984	60,541	,305
time * lightcolour	Pillai's Trace	.	.	.	.
	Wilks' Lambda	.	.	.	.
	Hotelling's Trace	.	.	.	.
	Roy's Largest Root	.	.	.	.

a. Temperature = 2,00

b. Design: Intercept
Within Subjects Design: time + lightcolour + time * lightcolour

c. Exact statistic

d. Cannot produce multivariate test statistics because of insufficient residual degrees of freedom.

e. Computed using alpha = ,05

Mauchly's Test of Sphericity[a,b]

Measure: MEASURE_1

Within Subjects Effect	Mauchly's W	Approx. Chi-Square	df	Sig.	Epsilon[c] Greenhouse-Geisser
time	,014	4,294	2	,117	,503
lightcolour	,516	,661	2	,718	,674
time * lightcolour	,000	.	9	.	,270

Mauchly's Test of Sphericity[a,b]

Measure: MEASURE_1

Within Subjects Effect	Epsilon[c] Huynh-Feldt	Lower-bound
time	,514	,500
lightcolour	1,000	,500
time * lightcolour	,337	,250

Tests the null hypothesis that the error covariance matrix of the orthonormalized transformed dependent variables is proportional to an identity matrix.

a. Temperature = 2,00

b. Design: Intercept
Within Subjects Design: time + lightcolour + time * lightcolour

c. May be used to adjust the degrees of freedom for the averaged tests of significance. Corrected tests are displayed in the Tests of Within-Subjects Effects table.

Tests of Within-Subjects Effects[a]

Measure: MEASURE_1

Source		Type III Sum of Squares	df	Mean Square
time	Sphericity Assumed	10,454	2	5,227
	Greenhouse-Geisser	10,454	1,007	10,382
	Huynh-Feldt	10,454	1,028	10,172
	Lower-bound	10,454	1,000	10,454
Error(time)	Sphericity Assumed	,012	4	,003
	Greenhouse-Geisser	,012	2,014	,006
	Huynh-Feldt	,012	2,055	,006
	Lower-bound	,012	2,000	,006
lightcolour	Sphericity Assumed	,957	2	,479
	Greenhouse-Geisser	,957	1,348	,710
	Huynh-Feldt	,957	2,000	,479
	Lower-bound	,957	1,000	,957
Error(lightcolour)	Sphericity Assumed	,052	4	,013
	Greenhouse-Geisser	,052	2,696	,019
	Huynh-Feldt	,052	4,000	,013
	Lower-bound	,052	2,000	,026
time * lightcolour	Sphericity Assumed	,385	4	,096
	Greenhouse-Geisser	,385	1,080	,357
	Huynh-Feldt	,385	1,348	,286
	Lower-bound	,385	1,000	,385
Error(time*lightcolour)	Sphericity Assumed	,048	8	,006
	Greenhouse-Geisser	,048	2,160	,022
	Huynh-Feldt	,048	2,696	,018
	Lower-bound	,048	2,000	,024

Tests of Within-Subjects Effects[a]

Measure: MEASURE_1

Source		F	Sig.	Partial Eta Squared
time	Sphericity Assumed	1772,899	,000	,999
	Greenhouse-Geisser	1772,899	,001	,999
	Huynh-Feldt	1772,899	,000	,999
	Lower-bound	1772,899	,001	,999
Error(time)	Sphericity Assumed			
	Greenhouse-Geisser			
	Huynh-Feldt			
	Lower-bound			
lightcolour	Sphericity Assumed	36,821	,003	,948
	Greenhouse-Geisser	36,821	,012	,948
	Huynh-Feldt	36,821	,003	,948
	Lower-bound	36,821	,026	,948
Error(lightcolour)	Sphericity Assumed			
	Greenhouse-Geisser			
	Huynh-Feldt			
	Lower-bound			
time * lightcolour	Sphericity Assumed	16,042	,001	,889
	Greenhouse-Geisser	16,042	,050	,889
	Huynh-Feldt	16,042	,033	,889
	Lower-bound	16,042	,057	,889
Error(time*lightcolour)	Sphericity Assumed			
	Greenhouse-Geisser			
	Huynh-Feldt			
	Lower-bound			

Tests of Within-Subjects Effects[a]

Measure: MEASURE_1

Source		Noncent. Parameter	Observed Power[b]
time	Sphericity Assumed	3545,799	1,000
	Greenhouse-Geisser	1785,083	1,000
	Huynh-Feldt	1821,970	1,000
	Lower-bound	1772,899	1,000
Error(time)	Sphericity Assumed		
	Greenhouse-Geisser		
	Huynh-Feldt		
	Lower-bound		
lightcolour	Sphericity Assumed	73,642	,998
	Greenhouse-Geisser	49,631	,960
	Huynh-Feldt	73,642	,998
	Lower-bound	36,821	,842
Error(lightcolour)	Sphericity Assumed		
	Greenhouse-Geisser		
	Huynh-Feldt		
	Lower-bound		
time * lightcolour	Sphericity Assumed	64,167	,999
	Greenhouse-Geisser	17,325	,609
	Huynh-Feldt	21,624	,734
	Lower-bound	16,042	,565
Error(time*lightcolour)	Sphericity Assumed		
	Greenhouse-Geisser		
	Huynh-Feldt		
	Lower-bound		

a. Temperature = 2,00

b. Computed using alpha = ,05

Tests of Within-Subjects Contrasts[a]

Measure: MEASURE_1

Source	time	lightcolour	Type III Sum of Squares	df	Mean Square
time	Linear		3,365	1	3,365
	Quadratic		,120	1	,120
Error(time)	Linear		,003	2	,002
	Quadratic		,001	2	,000
lightcolour		Level 2 vs. Level 1	,364	1	,364
		Level 3 vs. Level 1	1,904	1	1,904
Error(lightcolour)		Level 2 vs. Level 1	,075	2	,037
		Level 3 vs. Level 1	,065	2	,032
time * lightcolour	Linear	Level 2 vs. Level 1	,038	1	,038
		Level 3 vs. Level 1	,687	1	,687
	Quadratic	Level 2 vs. Level 1	2,222E-5	1	2,222E-5
		Level 3 vs. Level 1	,014	1	,014
Error(time*lightcolour)	Linear	Level 2 vs. Level 1	,069	2	,034
		Level 3 vs. Level 1	,041	2	,020
	Quadratic	Level 2 vs. Level 1	,018	2	,009
		Level 3 vs. Level 1	,007	2	,003

Tests of Within-Subjects Contrasts[a]

Measure: MEASURE_1

Source	time	lightcolour	F	Sig.	Partial Eta Squared
time	Linear		2240,572	,000	,999
	Quadratic		257,790	,004	,992
Error(time)	Linear				
	Quadratic				
lightcolour		Level 2 vs. Level 1	9,730	,089	,829
		Level 3 vs. Level 1	58,717	,017	,967
Error(lightcolour)		Level 2 vs. Level 1			
		Level 3 vs. Level 1			
time * lightcolour	Linear	Level 2 vs. Level 1	1,116	,401	,358
		Level 3 vs. Level 1	33,889	,028	,944
	Quadratic	Level 2 vs. Level 1	,003	,965	,001
		Level 3 vs. Level 1	4,168	,178	,676
Error(time*lightcolour)	Linear	Level 2 vs. Level 1			
		Level 3 vs. Level 1			
	Quadratic	Level 2 vs. Level 1			
		Level 3 vs. Level 1			

Tests of Within-Subjects Contrasts[a]

Measure: MEASURE_1

Source	time	lightcolour	Noncent. Parameter	Observed Power[b]
time	Linear		2240,572	1,000
	Quadratic		257,790	1,000
Error(time)	Linear			
	Quadratic			
lightcolour		Level 2 vs. Level 1	9,730	,409
		Level 3 vs. Level 1	58,717	,946
Error(lightcolour)		Level 2 vs. Level 1		
		Level 3 vs. Level 1		
time * lightcolour	Linear	Level 2 vs. Level 1	1,116	,100
		Level 3 vs. Level 1	33,889	,818
	Quadratic	Level 2 vs. Level 1	,003	,050
		Level 3 vs. Level 1	4,168	,225
Error(time*lightcolour)	Linear	Level 2 vs. Level 1		
		Level 3 vs. Level 1		
	Quadratic	Level 2 vs. Level 1		
		Level 3 vs. Level 1		

a. Temperature = 2,00

b. Computed using alpha = ,05

Tests of Between-Subjects Effects[a]

Measure: MEASURE_1

Transformed Variable: Average

Source	Type III Sum of Squares	df	Mean Square	F	Sig.	Partial Eta Squared
Intercept	13,412	1	13,412	2531,721	,000	,999
Error	,011	2	,005			

Tests of Between-Subjects Effects[a]

Measure: MEASURE_1

Transformed Variable: Average

Source	Noncent. Parameter	Observed Power[b]
Intercept	2531,721	1,000
Error		

a. Temperature = 2,00

b. Computed using alpha = ,05

Temperature = 3,00

Between-Subjects Factors[a]

a. Temperature = 3,00

Descriptive Statistics[a]

	Mean	Std. Deviation	N
CDW_red_T1	,5367	,04726	3
CDW_green_T1	,4433	,04041	3
CDW_blue_T1	,4033	,01155	3
CDW_red_T2	1,1467	,04726	3
CDW_green_T2	,9567	,02082	3
CDW_blue_T2	,7700	,04359	3
CDW_red_T3	2,1267	,12503	3
CDW_green_T3	1,8600	,05196	3
CDW_blue_T3	1,3433	,04509	3

a. Temperature = 3,00

Multivariate Tests[a,b]

Effect		Value	F	Hypothesis df	Error df
time	Pillai's Trace	1,000	146630,333[c]	2,000	1,000
	Wilks' Lambda	,000	146630,333[c]	2,000	1,000
	Hotelling's Trace	293260,667	146630,333[c]	2,000	1,000
	Roy's Largest Root	293260,667	146630,333[c]	2,000	1,000
lightcolour	Pillai's Trace	,998	294,453[c]	2,000	1,000
	Wilks' Lambda	,002	294,453[c]	2,000	1,000
	Hotelling's Trace	588,906	294,453[c]	2,000	1,000
	Roy's Largest Root	588,906	294,453[c]	2,000	1,000
time * lightcolour	Pillai's Trace	.[d]	.	.	.
	Wilks' Lambda	.[d]	.	.	.
	Hotelling's Trace	.[d]	.	.	.
	Roy's Largest Root	.[d]	.	.	.

Multivariate Tests[a,b]

Effect		Sig.	Partial Eta Squared	Noncent. Parameter	Observed Power[e]
time	Pillai's Trace	,002	1,000	293260,667	1,000
	Wilks' Lambda	,002	1,000	293260,667	1,000
	Hotelling's Trace	,002	1,000	293260,667	1,000
	Roy's Largest Root	,002	1,000	293260,667	1,000
lightcolour	Pillai's Trace	,041	,998	588,906	,775
	Wilks' Lambda	,041	,998	588,906	,775
	Hotelling's Trace	,041	,998	588,906	,775
	Roy's Largest Root	,041	,998	588,906	,775
time * lightcolour	Pillai's Trace	.	.	.	.
	Wilks' Lambda	.	.	.	.
	Hotelling's Trace	.	.	.	.
	Roy's Largest Root	.	.	.	.

a. Temperature = 3,00

b. Design: Intercept
Within Subjects Design: time + lightcolour + time * lightcolour

c. Exact statistic

d. Cannot produce multivariate test statistics because of insufficient residual degrees of freedom.

e. Computed using alpha = ,05

Mauchly's Test of Sphericity[a,b]

Measure: MEASURE_1

Within Subjects Effect	Mauchly's W	Approx. Chi-Square	df	Sig.	Epsilon[c] Greenhouse-Geisser
time	,000	8,140	2	,017	,500
lightcolour	,156	1,858	2	,395	,542
time * lightcolour	,000	.	9	.	,323

Mauchly's Test of Sphericity[a,b]

Measure: MEASURE_1

Within Subjects Effect	Epsilon[c] Huynh-Feldt	Lower-bound
time	,500	,500
lightcolour	,685	,500
time * lightcolour	,666	,250

Tests the null hypothesis that the error covariance matrix of the orthonormalized transformed dependent variables is proportional to an identity matrix.

a. Temperature = 3,00

b. Design: Intercept
Within Subjects Design: time + lightcolour + time * lightcolour

c. May be used to adjust the degrees of freedom for the averaged tests of significance. Corrected tests are displayed in the Tests of Within-Subjects Effects table.

Tests of Within-Subjects Effects[a]

Measure: MEASURE_1

Source		Type III Sum of Squares	df	Mean Square
time	Sphericity Assumed	7,944	2	3,972
	Greenhouse-Geisser	7,944	1,000	7,943
	Huynh-Feldt	7,944	1,001	7,939
	Lower-bound	7,944	1,000	7,944
Error(time)	Sphericity Assumed	,004	4	,001
	Greenhouse-Geisser	,004	2,000	,002
	Huynh-Feldt	,004	2,001	,002
	Lower-bound	,004	2,000	,002
lightcolour	Sphericity Assumed	,843	2	,421
	Greenhouse-Geisser	,843	1,085	,777
	Huynh-Feldt	,843	1,369	,615
	Lower-bound	,843	1,000	,843
Error(lightcolour)	Sphericity Assumed	,019	4	,005
	Greenhouse-Geisser	,019	2,169	,009
	Huynh-Feldt	,019	2,739	,007
	Lower-bound	,019	2,000	,010
time * lightcolour	Sphericity Assumed	,350	4	,087
	Greenhouse-Geisser	,350	1,294	,271
	Huynh-Feldt	,350	2,665	,131
	Lower-bound	,350	1,000	,350
Error(time*lightcolour)	Sphericity Assumed	,012	8	,002
	Greenhouse-Geisser	,012	2,588	,005
	Huynh-Feldt	,012	5,329	,002
	Lower-bound	,012	2,000	,006

Tests of Within-Subjects Effects[a]

Measure: MEASURE_1

Source		F	Sig.	Partial Eta Squared
time	Sphericity Assumed	4069,894	,000	1,000
	Greenhouse-Geisser	4069,894	,000	1,000
	Huynh-Feldt	4069,894	,000	1,000
	Lower-bound	4069,894	,000	1,000
Error(time)	Sphericity Assumed			
	Greenhouse-Geisser			
	Huynh-Feldt			
	Lower-bound			
lightcolour	Sphericity Assumed	86,798	,001	,977
	Greenhouse-Geisser	86,798	,009	,977
	Huynh-Feldt	86,798	,004	,977
	Lower-bound	86,798	,011	,977
Error(lightcolour)	Sphericity Assumed			
	Greenhouse-Geisser			
	Huynh-Feldt			
	Lower-bound			
time * lightcolour	Sphericity Assumed	57,030	,000	,966
	Greenhouse-Geisser	57,030	,008	,966
	Huynh-Feldt	57,030	,000	,966
	Lower-bound	57,030	,017	,966
Error(time*lightcolour)	Sphericity Assumed			
	Greenhouse-Geisser			
	Huynh-Feldt			
	Lower-bound			

Tests of Within-Subjects Effects[a]

Measure: MEASURE_1

Source		Noncent. Parameter	Observed Power[b]
time	Sphericity Assumed	8139,787	1,000
	Greenhouse-Geisser	4070,487	1,000
	Huynh-Feldt	4072,268	1,000
	Lower-bound	4069,894	1,000
Error(time)	Sphericity Assumed		
	Greenhouse-Geisser		
	Huynh-Feldt		
	Lower-bound		
lightcolour	Sphericity Assumed	173,596	1,000
	Greenhouse-Geisser	94,138	,994
	Huynh-Feldt	118,869	1,000
	Lower-bound	86,798	,986
Error(lightcolour)	Sphericity Assumed		
	Greenhouse-Geisser		
	Huynh-Feldt		
	Lower-bound		
time * lightcolour	Sphericity Assumed	228,118	1,000
	Greenhouse-Geisser	73,788	,991
	Huynh-Feldt	151,958	1,000
	Lower-bound	57,030	,941
Error(time*lightcolour)	Sphericity Assumed		
	Greenhouse-Geisser		
	Huynh-Feldt		
	Lower-bound		

a. Temperature = 3,00

b. Computed using alpha = ,05

Tests of Within-Subjects Contrasts[a]

Measure: MEASURE_1

Source	time	lightcolour	Type III Sum of Squares	df	Mean Square
time	Linear		2,596	1	2,596
	Quadratic		,052	1	,052
Error(time)	Linear		,001	2	,001
	Quadratic		7,531E-5	2	3,765E-5
lightcolour		Level 2 vs. Level 1	,303	1	,303
		Level 3 vs. Level 1	1,673	1	1,673
Error(lightcolour)		Level 2 vs. Level 1	,034	2	,017
		Level 3 vs. Level 1	,021	2	,011
time * lightcolour	Linear	Level 2 vs. Level 1	,045	1	,045
		Level 3 vs. Level 1	,634	1	,634
	Quadratic	Level 2 vs. Level 1	,000	1	,000
		Level 3 vs. Level 1	,013	1	,013
Error(time*lightcolour)	Linear	Level 2 vs. Level 1	,003	2	,002
		Level 3 vs. Level 1	,011	2	,006
	Quadratic	Level 2 vs. Level 1	,003	2	,002
		Level 3 vs. Level 1	,010	2	,005

Tests of Within-Subjects Contrasts[a]

Measure: MEASURE_1

Source	time	lightcolour	F	Sig.	Partial Eta Squared
time	Linear		4235,215	,000	1,000
	Quadratic		1378,689	,001	,999
Error(time)	Linear				
	Quadratic				
lightcolour		Level 2 vs. Level 1	17,899	,052	,899
		Level 3 vs. Level 1	156,653	,006	,987
Error(lightcolour)		Level 2 vs. Level 1			
		Level 3 vs. Level 1			
time * lightcolour	Linear	Level 2 vs. Level 1	26,252	,036	,929
		Level 3 vs. Level 1	114,189	,009	,983
	Quadratic	Level 2 vs. Level 1	,129	,754	,061
		Level 3 vs. Level 1	2,579	,250	,563
Error(time*lightcolour)	Linear	Level 2 vs. Level 1			
		Level 3 vs. Level 1			
	Quadratic	Level 2 vs. Level 1			
		Level 3 vs. Level 1			

Tests of Within-Subjects Contrasts[a]

Measure: MEASURE_1

Source	time	lightcolour	Noncent. Parameter	Observed Power[b]
time	Linear		4235,215	1,000
	Quadratic		1378,689	1,000
Error(time)	Linear			
	Quadratic			
lightcolour		Level 2 vs. Level 1	17,899	,603
		Level 3 vs. Level 1	156,653	1,000
Error(lightcolour)		Level 2 vs. Level 1		
		Level 3 vs. Level 1		
time * lightcolour	Linear	Level 2 vs. Level 1	26,252	,736
		Level 3 vs. Level 1	114,189	,996
	Quadratic	Level 2 vs. Level 1	,129	,056
		Level 3 vs. Level 1	2,579	,162
Error(time*lightcolour)	Linear	Level 2 vs. Level 1		
		Level 3 vs. Level 1		
	Quadratic	Level 2 vs. Level 1		
		Level 3 vs. Level 1		

a. Temperature = 3,00

b. Computed using alpha = ,05

Tests of Between-Subjects Effects[a]

Measure: MEASURE_1

Transformed Variable: Average

Source	Type III Sum of Squares	df	Mean Square	F	Sig.	Partial Eta Squared
Intercept	10,212	1	10,212	2750,707	,000	,999
Error	,007	2	,004			

Tests of Between-Subjects Effects[a]

Measure: MEASURE_1

Transformed Variable: Average

Source	Noncent. Parameter	Observed Power[b]
Intercept	2750,707	1,000
Error		

a. Temperature = 3,00

b. Computed using alpha = ,05

```
GLM FA_red_T1 FA_green_T1 FA_blue_T1 FA_red_T2 FA_green_T2 FA_blue_T2 FA_red_T3 FA_green_T3 FA_blue_T3
  /WSFACTOR=time 3 Polynomial lightcolour 3 Simple(1)
  /METHOD=SSTYPE(3)
  /PRINT=DESCRIPTIVE ETASQ OPOWER
  /CRITERIA=ALPHA(.05)
  /WSDESIGN=time lightcolour time*lightcolour.
```

General Linear Model

Notes

Output Created		28-FEB-2021 15:03:45
Comments		
Input	Data	C:\Users\Frieda\Downloads\Mark\Data.sav
	Active Dataset	DataSet1
	Filter	<none>
	Weight	<none>
	Split File	Temperature
	N of Rows in Working Data File	9
Missing Value Handling	Definition of Missing	User-defined missing values are treated as missing.
	Cases Used	Statistics are based on all cases with valid data for all variables in the model.
Syntax		GLM FA_red_T1 FA_green_T1 FA_blue_T1 FA_red_T2 FA_green_T2 FA_blue_T2 FA_red_T3 FA_green_T3 FA_blue_T3 /WSFACTOR=time 3 Polynomial lightcolour 3 Simple(1) /METHOD=SSTYPE(3) /PRINT=DESCRIPTIVE ETASQ OPOWER /CRITERIA=ALPHA(.05) /WSDESIGN=time lightcolour time*lightcolour.
Resources	Processor Time	00:00:00,06
	Elapsed Time	00:00:00,06

Within-Subjects Factors

Measure: MEASURE_1

time	lightcolour	Dependent Variable
1	1	FA_red_T1
	2	FA_green_T1
	3	FA_blue_T1
2	1	FA_red_T2
	2	FA_green_T2
	3	FA_blue_T2
3	1	FA_red_T3
	2	FA_green_T3
	3	FA_blue_T3

Temperature = 1,00

Between-Subjects Factors[a]

a. Temperature = 1,00

Descriptive Statistics[a]

	Mean	Std. Deviation	N
FA_red_T1	20,5894	,63431	3
FA_green_T1	26,2144	3,82042	3
FA_blue_T1	23,7375	4,16058	3
FA_red_T2	14,6660	,41779	3
FA_green_T2	20,9458	,39310	3
FA_blue_T2	20,1901	,15935	3
FA_red_T3	12,5158	,05514	3
FA_green_T3	19,4401	,44268	3
FA_blue_T3	18,0007	,29083	3

a. Temperature = 1,00

Multivariate Tests[a,b]

Effect		Value	F	Hypothesis df	Error df
time	Pillai's Trace	1,000	2884,336[c]	2,000	1,000
	Wilks' Lambda	,000	2884,336[c]	2,000	1,000
	Hotelling's Trace	5768,673	2884,336[c]	2,000	1,000
	Roy's Largest Root	5768,673	2884,336[c]	2,000	1,000
lightcolour	Pillai's Trace	,995	100,812[c]	2,000	1,000
	Wilks' Lambda	,005	100,812[c]	2,000	1,000
	Hotelling's Trace	201,624	100,812[c]	2,000	1,000
	Roy's Largest Root	201,624	100,812[c]	2,000	1,000
time * lightcolour	Pillai's Trace	.[d]	.	.	.
	Wilks' Lambda	.[d]	.	.	.
	Hotelling's Trace	.[d]	.	.	.
	Roy's Largest Root	.[d]	.	.	.

Multivariate Tests[a,b]

Effect		Sig.	Partial Eta Squared	Noncent. Parameter	Observed Power[e]
time	Pillai's Trace	,013	1,000	5768,673	1,000
	Wilks' Lambda	,013	1,000	5768,673	1,000
	Hotelling's Trace	,013	1,000	5768,673	1,000
	Roy's Largest Root	,013	1,000	5768,673	1,000
lightcolour	Pillai's Trace	,070	,995	201,624	,523
	Wilks' Lambda	,070	,995	201,624	,523
	Hotelling's Trace	,070	,995	201,624	,523
	Roy's Largest Root	,070	,995	201,624	,523
time * lightcolour	Pillai's Trace	.	.	.	.
	Wilks' Lambda	.	.	.	.
	Hotelling's Trace	.	.	.	.
	Roy's Largest Root	.	.	.	.

a. Temperature = 1,00

b. Design: Intercept
Within Subjects Design: time + lightcolour + time * lightcolour

c. Exact statistic

d. Cannot produce multivariate test statistics because of insufficient residual degrees of freedom.

e. Computed using alpha = ,05

Mauchly's Test of Sphericity[a,b]

Measure: MEASURE_1

Within Subjects Effect	Mauchly's W	Approx. Chi-Square	df	Sig.	Epsilon[c] Greenhouse-Geisser
time	,001	6,520	2	,038	,500
lightcolour	,160	1,835	2	,400	,543
time * lightcolour	,000	.	9	.	,325

Mauchly's Test of Sphericity[a,b]

Measure: MEASURE_1

Within Subjects Effect	Epsilon[c] Huynh-Feldt	Lower-bound
time	,501	,500
lightcolour	,690	,500
time * lightcolour	,682	,250

Tests the null hypothesis that the error covariance matrix of the orthonormalized transformed dependent variables is proportional to an identity matrix.

a. Temperature = 1,00

b. Design: Intercept
Within Subjects Design: time + lightcolour + time * lightcolour

c. May be used to adjust the degrees of freedom for the averaged tests of significance. Corrected tests are displayed in the Tests of Within-Subjects Effects table.

Tests of Within-Subjects Effects[a]

Measure: MEASURE_1

Source		Type III Sum of Squares	df	Mean Square	F
time	Sphericity Assumed	225,049	2	112,525	45,487
	Greenhouse-Geisser	225,049	1,001	224,884	45,487
	Huynh-Feldt	225,049	1,003	224,387	45,487
	Lower-bound	225,049	1,000	225,049	45,487
Error(time)	Sphericity Assumed	9,895	4	2,474	
	Greenhouse-Geisser	9,895	2,001	4,944	
	Huynh-Feldt	9,895	2,006	4,933	
	Lower-bound	9,895	2,000	4,948	
lightcolour	Sphericity Assumed	192,262	2	96,131	18,545
	Greenhouse-Geisser	192,262	1,087	176,915	18,545
	Huynh-Feldt	192,262	1,380	139,325	18,545
	Lower-bound	192,262	1,000	192,262	18,545
Error(lightcolour)	Sphericity Assumed	20,735	4	5,184	
	Greenhouse-Geisser	20,735	2,173	9,540	
	Huynh-Feldt	20,735	2,760	7,513	
	Lower-bound	20,735	2,000	10,367	
time * lightcolour	Sphericity Assumed	6,049	4	1,512	,414
	Greenhouse-Geisser	6,049	1,302	4,647	,414
	Huynh-Feldt	6,049	2,728	2,218	,414
	Lower-bound	6,049	1,000	6,049	,414
Error(time*lightcolour)	Sphericity Assumed	29,227	8	3,653	
	Greenhouse-Geisser	29,227	2,603	11,227	
	Huynh-Feldt	29,227	5,455	5,357	
	Lower-bound	29,227	2,000	14,613	

Tests of Within-Subjects Effects[a]

Measure: MEASURE_1

Source		Sig.	Partial Eta Squared	Noncent. Parameter
time	Sphericity Assumed	,002	,958	90,974
	Greenhouse-Geisser	,021	,958	45,520
	Huynh-Feldt	,021	,958	45,621
	Lower-bound	,021	,958	45,487
Error(time)	Sphericity Assumed			
	Greenhouse-Geisser			
	Huynh-Feldt			
	Lower-bound			
lightcolour	Sphericity Assumed	,009	,903	37,090
	Greenhouse-Geisser	,043	,903	20,154
	Huynh-Feldt	,026	,903	25,591
	Lower-bound	,050	,903	18,545
Error(lightcolour)	Sphericity Assumed			
	Greenhouse-Geisser			
	Huynh-Feldt			
	Lower-bound			
time * lightcolour	Sphericity Assumed	,794	,171	1,656
	Greenhouse-Geisser	,623	,171	,539
	Huynh-Feldt	,734	,171	1,129
	Lower-bound	,586	,171	,414
Error(time*lightcolour)	Sphericity Assumed			
	Greenhouse-Geisser			
	Huynh-Feldt			
	Lower-bound			

Tests of Within-Subjects Effects[a]

Measure: MEASURE_1

Source		Observed Power[b]
time	Sphericity Assumed	1,000
	Greenhouse-Geisser	,897
	Huynh-Feldt	,898
	Lower-bound	,897
Error(time)	Sphericity Assumed	
	Greenhouse-Geisser	
	Huynh-Feldt	
	Lower-bound	
lightcolour	Sphericity Assumed	,945
	Greenhouse-Geisser	,664
	Huynh-Feldt	,799
	Lower-bound	,615
Error(lightcolour)	Sphericity Assumed	
	Greenhouse-Geisser	
	Huynh-Feldt	
	Lower-bound	
time * lightcolour	Sphericity Assumed	,105
	Greenhouse-Geisser	,074
	Huynh-Feldt	,092
	Lower-bound	,069
Error(time*lightcolour)	Sphericity Assumed	
	Greenhouse-Geisser	
	Huynh-Feldt	
	Lower-bound	

a. Temperature = 1,00

b. Computed using alpha = ,05

Tests of Within-Subjects Contrasts[a]

Measure: MEASURE_1

Source	time	lightcolour	Type III Sum of Squares	df	Mean Square
time	Linear		70,622	1	70,622
	Quadratic		4,395	1	4,395
Error(time)	Linear		2,383	2	1,192
	Quadratic		,915	2	,458
lightcolour		Level 2 vs. Level 1	354,535	1	354,535
		Level 3 vs. Level 1	200,424	1	200,424
Error(lightcolour)		Level 2 vs. Level 1	13,940	2	6,970
		Level 3 vs. Level 1	8,759	2	4,379
time * lightcolour	Linear	Level 2 vs. Level 1	2,532	1	2,532
		Level 3 vs. Level 1	8,192	1	8,192
	Quadratic	Level 2 vs. Level 1	5,360E-5	1	5,360E-5
		Level 3 vs. Level 1	2,917	1	2,917
Error(time*lightcolour)	Linear	Level 2 vs. Level 1	13,243	2	6,621
		Level 3 vs. Level 1	10,631	2	5,315
	Quadratic	Level 2 vs. Level 1	6,737	2	3,368
		Level 3 vs. Level 1	6,362	2	3,181

Tests of Within-Subjects Contrasts[a]

Measure: MEASURE_1

Source	time	lightcolour	F	Sig.	Partial Eta Squared
time	Linear		59,264	,016	,967
	Quadratic		9,605	,090	,828
Error(time)	Linear				
	Quadratic				
lightcolour		Level 2 vs. Level 1	50,865	,019	,962
		Level 3 vs. Level 1	45,766	,021	,958
Error(lightcolour)		Level 2 vs. Level 1			
		Level 3 vs. Level 1			
time * lightcolour	Linear	Level 2 vs. Level 1	,382	,599	,161
		Level 3 vs. Level 1	1,541	,340	,435
	Quadratic	Level 2 vs. Level 1	,000	,997	,000
		Level 3 vs. Level 1	,917	,439	,314
Error(time*lightcolour)	Linear	Level 2 vs. Level 1			
		Level 3 vs. Level 1			
	Quadratic	Level 2 vs. Level 1			
		Level 3 vs. Level 1			

Tests of Within-Subjects Contrasts[a]

Measure: MEASURE_1

Source	time	lightcolour	Noncent. Parameter	Observed Power[b]
time	Linear		59,264	,947
	Quadratic		9,605	,405
Error(time)	Linear			
	Quadratic			
lightcolour		Level 2 vs. Level 1	50,865	,920
		Level 3 vs. Level 1	45,766	,898
Error(lightcolour)		Level 2 vs. Level 1		
		Level 3 vs. Level 1		
time * lightcolour	Linear	Level 2 vs. Level 1	,382	,068
		Level 3 vs. Level 1	1,541	,119
	Quadratic	Level 2 vs. Level 1	,000	,050
		Level 3 vs. Level 1	,917	,092
Error(time*lightcolour)	Linear	Level 2 vs. Level 1		
		Level 3 vs. Level 1		
	Quadratic	Level 2 vs. Level 1		
		Level 3 vs. Level 1		

a. Temperature = 1,00

b. Computed using alpha = ,05

Tests of Between-Subjects Effects[a]

Measure: MEASURE_1

Transformed Variable: Average

Source	Type III Sum of Squares	df	Mean Square	F	Sig.	Partial Eta Squared
Intercept	3453,516	1	3453,516	3432,909	,000	,999
Error	2,012	2	1,006			

Tests of Between-Subjects Effects[a]

Measure: MEASURE_1

Transformed Variable: Average

Source	Noncent. Parameter	Observed Power[b]
Intercept	3432,909	1,000
Error		

a. Temperature = 1,00

b. Computed using alpha = ,05

Temperature = 2,00

Between-Subjects Factors[a]

a. Temperature = 2,00

Descriptive Statistics[a]

	Mean	Std. Deviation	N
FA_red_T1	28,4008	1,56241	3
FA_green_T1	33,3962	,91956	3
FA_blue_T1	33,9708	,33144	3
FA_red_T2	27,5088	,40067	3
FA_green_T2	34,4777	,16659	3
FA_blue_T2	34,3234	,36182	3
FA_red_T3	23,4384	,05918	3
FA_green_T3	32,9734	,21343	3
FA_blue_T3	31,6424	,29431	3

a. Temperature = 2,00

Multivariate Tests[a,b]

Effect		Value	F	Hypothesis df	Error df
time	Pillai's Trace	1,000	106872,031[c]	2,000	1,000
	Wilks' Lambda	,000	106872,031[c]	2,000	1,000
	Hotelling's Trace	213744,062	106872,031[c]	2,000	1,000
	Roy's Largest Root	213744,062	106872,031[c]	2,000	1,000
lightcolour	Pillai's Trace	,997	183,248[c]	2,000	1,000
	Wilks' Lambda	,003	183,248[c]	2,000	1,000
	Hotelling's Trace	366,497	183,248[c]	2,000	1,000
	Roy's Largest Root	366,497	183,248[c]	2,000	1,000
time * lightcolour	Pillai's Trace	.[d]	.	.	.
	Wilks' Lambda	.[d]	.	.	.
	Hotelling's Trace	.[d]	.	.	.
	Roy's Largest Root	.[d]	.	.	.

Multivariate Tests[a,b]

Effect		Sig.	Partial Eta Squared	Noncent. Parameter	Observed Power[e]
time	Pillai's Trace	,002	1,000	213744,062	1,000
	Wilks' Lambda	,002	1,000	213744,062	1,000
	Hotelling's Trace	,002	1,000	213744,062	1,000
	Roy's Largest Root	,002	1,000	213744,062	1,000
lightcolour	Pillai's Trace	,052	,997	366,497	,662
	Wilks' Lambda	,052	,997	366,497	,662
	Hotelling's Trace	,052	,997	366,497	,662
	Roy's Largest Root	,052	,997	366,497	,662
time * lightcolour	Pillai's Trace	.	.	.	.
	Wilks' Lambda	.	.	.	.
	Hotelling's Trace	.	.	.	.
	Roy's Largest Root	.	.	.	.

a. Temperature = 2,00

b. Design: Intercept
Within Subjects Design: time + lightcolour + time * lightcolour

c. Exact statistic

d. Cannot produce multivariate test statistics because of insufficient residual degrees of freedom.

e. Computed using alpha = ,05

Mauchly's Test of Sphericity[a,b]

Measure: MEASURE_1

Within Subjects Effect	Mauchly's W	Approx. Chi-Square	df	Sig.	Epsilon[c] Greenhouse-Geisser
time	,000	8,510	2	,014	,500
lightcolour	,606	,501	2	,778	,717
time * lightcolour	,000	.	9	.	,292

Mauchly's Test of Sphericity[a,b]

Measure: MEASURE_1

Within Subjects Effect	Epsilon[c] Huynh-Feldt	Lower-bound
time	,500	,500
lightcolour	1,000	,500
time * lightcolour	,450	,250

Tests the null hypothesis that the error covariance matrix of the orthonormalized transformed dependent variables is proportional to an identity matrix.

a. Temperature = 2,00

b. Design: Intercept
Within Subjects Design: time + lightcolour + time * lightcolour

c. May be used to adjust the degrees of freedom for the averaged tests of significance. Corrected tests are displayed in the Tests of Within-Subjects Effects table.

Tests of Within-Subjects Effects[a]

Measure: MEASURE_1

Source		Type III Sum of Squares	df	Mean Square	F
time	Sphericity Assumed	42,650	2	21,325	30,923
	Greenhouse-Geisser	42,650	1,000	42,645	30,923
	Huynh-Feldt	42,650	1,000	42,632	30,923
	Lower-bound	42,650	1,000	42,650	30,923
Error(time)	Sphericity Assumed	2,758	4	,690	
	Greenhouse-Geisser	2,758	2,000	1,379	
	Huynh-Feldt	2,758	2,001	1,379	
	Lower-bound	2,758	2,000	1,379	
lightcolour	Sphericity Assumed	295,649	2	147,824	308,400
	Greenhouse-Geisser	295,649	1,435	206,080	308,400
	Huynh-Feldt	295,649	2,000	147,824	308,400
	Lower-bound	295,649	1,000	295,649	308,400
Error(lightcolour)	Sphericity Assumed	1,917	4	,479	
	Greenhouse-Geisser	1,917	2,869	,668	
	Huynh-Feldt	1,917	4,000	,479	
	Lower-bound	1,917	2,000	,959	
time * lightcolour	Sphericity Assumed	15,684	4	3,921	16,587
	Greenhouse-Geisser	15,684	1,167	13,442	16,587
	Huynh-Feldt	15,684	1,800	8,711	16,587
	Lower-bound	15,684	1,000	15,684	16,587
Error(time*lightcolour)	Sphericity Assumed	1,891	8	,236	
	Greenhouse-Geisser	1,891	2,333	,810	
	Huynh-Feldt	1,891	3,601	,525	
	Lower-bound	1,891	2,000	,946	

Tests of Within-Subjects Effects[a]

Measure: MEASURE_1

Source		Sig.	Partial Eta Squared	Noncent. Parameter
time	Sphericity Assumed	,004	,939	61,847
	Greenhouse-Geisser	,031	,939	30,926
	Huynh-Feldt	,031	,939	30,936
	Lower-bound	,031	,939	30,923
Error(time)	Sphericity Assumed			
	Greenhouse-Geisser			
	Huynh-Feldt			
	Lower-bound			
lightcolour	Sphericity Assumed	,000	,994	616,800
	Greenhouse-Geisser	,000	,994	442,440
	Huynh-Feldt	,000	,994	616,800
	Lower-bound	,003	,994	308,400
Error(lightcolour)	Sphericity Assumed			
	Greenhouse-Geisser			
	Huynh-Feldt			
	Lower-bound			
time * lightcolour	Sphericity Assumed	,001	,892	66,347
	Greenhouse-Geisser	,042	,892	19,352
	Huynh-Feldt	,016	,892	29,863
	Lower-bound	,055	,892	16,587
Error(time*lightcolour)	Sphericity Assumed			
	Greenhouse-Geisser			
	Huynh-Feldt			
	Lower-bound			

Tests of Within-Subjects Effects[a]

Measure: MEASURE_1

Source		Observed Power[b]
time	Sphericity Assumed	,995
	Greenhouse-Geisser	,790
	Huynh-Feldt	,790
	Lower-bound	,790
Error(time)	Sphericity Assumed	
	Greenhouse-Geisser	
	Huynh-Feldt	
	Lower-bound	
lightcolour	Sphericity Assumed	1,000
	Greenhouse-Geisser	1,000
	Huynh-Feldt	1,000
	Lower-bound	1,000
Error(lightcolour)	Sphericity Assumed	
	Greenhouse-Geisser	
	Huynh-Feldt	
	Lower-bound	
time * lightcolour	Sphericity Assumed	,999
	Greenhouse-Geisser	,665
	Huynh-Feldt	,885
	Lower-bound	,577
Error(time*lightcolour)	Sphericity Assumed	
	Greenhouse-Geisser	
	Huynh-Feldt	
	Lower-bound	

a. Temperature = 2,00

b. Computed using alpha = ,05

Tests of Within-Subjects Contrasts[a]

Measure: MEASURE_1

Source	time	lightcolour	Type III Sum of Squares	df	Mean Square
time	Linear		9,917	1	9,917
	Quadratic		4,300	1	4,300
Error(time)	Linear		,777	2	,388
	Quadratic		,143	2	,071
lightcolour		Level 2 vs. Level 1	462,225	1	462,225
		Level 3 vs. Level 1	423,892	1	423,892
Error(lightcolour)		Level 2 vs. Level 1	1,330	2	,665
		Level 3 vs. Level 1	3,121	2	1,560
time * lightcolour	Linear	Level 2 vs. Level 1	30,911	1	30,911
		Level 3 vs. Level 1	10,407	1	10,407
	Quadratic	Level 2 vs. Level 1	,176	1	,176
		Level 3 vs. Level 1	,011	1	,011
Error(time*lightcolour)	Linear	Level 2 vs. Level 1	,649	2	,325
		Level 3 vs. Level 1	3,081	2	1,540
	Quadratic	Level 2 vs. Level 1	,252	2	,126
		Level 3 vs. Level 1	,597	2	,299

Tests of Within-Subjects Contrasts[a]

Measure: MEASURE_1

Source	time	lightcolour	F	Sig.	Partial Eta Squared
time	Linear		25,532	,037	,927
	Quadratic		60,278	,016	,968
Error(time)	Linear				
	Quadratic				
lightcolour		Level 2 vs. Level 1	695,241	,001	,997
		Level 3 vs. Level 1	271,655	,004	,993
Error(lightcolour)		Level 2 vs. Level 1			
		Level 3 vs. Level 1			
time * lightcolour	Linear	Level 2 vs. Level 1	95,256	,010	,979
		Level 3 vs. Level 1	6,756	,122	,772
	Quadratic	Level 2 vs. Level 1	1,393	,359	,411
		Level 3 vs. Level 1	,035	,869	,017
Error(time*lightcolour)	Linear	Level 2 vs. Level 1			
		Level 3 vs. Level 1			
	Quadratic	Level 2 vs. Level 1			
		Level 3 vs. Level 1			

Tests of Within-Subjects Contrasts[a]

Measure: MEASURE_1

Source	time	lightcolour	Noncent. Parameter	Observed Power[b]
time	Linear		25,532	,726
	Quadratic		60,278	,950
Error(time)	Linear			
	Quadratic			
lightcolour		Level 2 vs. Level 1	695,241	1,000
		Level 3 vs. Level 1	271,655	1,000
Error(lightcolour)		Level 2 vs. Level 1		
		Level 3 vs. Level 1		
time * lightcolour	Linear	Level 2 vs. Level 1	95,256	,991
		Level 3 vs. Level 1	6,756	,317
	Quadratic	Level 2 vs. Level 1	1,393	,112
		Level 3 vs. Level 1	,035	,052
Error(time*lightcolour)	Linear	Level 2 vs. Level 1		
		Level 3 vs. Level 1		
	Quadratic	Level 2 vs. Level 1		
		Level 3 vs. Level 1		

a. Temperature = 2,00

b. Computed using alpha = ,05

Tests of Between-Subjects Effects[a]

Measure: MEASURE_1

Transformed Variable: Average

Source	Type III Sum of Squares	df	Mean Square	F	Sig.	Partial Eta Squared
Intercept	8719,315	1	8719,315	46048,900	,000	1,000
Error	,379	2	,189			

Tests of Between-Subjects Effects[a]

Measure: MEASURE_1

Transformed Variable: Average

Source	Noncent. Parameter	Observed Power[b]
Intercept	46048,900	1,000
Error		

a. Temperature = 2,00

b. Computed using alpha = ,05

Temperature = 3,00

Between-Subjects Factors[a]

a. Temperature = 3,00

Descriptive Statistics[a]

	Mean	Std. Deviation	N
FA_red_T1	17,5646	,54405	3
FA_green_T1	21,2814	,62141	3
FA_blue_T1	19,0762	,17063	3
FA_red_T2	11,2283	,27005	3
FA_green_T2	15,2246	,46845	3
FA_blue_T2	14,2655	3,29286	3
FA_red_T3	13,9476	1,07250	3
FA_green_T3	16,5690	,13421	3
FA_blue_T3	14,3361	1,50780	3

a. Temperature = 3,00

Multivariate Tests[a,b]

Effect		Value	F	Hypothesis df	Error df
time	Pillai's Trace	1,000	1354,119[c]	2,000	1,000
	Wilks' Lambda	,000	1354,119[c]	2,000	1,000
	Hotelling's Trace	2708,238	1354,119[c]	2,000	1,000
	Roy's Largest Root	2708,238	1354,119[c]	2,000	1,000
lightcolour	Pillai's Trace	,998	226,330[c]	2,000	1,000
	Wilks' Lambda	,002	226,330[c]	2,000	1,000
	Hotelling's Trace	452,661	226,330[c]	2,000	1,000
	Roy's Largest Root	452,661	226,330[c]	2,000	1,000
time * lightcolour	Pillai's Trace	.[d]	.	.	.
	Wilks' Lambda	.[d]	.	.	.
	Hotelling's Trace	.[d]	.	.	.
	Roy's Largest Root	.[d]	.	.	.

Multivariate Tests[a,b]

Effect		Sig.	Partial Eta Squared	Noncent. Parameter	Observed Power[e]
time	Pillai's Trace	,019	1,000	2708,238	,991
	Wilks' Lambda	,019	1,000	2708,238	,991
	Hotelling's Trace	,019	1,000	2708,238	,991
	Roy's Largest Root	,019	1,000	2708,238	,991
lightcolour	Pillai's Trace	,047	,998	452,661	,713
	Wilks' Lambda	,047	,998	452,661	,713
	Hotelling's Trace	,047	,998	452,661	,713
	Roy's Largest Root	,047	,998	452,661	,713
time * lightcolour	Pillai's Trace	.	.	.	.
	Wilks' Lambda	.	.	.	.
	Hotelling's Trace	.	.	.	.
	Roy's Largest Root	.	.	.	.

a. Temperature = 3,00

b. Design: Intercept
Within Subjects Design: time + lightcolour + time * lightcolour

c. Exact statistic

d. Cannot produce multivariate test statistics because of insufficient residual degrees of freedom.

e. Computed using alpha = ,05

Mauchly's Test of Sphericity[a,b]

Measure: MEASURE_1

Within Subjects Effect	Mauchly's W	Approx. Chi-Square	df	Sig.	Epsilon[c] Greenhouse-Geisser
time	,022	3,805	2	,149	,506
lightcolour	,070	2,664	2	,264	,518
time * lightcolour	,000	.	9	.	,377

Mauchly's Test of Sphericity[a,b]

Measure: MEASURE_1

	Epsilon[c]	
Within Subjects Effect	Huynh-Feldt	Lower-bound
time	,523	,500
lightcolour	,575	,500
time * lightcolour	1,000	,250

Tests the null hypothesis that the error covariance matrix of the orthonormalized transformed dependent variables is proportional to an identity matrix.

a. Temperature = 3,00

b. Design: Intercept
Within Subjects Design: time + lightcolour + time * lightcolour

c. May be used to adjust the degrees of freedom for the averaged tests of significance. Corrected tests are displayed in the Tests of Within-Subjects Effects table.

Tests of Within-Subjects Effects[a]

Measure: MEASURE_1

Source		Type III Sum of Squares	df	Mean Square	F
time	Sphericity Assumed	161,292	2	80,646	47,962
	Greenhouse-Geisser	161,292	1,011	159,496	47,962
	Huynh-Feldt	161,292	1,046	154,266	47,962
	Lower-bound	161,292	1,000	161,292	47,962
Error(time)	Sphericity Assumed	6,726	4	1,681	
	Greenhouse-Geisser	6,726	2,023	3,325	
	Huynh-Feldt	6,726	2,091	3,216	
	Lower-bound	6,726	2,000	3,363	
lightcolour	Sphericity Assumed	53,437	2	26,718	16,103
	Greenhouse-Geisser	53,437	1,036	51,576	16,103
	Huynh-Feldt	53,437	1,150	46,479	16,103
	Lower-bound	53,437	1,000	53,437	16,103
Error(lightcolour)	Sphericity Assumed	6,637	4	1,659	
	Greenhouse-Geisser	6,637	2,072	3,203	
	Huynh-Feldt	6,637	2,299	2,886	
	Lower-bound	6,637	2,000	3,318	
time * lightcolour	Sphericity Assumed	5,650	4	1,412	,705
	Greenhouse-Geisser	5,650	1,508	3,746	,705
	Huynh-Feldt	5,650	4,000	1,412	,705
	Lower-bound	5,650	1,000	5,650	,705
Error(time*lightcolour)	Sphericity Assumed	16,022	8	2,003	
	Greenhouse-Geisser	16,022	3,016	5,312	
	Huynh-Feldt	16,022	8,000	2,003	
	Lower-bound	16,022	2,000	8,011	

Tests of Within-Subjects Effects[a]

Measure: MEASURE_1

Source		Sig.	Partial Eta Squared	Noncent. Parameter
time	Sphericity Assumed	,002	,960	95,924
	Greenhouse-Geisser	,020	,960	48,502
	Huynh-Feldt	,018	,960	50,146
	Lower-bound	,020	,960	47,962
Error(time)	Sphericity Assumed			
	Greenhouse-Geisser			
	Huynh-Feldt			
	Lower-bound			
lightcolour	Sphericity Assumed	,012	,890	32,206
	Greenhouse-Geisser	,054	,890	16,684
	Huynh-Feldt	,045	,890	18,514
	Lower-bound	,057	,890	16,103
Error(lightcolour)	Sphericity Assumed			
	Greenhouse-Geisser			
	Huynh-Feldt			
	Lower-bound			
time * lightcolour	Sphericity Assumed	,610	,261	2,821
	Greenhouse-Geisser	,523	,261	1,064
	Huynh-Feldt	,610	,261	2,821
	Lower-bound	,489	,261	,705
Error(time*lightcolour)	Sphericity Assumed			
	Greenhouse-Geisser			
	Huynh-Feldt			
	Lower-bound			

Tests of Within-Subjects Effects[a]

Measure: MEASURE_1

Source		Observed Power[b]
time	Sphericity Assumed	1,000
	Greenhouse-Geisser	,913
	Huynh-Feldt	,926
	Lower-bound	,908
Error(time)	Sphericity Assumed	
	Greenhouse-Geisser	
	Huynh-Feldt	
	Lower-bound	
lightcolour	Sphericity Assumed	,915
	Greenhouse-Geisser	,586
	Huynh-Feldt	,646
	Lower-bound	,567
Error(lightcolour)	Sphericity Assumed	
	Greenhouse-Geisser	
	Huynh-Feldt	
	Lower-bound	
time * lightcolour	Sphericity Assumed	,149
	Greenhouse-Geisser	,096
	Huynh-Feldt	,149
	Lower-bound	,082
Error(time*lightcolour)	Sphericity Assumed	
	Greenhouse-Geisser	
	Huynh-Feldt	
	Lower-bound	

a. Temperature = 3,00

b. Computed using alpha = ,05

Tests of Within-Subjects Contrasts[a]

Measure: MEASURE_1

Source	time	lightcolour	Type III Sum of Squares	df	Mean Square
time	Linear		28,469	1	28,469
	Quadratic		25,295	1	25,295
Error(time)	Linear		,036	2	,018
	Quadratic		2,206	2	1,103
lightcolour		Level 2 vs. Level 1	106,803	1	106,803
		Level 3 vs. Level 1	24,376	1	24,376
Error(lightcolour)		Level 2 vs. Level 1	,331	2	,165
		Level 3 vs. Level 1	10,743	2	5,372
time * lightcolour	Linear	Level 2 vs. Level 1	1,800	1	1,800
		Level 3 vs. Level 1	1,892	1	1,892
	Quadratic	Level 2 vs. Level 1	1,369	1	1,369
		Level 3 vs. Level 1	8,712	1	8,712
Error(time*lightcolour)	Linear	Level 2 vs. Level 1	4,433	2	2,216
		Level 3 vs. Level 1	9,219	2	4,610
	Quadratic	Level 2 vs. Level 1	,766	2	,383
		Level 3 vs. Level 1	15,584	2	7,792

Tests of Within-Subjects Contrasts[a]

Measure: MEASURE_1

Source	time	lightcolour	F	Sig.	Partial Eta Squared
time	Linear		1602,430	,001	,999
	Quadratic		22,929	,041	,920
Error(time)	Linear				
	Quadratic				
lightcolour		Level 2 vs. Level 1	646,100	,002	,997
		Level 3 vs. Level 1	4,538	,167	,694
Error(lightcolour)		Level 2 vs. Level 1			
		Level 3 vs. Level 1			
time * lightcolour	Linear	Level 2 vs. Level 1	,812	,463	,289
		Level 3 vs. Level 1	,410	,587	,170
	Quadratic	Level 2 vs. Level 1	3,573	,199	,641
		Level 3 vs. Level 1	1,118	,401	,359
Error(time*lightcolour)	Linear	Level 2 vs. Level 1			
		Level 3 vs. Level 1			
	Quadratic	Level 2 vs. Level 1			
		Level 3 vs. Level 1			

Tests of Within-Subjects Contrasts[a]

Measure: MEASURE_1

Source	time	lightcolour	Noncent. Parameter	Observed Power[b]
time	Linear		1602,430	1,000
	Quadratic		22,929	,689
Error(time)	Linear			
	Quadratic			
lightcolour		Level 2 vs. Level 1	646,100	1,000
		Level 3 vs. Level 1	4,538	,239
Error(lightcolour)		Level 2 vs. Level 1		
		Level 3 vs. Level 1		
time * lightcolour	Linear	Level 2 vs. Level 1	,812	,087
		Level 3 vs. Level 1	,410	,069
	Quadratic	Level 2 vs. Level 1	3,573	,202
		Level 3 vs. Level 1	1,118	,100
Error(time*lightcolour)	Linear	Level 2 vs. Level 1		
		Level 3 vs. Level 1		
	Quadratic	Level 2 vs. Level 1		
		Level 3 vs. Level 1		

a. Temperature = 3,00

b. Computed using alpha = ,05

Tests of Between-Subjects Effects[a]

Measure: MEASURE_1

Transformed Variable: Average

Source	Type III Sum of Squares	df	Mean Square	F	Sig.	Partial Eta Squared
Intercept	2287,817	1	2287,817	11517,368	,000	1,000
Error	,397	2	,199			

Tests of Between-Subjects Effects[a]

Measure: MEASURE_1

Transformed Variable: Average

Source	Noncent. Parameter	Observed Power[b]
Intercept	11517,368	1,000
Error		

a. Temperature = 3,00

b. Computed using alpha = ,05

```
GLM Cis_iso_red_T1 Cis_iso_green_T1 Cis_iso_blue_T1 Cis_iso_red_T2 Cis_iso_
green_T2 Cis_iso_blue_T2 Cis_iso_red_T3 Cis_iso_green_T3 Cis_iso_blue_T3
  /WSFACTOR=time 3 Polynomial lightcolour 3 Simple(1)
  /METHOD=SSTYPE(3)
  /PRINT=DESCRIPTIVE ETASQ OPOWER
  /CRITERIA=ALPHA(.05)
  /WSDESIGN=time lightcolour time*lightcolour.
```

General Linear Model

Notes

Output Created		28-FEB-2021 15:03:46
Comments		
Input	Data	C:\Users\Frieda\Downloads\Mark\Data.sav
	Active Dataset	DataSet1
	Filter	<none>
	Weight	<none>
	Split File	Temperature
	N of Rows in Working Data File	9
Missing Value Handling	Definition of Missing	User-defined missing values are treated as missing.
	Cases Used	Statistics are based on all cases with valid data for all variables in the model.

Notes

Syntax		GLM Cis_iso_red_T1 Cis_iso_green_T1 Cis_iso_blue_T1 Cis_iso_red_T2 Cis_iso_green_T2 Cis_iso_blue_T2 Cis_iso_red_T3 Cis_iso_green_T3 Cis_iso_blue_T3 /WSFACTOR=time 3 Polynomial lightcolour 3 Simple(1) /METHOD=SSTYPE(3) /PRINT=DESCRIPTIVE ETASQ OPOWER /CRITERIA=ALPHA(.05) /WSDESIGN=time lightcolour time*lightcolour.
Resources	Processor Time	00:00:00,06
	Elapsed Time	00:00:00,08

Within-Subjects Factors

Measure: MEASURE_1

time	lightcolour	Dependent Variable
1	1	cis_iso_red_T1
	2	cis_iso_green_T1
	3	cis_iso_blue_T1
2	1	cis_iso_red_T2
	2	cis_iso_green_T2
	3	cis_iso_blue_T2
3	1	cis_iso_red_T3
	2	cis_iso_green_T3
	3	cis_iso_blue_T3

Temperature = 1,00

Between-Subjects Factors[a]

a. Temperature = 1,00

Descriptive Statistics[a]

	Mean	Std. Deviation	N
cis_iso_red_T1	37,0100	2,22919	3
cis_iso_green_T1	72,6333	1,34448	3
cis_iso_blue_T1	66,1300	3,39044	3
cis_iso_red_T2	23,3367	,91139	3
cis_iso_green_T2	44,0100	,81191	3
cis_iso_blue_T2	39,6867	,95196	3
cis_iso_red_T3	22,5667	,93500	3
cis_iso_green_T3	37,1633	,80351	3
cis_iso_blue_T3	39,2733	,35557	3

a. Temperature = 1,00

Multivariate Tests[a,b]

Effect		Value	F	Hypothesis df	Error df
time	Pillai's Trace	1,000	3886,643[c]	2,000	1,000
	Wilks' Lambda	,000	3886,643[c]	2,000	1,000
	Hotelling's Trace	7773,287	3886,643[c]	2,000	1,000
	Roy's Largest Root	7773,287	3886,643[c]	2,000	1,000
lightcolour	Pillai's Trace	1,000	1958,554[c]	2,000	1,000
	Wilks' Lambda	,000	1958,554[c]	2,000	1,000
	Hotelling's Trace	3917,108	1958,554[c]	2,000	1,000
	Roy's Largest Root	3917,108	1958,554[c]	2,000	1,000
time * lightcolour	Pillai's Trace	.[d]	.	.	.
	Wilks' Lambda	.[d]	.	.	.
	Hotelling's Trace	.[d]	.	.	.
	Roy's Largest Root	.[d]	.	.	.

Multivariate Tests[a,b]

Effect		Sig.	Partial Eta Squared	Noncent. Parameter	Observed Power[e]
time	Pillai's Trace	,011	1,000	7773,287	1,000
	Wilks' Lambda	,011	1,000	7773,287	1,000
	Hotelling's Trace	,011	1,000	7773,287	1,000
	Roy's Largest Root	,011	1,000	7773,287	1,000
lightcolour	Pillai's Trace	,016	1,000	3917,108	,998
	Wilks' Lambda	,016	1,000	3917,108	,998
	Hotelling's Trace	,016	1,000	3917,108	,998
	Roy's Largest Root	,016	1,000	3917,108	,998
time * lightcolour	Pillai's Trace	.	.	.	.
	Wilks' Lambda	.	.	.	.
	Hotelling's Trace	.	.	.	.
	Roy's Largest Root	.	.	.	.

a. Temperature = 1,00

b. Design: Intercept
Within Subjects Design: time + lightcolour + time * lightcolour

c. Exact statistic

d. Cannot produce multivariate test statistics because of insufficient residual degrees of freedom.

e. Computed using alpha = ,05

Mauchly's Test of Sphericity[a,b]

Measure: MEASURE_1

Within Subjects Effect	Mauchly's W	Approx. Chi-Square	df	Sig.	Epsilon[c] Greenhouse-Geisser
time	,010	4,591	2	,101	,503
lightcolour	,959	,042	2	,979	,960
time * lightcolour	,000	.	9	.	,261

Mauchly's Test of Sphericity[a,b]

Measure: MEASURE_1

Within Subjects Effect	Epsilon[c] Huynh-Feldt	Lower-bound
time	,510	,500
lightcolour	1,000	,500
time * lightcolour	,297	,250

Tests the null hypothesis that the error covariance matrix of the orthonormalized transformed dependent variables is proportional to an identity matrix.

a. Temperature = 1,00

b. Design: Intercept
Within Subjects Design: time + lightcolour + time * lightcolour

c. May be used to adjust the degrees of freedom for the averaged tests of significance. Corrected tests are displayed in the Tests of Within-Subjects Effects table.

Tests of Within-Subjects Effects[a]

Measure: MEASURE_1

Source		Type III Sum of Squares	df	Mean Square
time	Sphericity Assumed	3561,100	2	1780,550
	Greenhouse-Geisser	3561,100	1,005	3543,041
	Huynh-Feldt	3561,100	1,020	3489,589
	Lower-bound	3561,100	1,000	3561,100
Error(time)	Sphericity Assumed	14,204	4	3,551
	Greenhouse-Geisser	14,204	2,010	7,066
	Huynh-Feldt	14,204	2,041	6,959
	Lower-bound	14,204	2,000	7,102
lightcolour	Sphericity Assumed	2989,261	2	1494,630
	Greenhouse-Geisser	2989,261	1,921	1556,418
	Huynh-Feldt	2989,261	2,000	1494,630
	Lower-bound	2989,261	1,000	2989,261
Error(lightcolour)	Sphericity Assumed	1,292	4	,323
	Greenhouse-Geisser	1,292	3,841	,336
	Huynh-Feldt	1,292	4,000	,323
	Lower-bound	1,292	2,000	,646
time * lightcolour	Sphericity Assumed	380,057	4	95,014
	Greenhouse-Geisser	380,057	1,045	363,659
	Huynh-Feldt	380,057	1,189	319,675
	Lower-bound	380,057	1,000	380,057
Error(time*lightcolour)	Sphericity Assumed	8,604	8	1,075
	Greenhouse-Geisser	8,604	2,090	4,116
	Huynh-Feldt	8,604	2,378	3,618
	Lower-bound	8,604	2,000	4,302

Tests of Within-Subjects Effects[a]

Measure: MEASURE_1

Source		F	Sig.	Partial Eta Squared
time	Sphericity Assumed	501,428	,000	,996
	Greenhouse-Geisser	501,428	,002	,996
	Huynh-Feldt	501,428	,002	,996
	Lower-bound	501,428	,002	,996
Error(time)	Sphericity Assumed			
	Greenhouse-Geisser			
	Huynh-Feldt			
	Lower-bound			
lightcolour	Sphericity Assumed	4628,931	,000	1,000
	Greenhouse-Geisser	4628,931	,000	1,000
	Huynh-Feldt	4628,931	,000	1,000
	Lower-bound	4628,931	,000	1,000
Error(lightcolour)	Sphericity Assumed			
	Greenhouse-Geisser			
	Huynh-Feldt			
	Lower-bound			
time * lightcolour	Sphericity Assumed	88,348	,000	,978
	Greenhouse-Geisser	88,348	,010	,978
	Huynh-Feldt	88,348	,006	,978
	Lower-bound	88,348	,011	,978
Error(time*lightcolour)	Sphericity Assumed			
	Greenhouse-Geisser			
	Huynh-Feldt			
	Lower-bound			

Tests of Within-Subjects Effects[a]

Measure: MEASURE_1

Source		Noncent. Parameter	Observed Power[b]
time	Sphericity Assumed	1002,855	1,000
	Greenhouse-Geisser	503,984	1,000
	Huynh-Feldt	511,703	1,000
	Lower-bound	501,428	1,000
Error(time)	Sphericity Assumed		
	Greenhouse-Geisser		
	Huynh-Feldt		
	Lower-bound		
lightcolour	Sphericity Assumed	9257,863	1,000
	Greenhouse-Geisser	8890,342	1,000
	Huynh-Feldt	9257,863	1,000
	Lower-bound	4628,931	1,000
Error(lightcolour)	Sphericity Assumed		
	Greenhouse-Geisser		
	Huynh-Feldt		
	Lower-bound		
time * lightcolour	Sphericity Assumed	353,391	1,000
	Greenhouse-Geisser	92,332	,992
	Huynh-Feldt	105,035	,998
	Lower-bound	88,348	,987
Error(time*lightcolour)	Sphericity Assumed		
	Greenhouse-Geisser		
	Huynh-Feldt		
	Lower-bound		

a. Temperature = 1,00

b. Computed using alpha = ,05

Tests of Within-Subjects Contrasts[a]

Measure: MEASURE_1

Source	time	lightcolour	Type III Sum of Squares	df	Mean Square
time	Linear		982,272	1	982,272
	Quadratic		204,761	1	204,761
Error(time)	Linear		2,728	2	1,364
	Quadratic		2,006	2	1,003
lightcolour		Level 2 vs. Level 1	5025,865	1	5025,865
		Level 3 vs. Level 1	3865,938	1	3865,938
Error(lightcolour)		Level 2 vs. Level 1	1,529	2	,765
		Level 3 vs. Level 1	1,270	2	,635
time * lightcolour	Linear	Level 2 vs. Level 1	663,181	1	663,181
		Level 3 vs. Level 1	231,136	1	231,136
	Quadratic	Level 2 vs. Level 1	39,368	1	39,368
		Level 3 vs. Level 1	86,155	1	86,155
Error(time*lightcolour)	Linear	Level 2 vs. Level 1	,848	2	,424
		Level 3 vs. Level 1	3,246	2	1,623
	Quadratic	Level 2 vs. Level 1	,198	2	,099
		Level 3 vs. Level 1	6,242	2	3,121

Tests of Within-Subjects Contrasts[a]

Measure: MEASURE_1

Source	time	lightcolour	F	Sig.	Partial Eta Squared
time	Linear		720,079	,001	,997
	Quadratic		204,110	,005	,990
Error(time)	Linear				
	Quadratic				
lightcolour		Level 2 vs. Level 1	6573,672	,000	1,000
		Level 3 vs. Level 1	6089,263	,000	1,000
Error(lightcolour)		Level 2 vs. Level 1			
		Level 3 vs. Level 1			
time * lightcolour	Linear	Level 2 vs. Level 1	1564,045	,001	,999
		Level 3 vs. Level 1	142,394	,007	,986
	Quadratic	Level 2 vs. Level 1	396,700	,003	,995
		Level 3 vs. Level 1	27,605	,034	,932
Error(time*lightcolour)	Linear	Level 2 vs. Level 1			
		Level 3 vs. Level 1			
	Quadratic	Level 2 vs. Level 1			
		Level 3 vs. Level 1			

Tests of Within-Subjects Contrasts[a]

Measure: MEASURE_1

Source	time	lightcolour	Noncent. Parameter	Observed Power[b]
time	Linear		720,079	1,000
	Quadratic		204,110	1,000
Error(time)	Linear			
	Quadratic			
lightcolour		Level 2 vs. Level 1	6573,672	1,000
		Level 3 vs. Level 1	6089,263	1,000
Error(lightcolour)		Level 2 vs. Level 1		
		Level 3 vs. Level 1		
time * lightcolour	Linear	Level 2 vs. Level 1	1564,045	1,000
		Level 3 vs. Level 1	142,394	,999
	Quadratic	Level 2 vs. Level 1	396,700	1,000
		Level 3 vs. Level 1	27,605	,753
Error(time*lightcolour)	Linear	Level 2 vs. Level 1		
		Level 3 vs. Level 1		
	Quadratic	Level 2 vs. Level 1		
		Level 3 vs. Level 1		

a. Temperature = 1,00

b. Computed using alpha = ,05

Tests of Between-Subjects Effects[a]

Measure: MEASURE_1

Transformed Variable: Average

Source	Type III Sum of Squares	df	Mean Square	F	Sig.	Partial Eta Squared
Intercept	16197,653	1	16197,653	4733,905	,000	1,000
Error	6,843	2	3,422			

Tests of Between-Subjects Effects[a]

Measure: MEASURE_1

Transformed Variable: Average

Source	Noncent. Parameter	Observed Power[b]
Intercept	4733,905	1,000
Error		

a. Temperature = 1,00

b. Computed using alpha = ,05

Temperature = 2,00

Between-Subjects Factors[a]

a. Temperature = 2,00

Descriptive Statistics[a]

	Mean	Std. Deviation	N
cis_iso_red_T1	61,3767	4,08000	3
cis_iso_green_T1	79,0767	,84441	3
cis_iso_blue_T1	82,1100	,49790	3
cis_iso_red_T2	54,2400	2,71232	3
cis_iso_green_T2	83,5900	,81505	3
cis_iso_blue_T2	84,1500	,46872	3
cis_iso_red_T3	37,8633	,20502	3
cis_iso_green_T3	76,3767	,87535	3
cis_iso_blue_T3	71,3467	,20841	3

a. Temperature = 2,00

Multivariate Tests[a,b]

Effect		Value	F	Hypothesis df	Error df
time	Pillai's Trace	1,000	403986,705[c]	2,000	1,000
	Wilks' Lambda	,000	403986,705[c]	2,000	1,000
	Hotelling's Trace	807973,411	403986,705[c]	2,000	1,000
	Roy's Largest Root	807973,411	403986,705[c]	2,000	1,000
lightcolour	Pillai's Trace	1,000	11057,721[c]	2,000	1,000
	Wilks' Lambda	,000	11057,721[c]	2,000	1,000
	Hotelling's Trace	22115,441	11057,721[c]	2,000	1,000
	Roy's Largest Root	22115,441	11057,721[c]	2,000	1,000
time * lightcolour	Pillai's Trace	.[d]	.	.	.
	Wilks' Lambda	.[d]	.	.	.
	Hotelling's Trace	.[d]	.	.	.
	Roy's Largest Root	.[d]	.	.	.

Multivariate Tests[a,b]

Effect		Sig.	Partial Eta Squared	Noncent. Parameter	Observed Power[e]
time	Pillai's Trace	,001	1,000	807973,411	1,000
	Wilks' Lambda	,001	1,000	807973,411	1,000
	Hotelling's Trace	,001	1,000	807973,411	1,000
	Roy's Largest Root	,001	1,000	807973,411	1,000
lightcolour	Pillai's Trace	,007	1,000	22115,441	1,000
	Wilks' Lambda	,007	1,000	22115,441	1,000
	Hotelling's Trace	,007	1,000	22115,441	1,000
	Roy's Largest Root	,007	1,000	22115,441	1,000
time * lightcolour	Pillai's Trace	.	.	.	.
	Wilks' Lambda	.	.	.	.
	Hotelling's Trace	.	.	.	.
	Roy's Largest Root	.	.	.	.

a. Temperature = 2,00

b. Design: Intercept
Within Subjects Design: time + lightcolour + time * lightcolour

c. Exact statistic

d. Cannot produce multivariate test statistics because of insufficient residual degrees of freedom.

e. Computed using alpha = ,05

Mauchly's Test of Sphericity[a,b]

Measure: MEASURE_1

Within Subjects Effect	Mauchly's W	Approx. Chi-Square	df	Sig.	Epsilon[c] Greenhouse-Geisser
time	,000	9,534	2	,009	,500
lightcolour	,001	7,203	2	,027	,500
time * lightcolour	,000	.	9	.	,331

Mauchly's Test of Sphericity[a,b]

Measure: MEASURE_1

Within Subjects Effect	Epsilon[c] Huynh-Feldt	Lower-bound
time	,500	,500
lightcolour	,501	,500
time * lightcolour	,725	,250

Tests the null hypothesis that the error covariance matrix of the orthonormalized transformed dependent variables is proportional to an identity matrix.

a. Temperature = 2,00

b. Design: Intercept
Within Subjects Design: time + lightcolour + time * lightcolour

c. May be used to adjust the degrees of freedom for the averaged tests of significance. Corrected tests are displayed in the Tests of Within-Subjects Effects table.

Tests of Within-Subjects Effects[a]

Measure: MEASURE_1

Source		Type III Sum of Squares	df	Mean Square	F
time	Sphericity Assumed	897,363	2	448,681	134,632
	Greenhouse-Geisser	897,363	1,000	897,330	134,632
	Huynh-Feldt	897,363	1,000	897,233	134,632
	Lower-bound	897,363	1,000	897,363	134,632
Error(time)	Sphericity Assumed	13,331	4	3,333	
	Greenhouse-Geisser	13,331	2,000	6,665	
	Huynh-Feldt	13,331	2,000	6,664	
	Lower-bound	13,331	2,000	6,665	
lightcolour	Sphericity Assumed	4800,148	2	2400,074	451,333
	Greenhouse-Geisser	4800,148	1,000	4798,362	451,333
	Huynh-Feldt	4800,148	1,001	4793,009	451,333
	Lower-bound	4800,148	1,000	4800,148	451,333
Error(lightcolour)	Sphericity Assumed	21,271	4	5,318	
	Greenhouse-Geisser	21,271	2,001	10,632	
	Huynh-Feldt	21,271	2,003	10,620	
	Lower-bound	21,271	2,000	10,635	
time * lightcolour	Sphericity Assumed	338,270	4	84,567	63,852
	Greenhouse-Geisser	338,270	1,322	255,854	63,852
	Huynh-Feldt	338,270	2,901	116,614	63,852
	Lower-bound	338,270	1,000	338,270	63,852
Error(time*lightcolour)	Sphericity Assumed	10,595	8	1,324	
	Greenhouse-Geisser	10,595	2,644	4,007	
	Huynh-Feldt	10,595	5,802	1,826	
	Lower-bound	10,595	2,000	5,298	

Tests of Within-Subjects Effects[a]

Measure: MEASURE_1

Source		Sig.	Partial Eta Squared	Noncent. Parameter
time	Sphericity Assumed	,000	,985	269,263
	Greenhouse-Geisser	,007	,985	134,636
	Huynh-Feldt	,007	,985	134,651
	Lower-bound	,007	,985	134,632
Error(time)	Sphericity Assumed			
	Greenhouse-Geisser			
	Huynh-Feldt			
	Lower-bound			
lightcolour	Sphericity Assumed	,000	,996	902,666
	Greenhouse-Geisser	,002	,996	451,501
	Huynh-Feldt	,002	,996	452,005
	Lower-bound	,002	,996	451,333
Error(lightcolour)	Sphericity Assumed			
	Greenhouse-Geisser			
	Huynh-Feldt			
	Lower-bound			
time * lightcolour	Sphericity Assumed	,000	,970	255,408
	Greenhouse-Geisser	,006	,970	84,420
	Huynh-Feldt	,000	,970	185,219
	Lower-bound	,015	,970	63,852
Error(time*lightcolour)	Sphericity Assumed			
	Greenhouse-Geisser			
	Huynh-Feldt			
	Lower-bound			

Tests of Within-Subjects Effects[a]

Measure: MEASURE_1

Source		Observed Power[b]
time	Sphericity Assumed	1,000
	Greenhouse-Geisser	,999
	Huynh-Feldt	,999
	Lower-bound	,999
Error(time)	Sphericity Assumed	
	Greenhouse-Geisser	
	Huynh-Feldt	
	Lower-bound	
lightcolour	Sphericity Assumed	1,000
	Greenhouse-Geisser	1,000
	Huynh-Feldt	1,000
	Lower-bound	1,000
Error(lightcolour)	Sphericity Assumed	
	Greenhouse-Geisser	
	Huynh-Feldt	
	Lower-bound	
time * lightcolour	Sphericity Assumed	1,000
	Greenhouse-Geisser	,996
	Huynh-Feldt	1,000
	Lower-bound	,958
Error(time*lightcolour)	Sphericity Assumed	
	Greenhouse-Geisser	
	Huynh-Feldt	
	Lower-bound	

a. Temperature = 2,00

b. Computed using alpha = ,05

Tests of Within-Subjects Contrasts[a]

Measure: MEASURE_1

Source	time	lightcolour	Type III Sum of Squares	df	Mean Square
time	Linear		227,879	1	227,879
	Quadratic		71,242	1	71,242
Error(time)	Linear		4,441	2	2,220
	Quadratic		,003	2	,001
lightcolour		Level 2 vs. Level 1	7321,084	1	7321,084
		Level 3 vs. Level 1	7077,296	1	7077,296
Error(lightcolour)		Level 2 vs. Level 1	36,853	2	18,427
		Level 3 vs. Level 1	26,009	2	13,005
time * lightcolour	Linear	Level 2 vs. Level 1	649,792	1	649,792
		Level 3 vs. Level 1	243,844	1	243,844
	Quadratic	Level 2 vs. Level 1	3,092	1	3,092
		Level 3 vs. Level 1	15,699	1	15,699
Error(time*lightcolour)	Linear	Level 2 vs. Level 1	8,060	2	4,030
		Level 3 vs. Level 1	14,559	2	7,280
	Quadratic	Level 2 vs. Level 1	2,814	2	1,407
		Level 3 vs. Level 1	1,847	2	,923

Tests of Within-Subjects Contrasts[a]

Measure: MEASURE_1

Source	time	lightcolour	F	Sig.	Partial Eta Squared
time	Linear		102,633	,010	,981
	Quadratic		49511,819	,000	1,000
Error(time)	Linear				
	Quadratic				
lightcolour		Level 2 vs. Level 1	397,312	,003	,995
		Level 3 vs. Level 1	544,212	,002	,996
Error(lightcolour)		Level 2 vs. Level 1			
		Level 3 vs. Level 1			
time * lightcolour	Linear	Level 2 vs. Level 1	161,238	,006	,988
		Level 3 vs. Level 1	33,497	,029	,944
	Quadratic	Level 2 vs. Level 1	2,197	,276	,524
		Level 3 vs. Level 1	17,002	,054	,895
Error(time*lightcolour)	Linear	Level 2 vs. Level 1			
		Level 3 vs. Level 1			
	Quadratic	Level 2 vs. Level 1			
		Level 3 vs. Level 1			

Tests of Within-Subjects Contrasts[a]

Measure: MEASURE_1

Source	time	lightcolour	Noncent. Parameter	Observed Power[b]
time	Linear		102,633	,994
	Quadratic		49511,819	1,000
Error(time)	Linear			
	Quadratic			
lightcolour		Level 2 vs. Level 1	397,312	1,000
		Level 3 vs. Level 1	544,212	1,000
Error(lightcolour)		Level 2 vs. Level 1		
		Level 3 vs. Level 1		
time * lightcolour	Linear	Level 2 vs. Level 1	161,238	1,000
		Level 3 vs. Level 1	33,497	,814
	Quadratic	Level 2 vs. Level 1	2,197	,147
		Level 3 vs. Level 1	17,002	,585
Error(time*lightcolour)	Linear	Level 2 vs. Level 1		
		Level 3 vs. Level 1		
	Quadratic	Level 2 vs. Level 1		
		Level 3 vs. Level 1		

a. Temperature = 2,00

b. Computed using alpha = ,05

Tests of Between-Subjects Effects[a]

Measure: MEASURE_1

Transformed Variable: Average

Source	Type III Sum of Squares	df	Mean Square	F	Sig.	Partial Eta Squared
Intercept	44118,202	1	44118,202	32271,903	,000	1,000
Error	2,734	2	1,367			

Tests of Between-Subjects Effects[a]

Measure: MEASURE_1

Transformed Variable: Average

Source	Noncent. Parameter	Observed Power[b]
Intercept	32271,903	1,000
Error		

a. Temperature = 2,00

b. Computed using alpha = ,05

Temperature = 3,00

Between-Subjects Factors[a]

a. Temperature = 3,00

Descriptive Statistics[a]

	Mean	Std. Deviation	N
cis_iso_red_T1	31,0433	,85705	3
cis_iso_green_T1	50,3867	,09074	3
cis_iso_blue_T1	44,2200	1,32000	3
cis_iso_red_T2	21,9033	1,45960	3
cis_iso_green_T2	35,8667	,37528	3
cis_iso_blue_T2	40,7633	,31070	3
cis_iso_red_T3	31,5500	6,94000	3
cis_iso_green_T3	28,1400	,30512	3
cis_iso_blue_T3	33,2367	7,49318	3

a. Temperature = 3,00

Multivariate Tests[a,b]

Effect		Value	F	Hypothesis df	Error df	Sig.
time	Pillai's Trace	,998	297,117[c]	2,000	1,000	,041
	Wilks' Lambda	,002	297,117[c]	2,000	1,000	,041
	Hotelling's Trace	594,233	297,117[c]	2,000	1,000	,041
	Roy's Largest Root	594,233	297,117[c]	2,000	1,000	,041
lightcolour	Pillai's Trace	,998	218,610[c]	2,000	1,000	,048
	Wilks' Lambda	,002	218,610[c]	2,000	1,000	,048
	Hotelling's Trace	437,220	218,610[c]	2,000	1,000	,048
	Roy's Largest Root	437,220	218,610[c]	2,000	1,000	,048
time * lightcolour	Pillai's Trace	.[d]	.	.	.	.
	Wilks' Lambda	.[d]	.	.	.	.
	Hotelling's Trace	.[d]	.	.	.	.
	Roy's Largest Root	.[d]	.	.	.	.

Multivariate Tests[a,b]

Effect		Partial Eta Squared	Noncent. Parameter	Observed Power[e]
time	Pillai's Trace	,998	594,233	,777
	Wilks' Lambda	,998	594,233	,777
	Hotelling's Trace	,998	594,233	,777
	Roy's Largest Root	,998	594,233	,777
lightcolour	Pillai's Trace	,998	437,220	,705
	Wilks' Lambda	,998	437,220	,705
	Hotelling's Trace	,998	437,220	,705
	Roy's Largest Root	,998	437,220	,705
time * lightcolour	Pillai's Trace	.	.	.
	Wilks' Lambda	.	.	.
	Hotelling's Trace	.	.	.
	Roy's Largest Root	.	.	.

a. Temperature = 3,00

b. Design: Intercept
Within Subjects Design: time + lightcolour + time * lightcolour

c. Exact statistic

d. Cannot produce multivariate test statistics because of insufficient residual degrees of freedom.

e. Computed using alpha = ,05

Mauchly's Test of Sphericity[a,b]

Measure: MEASURE_1

Within Subjects Effect	Mauchly's W	Approx. Chi-Square	df	Sig.	Epsilon[c] Greenhouse-Geisser
time	,860	,151	2	,927	,877
lightcolour	,029	3,550	2	,169	,507
time * lightcolour	,000	.	9	.	,264

Mauchly's Test of Sphericity[a,b]

Measure: MEASURE_1

	Epsilon[c]	
Within Subjects Effect	Huynh-Feldt	Lower-bound
time	1,000	,500
lightcolour	,530	,500
time * lightcolour	,309	,250

Tests the null hypothesis that the error covariance matrix of the orthonormalized transformed dependent variables is proportional to an identity matrix.

a. Temperature = 3,00

b. Design: Intercept
Within Subjects Design: time + lightcolour + time * lightcolour

c. May be used to adjust the degrees of freedom for the averaged tests of significance. Corrected tests are displayed in the Tests of Within-Subjects Effects table.

Tests of Within-Subjects Effects[a]

Measure: MEASURE_1

Source		Type III Sum of Squares	df	Mean Square	F
time	Sphericity Assumed	612,522	2	306,261	401,982
	Greenhouse-Geisser	612,522	1,754	349,289	401,982
	Huynh-Feldt	612,522	2,000	306,261	401,982
	Lower-bound	612,522	1,000	612,522	401,982
Error(time)	Sphericity Assumed	3,048	4	,762	
	Greenhouse-Geisser	3,048	3,507	,869	
	Huynh-Feldt	3,048	4,000	,762	
	Lower-bound	3,048	2,000	1,524	
lightcolour	Sphericity Assumed	681,906	2	340,953	21,275
	Greenhouse-Geisser	681,906	1,015	672,111	21,275
	Huynh-Feldt	681,906	1,059	643,819	21,275
	Lower-bound	681,906	1,000	681,906	21,275
Error(lightcolour)	Sphericity Assumed	64,105	4	16,026	
	Greenhouse-Geisser	64,105	2,029	31,592	
	Huynh-Feldt	64,105	2,118	30,262	
	Lower-bound	64,105	2,000	32,052	
time * lightcolour	Sphericity Assumed	519,012	4	129,753	6,911
	Greenhouse-Geisser	519,012	1,056	491,479	6,911
	Huynh-Feldt	519,012	1,237	419,446	6,911
	Lower-bound	519,012	1,000	519,012	6,911
Error(time*lightcolour)	Sphericity Assumed	150,188	8	18,774	
	Greenhouse-Geisser	150,188	2,112	71,110	
	Huynh-Feldt	150,188	2,475	60,688	
	Lower-bound	150,188	2,000	75,094	

Tests of Within-Subjects Effects[a]

Measure: MEASURE_1

Source		Sig.	Partial Eta Squared	Noncent. Parameter
time	Sphericity Assumed	,000	,995	803,963
	Greenhouse-Geisser	,000	,995	704,925
	Huynh-Feldt	,000	,995	803,963
	Lower-bound	,002	,995	401,982
Error(time)	Sphericity Assumed			
	Greenhouse-Geisser			
	Huynh-Feldt			
	Lower-bound			
lightcolour	Sphericity Assumed	,007	,914	42,549
	Greenhouse-Geisser	,043	,914	21,585
	Huynh-Feldt	,039	,914	22,533
	Lower-bound	,044	,914	21,275
Error(lightcolour)	Sphericity Assumed			
	Greenhouse-Geisser			
	Huynh-Feldt			
	Lower-bound			
time * lightcolour	Sphericity Assumed	,010	,776	27,646
	Greenhouse-Geisser	,113	,776	7,299
	Huynh-Feldt	,096	,776	8,552
	Lower-bound	,119	,776	6,911
Error(time*lightcolour)	Sphericity Assumed			
	Greenhouse-Geisser			
	Huynh-Feldt			
	Lower-bound			

Tests of Within-Subjects Effects[a]

Measure: MEASURE_1

Source		Observed Power[b]
time	Sphericity Assumed	1,000
	Greenhouse-Geisser	1,000
	Huynh-Feldt	1,000
	Lower-bound	1,000
Error(time)	Sphericity Assumed	
	Greenhouse-Geisser	
	Huynh-Feldt	
	Lower-bound	
lightcolour	Sphericity Assumed	,967
	Greenhouse-Geisser	,672
	Huynh-Feldt	,698
	Lower-bound	,663
Error(lightcolour)	Sphericity Assumed	
	Greenhouse-Geisser	
	Huynh-Feldt	
	Lower-bound	
time * lightcolour	Sphericity Assumed	,897
	Greenhouse-Geisser	,339
	Huynh-Feldt	,393
	Lower-bound	,322
Error(time*lightcolour)	Sphericity Assumed	
	Greenhouse-Geisser	
	Huynh-Feldt	
	Lower-bound	

a. Temperature = 3,00

b. Computed using alpha = ,05

Tests of Within-Subjects Contrasts[a]

Measure: MEASURE_1

Source	time	lightcolour	Type III Sum of Squares	df	Mean Square
time	Linear		178,469	1	178,469
	Quadratic		25,704	1	25,704
Error(time)	Linear		,493	2	,246
	Quadratic		,523	2	,262
lightcolour		Level 2 vs. Level 1	893,811	1	893,811
		Level 3 vs. Level 1	1137,263	1	1137,263
Error(lightcolour)		Level 2 vs. Level 1	17,646	2	8,823
		Level 3 vs. Level 1	124,411	2	62,206
time * lightcolour	Linear	Level 2 vs. Level 1	776,571	1	776,571
		Level 3 vs. Level 1	198,030	1	198,030
	Quadratic	Level 2 vs. Level 1	71,920	1	71,920
		Level 3 vs. Level 1	261,214	1	261,214
Error(time*lightcolour)	Linear	Level 2 vs. Level 1	57,258	2	28,629
		Level 3 vs. Level 1	216,533	2	108,267
	Quadratic	Level 2 vs. Level 1	20,216	2	10,108
		Level 3 vs. Level 1	82,037	2	41,018

Tests of Within-Subjects Contrasts[a]

Measure: MEASURE_1

Source	time	lightcolour	F	Sig.	Partial Eta Squared
time	Linear		724,743	,001	,997
	Quadratic		98,234	,010	,980
Error(time)	Linear				
	Quadratic				
lightcolour		Level 2 vs. Level 1	101,303	,010	,981
		Level 3 vs. Level 1	18,282	,051	,901
Error(lightcolour)		Level 2 vs. Level 1			
		Level 3 vs. Level 1			
time * lightcolour	Linear	Level 2 vs. Level 1	27,125	,035	,931
		Level 3 vs. Level 1	1,829	,309	,478
	Quadratic	Level 2 vs. Level 1	7,115	,116	,781
		Level 3 vs. Level 1	6,368	,128	,761
Error(time*lightcolour)	Linear	Level 2 vs. Level 1			
		Level 3 vs. Level 1			
	Quadratic	Level 2 vs. Level 1			
		Level 3 vs. Level 1			

Tests of Within-Subjects Contrasts[a]

Measure: MEASURE_1

Source	time	lightcolour	Noncent. Parameter	Observed Power[b]
time	Linear		724,743	1,000
	Quadratic		98,234	,992
Error(time)	Linear			
	Quadratic			
lightcolour		Level 2 vs. Level 1	101,303	,993
		Level 3 vs. Level 1	18,282	,610
Error(lightcolour)		Level 2 vs. Level 1		
		Level 3 vs. Level 1		
time * lightcolour	Linear	Level 2 vs. Level 1	27,125	,747
		Level 3 vs. Level 1	1,829	,131
	Quadratic	Level 2 vs. Level 1	7,115	,328
		Level 3 vs. Level 1	6,368	,304
Error(time*lightcolour)	Linear	Level 2 vs. Level 1		
		Level 3 vs. Level 1		
	Quadratic	Level 2 vs. Level 1		
		Level 3 vs. Level 1		

a. Temperature = 3,00

b. Computed using alpha = ,05

Tests of Between-Subjects Effects[a]

Measure: MEASURE_1

Transformed Variable: Average

Source	Type III Sum of Squares	df	Mean Square	F	Sig.	Partial Eta Squared
Intercept	11173,195	1	11173,195	57080,520	,000	1,000
Error	,391	2	,196			

Tests of Between-Subjects Effects[a]

Measure: MEASURE_1

Transformed Variable: Average

Source	Noncent. Parameter	Observed Power[b]
Intercept	57080,520	1,000
Error		

a. Temperature = 3,00

b. Computed using alpha = ,05

Tab.4. Results of planned contrasts/comparison to red light conditions. Cell dry weight [CDW], fatty acid [FA].

Temperature	Variable	light spectrum	F	p	partial eta²
20	CDW	green vs. red	10,91	0,08	0,85
		blue vs. red	63,28	0,02	0,97
	FA	green vs. red	50,87	0,02	0,96
		blue vs. red	45,77	0,02	0,96
	16:1 cis	green vs. red	6573,67	0,00	1,00
		blue vs. red	6089,26	0,00	1,00
30	CDW	green vs. red	9,73	0,09	0,83
		blue vs. red	58,72	0,02	0,97
	FA	green vs. red	695,24	0,00	1,00
		blue vs. red	271,65	0,00	0,99
	16:1 cis	green vs. red	397,31	0,00	0,99
		blue vs. red	544,21	0,00	1,00
35	CDW	green vs. red	17,90	0,05	0,90
		blue vs. red	156,65	0,01	0,99
	FA	green vs. red	646,10	0,00	1,00
		blue vs. red	4,54	0,17	0,69
	16:1 cis	green vs. red	101,30	0,01	0,98
		blue vs. red	18,28	0,05	0,90

Tab.5. Results oft two-way repeated-measures ANNOVA. Cell dry weight [CDW], fatty acid [FA].

		ANOVA								
		timepoint			lightwave			timepoint*lightwave		
		F	p	partial eta²	F	p	partial eta²	F	p	partial eta²
Temperature	Variable									
20	CDW	1233,35	0,00	1,00	25,77	0,01	0,93	20,84	0,00	0,91
	FA	45,49	0,02	0,96	18,54	0,04	0,90	0,41	0,62	0,17
	16:1 cis	501,43	0,00	1,00	4628,93	0,00	1,00	88,35	0,01	0,98
30	CDW	1772,90	0,00	1,00	36,82	0,01	0,95	16,04	0,05	0,89
	FA	30,92	0,03	0,94	308,40	0,00	0,99	16,59	0,04	0,89
	ISO	134,63	0,01	0,99	451,33	0,00	1,00	63,85	0,01	0,97
35	CDW	4069,89	0,00	1,00	86,80	0,01	0,98	57,03	0,01	0,97
	FS	47,96	0,02	0,96	16,10	0,05	0,89	0,71	0,52	0,26
	16:1 cis	401,98	0,00	1,00	21,27	0,04	0,91	6,91	0,11	0,78

Publikation 2

Blue-green light is required for a maximized fatty acid unsaturation and pigment concentration in the microalga *Acutodesmus obliquus*

Mark Helamieh; Marco Reich; Sophie Bory; Philipp Rohne; Martin Kerner; Klaus Kümmerer

2022

Lipids, *57*(4-5), 221-232.

DOI: 10.1002/lipd.12343.

Received: 1 February 2022 | Revised: 5 April 2022 | Accepted: 5 April 2022

DOI: 10.1002/lipd.12343

ORIGINAL ARTICLE

AOCS WILEY

Blue-green light is required for a maximized fatty acid unsaturation and pigment concentration in the microalga *Acutodesmus obliquus*

Mark Helamieh[1,2] | **Marco Reich**[1] | **Sophie Bory**[1] | **Philipp Rohne**[3] | **Ulf Riebesell**[4] | **Martin Kerner**[2] | **Klaus Kümmerer**[1]

[1]Institute of Sustainable Chemistry, Leuphana University of Lueneburg, Lueneburg, Germany

[2]Strategic Science Consult Ltd, Hamburg, Germany

[3]Institute of Pharmacy and Biochemistry, Therapeutical Life Sciences, Johannes Gutenberg-University Mainz, Mainz, Germany

[4]GEOMAR Helmholtz Centre for Ocean Research Kiel, Kiel, Germany

Correspondence
Mark Helamieh, Institute of Sustainable Chemistry, Leuphana University Lueneburg, Universitaetsallee 1, 21335 Lueneburg, Germany.
Email: mark.helamieh@stud.leuphana.de and markhelamieh@web.de

Funding information
Federal Institute for Research on Building, Urban Affairs and Spatial Development, Initiative Future Building, Germany, Grant/Award Number: SWD-10.08.18.7-17.02

Abstract

Blue-green light is known to maximize the degree of fatty acid (FA) unsaturation in microalgae. However, knowledge on the particular waveband responsible for this stimulation of FA desaturation and its impact on the pigment composition in microalgae remains limited. In this study, *Acutodesmus obliquus* was cultivated for 96 h at 15°C with different light spectra (380–700 nm, 470–700 nm, 520–700 nm, 600–700 nm, and dark controls). Growth was monitored daily, and qualitative characterization of the microalgal FA composition was achieved via gas chromatography coupled with electron impact ionization mass spectrometry (GC-EI/MS). Additionally, a quantitative analysis of microalgal pigments was performed using high-performance liquid chromatography with diode array detection (HPLC-DAD). Spectra that included wavelengths between 470 and 520 nm led to a significantly higher percentage of the polyunsaturated fatty acids (PUFA) 18:3 and 16:4, compared to all other light conditions. However, no significant differences between the red light cultivations and the heterotrophic dark controls were observed for the FA 18:3 and 16:4. These results indicate, that exclusively the blue-green light waveband between 470 and 520 nm is responsible for a maximized FA unsaturation in *A. obliquus*. Furthermore, the growth and production of pigments were impaired if blue-green light (380–520 nm) was absent in the light spectrum. This knowledge can contribute to achieving a suitable microalgal pigment and FA composition for industrial purposes and must be considered in spectrally selective microalgae cultivation systems.

KEYWORDS
blue-green light, fatty acid, lutein, microalgae, photosynthetic pigment

INTRODUCTION

Microalgae are considered a promising source of products for the food and fuel industry (Adarme-Vega et al., 2012; Ahmad et al., 2011; Rösch et al., 2019; Schenk et al., 2008; Singh et al., 2011; Tang et al., 2020). Compared to land-based crops, microalgae have several advantages, such as higher growth rates, a lower water demand, and no requirement for

Abbreviations: CDW, cell dry weight; DAD, diode array detector; EI, electron impact; FA, fatty acid; FAME, fatty acid methyl ester; GC, gas chromatography; HPLC, high-performance liquid chromatography; IS, internal standard; MS, mass spectrometry; MUFA, monounsaturated fatty acids; PUFA, polyunsaturated fatty acids; rpm, rounds per minute; RT, retention time; SFA, saturated fatty acids; SIM, selected ion monitoring.

arable land (Ho et al., 2014; Miranda et al., 2018). Microalgal biomass can be used to produce green biofuels (Anto et al., 2020). Different components of the microalgal biomass are suitable for biogas production via anaerobic digestion, whereas lipids can be used to produce biodiesel (Chhandama et al., 2021; Zabed et al., 2020). For the production of biodiesel, a higher degree of fatty acid (FA) saturation is desirable (Piligaev et al., 2015). Additionally, microalgae might also serve as a production platform for valuable bioactive compounds in food and feed production (Goiris et al., 2012; Gong et al., 2011; Kusmayadi et al., 2021). For instance, carotenoids such as astaxanthin, lutein, and beta carotene are produced by microalgae and have a high value as supplements in the food, feed, and pharmaceutical industry (Gong et al., 2011; Vaz et al., 2016). Primarily lutein is frequently found in several microalgal species (Ho et al., 2014). Owing to its color and antioxidative properties, it has many different applications in the food, pharmaceutical, and cosmetic industry (Sun et al., 2014). Another group of essential components for the human diet, produced by microalgae, are specific FA (Behrens & Kyle, 1996). The optimal FA composition is a decisive factor for the nutritional value of food products. A high ratio of omega-3/omega-6 FA is required for healthy nutrition, whereas a lower omega-3/omega-6 ratio is supposedly associated with adverse health effects (Fabiani et al., 2021; Simopoulos, 2002). In western diets, high contents of omega-6 FA are prevailing, which might be related to several diseases of affluence, such as cardiovascular diseases, cancer, and autoimmune diseases (Shanab et al., 2018; Simopoulos, 2002). In contrast, higher chained omega-3 FA, such as eicosapentaenoic acid and docosahexaenoic acid, are important precursors of hormones and can be protective against neurodegenerative diseases such as Alzheimer's, Parkinson's, and multiple sclerosis disease (Shanab et al., 2018). These higher chained polyunsaturated fatty acids (PUFA) are biosynthesized from linoleic acid (18:2) and linolenic acid (18:3) precursors. A relatively high content of these FA can be found in fish oil (Shanab et al., 2018). However, several adverse environmental effects are related to the fishery industry (Blanco Gonzalez et al., 2017; Worm et al., 2006). Therefore, novel approaches for the production of PUFA are required.

The use of microalgae for PUFA production is viewed as a greener alternative in the food industry (Adarme-Vega et al., 2012). Furthermore, the metabolism of microalgae can be influenced by cultivation parameters (Aussant et al., 2018; El-Sheekh et al., 2012; Hultberg et al., 2014). This, in turn, may be used for the targeted production of specific FA and other valuable compounds (Abomohra et al., 2013; Abomohra & Almutairi, 2020; El-Sheekh et al., 2012). For example, phytohormones and the pretreatment of microalgae with low-dose atmospheric plasma can increase growth and FA production (Almarashi et al., 2020; Esakkimuthu et al., 2020). It is also well-known that the cultivation temperature greatly impacts the FA composition of microalgae, whereby lower cultivation temperatures are related to a higher PUFA concentration and a higher degree of FA unsaturation (Degraeve-Guilbault et al., 2021; Patterson, 1970). Another abiotic parameter that impacts the FA composition is the intensity and spectral composition of light (Hultberg et al., 2014; Nzayisenga et al., 2020; Shu et al., 2012). A recent study showed that different light intensities strongly impact the PUFA and pigment composition in the microalga *Chlorella sorokiniana* (Krimech et al., 2022). Moreover, blue and green light can influence FA composition and content in microalgae (Hultberg et al., 2014; Shu et al., 2012). This coincides with a higher observed content of photosynthetic pigments and xanthophylls upon blue light treatment (Fu et al., 2013; Ho et al., 2014; Sharmila et al., 2018). Furthermore, it was postulated that a maximum FA unsaturation in microalgae requires blue or blue-green light (Helamieh et al., 2021; Poliner et al., 2021). However, the detailed activating waveband was only roughly estimated between 450 and 550 nm (Helamieh et al., 2021). Although the underlying cause is unclear, it is assumed that the higher degree of FA desaturation upon blue-green light treatment might be caused by a rearrangement of the thylakoid system of the microalgal chloroplasts, which contain high percentages of highly unsaturated FA (Helamieh et al., 2021; Hugly & Somerville, 1992; Hultberg et al., 2014). If this is the case, the increase of highly unsaturated FA should be coupled with increased photosynthetic pigments. Besides the effects of blue light, the impact of red light on many metabolic processes and the FA composition in eukaryotic microalgae is not yet well understood (Helamieh et al., 2021; Poliner et al., 2021).

In addition to the fundamental scientific interest in a detailed understanding of the spectral impact on microalgal metabolism, this knowledge can be practically applied in photovoltaic-photosynthesis hybrid systems. These systems combine spectrally selective solar cells with photobioreactors to concomitantly harvest sunlight to produce microalgal biomass and electricity in one comprehensive system. For example, a recently developed, germanium-based semitransparent solar cell enables a high transmission of specific wavebands and can be spectrally adjusted, depending on the layer thickness (Osterthun, Neugebohrn, et al., 2021). Thus, detailed knowledge of the stimulating light waveband is required to adjust the transmission of the photovoltaic to the microalgal demands accordingly. Besides producing electricity and biomass in these systems, selected light wavelengths might modulate microalgal metabolism to produce a desirable FA and pigment composition for biofuel, food, and feed applications.

To close this knowledge gap, the impact of different light spectra on the growth, FA, and pigment composition of the microalga *Acutodesmus obliquus* was studied. The respective light spectra were chosen to identify the stimulating light wavebands that trigger a high degree of unsaturation and pigment production in microalgae. Biomass production of *A. obliquus* was assessed, and qualitative characterization of the FA profiles was analyzed by gas chromatography coupled with electron impact ionization mass spectrometry (GC-EI/MS). Additionally, the pigment composition was determined by high-performance liquid chromatography with diode array detection (HPLC-DAD).

MATERIAL AND METHODS

Microalgae preparation

The microalga strain *A. obliquus* (syn. *Scenedesmus obliquus; Tetradesmus obliquus*) (No. U169) from the Microalgae and Zygnematophyceae Collection Hamburg (MZCH, previously SVCK) of the University of Hamburg was used (von Schwartzenberg et al., 2013). The cultivation medium was composed of Flory Basis Fertilizer 1 (Euflor, Germany) and KNO_3 (Fisher Scientific, Germany). The pH was adjusted at 7.0 using HCl (Fisher Scientific, Germany) and NaOH (Fisher Scientific, Germany). To study heterotrophic growth, 2 g L^{-1} of glucose (Sigma-Aldrich, Taufkirchen, Germany) was added in the heterotrophic dark control. The determination of cell dry weight (CDW) was done gravimetrically. Microalgae inoculum was obtained in a pre-culture in 1 L Schott flasks at 25°C and a constant photon flux density of 150 μmol m^{-2} s^{-1} emitted by a Sylvania T9 circline 32 W fluorescent tube with a white light spectrum. A CO_2-enriched air (5% v/v) was used for the aeration of the pre-culture. A magnetic stirrer constantly homogenized the microalgae suspension at 200 rpm stirring speed. In order to obtain a factor to convert optical density into dry weight, a defined volume, depending on the optical density, of algae suspension was taken from each pre-culture and four dilution steps of the sample were prepared. The dilutions were filtered and subsequently dried at 80°C for 24 h. It was previously tested that a constant weight was reached after 3–8 h. In parallel, a subsample of each dilution was used to measure the optical density at 750 nm(OD_{750}). A conversion factor was calculated from the linear correlation between OD_{750} and dry weight.

Cultivation unit

Microalgae were cultivated as a batch in bubble column reactors. For that purpose, glass tubes of a length of 490 mm and a diameter of 40 mm each holding a volume of 350 ml, were used. Twelve glass tubes were submerged into an optical transparent acrylic glass water bath in black acrylic brackets. These brackets kept the tubes vertically and prevented ambient light from reaching the back and the sides of the tubes. All tubes were exclusively irradiated from the front side of the water bath with metal halide lamps (Philips MSR HR CT, 575 W), with a sun-like light spectrum (Figure 1a) (Helamieh et al., 2021; Osterthun, Helamieh, et al., 2021). The metal halide lamps generated the applied white light spectrum (380–700 nm). All wavelengths below 380 nm emitted by the metal halide lamps were absorbed by the acrylic glass water bath. For all other spectra, the optical filter foils "light red," "deep straw," and "medium yellow" (LEE-Filters, England) were used in combination with the metal halide lamps. These optical filters were fixed to the outer front side of the water bath. The resulting light spectra are further referred to as "red light" (600–700 nm), "orange light" (520–700 nm), and "yellow light" (470–700 nm) (Figure 1b–d). All spectra were measured and adjusted to the same photon flux density for each experiment (Table 1). Absolute photon fluxes were determined by a UV–Vis spectrometer (BLACK-Comet, StellarNET, Tampa, USA) within a range of 400–700 nm. Additionally, one section of the front side was shaded with aluminum foil for the dark control samples.

Test conditions

Pre-cultures were diluted to an OD_{750} of 0.5 for each experiment, measured with a UV/VIS spectrometer (Pharmacia LKB Ultrospec III). All cultivation experiments were started by using a volume of 350 ml of microalgae suspension. The growth was monitored via the OD_{750}, which was measured directly after sampling (Admirasari et al., 2022; Helamieh et al., 2021; Osterthun, Helamieh, et al., 2021; Reymann et al., 2020). The CDW was determined via the linear correlation between OD_{750} and CDW as established by the measurements.

$$CDW = 0.873 \times OD_{750} - 0.156$$

All experiments were performed as batch experiments for 96 h, with triplicates for each test condition in two experiments. The microalgae were irradiated constantly with a photon flux density of 195 ± 20 μmol m^{-2} s^{-1} in experiment 1 and 209 ± 24 μmol m^{-2} s^{-1} in experiment 2 for all light spectra, respectively (Table 1). The dark control was cultivated in the absence of light. In one dark control, 1 g L^{-1} of glucose was added at the start to compensate for the absence of light and enable a heterotrophic microalgal growth. In previous tests, under similar conditions, it was observed that glucose was depleted after 72 h of cultivation. Therefore, 1 g L^{-1}

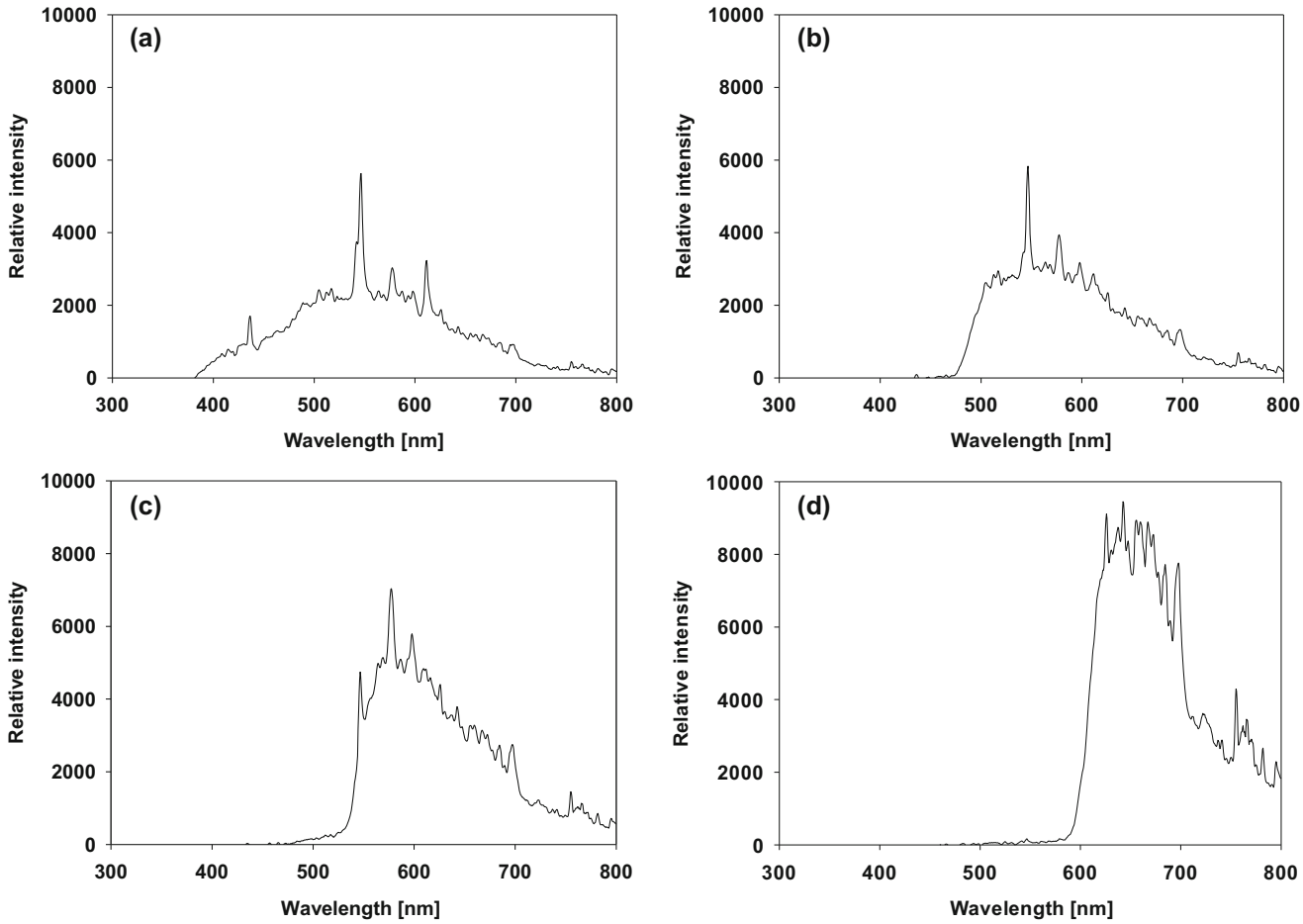

FIGURE 1 The light spectrum of the MSR 575 HR CT metal halide lamp. Unfiltered (white light) (a); in combination with the optical foils: medium yellow (yellow light) (b); deep straw (orange light) (c), and light red (red light) (d) (Lee filters, England). The relative emission spectra (Jλ,rel in counts) were determined by a UV–vis spectrometer (Black-comet, StellarNET, Tampa, USA) within a range of $\lambda = 300$–800 nm (integration time = 10 ms)

TABLE 1 Test conditions during the different experiments

Experiment	Light conditions	White light	Yellow light	Orange light	Red light	Repeated
1	Photon flux [μmol m^{-2} s^{-1}]	188 ± 11	195 ± 20	195 ± 10	184 ± 10	2×
Exp.	Light conditions	White light	Dark control	Dark + GLc	Red light	Repeated
2	Photon flux [μmol m^{-2} s^{-1}]	209 ± 24	0	0	210 ± 1	3×

Note: The temperatures and the estimated accuracies of measurement. Values for the photon fluxes represent the means ± standard deviation of triplicates.

of glucose was added at 72 h upon cultivation started. These dark controls were used to observe if red light impacts the FA and pigment composition. A detailed description of all conditions is summarized in Table 1. The bubble column reactors were aerated and mixed by humidified and CO_2-enriched air (5% v/v) at an airflow of 0.2 L min^{-1}. The temperature in the water bath was kept at 15° ± 0.5°C by a chiller (AD15R-30, VWR, Pennsylvania, USA) in all experiments to enable a maximum of unsaturated FA. Samples for the FA analysis were taken from the pre-culture. After the cultivation was started, 3–20 ml (depending on the biomass concentration) samples were taken after 24 h and 96 h of cultivation for FA and pigment analysis and subsequently stored at −80°C prior to analysis. The FA compositions of samples taken after 24 h and 96 h of cultivation were subsequently analyzed by GC-EI/MS. Additionally, the pigment composition of the samples taken after 96 h of cultivation was analyzed by HPLC-DAD.

Fatty acid analysis

Details of the analytical method can be found elsewhere (Helamieh et al., 2021).

FA extraction: The frozen samples were thawed and 0.0025 g CDW was used for the FA-extractions. 20 μmol heptadecanoic acid (Sigma Aldrich, Taufkirchen, Germany) dissolved in hexane was used as internal standard (IS). A modified Folch extraction was employed to extract the FA (Ichihara & Fukubayashi, 2010; Reich et al., 2012, 2013). The solvents of the extraction were evaporated under a constant and gentle stream of nitrogen and the transesterification was done according to (Helamieh et al., 2021).

Instrumental conditions (GC): The samples were analyzed according to (Helamieh et al., 2021).

GC/EI-MS was performed with a Thermo Scientific™ ISQ™ 7000 Single Quadrupole GC–MS system. The samples (1 μl) were injected with a sampler and the injector was operated in splitless mode and kept at 260°C. To separate the target compounds, a TRACE™ TR FAME fused silica capillary column (0.25 mm, 0.25 μm × 30 m) with helium as carrier gas was used with a constant pressure of 100 kPa, with a flow rate of 1.5 ml min^{-1}. The oven temperature was set to start at 60°C, plateau for 1 min, followed by a ramp rate of 6.5°C min^{-1} until the final temperature of 260°C was reached and then held for 8 min. The electron energy was 70 eV. The ion source was set to 270°C and the mass range of *m*/*z* 60–400 was recorded in the full scan mode. Fragment ions included *m*/*z* 74, *m*/*z* 79, *m*/*z* 81, and *m*/*z* 87 for the fatty acid methyl ester (FAME) detected during the measurement in the GC/EI-MS selected ion monitoring (SIM) mode.

Pigment analysis

The microalgal pigments were analyzed by HPLC according to (van Heukelem & Thomas, 2001). A HPLC Ultimate 3000 (Thermo Fisher) equipped with a DAD-3000 diode array detector, an FLD-3400RS fluorescence detector, a pre-column (Eclipse XDB-C8 Grd Crtds 4.6 × 12.5), and a separation column (Eclipse XDB-C8 3.5u 4.6 × 150) were used for the analysis of pigments. Spectra were recorded with a wavelength range of 380–800 nm. Separation was done isocratic, whereby solvent A (70:30 Methanol: 28 mM Tetrabutylammonium acetate, pH 6.5) and solvent B (100% Methanol) were added linearly with a flow-rate of 1.1 ml min^{-1}, from 5% to 95% within 22 min. The column oven temperature (TCC-3000SD) was set at 60°C.

Data evaluation and statistical analyses

The mass spectra and the RT were used for the qualitative analysis of the separated FAME. The data obtained from the SIM mode measurement were used to set the peak area ratios (sum of the four recorded *m*/*z* values) of the identified FAME into relation with the respective area of the IS. Heptadecanoic acid was used as IS. Finally, the proportion of each FA (in %) was calculated. All samples were taken in triplicates. The mean values ± standard error were calculated. Experiment 1 was repeated three times, and experiment 2 was repeated twice for the biomass production and FA analysis. The pigment analysis was repeated twice for experiment 1 (Table 4) and once for experiment 2 (Table 5). Statistical analyses were carried out using RStudio (version 1.2.5033), and the programming language R (version 3.6.2). Data import, visualization, and analysis were supported using the tidyverse, ggpubr, and rstatix packages. To examine whether the observed effects are statistically significant, a One-way ANOVA with Tukey post hoc test was performed.

RESULTS

Growth of *A. obliquus*

The produced biomass of *A. obliquus*, cultivated under all light conditions, was compared in two experiments. In experiment 1, the CDW reached a maximum value of 1.4 g L^{-1} for the white light treated samples after 96 h of cultivation. However, the maximum CDW of the red light treated samples reached a slightly but significantly lower value during the same cultivation time (Figure 2a). In the dark control, to which glucose was added to partially compensate for a decreased synthesis in the absence of light, a CDW of 1 g L^{-1} was reached after 96 h. No biomass increase was observed in the absence of light without glucose (Figure 2a). In experiment 2, the red light treated approaches reached a significantly lower maximum CDW, compared to all other tested spectral approaches, accordingly (Figure 2b).

Impact of the light conditions on the fatty acid composition

In this study, 15 FA were identified in *A. obliquus* (see supplementary). The main variations were observed in the FA 16:1, 16:2, 16:3, 16:4, 18:1, 18:2, and 18:3. Therefore, the focus was set on these FA.

It was found that the tested light conditions had a significant effect on the FA composition of *A. obliquus* (Figure 3, Tables 2, and 3). In experiment 1, the highest relative percentages of the FA 16:4 and 18:3 were observed upon cultivation with white light, compared to all other conditions. The dark controls and red light treated cultivations reached a significantly lower percentage of 16:4 and 18:3 at the same time (Figure 3a and b). In experiment 2, the highest relative percentages of the FA 16:4, and 18:3 were observed upon cultivation with white light and yellow light, compared to the red light and orange light treated approaches (Table 3, Figure 3a and b).

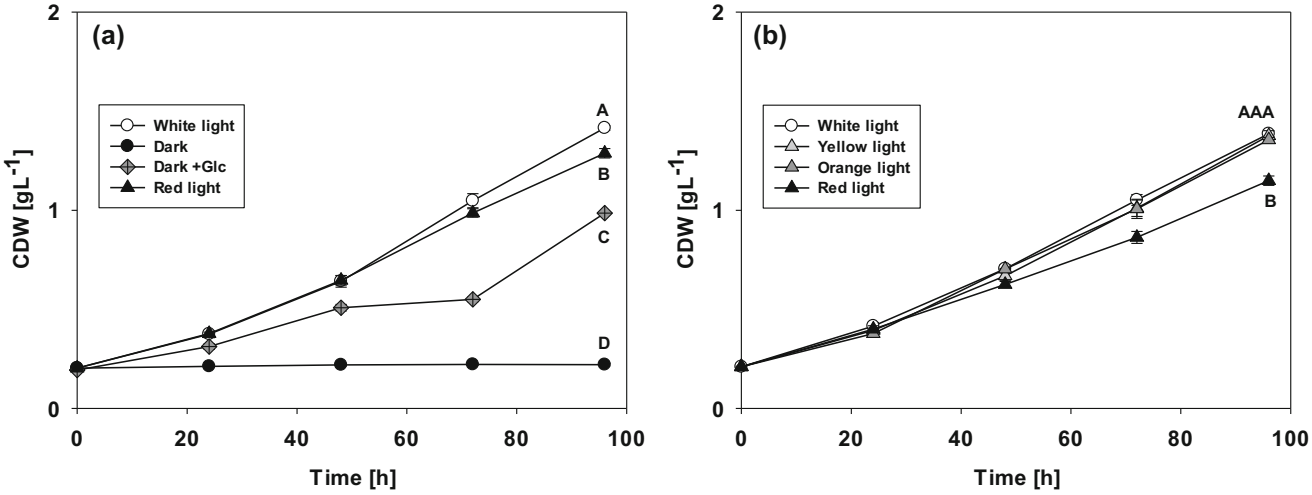

FIGURE 2 Biomass production of *A. obliquus* exposed to (a) white light (380–700 nm), red light (600–700 nm), dark controls with, and without 2 gL^{-1} glucose (experiment 1), and (b) white light (380–700 nm), yellow light (470–700 nm), orange light (520–700 nm), and red light (600–700 nm) (experiment 2). Both experiments were done at 210 μmol m^{-2} s^{-1} (if light was applied) and 15°C temperature. The cell dry weight (CDW) was determined by a correlation with the optical density at 750 nm. Values represent means and standard errors. Experiment 1 was repeated three times and experiment 2 was repeated two times. Different superscript letters (A–D) mean significant differences between groups ($p < 0.05$)

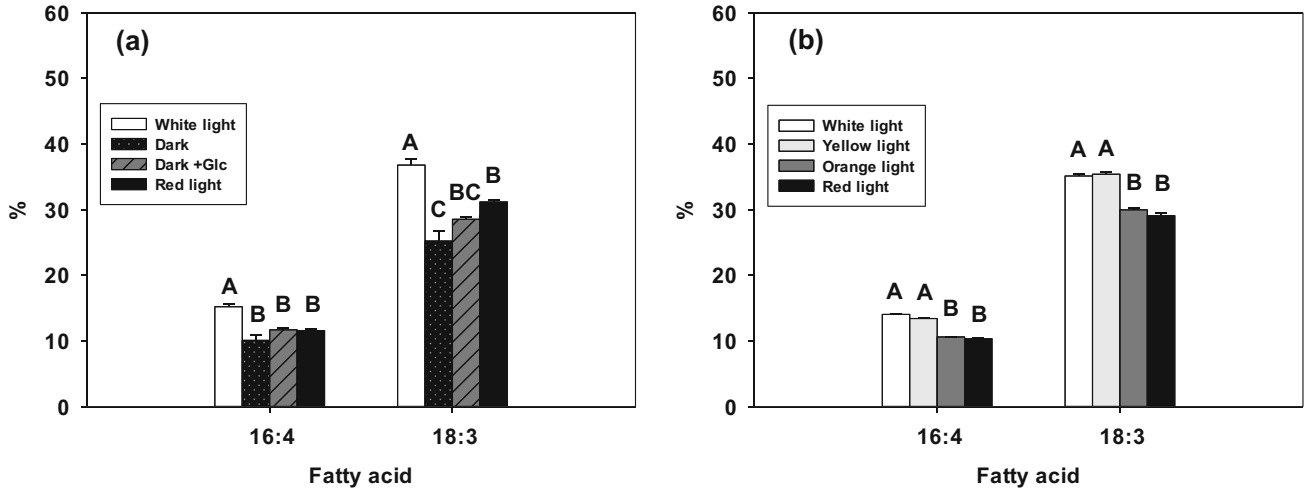

FIGURE 3 Relative percentage of the fatty acids 16:4 and 18:3 in *A. obliquus* exposed to (a) white light (380–700 nm), red light (600–700 nm), dark controls with, and without 2 gL^{-1} glucose (experiment 1), and (b) white light (380–700 nm), yellow light (470–700 nm), orange light (520–700 nm), and red light (600–700 nm) (experiment 2). Both experiments were done at 210 μmol m^{-2} s^{-1} (if light was applied) and 15°C temperature. The measurement of fatty acid were carried using GS-MS. all values shown are the means ± standard errors of two (experiment 1) and three independent experiments (experiment 2). Data were analyzed by using one-way ANOVA, followed by Tukey's multiple comparison test. Different superscript letters (A–C) mean significant differences between groups ($p < 0.05$)

Notably, no significant differences could be observed between the white light and yellow light treated cultivations, as well as between the red and orange light treated groups (Figure 3a and b). Furthermore, no significant differences were observed between the red light treated samples and the heterotrophic dark control samples (Figure 3a). No significant impact of the light conditions on the relative percentage of 18:4 in *A. obliquus* was observed (data not shown). Additionally, the percentage of 16:1 increased considerably after adding glucose in the absence of light (Table 2).

Impact of the light conditions on the pigment concentration

In the pigment analysis, two photosynthetic pigments (chlorophyll a and chlorophyll b) and four xanthophylls (lutein, violaxanthin, neoxanthin, and beta carotene)

TABLE 2 Fatty acids. Results of the fatty acid analysis of experiment 1. The analysis was repeated three

	16:1 [%]	16:2 [%]	16:3 [%]	16:4 [%]	18:1 [%]
W	1.4 ± 0.1^{bc}	0.1 ± 0.1^{c}	2.3 ± 0.1^{c}	15.2 ± 0.4^{a}	2.3 ± 0.1^{b}
D	2.0 ± 0.2^{b}	0.4 ± 0.1^{b}	4.8 ± 0.3^{a}	10.1 ± 0.8^{b}	4.8 ± 0.2^{a}
D + Glc	4.8 ± 0.1^{a}	0.7 ± 0.1^{a}	3.7 ± 0.1^{b}	11.7 ± 0.2^{b}	4.8 ± 0.1^{a}
R	1.3 ± 0.1^{c}	0.3 ± 0.1^{b}	4.5 ± 0.1^{ab}	11.6 ± 0.2^{b}	4.8 ± 0.3^{a}
	18:2 [%]	**18:3 [%]**	**SFA [%]**	**MUFA [%]**	**PUFA [%]**
W	1.7 ± 0.1^{c}	36.8 ± 0.9^{a}	37.7 ± 0.1	3.7 ± 0.1^{c}	58.6 ± 0.9^{a}
D	7.4 ± 0.4^{a}	25.2 ± 1.5^{c}	43.0 ± 1.0	6.8 ± 0.2^{b}	50.2 ± 1.0^{b}
D + Glc	5.7 ± 0.1^{b}	28.67 ± 0.3^{bc}	37.8 ± 0.3	9.5 ± 0.1^{a}	52.6 ± 0.1^{ab}
R	5.5 ± 0.1^{b}	31.2 ± 0.3^{b}	38.0 ± 0.1	6.1 ± 0.2^{b}	55.9 ± 0.3^{ab}

Note: Values represent the means ± standard errors. W, white light; D, dark control; D + Glc, dark with additional glucose. The isomers (c/t) of 16:1 were summed up. Different superscript letters (a–c) mean significant differences between groups ($P < 0.05$).

TABLE 3 Fatty acids. Results of the fatty acid analysis of experiment 2

	16:1 [%]	16:2 [%]	16:3 [%]	16:4 [%]	18:1 [%]
W	1.3 ± 0.1	0.1 ± 0.1^{c}	2.4 ± 0.1^{c}	14.1 ± 0.1^{a}	2.4 ± 0.1^{b}
Y	1.1 ± 0.1	0.2 ± 0.1^{b}	3.1 ± 0.2^{b}	13.4 ± 0.1^{a}	2.8 ± 0.1^{b}
O	1.2 ± 0.1	0.4 ± 0.1^{a}	4.7 ± 0.1^{a}	10.7 ± 0.1^{b}	4.8 ± 0.3^{a}
R	1.3 ± 0.1	0.4 ± 0.1^{a}	4.9 ± 0.1^{a}	10.4 ± 0.2^{b}	5.2 ± 0.2^{a}
	18:2 [%]	**18:3 [%]**	**SFA [%]**	**MUFA [%]**	**PUFA [%]**
W	1.8 ± 0.1^{d}	35.1 ± 0.3^{a}	40.5 ± 0.2	3.7 ± 0.1^{b}	55.8 ± 0.2
Y	2.9 ± 0.1^{c}	35.4 ± 0.4^{a}	38.4 ± 0.5	4.0 ± 0.1^{b}	57.7 ± 0.4
O	5.7 ± 0.1^{b}	30.1 ± 0.2^{b}	39.8 ± 0.4	6.0 ± 0.2^{a}	54.2 ± 0.2
R	6.4 ± 0.1^{a}	29.1 ± 0.5^{b}	39.6 ± 0.6	6.5 ± 0.1^{a}	53.9 ± 0.4

Note: The analysis was repeated two times. Values represent the means ± standard errors. W, white light; R, red light; O, orange light; Y, yellow light. The isomers (c/t) of 16:1 were summed up. Different superscript letters (a–d) mean significant differences between groups ($P < 0.05$).

TABLE 4 Results of the pigment analysis of experiment 1

	Chl a μg g^{-1} CDW	Chl b μg g^{-1} CDW	Lutein μg g^{-1} CDW	Vio μg g^{-1} CDW	Neo μg g^{-1} CDW	Beta μg g^{-1} CDW
W	18,003 ± 2099	5345 ± 579	1594 ± 250	300 ± 45	857 ± 119	855 ± 141
D	14,049 ± 404	4345 ± 164	975 ± 135	219 ± 32	769 ± 73	372 ± 83
D + Glc	6720 ± 679	2249 ± 249	449 ± 35	85 ± 11	390 ± 36	132 ± 2
R	15,646 ± 5408	4549 ± 1620	1188 ± 356	250 ± 80	805 ± 260	651 ± 87

Note: The analysis was performed once. Values represent means of triplicates ± standard deviation. Chl a, Chlorophyll-a; Chl b, Chlorophyll-b; Vio, Violaxanthin; neo, Neoxanthin, beta, Beta carotene; W, white light; D, dark control; D + Glc, dark with additional glucose; R, red light; O, orange light; Y, yellow light.

were identified in *A. obliquus* (Tables 4 and 5). The pigment composition in *A. obliquus* is explained in detail for experiment 2. Under white light treatment in experiment 2 the photosynthetic pigment, chlorophyll-a, was identified in concentrations of 14,939 ± 332 μg g^{-1} CDW. The second porphyrin pigment, chlorophyll b, was identified in concentrations of 5794 ± 309 μg g^{-1} CDW. Lutein was found in concentrations of 1529 ± 58 μg g^{-1} CDW. It is known that *A. obliquus* is a lutein-rich microalga (Ho et al., 2014). Furthermore, the xanthophylls violaxanthin, neoxanthin, and beta carotene were identified in amounts of 269 ± 31 μg g^{-1} CDW, 907 ± 78 μg g^{-1} CDW, and 428 ± 18 μg g^{-1} CDW, respectively (Table 5). A similar pigment composition was also observed in experiment 1 (Table 4).

Similar to the results received for the FA, a strong impact of the light spectrum on the pigment concentration was observed. The concentration decreased successively with the decreasing share of blue light in the yellow, orange, and red light spectra, respectively (Table 5, Figure 1). Under red light conditions, only 47.1% of the lutein concentration was found, compared to white light conditions (Table 5). The same tendency was also observed for the pigments chlorophyll a, violaxanthin, neoxanthin, and beta carotene (Table 4). A similar effect was also observed in the pigment data

TABLE 5 Results of the pigment analysis of experiment 2

	Chl a µg g^{-1} CDW	Chl b µg g^{-1} CDW	Lutein µg g^{-1} CDW	Vio µg g^{-1} CDW	Neo µg g^{-1} CDW	Beta µg g^{-1} CDW
W	14,939 ± 332	5794 ± 309	1529 ± 58	269 ± 31	907 ± 78	428 ± 18
Y	10,490 ± 2085	4265 ± 520	1034 ± 216	188 ± 46	603 ± 170	326 ± 100
O	7910 ± 1835	3435 ± 251	747 ± 157	132 ± 28	464 ± 119	207 ± 64
R	8355 ± 2572	5090 ± 1082	721 ± 189	133 ± 33	541 ± 161	163 ± 44

Note: The analysis was repeated two times for the samples of experiment 2. Values represent the means ± standard error in the experiment. Chl a, Chlorophyll-a; Chl b, Chlorophyll-b; Vio, Violaxanthin; neo, Neoxanthin, beta, Beta carotene; W, white light; D, dark control; D + Glc, dark with additional glucose; R, red light; O, orange light; Y, yellow light, CDW, cell dry weight.

of experiment 1. The highest concentrations were observed for the white light cultivation, compared to the red light and dark treatments (Table 4).

DISCUSSION

In this study, *A. obliquus* was cultivated at 15°C under different light conditions. The low temperature was chosen to maximize the FA-unsaturation. Microalgae raise the PUFA content with lowered environmental temperatures to maintain the fluidity of cell membranes (Degraeve-Guilbault et al., 2021; Patterson, 1970). However, the used cultivation temperature is lower than the optimum temperature of this species, which is around 30°C (Hindersin et al., 2012). Therefore, the biomass production was lower than in previous studies with the same strain, which were performed around the optimum temperature of this species (Admirasari et al., 2022; Helamieh et al., 2021; Reymann et al., 2020). In addition, the growth under monochromatic red light was significantly lower compared to all other tested light spectra (Figure 2). This finding is also supported by a recent study on the same algae strain. It was shown that wavelengths below 500 nm combined with red light (600–700 nm) lead to higher photosynthetic efficiency and growth in *A. obliquus*, compared to monochromatic red light (600–700 nm) (Osterthun, Helamieh, et al., 2021).

The FA composition is in accordance with several published data on the same microalgal strain (Abomohra et al., 2013; Helamieh et al., 2021). However, due to the lower cultivation temperature, a higher relative percentage of PUFA, such as 18:3 and 16:4 was observed in this study. The relative percentage of the PUFA 18:3 and 16:4 reached up to 36.8%, and 15.2% of the relative FA percentage under white light conditions (Table 2, Figure 3).

This study observed a significant impact on the FA composition (Figure 3, Tables 2 and 3). We have already postulated that light wavelengths between 450 and 550 nm are required for maximum FA unsaturation in *A. obliquus* (Helamieh et al., 2021). This was confirmed in the present study. Moreover, this study's results can contribute to localizing the required waveband with a higher spectral resolution. The highest percentages of the PUFA 16:4 and 18:3 were observed upon white light (380–700 nm) and yellow light (470–700 nm) treatments, whereas red light (600–700 nm), orange light (520–700 nm), and dark treated samples reached significantly lower values in all experiments (Figure 3a and b). The highest percentage of 16:4 and 18:3 were found upon white and yellow light treatment. Both light spectra share the wavelength range between 470 and 520 nm. Based on these data, it can be concluded that this 50 nm broad waveband is relevant for the FA unsaturation in *A. obliquus*.

Accordingly, the red light and orange light treated group, as well as the dark controls, showed the lowest percentage of 16:4 and 18:3. No significant differences could be observed between the red and orange light treated cultivations (Figure 3a and b). Additionally, no significant differences were observed between the red light treated samples and the heterotrophic dark control samples (Figure 3a). Therefore, no impact of the wavelengths between 520 and 700 nm (contained in orange and red light) on the FA desaturation was found.

The elevation of the FA16:1 in the heterotrophic dark treated samples is remarkable, even though no immediate explanation for it can be found in the literature. In addition, different from (Helamieh et al., 2021), no impact of the light conditions on the relative percentage of 18:4 in *A. obliquus* was observed (data not shown).

The photosynthetic pigments were identified in proportions and concentrations that are typical for *A. obliquus* (Admirasari et al., 2022; Ho et al., 2014; Wiltshire et al., 2000). Previous work showed that exposure to specific light spectra is decisive for the production of pigments in microalgae (Chainapong et al., 2012; Ho et al., 2014). Our results confirm that the light conditions strongly impact the pigment composition. A stable tendency was observed for the carotenoid, lutein. The highest concentration was detected under white light treatment. A higher concentration of pigments in microalgae upon white light exposition was already observed (Ho et al., 2014). We assume, that similar to the FA data, the blue light component in the white light spectrum is decisive for the maximum pigment production (Figure 1). Blue light is associated with the synthesis of chlorophyll-a and is additionally involved

in rearrangements of chloroplasts (Sánchez-Saavedra & Voltolina, 2002). The carotenoids and xanthophylls have their absorption maximum in the waveband between 400 and 500 nm (Peterman et al., 1997). The impact of the applied spectra on the pigment concentrations shows similar patterns to the described blue-green light effect on the FA unsaturation. Though different from the FA composition, the concentrations of the pigments decrease successively, rather than abruptly, with the decreasing blue light content in the spectra (Tables 2–5, Figure 1, Figure 3).

Blue-green light effects on the metabolism of *A. obliquus*

The results show that blue-green light has an important function in the metabolism of *A. obliquus*: The growth under red light was reduced compared to all other tested light spectra. It was reported that supplementation of blue light could substantially improve the growth of *A. obliquus* compared to monochromatic red light (Osterthun, Helamieh, et al., 2021). Although the physiological reason for this finding is not apparent, we assume that blue light has vital functions in the metabolism required for high biomass production. However, several functions of blue light in organisms are already known in literature and can give some insights into putative mechanisms behind the finding. For instance, it is already known that the cell division of microalgae is regulated via blue light (Münzner & Voigt, 1992). Furthermore, blue light is essential for the entrainment of the circadian clock in many organisms (Hajdu et al., 2018; Li et al., 2016).

If the spectrum contained blue light, not only the CDW but also the concentration of the carotenoids and chlorophyll a in *A. obliquus* reached higher values compared to the treatment with monochromatic red light (Tables 4 and 5). Furthermore, also the FA metabolism is impacted by blue-green light. Only if light with wavelengths between 470 and 520 nm was applied, a significantly higher percentage of the FA 16:4 and 18:3 was observed compared to all other light treatments (Figure 3). Moreover, the higher concentration of pigments upon blue-green appears to be paralleling with the increase of FA unsaturation. Both effects are putatively related to rearrangement processes in the chloroplasts (Ho et al., 2014; Sánchez-Saavedra & Voltolina, 2002). Higher unsaturated FA can be found in thylakoid membranes of chloroplasts in high percentages (Hugly & Somerville, 1992; Hultberg et al., 2014; Poliner et al., 2021). Therefore, this part of the light spectrum might increase the thylakoid membrane systems, with a concomitant elevation of pigments and specific PUFA in *A. obliquus*.

Blue light is also involved in posttranscriptional activations of different enzymes. For example, in the green microalga *Monoraphidium braunii*, the import of nitrate and the nitrate reductase is activated by blue light (Aparicio et al., 1976; Aparicio & Quiñones, 1991; Quiñones & Aparicio, 1990). Recently, a blue light-driven decarboxylation of FA to alkanes in *Chlorella variabilis* was reported (Huijbers et al., 2018). It was suggested that this spectrally selective photoactivation of the decarboxylase could be harnessed for the enzymatic production of biodiesel. Another group of light-dependent enzymes are FA desaturases. It is well known that these enzymes in plants and microorganisms are activated by environmental cues, such as light (Kis et al., 1998). In *A. obliquus* and the stramenopile microalga *Nannochloropsis oceanica*, this activation of FA desaturases is assumed to be triggered by blue-green light exclusively (Helamieh et al., 2021; Poliner et al., 2021). This study on *A. obliquus* also supports this assumption. Moreover, the responsible part of the light spectrum was further localized and narrowed down to a 50 nm broad waveband between 470 nm and 520 nm.

SUMMARY AND OUTLOOK

The variety of blue light effects on the metabolism of *A. obliquus* and the important function for FA desaturation shows the need for further research. Many light perceiving processes in organisms are highly conserved in the evolution of life. Therefore, it might be interesting to elucidate if the requirement of blue light for FA unsaturation is a widespread effect in plants and microalgae. Besides the basic scientific research, this knowledge can be used for industrial applications. For example, the selective illumination with supplementation of blue-green light can be harnessed for a maximized production of PUFA and bioactive compounds, such as lutein in microalgae. This is especially desirable for microalgal feed and food products. Vice versa, the relative percentage of PUFA can be reduced for the production of biofuels from microalgal FA, applying a spectrally selective illumination that lacks the waveband between 470 and 520 nm. One technical application of this knowledge is possible in photovoltaic-photosynthesis hybrid systems.

This study evaluated the impact of different light spectra on the growth, FA composition, and pigment concentration of *A. obliquus*. We were able to show that blue-green light (380–520 nm) is crucial for a maximized production of pigments and a high percentage of the PUFA 16:4 and 18:3. Especially, the narrow light waveband between 470 and 520 nm is important for a high degree of FA unsaturation. Therefore, the importance of blue-green light should be taken into account in spectrally selective illumination microalgae cultivation systems. This knowledge might be the base for a light stimulated production of microalgal pigments and specific FA for the food and biofuel production.

ACKNOWLEDGMENTS

This study was funded by the research initiative Zukunft Bau of the Federal Institute for Research on Building, Urban Affairs, and Spatial Development (No. SWD-10.08.18.7-17.02). A special thanks goes to Christoph Stegen of the technical support team of the Leuphana University Lüneburg for his excellent technical support and expertise to optimize the experimental setup for microalgae cultivation. We thank Kerstin Nachtigall of the GEOMAR Helmholtz Centre for Ocean Research Kiel, for performing the HPLC-DAD analysis. Finally, we want to thank Professor Dr. Dieter Hanelt, PD Dr. Klaus von Schwartzenberg, and the staff of the Microalgae and Zygnematophyceae Collection Hamburg (MZCH, previously SVCK) microalgae collection of the University of Hamburg for giving us the chance to work with one of their microalgae strains.

CONFLICT OF INTEREST

The authors declare that they have no conflict of interest.

CREDIT AUTHORSHIP CONTRIBUTION STATEMENT

All authors have made a scientific contribution and approved the final draft of the manuscript. **Mark Helamieh**: Conceived and designed the study. Carried out the research analysis and interpretation of data. Wrote the first draft of the manuscript. **Marco Reich**: Supervision and support in the methodology part. Analysis and interpretation of data. Contribution to the writing process. Editing and review of manuscript. **Sophie Bory**: Carried out the research. Analysis of data. **Philipp Rohne**: Analysis of data and made the statistical work. Contribution to the writing process. **Ulf Riebesell**: Carried out the research. Analysis of data. **Martin Kerner**: Analysis of data. Contribution to the writing process. Supervision of the study. **Klaus Kümmerer**: Supervision and support in the methodology part. Contribution to the writing process. Analysis and interpretation of data. Editing and review of the manuscript.

ETHICS STATEMENT

No human or animal subjects were used in this study.

REFERENCES

Abomohra AEF, Almutairi AW. A close-loop integrated approach for microalgae cultivation and efficient utilization of agar-free seaweed residues for enhanced biofuel recovery. Bioresour Technol. 2020; 317:124027. https://doi.org/10.1016/J.BIORTECH.2020.124027

Abomohra AEF, Wagner M, El-Sheekh M, Hanelt D. Lipid and total fatty acid productivity in photoautotrophic fresh water microalgae: screening studies towards biodiesel production. J Appl Phycol. 2013;25(4):931–6. https://doi.org/10.1007/s10811-012-9917-y

Adarme-Vega TC, Lim DKY, Timmins M, Vernen F, Li Y, Schenk PM. Microalgal biofactories: a promising approach towards sustainable omega-3 fatty acid production. Microb Cell Fact. 2012;11(1): 1–10. https://doi.org/10.1186/1475-2859-11-96

Admirasari R, Hindersin S, von Schwartzenberg K, Hanelt D. Nutritive capability of anaerobically digested black water increases productivity of *Tetradesmus obliquus*: domestic wastewater as an alternative nutrient resource. Bioresource Technol Rep. 2022; 17:100905. https://doi.org/10.1016/J.BITEB.2021.100905

Ahmad AL, Yasin NHM, Derek CJC, Lim JK. Microalgae as a sustainable energy source for biodiesel production: a review. Renew Sustain Energy Rev. 2011;15(1):584–93. https://doi.org/10.1016/J.RSER.2010.09.018

Almarashi JQM, El-Zohary SE, Ellabban MA, Abomohra AEF. Enhancement of lipid production and energy recovery from the green microalga Chlorella vulgaris by inoculum pretreatment with low-dose cold atmospheric pressure plasma (CAPP). Energ Conver Manage. 2020;204:112314. https://doi.org/10.1016/J.ENCONMAN.2019.112314

Anto S, Mukherjee SS, Muthappa R, Mathimani T, Deviram G, Kumar SS, et al. Algae as green energy reserve: technological outlook on biofuel production. Chemosphere. 2020;242:125079. https://doi.org/10.1016/J.CHEMOSPHERE.2019.125079

Aparicio PJ, Quiñones MA. Blue light, a positive switch signal for nitrate and nitrite uptake by the green alga *Monoraphidium braunii*. Plant Physiol. 1991;95(2):374–8. https://doi.org/10.1104/PP.95.2.374

Aparicio PJ, Roldán JM, Calero F. Blue light photoreactivation of nitrate reductase from green algae and higher plants. Biochem Biophys Res Commun. 1976;70(4):1071–7. https://doi.org/10.1016/0006-291X(76)91011-1

Aussant J, Guihéneuf F, Stengel DB. Impact of temperature on fatty acid composition and nutritional value in eight species of microalgae. Appl Microbiol Biotechnol. 2018;102(12):5279–97. doi:10.1007/S00253-018-9001-X

Behrens PW, Kyle DJ. Microalgae as a source of fatty acids. J Food Lipids. 1996;3(4):259–72. https://doi.org/10.1111/J.1745-4522.1996.TB00073.X

Blanco Gonzalez E, De Boer F. The development of the Norwegian wrasse fishery and the use of wrasses as cleaner fish in the salmon aquaculture industry. Fish Sci. 2017;83:661–70. https://doi.org/10.1007/s12562-017-1110-4

Chainapong T, Traichaiyaporn S, Richard L. Ceridão_Nascimento_ALICEpdf, 2012; 8(5): 1593–1604.

Chhandama MVL, Satyan KB, Changmai B, Vanlalveni C, Rokhum SL. Microalgae as a feedstock for the production of biodiesel: a review. Bioresource Technol Rep. 2021;15:100771. https://doi.org/10.1016/J.BITEB.2021.100771

Degraeve-Guilbault C, Pankasem N, Gueirrero M, Lemoigne C, Domergue F, Kotajima T, et al. Temperature acclimation of the picoalga *Ostreococcus tauri* triggers early fatty-acid variations and involves a plastidial ω3-desaturase. Front Plant Sci. 2021; 12:639330. https://doi.org/10.3389/FPLS.2021.639330

El-Sheekh M, Abomohra AE-F, Hanelt D. Optimization of biomass and fatty acid productivity of *Scenedesmus obliquus* as a promising microalga for biodiesel production. World J Microbiol Biotechnol. 2012;29(5):915–22. https://doi.org/10.1007/S11274-012-1248-2

Esakkimuthu S, Krishnamurthy V, Wang S, Hu X, Abomohra AEF. Application of p-coumaric acid for extraordinary lipid production in *Tetradesmus obliquus*: a sustainable approach towards enhanced biodiesel production. Renew Energy. 2020;157: 368–76. https://doi.org/10.1016/J.RENENE.2020.05.005

Fabiani H, Mudjihartini N, Lestari W. Dietary omega-6 to omega-3 fatty acids ratio is correlated with high molecular weight adiponectin level in Indonesian office workers. Int J Nutr Pharmacol Neurol Dis. 2021;11(1):64. https://doi.org/10.4103/IJNPND.IJNPND_89_20

Fu W, Guomundsson Ó, Paglia G, Herjólfsson G, Andrésson ÓS, Palsson BO, et al. Enhancement of carotenoid biosynthesis in the green microalga *Dunaliella salina* with light-emitting diodes and adaptive laboratory evolution. Appl Microbiol Biotechnol. 2013; 97(6):2395–403. https://doi.org/10.1007/s00253-012-4502-5

Goiris K, Muylaert K, Fraeye I, Foubert I, de Brabanter J, de Cooman L. Antioxidant potential of microalgae in relation to their phenolic and carotenoid content. J Appl Phycol. 2012;24(6):1477–86. https://doi.org/10.1007/s10811-012-9804-6

Gong Y, Hu H, Gao Y, Xu X, Gao H. Microalgae as platforms for production of recombinant proteins and valuable compounds: Progress and prospects. J Ind Microbiol Biotechnol. 2011;38(12):1879–90. https://doi.org/10.1007/s10295-011-1032-6

Hajdu A, Dobos O, Domijan M, Bálint B, Nagy I, Nagy F, et al. ELONGATED HYPOCOTYL 5 mediates blue light signalling to the *Arabidopsis circadian* clock. Plant J. 2018;96(6):1242–54. https://doi.org/10.1111/TPJ.14106

Helamieh M, Gebhardt A, Reich M, Kuhn F, Kerner M, Kümmerer K. Growth and fatty acid composition of *Acutodesmus obliquus* under different light spectra and temperatures. Lipids. 2021;56:485–98. https://doi.org/10.1002/lipd.12316

Hindersin S, Leupold M, Kerner M, Hanelt D. Irradiance optimization of outdoor microalgal cultures using solar tracked photobioreactors. Bioprocess Biosyst Eng. 2012;36(3):345–55. https://doi.org/10.1007/S00449-012-0790-5

Ho SH, Chan MC, Liu CC, Chen CY, Lee WL, Lee DJ, et al. Enhancing lutein productivity of an indigenous microalga *Scenedesmus obliquus* FSP-3 using light-related strategies. Bioresour Technol. 2014;152:275–82. https://doi.org/10.1016/j.biortech.2013.11.031

Hugly S, Somerville C. A role for membrane lipid polyunsaturation in chloroplast biogenesis at low temperature. Plant Physiol. 1992;99(1):197–202. https://doi.org/10.1104/PP.99.1.197

Huijbers MME, Zhang W, Tonin F, Hollmann F. Light-driven enzymatic decarboxylation of fatty acids. Angew Chem Int Ed. 2018;57(41):13648–51. https://doi.org/10.1002/ANIE.201807119

Hultberg M, Jönsson HL, Bergstrand KJ, Carlsson AS. Impact of light quality on biomass production and fatty acid content in the microalga *Chlorella vulgaris*. Bioresour Technol. 2014;159:465–7. https://doi.org/10.1016/J.BIORTECH.2014.03.092

Ichihara K, Fukubayashi Y. Preparation of fatty acid methyl esters for gas-liquid chromatography. J Lipid Res. 2010;51(3):635–40. https://doi.org/10.1194/JLR.D001065/ATTACHMENT/55D3C28E-DB2E-47F2-A45B-FB118C1DF3A0/MMC1.PDF

Kis M, Zsiros O, Farkas T, Wada H, Nagy F, Gombos Z. Light-induced expression of fatty acid desaturase genes. Proc Natl Acad Sci USA. 1998;95(8):4209–14. https://doi.org/10.1073/PNAS.95.8.4209

Krimech A, Helamieh M, Wulf M, Krohn I, Riebesell U, Cherifi O, et al. Differences in adaptation to light and temperature extremes of *Chlorella sorokiniana* strains isolated from a wastewater lagoon. Bioresour Technol. 2022;350:126931. https://doi.org/10.1016/J.BIORTECH.2022.126931

Kusmayadi A, Leong YK, Yen HW, Huang CY, Chang JS. Microalgae as sustainable food and feed sources for animals and humans – biotechnological and environmental aspects. Chemosphere. 2021;271:129800. https://doi.org/10.1016/J.CHEMOSPHERE.2021.129800

Li X, Ma D, Lu SX, Hu X, Huang R, Liang T, et al. Blue light- and low temperature-regulated COR27 and COR28 play roles in the Arabidopsis circadian clock. Plant Cell. 2016;28(11):2755–69. https://doi.org/10.1105/TPC.16.00354

Miranda MT, Sepúlveda FJ, Arranz JI, Montero I, Rojas C. Physical-energy characterization of microalgae Scenedesmus and experimental pellets. Fuel. 2018;226:121–6. https://doi.org/10.1016/J.FUEL.2018.03.097

Münzner P, Voigt J. Blue light regulation of cell division in Chlamydomonas reinhardtii. Plant Physiol. 1992;99(4):1370–5. https://doi.org/10.1104/PP.99.4.1370

Nzayisenga JC, Farge X, Groll SL, Sellstedt A. Effects of light intensity on growth and lipid production in microalgae grown in wastewater. Biotechnol Biofuels. 2020;13(1):1–8. https://doi.org/10.1186/s13068-019-1646-x

Osterthun N, Helamieh M, Berends D, Neugebohrn N, Vehse M, Kerner M, Agert C. Influence of spectrally selective solar cells on microalgae growth in photo-bioreactors. 2021:70001.

Osterthun N, Neugebohrn N, Gehrke K, Vehse M, Agert C. Spectral engineering of ultrathin germanium solar cells for combined photovoltaic and photosynthesis. Opt Express. 2021;29(2):938. https://doi.org/10.1364/oe.412101

Patterson GW. Effect of culture temperature on fatty acid composition of *Chlorella sorokiniana*. Lipids. 1970;5(7):597–600. https://doi.org/10.1007/BF02531336

Peterman EJG, Gradinaru CC, Calkoen F, Borst JC, van Grondelle R, van Amerongen H. Xanthophylls in light-harvesting complex II of higher plants: light harvesting and triplet quenching†. Biochemistry. 1997;36(40):12208–15. https://doi.org/10.1021/BI9711689

Piligaev AV, Sorokina KN, Bryanskaya AV, Peltek SE, Kolchanov NA, Parmon VN. Isolation of prospective microalgal strains with high saturated fatty acid content for biofuel production. Algal Res. 2015;12:368–76. https://doi.org/10.1016/J.ALGAL.2015.08.026

Poliner E, Busch AWU, Newton L, Kim YU, Clark R, Gonzalez-Martinez SC, et al. Aureochromes are necessary for maintaining polyunsaturated fatty acid content in *Nannochloropsis oceanica*. BioRxiv. 2021;2021(01):428447. https://doi.org/10.1101/2021.01.27.428447

Quiñones MA, Aparicio PJ. Blue light activation of nitrate reductase and blue light promotion of the biosynthesis of nitrite reductase in *Monoraphidium braunii*. In: Ullrich WR, Rigano C, Fuggi A, Aparicio PJ, (eds), *Inorganic Nitrogen in Plants and Microorganisms*. Berlin, Heidelberg: Springer; 1990;171–7. https://doi.org/10.1007/978-3-642-75812-6_26

Reich M, Hannig C, Al-Ahmad A, Bolek R, Kümmerer K. A comprehensive method for determination of fatty acids in the initial oral biofilm (pellicle). J Lipid Res. 2012;53(10):2226–30. https://doi.org/10.1194/JLR.D026260

Reich M, Kümmerer K, Al-Ahmad A, Hannig C. Fatty acid profile of the initial oral biofilm (pellicle): an in-situ study. Lipids. 2013;48(9):929–37. https://doi.org/10.1007/S11745-013-3822-2

Reymann T, Kerner M, Kümmerer K. Assessment of the biotic and abiotic elimination processes of five micropollutants during cultivation of the green microalgae *Acutodesmus obliquus*. Bioresource Technol Rep. 2020;11:100512. https://doi.org/10.1016/J.BITEB.2020.100512

Rösch C, Roßmann M, Weickert S. Microalgae for integrated food and fuel production. GCB Bioenergy. 2019;11(1):326–34. https://doi.org/10.1111/GCBB.12579

Sánchez-Saavedra MP, Voltolina D. Efecto de las tasas de flujo de fotones de luz blanca y azul-verde en la eficiencia del crecimiento y contenido de pigmentos de tres especies de diatomeas en cultivos terminales. Cienc Mar. 2002;28(3):273–9. https://doi.org/10.7773/cm.v28i3.225

Schenk PM, Thomas-Hall SR, Stephens E, Marx UC, Mussgnug JH, Posten C, et al. Second generation biofuels: high-efficiency microalgae for biodiesel production. Bioenergy Res. 2008;1(1):20–43. https://doi.org/10.1007/s12155-008-9008-8

Shanab SMM, Hafez RM, Fouad AS. A review on algae and plants as potential source of arachidonic acid. J Adv Res. 2018;11:3–13. https://doi.org/10.1016/J.JARE.2018.03.004

Sharmila D, Suresh A, Indhumathi J, Gowtham K, Velmurugan N. Impact of various color filtered LED lights on microalgae growth, pigments and lipid production. Eur J Biotechnol Biosci. 2018;6(6):1–7. www.biosciencejournals.com

Shu C-H, Tsai C-C, Liao W-H, Chen K-Y, Huang H-C. Effects of light quality on the accumulation of oil in a mixed culture of Chlorella sp. and *Saccharomyces cerevisiae*. Chem Technol Biotechnol. 2012;87:601–7. https://doi.org/10.1002/jctb.2750

Simopoulos AP. The importance of the ratio of omega-6/omega-3 essential fatty acids. Biomed Pharmacother. 2002;56(8):365–79. https://doi.org/10.1016/S0753-3322(02)00253-6

Singh A, Nigam PS, Murphy JD. Renewable fuels from algae: an answer to debatable land based fuels. Bioresour Technol. 2011; 102(1):10–6. https://doi.org/10.1016/J.BIORTECH.2010.06.032

Sun Z, Zhi-gang Z, Jiang Y. Microalgae as a source of lutein: chemistry, biosynthesis, and Carotenogenesis. Adv Biochem Eng Biotechnol. 2014;123(July):127–41. https://doi.org/10.1007/10

Tang DYY, Yew GY, Koyande AK, Chew KW, Vo DVN, Show PL. Green technology for the industrial production of biofuels and bioproducts from microalgae: a review. Environ Chem Lett. 2020;18(6):1967–85. https://doi.org/10.1007/s10311-020-01052-3

van Heukelem L, Thomas CS. Computer-assisted high-performance liquid chromatography method development with applications to the isolation and analysis of phytoplankton pigments. J Chromatogr A. 2001;910(1):31–49. https://doi.org/10.1016/S0378-4347(00)00603-4

Vaz B d S, Moreira JB, Morais MG d, Costa JAV. Microalgae as a new source of bioactive compounds in food supplements. Curr Opin Food Sci. 2016;7:73–7. https://doi.org/10.1016/J.COFS.2015.12.006

von Schwartzenberg K, Bornfleth S, Lindner A-C, Hanelt D. The microalgae and Zygnematophyceae collection Hamburg (MZCH) – living cultures for research on rare streptophytic algae. Algolog Stud. 2013;142:77–107. https://doi.org/10.1127/1864-1318/2013/0131

Wiltshire KH, Boersma M, Möller A, Buhtz H. Extraction of pigments and fatty acids from the green alga *Scenedesmus obliquus* (Chlorophyceae). Aquat Ecol. 2000;34(2):119–26. https://doi.org/10.1023/A:1009911418606

Worm B, Barbier EB, Beaumont N, Duffy JE, Folke C, Halpern BS, et al. Impacts of biodiversity loss on ocean ecosystem services. Science. 2006;314(5800):787–90. https://doi.org/10.1126/science.1132294

Zabed HM, Akter S, Yun J, Zhang G, Zhang Y, Qi X. Biogas from microalgae: technologies, challenges and opportunities. Renew Sustain Energy Rev. 2020;117:109503. https://doi.org/10.1016/J.RSER.2019.109503

SUPPORTING INFORMATION

Additional supporting information may be found in the online version of the article at the publisher's website.

How to cite this article: Helamieh M, Reich M, Bory S, Rohne P, Riebesell U, Kerner M, et al. Blue-green light is required for a maximized fatty acid unsaturation and pigment concentration in the microalga *Acutodesmus obliquus*. Lipids. 2022;57(4-5):221–32. https://doi.org/10.1002/lipd.12343

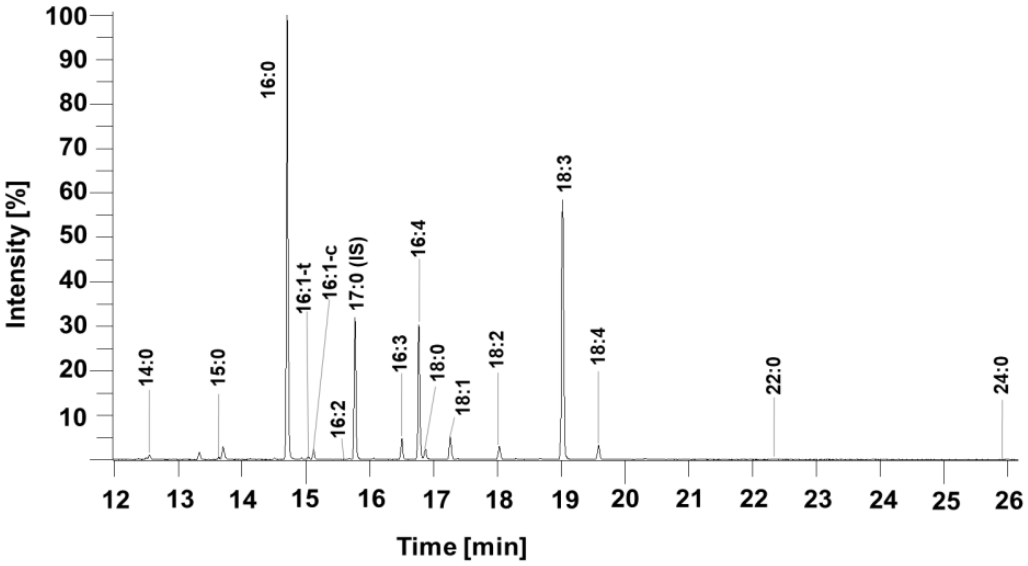

Supplementary Figure1. Fatty acid GC/MS chromatogram of *Acutodesmus obliquus* acquired in SIM mode. The sample was taken after 96 h of cultivation of *Acutodesmus obliquus* with 210 µmol m^{-2} $s^{-}1$ white light at 15°C.

Publikation 3

Impact of green and blue-green light on the growth, pigment concentration, and fatty acid unsaturation in the microalga *Monoraphidium braunii*

Mark Helamieh; Marco Reich; Philipp Rohne; Martin Kerner; Klaus Kümmerer

Im Oktober 2023 veröffentlicht bei *Photochemistry and Photobiology*.

DOI:10.1111/php.13873.

Received: 20 July 2023 | Revised: 4 October 2023 | Accepted: 4 October 2023

DOI: 10.1111/php.13873

RESEARCH ARTICLE

Impact of green and blue-green light on the growth, pigment concentration, and fatty acid unsaturation in the microalga *Monoraphidium braunii*

Mark Helamieh[1,2] | **Marco Reich**[1] | **Philipp Rohne**[3] | **Ulf Riebesell**[4] | **Martin Kerner**[2] | **Klaus Kümmerer**[1]

[1]Institute of Sustainable Chemistry, Leuphana University of Lueneburg, Lueneburg, Germany

[2]Strategic Science Consult Ltd., Hamburg, Germany

[3]Institute of Pharmacy and Biochemistry, Therapeutical Life Sciences, Johannes Gutenberg—University Mainz, Mainz, Germany

[4]GEOMAR Helmholtz Centre for Ocean Research Kiel, Kiel, Germany

Correspondence
Marco Reich, Institute of Sustainable Chemistry, Leuphana University of Lueneburg, Universitaetsallee 1, Lueneburg 21335, Germany.
Email: marco.reich@leuphana.de

Funding information
Bundesinstitut für Bau- Stadt- und Raumforschung, Grant/Award Number: SWD-10.08.18.7-17.02

Abstract

The spectral composition of light is an important factor for the metabolism of photosynthetic organisms. Several blue light-regulated metabolic processes have already been identified in the industrially relevant microalga *Monoraphidium braunii*. However, little is known about the spectral impact on this species' growth, fatty acid (FA), and pigment composition. In this study, *M. braunii* was cultivated under different light spectra (white light: 400–700 nm, blue light: 400–550 nm, green light: 450–600 nm, and red light: 580–700 nm) at 25°C for 96 h. The growth was monitored daily. Additionally, the FA composition, and pigment concentration was analyzed after 96 h. The highest biomass production was observed upon white light and red light irradiation. However, green light also led to comparably high biomass production, fueling the scientific debate about the contribution of weakly absorbed light wavelengths to microalgal biomass production. All light spectra (white, blue, and green) that comprised blue-green light (450–550 nm) led to a higher degree of FA unsaturation and a greater concentration of all identified pigments than red light. These results further contribute to the growing understanding that blue-green light is an essential trigger for maximized pigment concentration and FA unsaturation in green microalgae.

KEYWORDS

algal metabolism, fatty acid desaturase, green microalgae, photosynthetic pigment, polyunsaturated fatty acid, spectral light composition, thylakoid membrane

Abbreviations: ALA, alpha linolenic acid; CDW, cell dry weight; DAD, diode array detector; EI, electron impact; FA, fatty acid; FAME, fatty acid methyl ester; GC, gas chromatography; HPLC, high-performance liquid chromatography; IS, internal standard; LA, linoleic acid; MS, mass spectrometry; MUFA, monounsaturated fatty acids; PUFA, polyunsaturated fatty acids; rpm, rounds per minute; RT, retention time; SFA, saturated fatty acids; SIM, selected ion monitoring.

INTRODUCTION

Light is a vital parameter for the metabolism of photosynthetic organisms such as microalgae. The light intensity and light regime are crucial for growth and photosynthetic activity.[1] Additionally, the spectral composition of light is highly relevant for microalgal metabolism. The impact of different light spectra on the growth of microalgae has been controversially discussed in the latest literature.[2–5] Recent studies have reported a high biomass production upon green and yellow light under high light conditions as well as high culture densities. This is inconsistent with the common opinion that weakly absorbed light spectra only make a minor contribution to the growth of microalgae.[3–7]

Besides, the importance for photosynthetic energy intake and biomass production, blue and green light are important environmental triggers for regulating many metabolic processes in higher plants and algae.[8–11] For instance, it is known that blue light is required for the cell division of the microalga *Chlamydomonas reinhardtii*.[12] In the green microalga *Monoraphidium braunii*, many well-known blue light-induced processes have been identified. Blue light is a positive switch signal for the nitrate, nitrite, chloride, and hydrogen carbonate uptake in *M. braunii*.[13–15] Moreover, it is also an activation signal for enzymes involved in the nitrogen metabolism of this organism.[16] Activation of the enzyme nitrate reductase by blue light has also been reported in other algae species and is presumably widespread among green microalgae.[9,17] Furthermore, blue and green light can influence the composition of photosynthetic pigments and fatty acids (FA). Recently, we have reported that blue-green light between 450 and 550 nm is required for a maximized FA unsaturation and a maximized pigment concentration in the green microalga *Acutodesmus obliquus*.[18] These blue-green light-triggered physiological reactions might be related to a light activation of FA desaturase enzymes and the rearrangement processes of thylakoid membranes of chloroplasts.[5,19–21] Many of such light-triggered processes in organisms are highly conserved in the evolution of organisms.[22,23] Therefore, investigating the impact of blue-green light on the FA and pigment composition in photosynthetic organisms is of great interest, both phylogenetically and biochemically.

Besides this foundational knowledge, investigating these spectrally triggered metabolic processes in microalgae may have practical applications. The detailed data can be harnessed for the targeted production of valuable compounds, such as FA, for the food, feed, and biofuel industries. In particular, cultivation parameters can be used to influence microalgal metabolisms and enable the targeted industrial production of valuable compounds in microalgae.[24–28] Pigments are used as colorants and antioxidants in the food industry.[29–31] In particular, the pigment lutein is found in many microalgae and is highly valued in the pharmaceutical, cosmetic, and food industries.[32–34] Polyunsaturated fatty acids (PUFA), such as alpha-linolenic acid (ALA, 18:3n-3), are produced by different microalgae species.[35,36] The value of ALA for human nutrition is very high, due to its key function as a precursor for higher chained PUFA, which are in turn important for different physiological reactions in the human body.[37] Therefore, the food industry aims to produce products enriched in ALA.[38] But the n-3 /n-6 FA ratio is also vital for the nutritional value of food products. In particular, the ratio of the n-3 FA ALA toward the n-6 FA linoleic acid (LA, 18:2n-6) can have a strong impact on human health. A high ALA/LA ratio can even provide protection against several neurodegenerative diseases.[39–41] However, the supply of these PUFA from traditional sources, such as aquaculture and the fishery industry, is insufficient to satisfy global demand.[42] Moreover, these sources are associated with adverse environmental effects.[43,44] In contrast, microalgae are a renewable production platform for crop production and other agricultural demands.[45] Additionally, they have several advantages over land plants, such as no requirement for arable land, a lower water quality requirement, and higher growth rates.[46,47]

In this study, a combined investigation of the impact of different broad light spectra on the growth, FA, and pigment composition of *M. braunii* was conducted. It provides new insights into the light-related metabolic processes of green microalgae. The species was chosen due to the many already known blue light-triggered metabolic processes and its high industrial relevance.[5,48,49] Moreover, it has a close phylogenetic relation to *A. obliquus*, for which the impact of blue-green light on the FA composition and pigment concentration has already been described in detail Ref. [5,50].

MATERIALS AND METHODS

Microalgae preparation

The green microalga strain, *Monoraphidium braunii* SAG-202-7b (*M. braunii*) from the Culture Collection of Algae (SAG) of the University of Göttingen, Germany, was used for this study. Strain preservation was conducted in flasks on an orbital shaker (IKA KS 501 digital; 100–110 rpm), continuously illuminated by a fluorescent lamp with $50 \pm 10\,\mu mol\,photons\,m^{-2}\,s^{-1}$ (Osram Lumilux, cool white, 18W), resulting in a temperature of $25 \pm 1°C$. The flasks contained sterilized Flory Basis Fertilizer 1 (Euflor, Germany) and KNO_3 (Fisher Scientific, Germany) as described in Ref. [5,48]. The pre-cultivation and

determination of cell dry weight (CDW) were performed according to Ref. [5,18].

Cultivation device and test conditions

Only a brief description of the cultivation experiments and methodological differences is provided here since they have already been described in detail in Helamieh et al.[5].

Microalgae cultivation was carried out in column reactors as a batch culture for 96 h, with the cultivation temperature set at 25 ± 0.5°C to promote high growth and a high FA unsaturation. Two Philips MSR HR CT, 575 W metal halide lamps with a sun-like light spectrum provided the light. The metal halide lamps generated the white light spectrum, which was further referred to as "white light" (380–700 nm). The white light was additionally attenuated with a shading net (polyethylene, aperture size 2 × 10 mm, Hermann Meyer KG, Rellingen, Germany). Other light spectra were obtained using the optical filter foils "light red" "dark green," and "dark blue" (LEE-Filters, England) in combination with the metal halide lamps. These light spectra were named "red light" (580–700 nm), "green light" (450–600 nm), and "blue light" (400–550 nm). All microalgae experiments were conducted at a photon flux density of 210 µmol photons $m^{-2} s^{-1}$ for all tested light spectra (shown in the Appendix S1).

The cultivation experiments started at an optical density of 0.5 and were measured with a UV/VIS spectrometer at 750 nm (Pharmacia LKB Ultrospec III).[5,51] The cell dry weight (CDW) was calculated using a linear correlation between optical density at 750 nm (OD_{750}) and CDW, previously determined in measurements:

$$CDW = 0.436 \times OD_{750} - 0.099$$

Samples were taken daily and subsequently stored at −80°C for the FA and pigment analysis. The CDW was determined using the linear correlation by measuring the OD_{750} immediately after daily sampling.

Fatty acid analysis

The analytical method was performed according to Helamieh et al.[5]

In contrast, a volume equivalent to 0.015 g CDW of the thawed samples was used for the FA extractions and heneicosanoic acid (Sigma Aldrich, Taufkirchen, Germany) 20 µmol dissolved in hexane was employed as an internal standard (IS) in this study. The extraction and transesterification of all FA-containing lipids into fatty acid methyl ester (FAME) were carried out according to Ref. [5,52–54]. The retention times (RT) in a GC–MS chromatogram with the identified FA can be found in the Appendix S1. The ratio of the identified FAME was set into relation with the respective area of the IS, and the relative percentage of the total FAME was calculated.

Pigment analysis

The pigment analysis was performed according to Helamieh et al.[18]

Data evaluation and statistical analyses

The cultivations were performed in triplicates for each tested condition in two independent experiments, and the means ± standard errors were calculated from the values obtained. All statistical tests were done according to Helamieh et al.[18]

RESULTS

Growth

In the growth experiments, *M. braunii* was cultivated for 96 h at 25°C, with equal photon flux densities under white, red, green, and blue light conditions. Under white light treatment, the CDW reached 1.94 ± 0.04 g L^{-1}. With red light, a maximum of 1.62 ± 0.04 g L^{-1} CDW was reached. Green light and blue light treatment led to a maximum CDW of 1.37 ± 0.04 and 1.06 ± 0.01 g L^{-1}, respectively (Figure 1). The differences in biomass production after 96 h cultivation are significant ($p \leq 0.05$) for all spectra, except for the green light cultivation compared to the red light cultivation (Figure 1).

Fatty acids

All identified FA of *M. braunii* are shown in Table 1, and a chromatogram of the GC-EI/MS analysis is shown in the supplementary data (see Appendix S1). The FA 18:1, 16:1, and 16:3 were observed in different, not specifically characterized isomeric forms. Under white light, the dominant PUFA were 18:2 (18.2% ± 0.6%) and 18:3 (15.7% ± 0.6%), with a total PUFA percentage of 57.2% ± 0.6%. The rare PUFA 16:4 and 18:4 are typical for microalgae and were also identified in *M. braunii* (Table 1).[55]

The light spectrum had a strong effect on the FA composition. Higher proportions of the FA 18:3 were found in the white, green, and blue light cultivation compared to

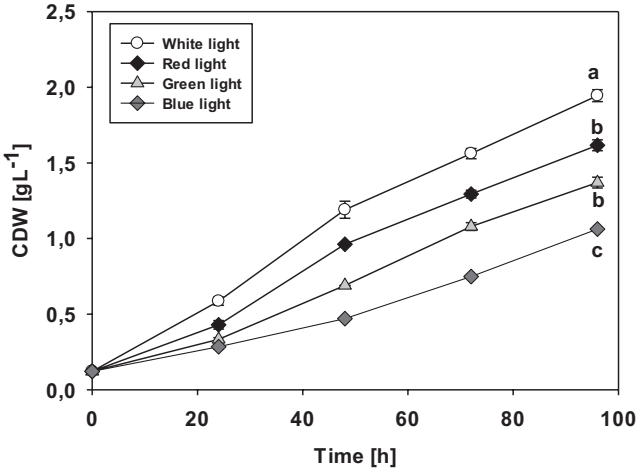

FIGURE 1 Biomass production of *Monoraphidium braunii* exposed to 210 µmol photons $m^{-2}s^{-1}$ white light (400–700 nm), red light (580–700 nm), green light (450–600 nm), and blue light (400–550 nm) at 25°C. The cell dry weight (CDW) was determined by a correlation with the optical density at 750 nm. Values represent means ± standard errors of two experiments. Different superscript letters (a–c) mean significant differences ($p \leq 0.05$) between the groups.

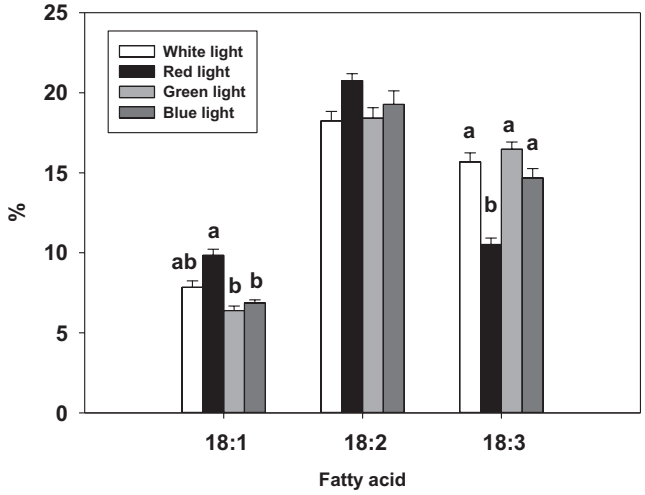

FIGURE 2 Relative proportions [%] of the fatty acids 18:1, 18:2; and 18:3 in *Monoraphidium braunii* exposed to 96 h with 210 µmol photons $m^{-2}s^{-1}$ white light (400–700 nm), red light (580–700 nm), green light (450–600 nm), and blue light (400–550 nm) at 25°C. The isomers of 18:1 were summed up. Values represent means ± standard errors of two experiments with triplicates of each light condition. Different superscript letters (a, b) mean significant differences ($p \leq 0.05$) between the groups.

TABLE 1 Fatty acid (FA) profile of *Monoraphidium braunii*.

FA	%	FA	%
14:0	≤1	18:1 isomer	≤1
15:0	≤1	$18:2^{\Delta 9,12}$	18.2 ± 0.6
16:0	30.7 ± 0.1	$18:3^{\Delta 9,12,15}$	15.7 ± 0.6
16:1 isomers	1.8	$18:4^{\Delta 6,9,12,15}$	2.2 ± 0.2
$16:2^{\Delta 7,10}$	7.5 ± 0.3	22:0	≤1
17:0	≤1	24:0	≤1
16:3 isomer	1.4 ± 0.1		
16:3 isomer	5.6 ± 0.2		
$16:4^{\Delta 4,7,10,13}$	6.4 ± 0.6	SFA	32.6 ± 0.1
18:0	≤1	MUFA	10.2 ± 0.6
18:1 isomer	7.8 ± 0.4	PUFA	57.2 ± 0.6

Note: The samples were taken after 96 h of cultivation with 210 µmol photons $m^{-2}s^{-1}$ white light at 25°C. Values represent means ± standard errors. The experiment was repeated twice in triplicates.

Abbreviations: MUFA, monounsaturated fatty acids; PUFA, polyunsaturated fatty acids; SFA, saturated fatty acids.

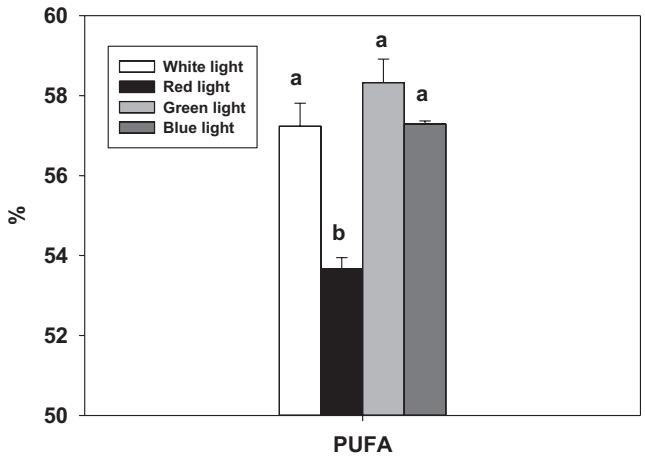

FIGURE 3 Relative proportions [%] of polyunsaturated fatty acids (PUFA) in *Monoraphidium braunii* exposed to 96 h with 210 µmol photons $m^{-2}s^{-1}$ white light (400–700 nm), red light (580–700 nm), green light (450–600 nm), and blue light (400–550 nm) at 25°C. Values represent means ± standard errors of two experiments with triplicates of each light condition. Different superscript letters (a, b) mean significant differences ($p \leq 0.05$) between the groups.

red light conditions (Figure 2). A similar pattern was also observed for the PUFA 16:4, even though these differences were not significant (see Figure S2).

Contrary to the aforementioned effect on the FA 18:3, a reverse tendency was observed for the lower desaturated n-C18 FA (18:1 and 18:2). Upon red light cultivation, a higher percentage of the 18:1 and 18:2 was detected, compared to the other spectral cultivations. Taken together, upon white, green, and blue light cultivation, a higher proportion of 18:3 toward 18:2 and 18:1 was identified, in comparison to red light cultivation (Figure 2). Additionally, a higher percentage of the summarized PUFA was also observed under white, green, and blue light, compared to red light cultivation (Figure 3). Therefore, the white, green, and blue light treatment led to a higher total degree of FA unsaturation than monochromatic red light.

Photosynthetic pigments

In the HPLC DAD analysis, six pigments were identified in *M. braunii* (Table 2). The following composition was found in the white light control after 96 h of cultivation. The primary photosynthetic pigments, chlorophyll a and b were found in concentrations of $9694 \pm 31\,\mu g\,g^{-1}$ CDW and $3370 \pm 45\,\mu g\,g^{-1}$ CDW, respectively. Lutein was found to be the major carotenoid in concentrations of $535 \pm 22\,\mu g\,g^{-1}$ CDW. Furthermore, the carotenoids and xanthophylls neoxanthin ($398\,\mu g\,g \pm 14\,\mu g\,g^{-1}$ CDW), violaxanthin ($228 \pm 8\,\mu g\,g^{-1}$ CDW), and alpha-carotene ($22 \pm 1\,\mu g\,g^{-1}$ CDW) were identified.

The light spectrum had an influence on the concentration of the identified photosynthetic pigments. Pigment concentrations for all identified pigments reached a higher value in the white, green, and blue light cultivations, compared to the red light cultivation (Table 2; Figure 4). For example, only 69.0% of lutein was found upon red light treatment compared to white light cultivation. Likewise, the values for the red light-treated samples reached 72.6% for neoxanthin, 78.5% for violaxanthin, 63.6% for alpha-carotene, and 80.0% and 87.9% for chlorophyll a and b, in comparison to white light. A similar relation of pigments can also be observed if red light treatment is compared to the green or blue light-cultivated samples (Table 2; Figure 4).

DISCUSSION

In the cultivation experiments, the biomass production of *M. braunii* was strongly affected by the light spectrum. This underlines the importance of the parameter light spectrum for the biomass production of microalgae. A comparably low growth upon blue light was also observed in recent studies on microalgae.[5,56] Even though the absorption spectrum of the primary photosynthetic pigment, chlorophyll *a*, has a high overlap with the blue light spectrum, this waveband is inefficiently used for the biomass production of *M. braunii* (Figure 1). Besides chlorophyll *a* and *b*, carotenoids and xanthophylls in *M. braunii* can also absorb blue light.[57] Xanthophylls and carotenoids mainly convert light energy into heat as a photoprotective mechanism, which might compromise biomass production.[58,59] This is one possible explanation for the low growth performance under blue light.

In contrast, the green light treatment led to higher biomass production than blue light (Figure 1). In classical plant physiology, the prevailing assumption of a low contribution of green light to photosynthetic production dominates.[60] However, a more complex understanding has emerged in very recent studies.[2–5,56] Due to the low absorptance, green light has a lower contribution to the photosynthetic production in plants and microalgae compared to red, and blue light at low photon flux densities. However, green light might efficiently contribute to biomass production under high and medium photon flux densities and high biomass concentrations. In this case, the low absorptance of green light is compensated by a more uniform absorption and more efficient use of light energy.[4] Green light can penetrate deeper layers, enabling better light dilution in the leaf tissue or microalgae solution. In contrast, red and blue light are strongly absorbed by the first layers of chloroplasts in leaf layers or microalgae solutions, whereas deeper layers remain unilluminated. This results in a lower photon quantum yield due to unequal illumination, a higher heat dissipation, and perhaps, even a higher degree of photoinhibition of the photosystems.[2,4,5,56] Very efficient use of red light and green light under medium photon flux densities was also observed in our study on *A. obliquus*.[5] Nevertheless, a combination of blue and red light was found to cause higher photosynthetic efficiencies compared to monochromatic red light in the same algae strain.[61] This was also observed in our recent study on the microalgae *A. obliquus* and might explain the high biomass production under white light, which contains red light and blue light (Figure 1).[18]

TABLE 2 Results of the HPLC-DAD pigment analysis in *Monoraphidium braunii*.

	Chl *a* ($\mu g\,g^{-1}$ CDW)	Chl *b* ($\mu g\,g^{-1}$ CDW)	Lutein ($\mu g\,g^{-1}$ CDW)	Neo ($\mu g\,g^{-1}$ CDW)	Vio ($\mu g\,g^{-1}$ CDW)	Alpha ($\mu g\,g^{-1}$ CDW)
W	9694 ± 31	3370 ± 45	535 ± 22	398 ± 14	228 ± 8	22 ± 1^{a}
R	7754 ± 923	2935 ± 405	369 ± 33	289 ± 31	179 ± 17	14 ± 1^{ab}
G	9881 ± 343	3234 ± 121	490 ± 10	360 ± 26	223 ± 5	17 ± 1^{ab}
B	9505 ± 808	3518 ± 420	475 ± 41	354 ± 1	222 ± 8	15 ± 1^{b}

Note: The analysis was repeated two times. Values represent the means ± standard errors. Different superscript letters (a, b) mean significant differences ($p \leq 0.05$) between the groups.

Abbreviations: Alpha, Alpha-Carotene; B, blue light; CDW, cell dry weight; Chl *a*, Chlorophyll *a*; Chl *b*, Chlorophyll *b*; G, green light; Neo, Neoxanthin; R, red light; Vio, Violaxanthin; W, white light.

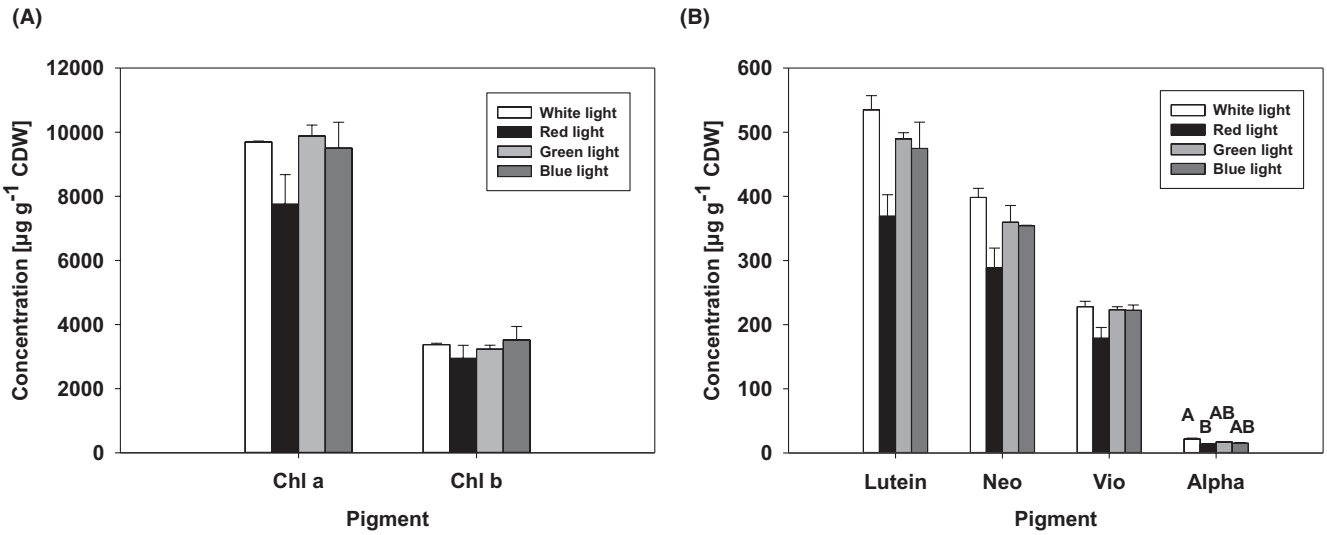

FIGURE 4 Results of the HPLC-DAD analysis of *Monoraphidium braunii*. Chl *a*: Chlorophyll *a*; Chl *b*: Chlorophyll *b* (A). Alpha, Alpha-Carotene; Neo, Neoxanthin; Vio, Violaxanthin (B). CDW, cell dry weight. The analysis was repeated two times. Values represent means ± standard error. Different superscript letters (A, B) mean significant differences ($p \leq 0.05$) between the groups.

The FA composition of *M. braunii* has a high content of PUFA, and therein a comparably high percentage of the FA 18:3 and 18:2 (Table 1). These are essential FA for human nutrition.[62] The FA composition is in accordance with other studies on the genus *Monoraphidium*.[49,55] A strong impact of the light spectrum on the FA composition of *M. braunii* was observed. The degree of FA unsaturation was higher upon white, green, and blue light treatment, compared to red light conditions. In our recent study on the green microalga *A. obliquus*, we observed a similar spectral effect. We hypothesized that blue-green light between 450 and 550 nm is required for a maximum FA unsaturation in *A. obliquus*.[5] The waveband between 450 and 550 nm was contained in all tested light spectra except red light. Therefore, the aforementioned FA desaturation effect is apparently also present in *M. braunii* and might explain the higher degree of unsaturation upon white, blue, and green light compared to red light in this study (Figures 2 and 3). This spectral waveband might be required for the maximum activity of FA-desaturase enzymes in green microalgae. Some of these FA-desaturases in photosynthetic organisms are regulated via different environmental cues, such as temperature and light.[63,64] However, it is not yet known which part of the light spectrum is required for the light regulation of FA-desaturases.

The changes in the ratio of the n-C18 FA indicate that the different light spectra impact the FA desaturation process (Figure 2). In particular, the desaturation of the FA 18:2, which is the last biochemical step in the biosynthesis of 18:3, seems to require blue-green light in *M. braunii*. It is well-known that the FA are desaturated step by step via FA-desaturases that are specific for each reaction.[21,64,65] Moreover, the activation of desaturases by light is already recognized as widespread in different phylogenetically distanced organisms.[21,63,64] Therefore, we assume that blue-green light (450–550 nm) is also required for a maximized degree of unsaturation in *M. braunii*, presumably by activating FA-desaturases.

In the pigment analysis, six photosynthetic pigments were analyzed (Figure 4a,b; Table 2). The pigment composition is in accordance with previous studies on this species.[66] Furthermore, a spectral influence on the pigment composition of *M. braunii* was observed in this study. It is already known that blue light triggers the production of xanthophylls and photosynthetic pigments.[34,67,68] This was also observed in this study for *M. braunii*. Similar to the higher FA unsaturation, the concentrations of all pigments were also higher upon white, green, and blue light treatment compared to the red light cultivation (Figure 4a,b; Table 2). Both, the different pigment concentrations and the different degrees of FA saturation, might be related to rearrangement processes of thylakoid membranes of chloroplasts.[5,19,20] These membrane systems are the locations of the photosynthetic complexes that contain the carotenoids and chlorophyll a and b.[8,69] Furthermore, the thylakoid membrane systems have high proportions of PUFA.[19–21] Therefore, the application of blue-green light might trigger an elevation of the thylakoid membrane system in *M. braunii*. This potentially explains the higher values of photosynthetic pigments and PUFA upon blue-green light-containing spectra.

Many light-regulated processes are highly conserved in the evolution of organisms.[22,23] Therefore, further investigation of the impact of blue-green light on the PUFA and pigments in different phylogenetically

distant organisms is required. This investigation might reveal the extend to which the light wavelength dependent effect on the FA and pigment composition is spread among photosynthetic organisms. To validate the hypothesized mechanism of thylakoid membrane rearrangements, additional research is necessary. For example, electron microscopic images of microalgae samples cultivated under specific light spectra might visualize blue-green light-triggered rearrangement processes in the chloroplasts of microalgae. To uncover the potential role of FA-desaturases, a detailed investigation of these enzymes is required. A transcriptome analysis of genes encoding FA-desaturases or enzyme assays involving FA-desaturases can provide insights into the role of these enzymes in blue-green light-triggered FA unsaturation. A detailed analysis can contribute to a deeper understanding of the light-regulated mechanisms in microalgae and plants. This knowledge can be leveraged for targeted industrial production of valuable compounds in microalgae.[24–28] Further practical applications of this knowledge are photovoltaic-photosynthesis hybrid systems with comprehensive spectral use of the sunlight for the production of electricity and biomass in one system.[61]

CONCLUSION AND IMPLICATIONS

Monochromatic red light and green light led to higher biomass production than monochromatic blue light. This underlines the high relevance of red and green light for microalgal growth. However, the highest biomass production was observed upon white light treatment. In addition, the strong impact of blue-green light on the FA and pigment composition of *M. braunii* was observed. Light spectra that contained blue-green light (450–550 nm) led to a maximized FA unsaturation and concentration of photosynthetic pigments. These results contribute to a growing understanding that blue-green light is a crucial environmental trigger for the lipid metabolism of photosynthetic organisms. The knowledge generated in this study may potentially be used to influence the metabolism of microalgae for industrial applications. It might pave the way for a targeted production of specific FA by light wavelength management for the biofuel and food industry. A lower degree of FA unsaturation is suitable for the production of biofuels, whereas a high content of specific PUFA is associated with beneficial nutritional effects. The degree of FA saturation in microalgae can be influenced by light wavelength management during microalgae cultivation, particularly by choosing a light spectrum that includes or excludes the waveband between 450 and 550 nm.

AUTHOR CONTRIBUTIONS

All authors have made a scientific contribution and approved the final draft of the article. Mark Helamieh—Conceived and designed the study. Carried out the research analysis and interpretation of data. Wrote the first draft of the article. Marco Reich—Supervision and support in the methodology part. Analysis and interpretation of the data. Contribution to the writing process. Editing and review of the article. Philipp Rohne—Analysis of data and statistical work. Contribution to the writing process. Ulf Riebesell—Supervised HPLC analysis and quality control of data. Martin Kerner—Analysis of data. Contribution to the writing process. Supervised the study. Klaus Kümmerer—Supervision and supported in the methodology part. Contribution to the writing process. Analysis and interpretation of data. Editing and review of the article.

ACKNOWLEDGMENTS

This study was funded by the research initiative Zukunft Bau of the Federal Institute for Research on Building, Urban Affairs, and Spatial Development (No. SWD-10.08.18.7-17.02). A special thanks to Christoph Stegen of the technical support team of the Leuphana University Lüneburg for his excellent technical support and expertise to optimize the experimental setup for microalgae cultivation. We thank Kerstin Nachtigall of the GEOMAR Helmholtz Centre for Ocean Research Kiel, for performing the HPLC-DAD analysis. Finally, we also thank Stina Krings for her contribution to microalgae cultivation and sampling. Open Access funding enabled and organized by Projekt DEAL.

CONFLICT OF INTEREST STATEMENT

The authors declare that they have no known competing financial interests or personal relationships that could have appeared to influence the work reported in this article.

ORCID

Mark Helamieh https://orcid.org/0000-0003-1865-3395

REFERENCES

1. Amini Khoeyi Z, Seyfabadi J, Ramezanpour Z. Effect of light intensity and photoperiod on biomass and fatty acid composition of the microalgae, *Chlorella vulgaris*. *Aquac Int*. 2012;20:41-49.
2. Mattos ER, Singh M, Cabrera ML, Das KC. Enhancement of biomass production in *Scenedesmus bijuga* high-density culture using weakly absorbed green light. *Biomass Bioenergy*. 2015;81:473-478.
3. de Mooij T, de Vries G, Latsos C, Wijffels RH, Janssen M. Impact of light color on photobioreactor productivity. *Algal Res*. 2016;15:32-42.
4. Ooms MD, Graham PJ, Nguyen B, Sargent EH, Sinton D. Light dilution via wavelength management for efficient high-density photobioreactors. *Biotechnol Bioeng*. 2017;114(6):1160-1169.

5. Helamieh M, Gebhardt A, Reich M, Kuhn F, Kerner M, Kümmerer K. Growth and fatty acid composition of *Acutodesmus obliquus* under different light spectra and temperatures. *Lipids*. 2021;56(5):485-498.
6. De Mooij T, Janssen M, Cerezo-Chinarro O, et al. Antenna size reduction as a strategy to increase biomass productivity: a great potential not yet realized. *J Appl Phycol*. 2015;27:1063-1077.
7. de Mooij T, Nejad ZR, van Buren L, Wijffels RH, Janssen M. Effect of photoacclimation on microalgae mass culture productivity. *Algal Res*. 2017;22:56-67.
8. Heldt HW, Piechulla B. *Pflanzenbiochemie*. Springer-Verlag; 2014.
9. Azuara MP, Aparicio PJ. In vivo blue-light activation of *Chlamydomonas reinhardii* nitrate reductase. *Plant Physiol*. 1983;71(2):286-290.
10. Christie JM, Briggs WR. Blue light sensing in higher plants. *J Biol Chem*. 2001;276(15):11457-11460.
11. Aparicio PJ, Witt FG, Ramirez JM, Quinones MA, Balandin T. Blue-light-induced pH changes associated with NO_3^-, NO_2^- and Cl^- uptake by the green alga *Monoraphidium braunii*. *Plant Cell Environ*. 1994;17(12):1323-1330.
12. Münzner P, Voigt J. Blue light regulation of cell division in *Chlamydomonas reinhardtii*. *Plant Physiol*. 1992;99(4):1370-1375.
13. Giráldez N, Aparicio PJ, Quiñones MA. Limiting CO_2 levels induce a blue light-dependent HCO_3^- uptake system in *Monoraphidium braunii*. *J Exp Bot*. 2000;51(345):807-815.
14. Giráldez N, Aparicio PJ, Quiñones MA. Blue light requirement for HCO_3 uptake and its action Spectrum in *Monoraphidium braunii*. *Photochem Photobiol*. 1998;68(3):420-426.
15. Aparicio PJ, Quiñones MA. Blue light, a positive switch signal for nitrate and nitrite uptake by the green alga *Monoraphidium braunii*. *Plant Physiol*. 1991;95(2):374-378.
16. Quiñones MA, Aparicio PJ. Blue light activation of nitrate reductase and blue light promotion of the biosynthesis of nitrite reductase in *Monoraphidium braunii*. *Inorganic Nitrogen in Plants and Microorganisms: Uptake and Metabolism*. Springer; 1990:171-177.
17. Corzo A, Niell FX. Nitrate-reductase activity and in vivo nitrate-reduction rate in *Ulva rigida* illuminated by blue light. *Mar Biol*. 1994;120:17-23.
18. Helamieh M, Reich M, Bory S, et al. Blue-green light is required for a maximized fatty acid unsaturation and pigment concentration in the microalga *Acutodesmus obliquus*. *Lipids*. 2022;57(4–5):221-232.
19. Hugly S, Somerville C. A role for membrane lipid polyunsaturation in chloroplast biogenesis at low temperature. *Plant Physiol*. 1992;99(1):197-202.
20. Hultberg M, Jönsson HL, Bergstrand KJ, Carlsson AS. Impact of light quality on biomass production and fatty acid content in the microalga *Chlorella vulgaris*. *Bioresour Technol*. 2014;159:465-467.
21. Poliner E, Busch AW, Newton L, et al. Aureochromes maintain polyunsaturated fatty acid content in *Nannochloropsis oceanica*. *Plant Physiol*. 2022;189(2):906-921.
22. Paul KN, Saafir TB, Tosini G. The role of retinal photoreceptors in the regulation of circadian rhythms. *Rev Endocr Metab Disord*. 2009;10:271-278.
23. Falciatore A, Bowler C. The evolution and function of blue and red light photoreceptors. *Curr Top Dev Biol*. 2005;68:317-350.
24. Abomohra AEF, Almutairi AW. A close-loop integrated approach for microalgae cultivation and efficient utilization of agar-free seaweed residues for enhanced biofuel recovery. *Bioresour Technol*. 2020;317:124027.
25. Almarashi JQ, El-Zohary SE, Ellabban MA, Abomohra AEF. Enhancement of lipid production and energy recovery from the green microalga *Chlorella vulgaris* by inoculum pretreatment with low-dose cold atmospheric pressure plasma (CAPP). *Energy Convers Manag*. 2020;204:112314.
26. Abomohra AEF, El-Naggar AH, Alaswad SO, Elsayed M, Li M, Li W. Enhancement of biodiesel yield from a halophilic green microalga isolated under extreme hypersaline conditions through stepwise salinity adaptation strategy. *Bioresour Technol*. 2020;310:123462.
27. Abomohra AEF, Shang H, El-Sheekh M, et al. Night illumination using monochromatic light-emitting diodes for enhanced microalgal growth and biodiesel production. *Bioresour Technol*. 2019;288:121514.
28. Abomohra AEF, Eladel H, El-Esawi M, et al. Effect of lipid-free microalgal biomass and waste glycerol on growth and lipid production of *Scenedesmus obliquus*: innovative waste recycling for extraordinary lipid production. *Bioresour Technol*. 2018;249:992-999.
29. Gong Y, Hu H, Gao Y, Xu X, Gao H. Microalgae as platforms for production of recombinant proteins and valuable compounds: progress and prospects. *J Ind Microbiol Biotechnol*. 2011;38(12):1879-1890.
30. Gong M, Bassi A. Carotenoids from microalgae: a review of recent developments. *Biotechnol Adv*. 2016;34(8):1396-1412.
31. da Silva Vaz B, Moreira JB, de Morais MG, Costa JAV. Microalgae as a new source of bioactive compounds in food supplements. *Curr Opin Food Sci*. 2016;7:73-77.
32. Granado F, Olmedilla B, Blanco I. Nutritional and clinical relevance of lutein in human health. *Br J Nutr*. 2003;90(3):487-502.
33. Sun Z, Li T, Zhou ZG, Jiang Y. Microalgae as a source of lutein: chemistry, biosynthesis, and carotenogenesis. *Adv Biochem Eng Biotechnol*. 2016;153:37-58.
34. Ho SH, Chan MC, Liu CC, et al. Enhancing lutein productivity of an indigenous microalga *Scenedesmus obliquus* FSP-3 using light-related strategies. *Bioresour Technol*. 2014;152:275-282.
35. Nagappan S, Kumar Verma S. Co-production of biodiesel and alpha-linolenic acid (omega-3 fatty acid) from microalgae, *Desmodesmus* sp. MCC34. *Energy Sources A: Recovery Util Environ Eff*. 2018;40(24):2933-2940.
36. Kumar BR, Deviram G, Mathimani T, Duc PA, Pugazhendhi A. Microalgae as rich source of polyunsaturated fatty acids. *Biocatal Agric Biotechnol*. 2019;17:583-588.
37. Burdge GC, Calder PC. Conversion of alpha-linolenic acid to longer-chain polyunsaturated fatty acids in human adults. *Reprod Nutr Dev*. 2005;45(5):581-597.
38. Kamal-Eldin A, Yanishlieva NV. N-3 fatty acids for human nutrition: stability considerations. *Eur J Lipid Sci Technol*. 2002;104(12):825-836.
39. Singh S, Nair V, Jain S, Gupta YK. Evaluation of anti-inflammatory activity of plant lipids containingα–linolenic acid. *Indian J Exp Biol*. 2008;46:553-556.
40. Simopoulos AP. The importance of the ratio of omega-6/omega-3 essential fatty acids. *Biomed Pharmacother*. 2002;56(8):365-379.
41. Shanab SM, Hafez RM, Fouad AS. A review on algae and plants as potential source of arachidonic acid. *J Adv Res*. 2018;11:3-13.

42. Tocher DR, Betancor MB, Sprague M, Olsen RE, Napier JA. Omega-3 long-chain polyunsaturated fatty acids, EPA and DHA: bridging the gap between supply and demand. *Nutrients*. 2019;11(1):89.
43. Worm B, Barbier EB, Beaumont N, et al. Impacts of biodiversity loss on ocean ecosystem services. *Science*. 2006;314(5800):787-790.
44. Blanco Gonzalez E, de Boer F. The development of the Norwegian wrasse fishery and the use of wrasses as cleaner fish in the salmon aquaculture industry. *Fish Sci*. 2017;83:661-670.
45. Alvarez AL, Weyers SL, Goemann HM, Peyton BM, Gardner RD. Microalgae, soil and plants: a critical review of microalgae as renewable resources for agriculture. *Algal Res*. 2021;54:102200.
46. Benedetti M, Vecchi V, Barera S, Dall'Osto L. Biomass from microalgae: the potential of domestication towards sustainable biofactories. *Microb Cell Factories*. 2018;17:1-18.
47. Amaro HM, Macedo ÂC, Malcata FX. Microalgae: an alternative as sustainable source of biofuels? *Energy*. 2012;44(1):158-166.
48. Lindner AV, Pleissner D. Removal of phenolic compounds from olive mill wastewater by microalgae grown under dark and light conditions. *Waste Biomass Valorization*. 2022;13(1):525-534.
49. Krienitz L, Wirth M. The high content of polyunsaturated fatty acids in *Nannochloropsis limnetica* (Eustigmatophyceae) and its implication for food web interactions, freshwater aquaculture and biotechnology. *Limnologica*. 2006;36(3):204-210.
50. Krienitz L, Ustinova I, Friedl T, Huss VA. Traditional generic concepts versus *18S rRNA* gene phylogeny in the green algal family Selenastraceae (Chlorophyceae, Chlorophyta). *J Phycol*. 2001;37(5):852-865.
51. Admirasari R, Hindersin S, von Schwartzenberg K, Hanelt D. Nutritive capability of anaerobically digested black water increases productivity *of Tetradesmus obliquus*: domestic wastewater as an alternative nutrient resource. *Biores Technol Rep*. 2022;17:100905.
52. Reich M, Hannig C, Al-Ahmad A, Bolek R, Kümmerer K. A comprehensive method for determination of fatty acids in the initial oral biofilm (pellicle). *J Lipid Res*. 2012;53(10):2226-2230.
53. Reich M, Kümmerer K, Al-Ahmad A, Hannig C. Fatty acid profile of the initial oral biofilm (pellicle): an in-situ study. *Lipids*. 2013;48:929-937.
54. Ichihara KI, Fukubayashi Y. Preparation of fatty acid methyl esters for gas-liquid chromatography [S]. *J Lipid Res*. 2010;51(3):635-640.
55. Řezanka T, Nedbalová L, Lukavský J, Střížek A, Sigler K. Pilot cultivation of the green alga *Monoraphidium* sp. producing a high content of polyunsaturated fatty acids in a low-temperature environment. *Algal Res*. 2017;22:160-165.
56. Liu J, Van Iersel MW. Photosynthetic physiology of blue, green, and red light: light intensity effects and underlying mechanisms. *Front Plant Sci*. 2021;12:328.
57. Ruban AV, Horton P, Young AJ. Aggregation of higher plant xanthophylls: differences in absorption spectra and in the dependency on solvent polarity. *J Photochem Photobiol*. 1993;21(2–3):229-234.
58. Jahns P, Latowski D, Strzalka K. Mechanism and regulation of the violaxanthin cycle: the role of antenna proteins and membrane lipids. *Biochim Biophys Acta Bioenerg*. 2009;1787(1):3-14.
59. Wilhelm C, Krámer P, Wild A. Effect of different light qualities on the ultrastructure, thylakoid membrane composition and assimilation metabolism of *Chlorella fusca*. *Physiol Plant*. 1985;64(3):359-364.
60. McCree KJ. The action spectrum, absorptance and quantum yield of photosynthesis in crop plants. *Agric Meteorol*. 1971;9:191-216.
61. Osterthun N, Helamieh M, Berends D, et al. Influence of spectrally selective solar cells on microalgae growth in photo-bioreactors. In *AIP Conference Proceedings*. 2361;No. 1:70001). AIP Publishing LLC; 2021.
62. Zhuang P, Shou Q, Wang W, et al. Essential fatty acids linoleic acid and α-linolenic acid sex-dependently regulate glucose homeostasis in obesity. *Mol Nutr Food Res*. 2018;62(17):1800448.
63. Collados R, Andreu V, Picorel R, Alfonso M. A light-sensitive mechanism differently regulates transcription and transcript stability of ω3 fatty-acid desaturases (FAD3, FAD7 and FAD8) in soybean photosynthetic cell suspensions. *FEBS Lett*. 2006;580(20):4934-4940.
64. Kis M, Zsiros O, Farkas T, Wada H, Nagy F, Gombos Z. Light-induced expression of fatty acid desaturase genes. *Proc Natl Acad Sci U S A*. 1998;95(8):4209-4214.
65. Lee KR, Jeon I, Yu H, et al. Increasing monounsaturated fatty acid contents in hexaploid *Camelina sativa* seed oil by *FAD2* gene knockout using CRISPR-Cas9. *Front Plant Sci*. 2021;12:702930.
66. Cordero BF, Obraztsova I, Couso I, Leon R, Vargas MA, Rodriguez H. Enhancement of lutein production in *Chlorella sorokiniana* (Chorophyta) by improvement of culture conditions and random mutagenesis. *Mar Drugs*. 2011;9(9):1607-1624.
67. Fu W, Guðmundsson Ó, Paglia G, et al. Enhancement of carotenoid biosynthesis in the green microalga *Dunaliella salina* with light-emitting diodes and adaptive laboratory evolution. *Appl Microbiol Biotechnol*. 2013;97:2395-2403.
68. Sharmila D, Suresh A, Indhumathi J, Gowtham K, Velmurugan N. Impact of various color filtered LED lights on microalgae growth, pigments and lipid production. *European J Biotechnol Biosci*. 2018;6(6):1-7.
69. Pribil M, Labs M, Leister D. Structure and dynamics of thylakoids in land plants. *J Exp Bot*. 2014;65(8):1955-1972.

SUPPORTING INFORMATION

Additional supporting information can be found online in the Supporting Information section at the end of this article.

How to cite this article: Helamieh M, Reich M, Rohne P, Riebesell U, Kerner M, Kümmerer K. Impact of green and blue-green light on the growth, pigment concentration, and fatty acid unsaturation in the microalga *Monoraphidium braunii*. *Photochem Photobiol*. 2023;00:1-9. doi:10.1111/php.13873